AN ABSTRACT OF THE THESIS OF

Lik Tong Tan for the degree of Doctor of Philosophy in Pharmacy presented on April 26 2001. Title: Bioactive Natural Products from Marine Algae.

Abstract approved: Redacted for Privacy
William H. Gerwick

This thesis is an account of my investigation on the natural products deriving from various marine algae and has resulted in the discovery of thirteen novel bioactive metabolites. Isolation and characterization of these unique molecules were carried out using different chromatographic techniques and by careful analyses of 1D and 2D NMR data, respectively.

Two new thiazole-containing cyclic heptapeptides, *cis,cis*- and *trans,trans*-ceratospongamide, were identified from an Indonesian red alga, *Ceratodictyon spongiosum* Zanardini. These are a pair of stable conformers differing only in the conformation of two proline amide bonds. The *trans,trans*-form was revealed to be a potent anti-inflammatory agent in the inhibition of $sPLA_2$ expression in a cell-based model.

The hermitamides are new malyngamide-type molecules isolated from a collection of the marine cyanobacterium *Lyngbya majuscula* Gomont made in Papua New Guinea. The semi-syntheses of these natural metabolites were achieved by coupling the free-occurring C-14 lyngbic acid isolated from the microalga and the commercially available aromatic amines. Two new semi-synthetic molecules, the *N*-methylated derivatives of the hermitamides, were also prepared. The biological properties of the hermitamides and synthetic derivatives were evaluated in several bioassays.

The organic extract of another collection of *L. majuscula* Gomont from Papua New Guinea was a prolific source of several novel cyclic depsipeptides, given the trivial names clairamides A and B, wewakamide, carliamide, and guinamides A and B. These molecules were characterized by having unique β-amino or β-hydroxy acid moieties,

one of which is being reported for the first time from the marine environment. The absolute stereochemistry in clairamide A of one such unit, 2-methyl-3-amino-pentanoic acid, is discussed. Clairamide B and carliamide exhibited moderate cytotoxic activities.

Investigation of another species of filamentous marine cyanobacterium, *L. bouillonii* Hoffmann and Demoulin from Papua New Guinea yielded three novel cytotoxic metabolites. These were two cyclic depsipeptides, bouillonamides A and B, and a glycosidic macrolide, lyngbouilloside. The cytotoxic activities of these molecules were evaluated in the neuro-2a mouse neuroblastoma cell assay. The isolation of these metabolites demonstrated that *L. bouillonii* is a rich source of novel and biologically active natural products.

BIOACTIVE NATURAL PRODUCTS FROM MARINE ALGAE

by

Lik Tong Tan

A THESIS

submitted to

Oregon State University

in partial fulfillment of
the requirements for the
degree of

Doctor of Philosophy

Presented April 26, 2001
Commencement June 2001

Doctor of Philosophy thesis of Lik Tong Tan presented on April 26, 2001

APPROVED:

Redacted for Privacy

Major Professor, Representing Pharmacy

Redacted for Privacy

Dean of the College of Pharmacy

Redacted for Privacy

Dean of Graduate School

I understand that my thesis will become part of the permanent collection of Oregon State University libraries. My signature below authorizes release of my thesis to any reader upon request.

Redacted for Privacy

Lik Tong Tan, Author

ACKNOWLEDGEMENTS

I would like to thank my major advisor, Dr. William H. Gerwick, for his generous support, academic guidance, and patience throughout the course of my graduate career at Oregon State University. My appreciation also goes out to my committee members, Dr. George Constantine, Dr. Philip Proteau, Dr. Victor Hsu, and Dr. Bruce Coblentz for their time and useful suggestions.

I am grateful to Brian Arbogast (Department of Chemistry, OSU) for mass spectral data. I would also like to acknowledge past and present colleagues.

I am indebted to my family for their support and encouragement and finally to my wife, Edith, for her unyielding love and patience throughout the entire process.

CONTRIBUTION OF AUTHORS

Anti-inflammatory bioassays in chapter two of my thesis were carried out by Kevin McGough in the laboratory of Professor Robert Jacob at University of California at Santa Barbara. Three dimensional molecular modeling of the natural products in the same chapter was carried out by Shawn Watts at the Department of Biochemistry and Biophysics, OSU. The various NMR experiments discussed in chapters two and five, were performed by Thomas Williamson and Brian Marquez, respectively. Dr. Tatsufumi Okino and Gloria Zeller provided the results of the neuro-2a mouse neuroblastoma cell toxicity bioassays presented in chapters three, four, and five. Pure samples of the (2*S*,3*R*) 2-methyl-3-amino-pentanoic acid used for the absolute stereochemical determination in chapter four were provided by Professor R. Bates at the University of Arizona.

TABLE OF CONTENTS

	PAGE
CHAPTER ONE: GENERAL INTRODUCTION	1
HIGHLIGHTS OF MARINE NATURAL PRODUCTS	3
BIOACTIVE SECONDARY METABOLITES FROM MARINE ALGAE	19
INVERTEBRATE NATURAL PRODUCTS DERIVING FROM MARINE CYANOBACTERIA	26
GENERAL THESIS CONTENTS	33
CHAPTER TWO: *CIS,CIS*- AND *TRANS,TRANS*-CERATOSPONGAMIDE, NEW BIOACTIVE CYCLIC HEPTAPEPTIDES FROM THE INDONESIAN RED ALGA *CERATODICTYON SPONGIOSUM* AND SYMBIOTIC SPONGE *SIGMADOCIA SYMBIOTICA*	
ABSTRACT	35
INTRODUCTION	36
RESULTS AND DISCUSSION	38
EXPERIMENTAL	55
CHAPTER THREE: HERMITAMIDES A AND B, TOXIC MALYNGAMIDE-TYPE NATURAL PRODUCTS FROM THE MARINE CYANOBACTERIUM *LYNGBYA MAJUSCULA* GOMONT	
ABSTRACT	59
INTRODUCTION	60
RESULTS AND DISCUSSION	65
EXPERIMENTAL	86
CHAPTER FOUR: NOVEL CYCLIC DEPSIPEPTIDES FROM A PAPUA NEW GUINEA COLLECTION OF *LYNGBYA MAJUSCULA* GOMONT	
ABSTRACT	90
INTRODUCTION	91
RESULTS AND DISCUSSION	98

TABLE OF CONTENTS (*continued*)

PAGE

EXPERIMENTAL 139

CHAPTER FIVE: A NOVEL CYTOTOXIC MACROLIDE AND CYCLIC DEPSIPEPTIDES FROM A PAPUA NEW GUINEA MARINE CYANOBACTERIUM *LYNGBYA BOUILLONII* HOFFMANN AND DEMOULIN

ABSTRACT 144

INTRODUCTION 145

RESULTS AND DISCUSSION 148

EXPERIMENTAL 184

CHAPTER SIX: CONCLUSIONS 188

BIBLIOGRAPHY 195

APPENDICES 206

APPENDIX A: ISOLATION OF MALYNGAMIDE C AND DERIVATIVES FROM A MARINE CYANOBACTERIUM, *LYNGBYA* SPECIES, COLLECTED FROM PAPUA NEW GUINEA 207

APPENDIX B: DETECTION OF DEBROMOAPLYSIATOXIN IN A MARINE CYANOBACTERIAL ASSEMBLAGE COLLECTED FROM FIJI 208

APPENDIX C: ISOLATION AND STRUCTURE DETERMINATION OF KNOWN ANTIFUNGAL NATURAL PRODUCTS FROM THE RED ALGA, *GELIDIUM PRISTIODES* 209

LIST OF FIGURES

FIGURE		PAGE
I.1	Marine toxins (I).	4
I.2	Largest non-proteinaceous marine toxin (II).	5
I.3	Marine toxins (III).	6
I.4	Anticancer marine natural products (I).	8
I.5	Anticancer marine natural products (II).	10
I.6	Natural (**21**) and synthetic (**22**) anticancer molecules.	11
I.7	Antiinflammatory marine natural products.	13
I.8	Marine natural products as molecular probes.	14
I.9	Antimalarial marine natural products.	15
I.10	AntiHIV marine natural product.	16
I.11	Insecticidal and antifouling marine natural products.	17
I.12	Natural products from marine algae.	21
I.13	Natural products from marine cyanobacteria (I).	23
I.14	Natural products from marine cyanobacteria (II).	24
I.15	Natural products from marine cyanobacteria (III).	25
II.1	New cyclic heptapeptides (**96** and **97**) from *Ceratodictyon spongiosum* Zanardini (IBI-4/Nov/94-15).	39
II.2	^{1}H NMR spectrum of *cis,cis*-ceratospongamide (**96**) in $CDCl_3$.	42
II.3	^{13}C NMR spectrum of *cis,cis*-ceratospongamide (**96**) in $CDCl_3$.	43
II.4	Selected correlations observed by ^{1}H-^{15}N HMBC of *cis,cis*-ceratospongamide (**96**).	46
II.5	FAB mass spectral fragmentations observed for *cis,cis*-ceratospongamide (**96**) and *trans,trans*-ceratospongamide (**97**).	46
II.6	^{1}H NMR spectrum of *trans,trans*-ceratospongamide (**97**) in $CDCl_3$.	48
II.7	^{13}C NMR spectrum of *trans,trans*-ceratospongamide (**97**) in $CDCl_3$.	49
II.8	Molecular modeling of the ceratospongamides: (A) view of **97** looking down on macrocycle, (B) orthogonal view of **97**, (C) view of **96** looking down on macrocycle, (D) orthogonal view of **96**.	54
III.1	Lyngbic acids.	61

FIGURE		PAGE
III.2	Malyngamides from marine cyanobacteria.	63
III.3	New and semi-synthetic hermitamides.	66
III.4	LR FABMS spectrum of hermitamide A (**123**).	67
III.5	1D NMR spectra of hermitamide A (**123**) in C_6D_6.	68
III.6	HSQC spectrum of hermitamide A (**123**) in C_6D_6.	70
III.7	HMBC spectrum of hermitamide A (**123**) in C_6D_6.	71
III.8	COSY spectrum of hermitamide A (**123**) in C_6D_6.	72
III.9	LR FABMS spectrum of hermitamide B (**124**).	74
III.10	1D NMR spectra of hermitamide B (**124**) in $CDCl_3$.	75
III.11	HSQC spectrum hermitamide B (**124**) in $CDCl_3$.	77
III.12	HMBC spectrum hermitamide B (**124**) in $CDCl_3$.	78
III.13	TOCSY spectrum hermitamide B (**124**) in $CDCl_3$.	79
III.14	Methods utilized in the syntheses of the hermitamides (**123** and **124**) and derivatives (**125** and **126**).	81
III.15	^{1}H NMR spectra of *N*-Me-hermitamides A (**125**) and B (**126**) in $CDCl_3$.	83
III.16	LR FABMS spectrum of *N*-Me-hermitamide A (**125**).	84
III.17	LR FABMS spectrum of *N*-Me-hermitamide B (**126**).	85
IV.1	Novel cyclic depsipeptides isolated from *Lyngbya majuscula* (PNSM-4/Sep/98-01).	99
IV.2	Isolation and purification of compounds **151** to **156**.	100
IV.3	^{1}H NMR spectrum of clairamide B (**152**) in $CDCl_3$.	101
IV.4	^{13}C NMR spectrum of clairamide B (**152**) in $CDCl_3$.	102
IV.5	Partial structures of clairamide B (**152**).	104
IV.6	HMBC correlations in clairamide B (**152**).	104
IV.7	HSQC spectrum of clairamide B (**152**) in $CDCl_3$.	105
IV.8	HMBC spectrum of clairamide B (**152**) in $CDCl_3$.	106
IV.9	TOCSY spectrum of clairamide B (**152**) in $CDCl_3$.	107
IV.10	^{1}H NMR spectrum of wewakamide (**153**) in DMSO-d_6.	110

FIGURE		PAGE
IV.11	^{13}C NMR spectrum of wewakamide (**153**) in DMSO-d_6.	111
IV.12	Partial structures of wewakamide (**153**).	113
IV.13	HMBC correlations in wewakamide (**153**).	113
IV.14	HSQC spectrum of wewakamide (**153**) in DMSO-d_6.	114
IV.15	HMBC spectrum of wewakamide (**153**) in DMSO-d_6.	115
IV.16	TOCSY spectrum of wewakamide (**153**) in DMSO-d_6.	116
IV.17	^{1}H NMR spectrum of guinamide A (**155**) in $CDCl_3$.	119
IV.18	^{13}C NMR spectrumof guinamide A (**155**) in $CDCl_3$.	120
IV.19	Partial structures of guinamide A (**155**).	122
IV.20	HMBC correlations in guinamide A (**155**).	122
IV.21	HSQC spectrum of guinamide A (**155**) in $CDCl_3$.	123
IV.22	HMBC spectrum of guinamide A (**155**) in $CDCl_3$.	124
IV.23	TOCSY spectrum of guinamide A (**155**) in $CDCl_3$.	125
IV.24	^{1}H NMR spectrum of guinamide B (**156**) in $CDCl_3$.	127
IV.25	^{13}C NMR spectrum of guinamide B (**156**) in $CDCl_3$.	128
IV.26	Partial structures of guinamide B (**156**).	130
IV.27	HMBC correlations in guinamide B (**156**).	130
IV.28	HSQC spectrum of guinamide B (**156**) in $CDCl_3$.	131
IV.29	HMBC spectrum of guinamide B (**156**) in $CDCl_3$.	132
IV.30	TOCSY spectrum of guinamide B (**156**) in $CDCl_3$.	133
IV.31	^{1}H NMR spectrum of clairamide A (**151**) in $CDCl_3$.	135
IV.32	Absolute stereochemical analysis of Mapa unit in clairamide A (**151**).	136
V.1	Picture of *Lyngbya bouillonii* Hoffmann and Demoulin in nature.	146
V.2	Secondary metabolites isolated from *Lyngbya bouillonii*.	147
V.3	Natural products from *Lyngbya bouillonii* (PNGRD 21/Aug/00-2).	149
V.4	^{1}H NMR spectrum of apratoxin (**164**) in $CDCl_3$.	150
V.5	^{1}H NMR spectrum of bouillonamide A (**161**) in $CDCl_3$.	152
V.6	^{13}C NMR spectrum of bouillonamide A (**161**) in $CDCl_3$.	153

FIGURE		PAGE
V.7	Partial structures of bouillonamide A (**161**).	155
V.8	Key HMBC correlations used to sequence the linkage of residues in bouillonamide A (**161**).	155
V.9	HSQC spectrum of bouillonamide A (**161**) in $CDCl_3$.	156
V.10	HMBC spectrum of bouillonamide A (**161**) in $CDCl_3$.	157
V.11	TOCSY spectrum of bouillonamide A (**161**) in $CDCl_3$.	158
V.12	^{1}H NMR spectrum of bouillonamide B (**162**) in $CDCl_3$.	160
V.13	^{13}C NMR spectrum of bouillonamide B (**162**) in $CDCl_3$.	161
V.14	Partial structures of bouillonamide B (**162**) showing selected HMBC correlations.	163
V.15	Key HMBC correlations used to sequence the linkage of residues in bouillonamide B (**162**).	163
V.16	HSQC spectrum of bouillonamide B (**162**) in $CDCl_3$.	164
V.17	HMBC spectrum of bouillonamide B (**162**) in $CDCl_3$.	165
V.18	COSY spectrum of bouillonamide B (**162**) in $CDCl_3$.	166
V.19	LR positive ion FABMS spectrum of lyngbouilloside (**163**).	168
V.20	LR negative ion FABMS spectrum of lyngbouilloside (**163**).	169
V.21	^{1}H NMR spectrum of lyngbouilloside (**163**) in $CDCl_3$.	170
V.22	^{13}C NMR spectrum of lyngbouilloside (**163**) in $CDCl_3$.	171
V.23	^{1}H NMR spectrum of acetylated lyngbouilloside (**169**) in $CDCl_3$.	172
V.24	2,4-Di-*O*-methylrhamnopyranoside moiety in lyngbouilloside (**163**).	174
V.25	Partial structures of lyngbouilloside (**163**).	175
V.26	Selected HMBC correlations in lyngbouilloside (**163**).	175
V.27	HSQC spectrum of lyngbouilloside (**163**) in $CDCl_3$.	176
V.28	HMBC spectrum of lyngbouilloside (**163**) in $CDCl_3$.	177
V.29	COSY spectrum of lyngbouilloside (**163**) in $CDCl_3$.	178
V.30	Six possible conformers for the asymmetric carbons at C-10 and C-11 of lyngbouilloside (**163**).	180

FIGURE PAGE

V.31 ^{1}H NMR spectra of clairamides A (**151**, top), B (**152**, middle), and bouillonamide B (**162**, bottom) in $CDCl_3$. 182

V.32 Glycosidic macrolides from marine invertebrates. 183

VI.1 Natural products from *Ceratodictyon spongiosum* (**96** and **97**) and *Lyngbya majuscula* (**123** and **124**). [Compounds **125** and **126** are synthetic *N*-methylated derivatives of the natural hermitamides] 191

VI.2 Natural products isolated and defined in this thesis from Papua New Guinea collections of *Lyngbya majuscula* (**151** to **156**). 192

VI.3 Natural products isolated and defined in this thesis from Papua New Guinea collections of *Lyngbya bouillonii* (**161** to **164**). 193

LIST OF TABLES

TABLE		PAGE
I.1	Anticancer marine natural products in clinical and preclinical testings.	7
I.2	Isolation of identical/related dolastatins from marine cyanobacteria.	28
I.3	β-Amino and β-hydroxy acid units in molluscan and cyanobacterial compounds.	29
II.1	^{1}H and ^{13}C NMR spectral data (in ppm) for *cis,cis*-ceratospongamide (**96**)[a] with HMBC and ROESY correlations.	44
II.2	^{1}H and ^{13}C NMR spectral data (in ppm) for *trans,trans*-ceratospongamide (**97**)[a] with HMBC and ROESY correlations.	50
III.1	Biological activities of the malyngamides.	64
III.2	^{1}H and ^{13}C NMR data for hermitamide A (**123**) in C_6D_6.[a]	69
III.3	^{1}H and ^{13}C NMR data for hermitamide B (**124**) in $CDCl_3$.[a]	76
IV.1	β-Amino acid moieties found in marine cyanobacterial and molluscan metabolites.	96
IV.2	β-Hydroxy acid moieties found in marine cyanobacterial and molluscan metabolites.	97
IV.3	NMR spectral data for clairamide B (**152**) at 600 MHz (^{1}H) and 100 MHz (^{13}C) in $CDCl_3$.	103
IV.4	NMR spectral data for wewakamide (**153**) at 600 MHz (^{1}H) and 100 MHz (^{13}C) in DMSO-d_6.	112
IV.5	NMR spectral data for guinamide A (**155**) at 400 MHz (^{1}H) and 100 MHz (^{13}C) in $CDCl_3$.	121
IV.6	NMR spectral data for guinamide B (**156**) at 400 MHz (^{1}H) and 100 MHz (^{13}C) in $CDCl_3$.	129
IV.7	Constituents of the *Lyngbya majuscula* cyclic depsipeptides (**151** to **156**).	138
V.1	NMR spectral data for bouillonamide A (**161**) at 400 MHz (^{1}H) and 100 MHz (^{13}C) in $CDCl_3$.	154
V.2	NMR spectral data for bouillonamide B (**162**) at 400 MHz (^{1}H) and 100 MHz (^{13}C) in $CDCl_3$.	162
V.3	NMR spectral data for lyngbouilloside (**163**) at 400 MHz (^{1}H) and 100 MHz (^{13}C) in $CDCl_3$.	173
VI.1	Biological activities of natural and semi-synthetic molecules presented in the thesis.	194

LIST OF ABBREVIATIONS

Abu	2-Amino-2-butenoic acid
Ahp	3-Amino-6-hydroxy-2-piperidone
Ala	Alanine
Amoya	3-Amino-2-methyl-oct-7-ynoic acid
Ara-A	Adenine arabinoside
Ara-C	Cytosine arabinoside
br	Broad
CI	Chemical Ionization
CNS	Central Nervous System
COSY	^{1}H-^{1}H Chemical Shift Correlation Spectroscopy
d	Doublet
DCC	*N,N'*-Dicyclohexylcarbodiimide
Dhoaa	2,2-Dimethyl-3-hydroxy-octanoic acid
Dhoya	2,2-Dimethyl-3-hydroxy-7-octynoic acid
Dmhha	2,2-Dimethyl-3-hydroxy-hexanoic acid
DMSO	Dimethylsulfoxide
ED	Effective Dosage
EIMS	Electron-Impact Mass Spectrometry
ELISA	Enzyme-Linked Immunosorbent Assay
EtOAc	Ethyl Acetate
FAB	Fast Atom Bombardment
FFDNB	1,5-Difluoro-2,4-dinitrobenzene
FDAA	*N*α-(2,4-dinitro-5-fluoro-phenyl)-*L*-alaninamide
GC	Gas Chromatography
Gly	Glycine
Hiv	2-Hydroxy-isovaleric acid
HIV	Human Immunodeficiency Virus
HMBC	Heteronuclear Multiple-Bond Coherence Spectroscopy
Hmha	5-Hydroxy-3-methyl-heptanoic acid

LIST OF ABBREVIATIONS (*continued*)

HPLC	High Performance Liquid Chromatography
HSQC	Heteronuclear Single Quantum Coherence
HSQMBC	Heteronuclear Single Quantum Multiple Bond Correlation
Hymo	3-Hydroxy-2-methyl-oct-7-ynoic acid
IC	Inhibitory Concentration
Ile	Isoleucine
IL	Interleukin
IR	Infrared Spectroscopy
Lac	Lactic acid
LD	Lethal Dose
m	Multiplet
Maba	2-Methyl-3-amino-butanoic acid
Maha	2-Methyl-3-amino-hexanoic acid
Mapa	2-Methyl-3-amino-pentanoic acid
Me	Methyl
MeOH	Methanol
Mmaha	2-Methyl-6-methylamino-hex-5-enoic acid
MS	Mass Spectroscopy
NMR	Nuclear Magnetic Resonance
NOESY	Nuclear Overhauser Exchange Spectroscopy
NRPS	Non-Ribosomal Polyketide Synthetase
Phe	Phenylalanine
PKS	Polyketide Synthase
Pro	Proline
q	Quartet
ROESY	Rotating Overhauser Exchange Spectroscopy
RT	Room Temperature
s	Singlet
SCUBA	Self-Contained Underwater Breathing Apparatus

$sPLA_2$	secreted Phospholipase A_2
t	Triplet
TCA	Trichloroacetonitrile
TFA	Trifluoroacetic acid
TLC	Thin Layer Chromatography
TOCSY	Total Correlation Spectroscopy
t_R	Retention Time
Tyr	Tyrosine
UV	Ultraviolet Spectroscopy
Val	Valine
VLC	Vacuum liquid chromatography

This thesis is dedicated to my wife, EDITH.

BIOACTIVE NATURAL PRODUCTS FROM MARINE ALGAE

CHAPTER ONE

GENERAL INTRODUCTION

Nature has been the traditional source of new pharmaceuticals. A recent survey has estimated that over 50% of the current drugs used are either harvested from natural sources or from synthetic compounds based on natural products templates.[1] The use of natural products in treatment of human ailments has its beginnings dating back to ancient times in both Eastern and Western cultures. Currently, there is a pressing need for new therapeutic agents and this is due mainly to the resurgence of pathogenic microorganisms and parasites that have developed resistance to traditional chemotherapies. There is also an urgent need to uncover new pharmaceuticals for treating different forms of cancer, viral and fungal infections, as well as inflammatory diseases. Scientists are therefore, relying on nature to provide them with solutions. Traditionally, terrestrial plants have been a main source for the discovery of new pharmaceuticals. However, scientists are beginning to focus their attention to the marine realm as an additional source of novel and useful natural products.

Historically, the first recorded research on marine natural products began in the early 1950s with the pioneering work of Bergman, which led to the discoveries of the nucleosides spongouridine (**1**) and spongothymidine (**2**) from marine sponges collected off the coast of Florida.[2] This initial serendipitous discovery led to the development of Ara-A (**3**) and Ara-C (**4**), which are based on these sponge nucleosides and are clinically available today. Ara-C (**4**) is an anticancer drug used for the treatment of acute myelocytic leukemia and non-Hodgkin's lymphoma while the antiviral drug, Ara-A (**3**), is used for the treatment of herpes infections.[3,4] However, it was only in the 1970s that an intensive search for useful secondary metabolites (i.e. compounds that do not have apparent involvement in primary metabolism) from marine plants and invertebrates

began in earnest that continues today. There are several reasons that drive this vigorous endeavor to search for drugs from the sea.

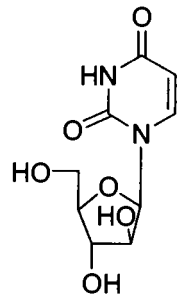

Spongouridine (1)

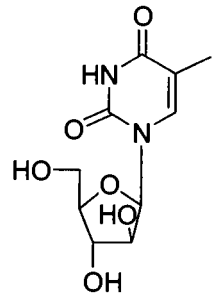

Spongothymidine (2)

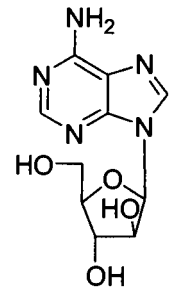

Ara-A (3)

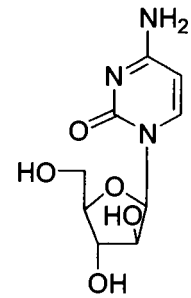

Ara-C (4)

The ocean covers nearly three-quarters of the earth's surface and is home to a tremendous variety of flora and fauna. It has been conservatively estimated that the number of marine species stands at half a million and was projected to be upwards of 10 million with the majority still undescribed.[5] The ocean thus represents a wealth of resources for biotechnology research. Coupled with the development of SCUBA in the 1940s, and more recently submersible vehicles, these have allowed relatively easy accessibility of both shallow and deep-water marine organisms for studies by natural products chemists.

In contrast to their terrestrial counterparts, many marine derived secondary metabolites are structurally complex with unique functionalities. This is due in part to the differences in the physicochemical nature of the two environments where higher pressures, lower temperatures, lack of light as well as high ionic concentrations present in the sea may account for the biosynthesis of highly functionalized and unusual molecules in these organisms. It is because of these structural novelties that natural products chemists hope to uncover new classes of therapeutic agents with unique pharmacophores which may potentially lead to defining novel sites of action in protein and enzymes that are involved in human illnesses.

Many marine organisms are engaged in chemical warfare. This is especially true for reef dwellers where space is at a premium and many different organisms are living in

close proximity to each other. Thus, many marine organisms, such as sessile species, produce toxic compounds for their survival by preventing predation and fouling by other organisms. Based on such ecological observations, natural products chemists are able to isolate and define numerous potent marine secondary metabolites with potential uses as therapeutic agents. This introduction serves to highlight some of the milestones and significant discoveries in the field of marine natural products chemistry. Attention is given to secondary metabolites that are increasingly becoming important as pharmaceuticals or as agrochemicals. A brief review on bioactive natural products from marine algae (with emphasis on marine cyanobacteria), the main focus of this thesis, is also presented. Some structural parallels between secondary metabolites from marine invertebrates and cyanobacteria will also be discussed. This introductory chapter concludes with a concise outline of the various chapters presented in the thesis.

HIGHLIGHTS OF MARINE NATURAL PRODUCTS

Since its inception in the early 1950s, more then 10,000 secondary metabolites have been defined from marine organisms (as compared with about 150,000 from terrestrial plants).[6] The predominant sources of marine organisms studied by natural products chemists are sponges, soft corals, seaweeds, sea squirts, and bryozoans. The types of compounds characterized from these organisms are diverse and represent many different structural classes, including terpenoids, acetogenins, alkaloids, and polyphenolics. In addition, these metabolites possess a wide spectrum of bioactivities, ranging from antifeedant to cytotoxicity. Such diverse marine secondary metabolites are being compiled yearly in a series of comprehensive reviews by Faulkner.[7]

An important class of marine macromolecules, belonging mainly to the polyether structural class, forms the basis of a majority of marine toxins. Some of the well known marine polyether toxins are: brevetoxin B (**5**), isolated from the dinoflagellate *Gymnodinium breve*;[8] ciguatoxin (**6**), initially reported from moray eels and a toxic constituent implicated in ciguateric seafood poisoning;[9] maitotoxin (**7**), isolated from *Gambierdiscus toxicus*;[10,11] and okadaic acid (**8**), a potent tumor promoter and major

causative agent of diarrhetic shellfish poisoning, found from two species of dinoflagellates, *Prorocentrum lima* and *Dinophysis* species.[12,13] Palytoxin (**9**), a complex polyol, is another well known toxic macromolecule isolated from the zoanthid, *Palythoa toxicus*.[14] Of these macromolecules, maitotoxin is the largest (MW 3422), and most likely, the most lethal non-proteinaceous toxin (LD_{50} of ca. 50 ng/kg in mice) characterized from a marine microorganism. Many of these toxic macromolecules have also proven to be invaluable as molecular tools for dissecting cellular processes by molecular pharmacologists.

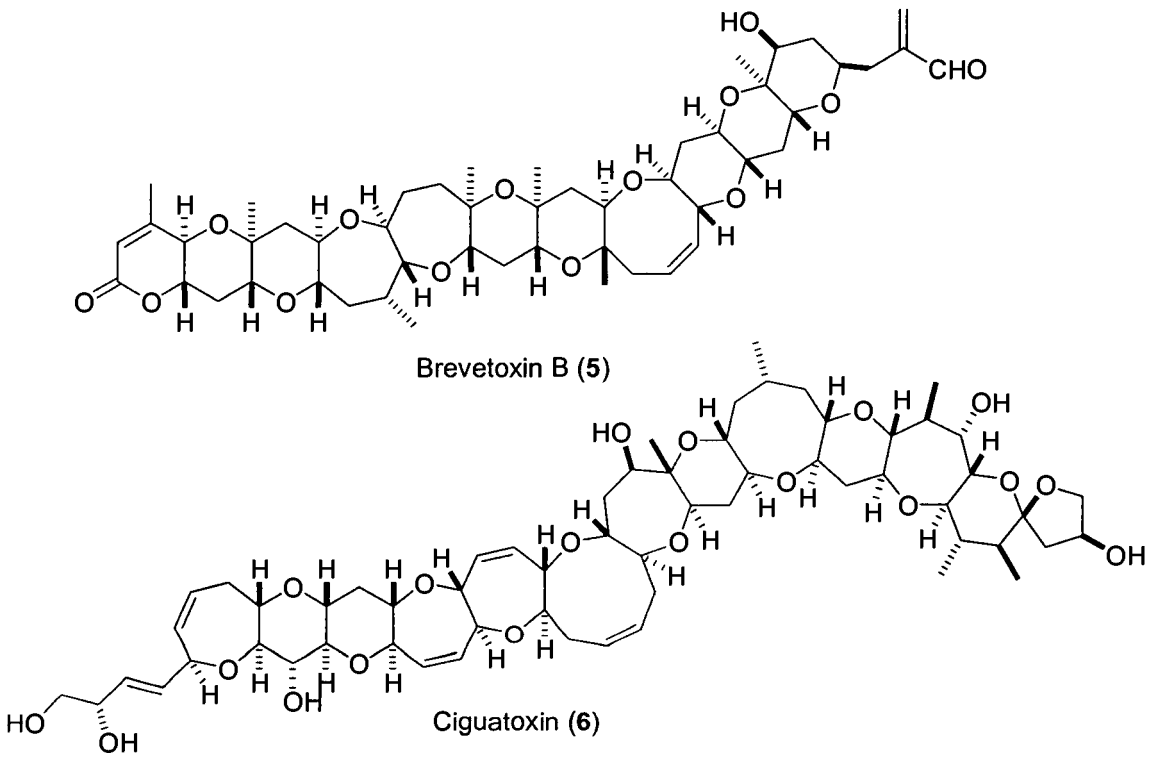

Figure I.1 Marine toxins (I).

The main objective of any marine natural products program is to discover secondary metabolites of therapeutic utility. This is especially so in the area of cancer research where numerous marine natural products are being screened for anticancer

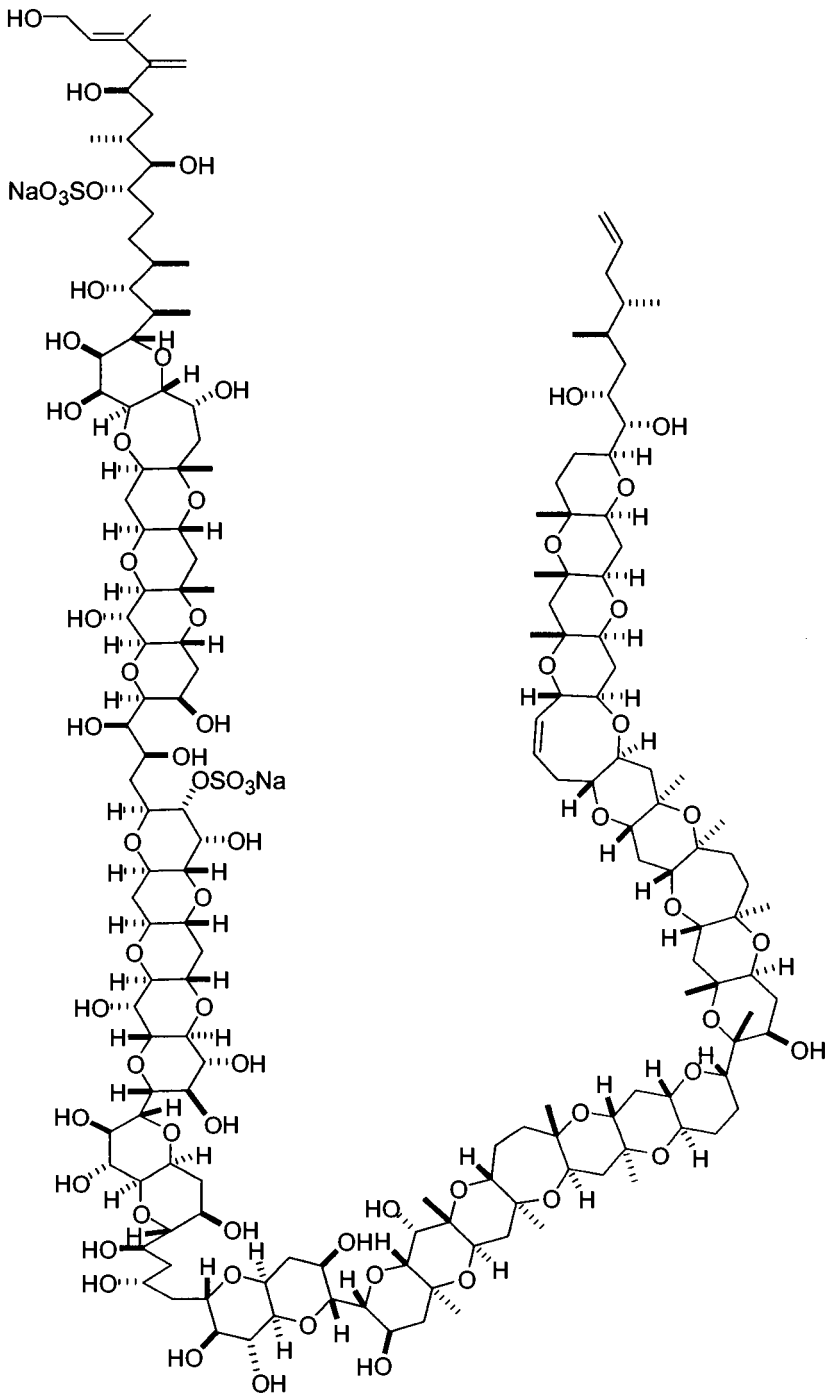

Maitotoxin (**7**)

Figure I.2 Largest non-proteinaceous marine toxin (II).

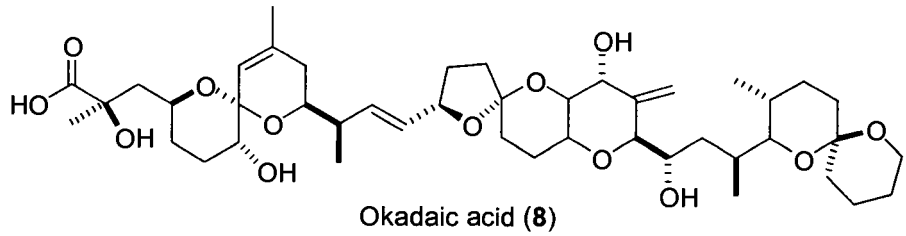

Okadaic acid (**8**)

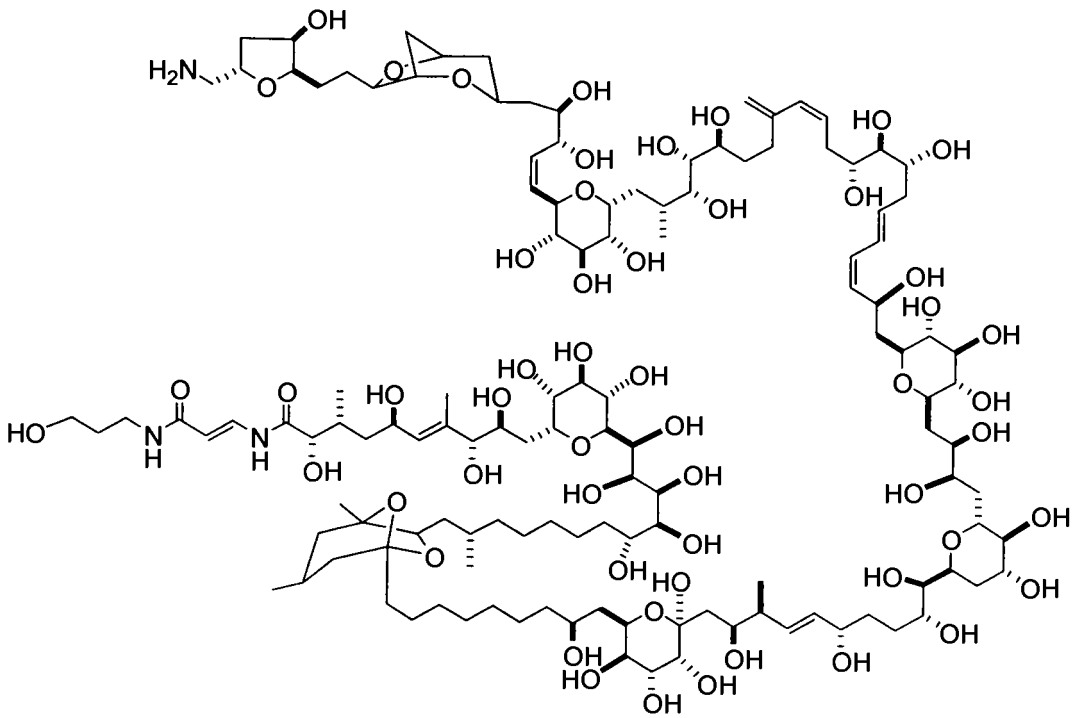

Palytoxin (**9**)

Figure I.3 Marine toxins (III).

properties. Although none of the discoveries since the 1970s has led to a clinical product, there are a number of potential candidates currently under intense investigation that will eventually do so. Among the more promising natural products are bryostatin 1 (**10**) and ecteinascidin 743 (**11**) (Table I.1). The former compound is a polyketide first isolated in minute quantity from the bryozoan, *Bugula neritina* collected from the Gulf of California in the 1970's.[15] It is currently in phase II clinical trials for the treatment of various leukemias, lymphomas, melanoma, and solid tumors. The biological profiles of bryostatin 1 (**10**) are interesting in that not only does it inhibit tumor growth but it stimulates bone marrow growth, increasing red blood cell production.[16] Recent research

has found that this cytotoxic macrolide shows potential in the treatment of ovarian and breast cancer and it also enhances lymphocyte survival in patients undergoing radiation treatment.[17] To date, eighteen bryostatins have been defined and some members of this family (e.g. bryostatin 5 and 8) exhibit biological activities equivalent to or better than bryostatin 1 (**10**).[18]

Table I.1 Anticancer marine natural products in clinical and preclinical testing.

Status	Compounds	Organisms
Phase II	Ecteinascidin 743	*Ecteinascidia turbinata* (ascidian)
	Bryostatin 1	*Bugula neritina* (bryozoan)
Phase I	Aplidine (dehydrodidemnin B)	*Aplidium albicans* (ascidian)
	Dolastatin 10	*Dolabella auricularia* (seahare) (Cyanobacteria implicated as true producer)
	Bengamide derivative	Based on the bengamides reported from the sponge *Jaspis cf. coriacea*
Pre-clinical	Halichondrin B	*Axinella* sp. (sponge)
	Isohomohalichondrin B	*Axinella* sp. (sponge)
	Aplyronine A	*Aplysia kurodai* (seahare)
	Discodermolide	*Discodermia dissolute* (sponge)
	Eleutherobin	*Eleutherobia albifora* (soft coral)
	Sarcodictyin A	*Sarcodictyon roseum* (soft coral)
	Curacin A	*Lyngbya majuscula* (cyanobacterium)
	Kahalalide F	*Elysia rufescens* (mollusk)

One major obstacle that may prevent the development of bryostatin 1 (**10**) to a clinically useful anticancer agent is the supply issue. The yield of bryostatin 1 (**10**) from *B. neritina* is low in the range of about 1.4 μg per gram of wet weight of the organism.[19] Another complication is the unpredictable production of the molecule by the bryozoan. One of the ways to meet the demand issue is through aquaculture which was undertaken by CalBioMarine Technologies in California, and has since proven to be a commercially viable source of the molecule. However, a recent report presented evidence that suggests

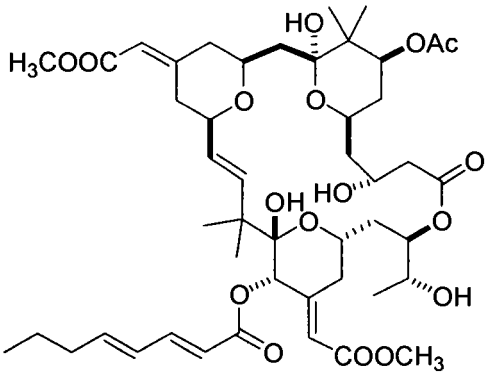

Bryostatin 1 (**10**)

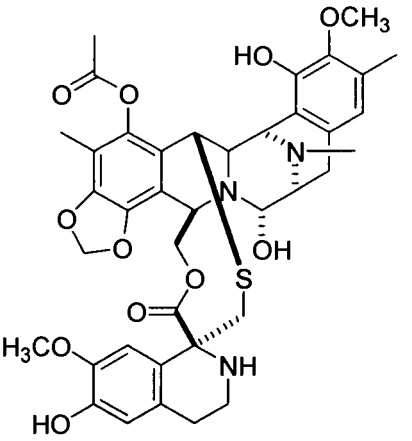

Ecteinascidin 743 (**11**)

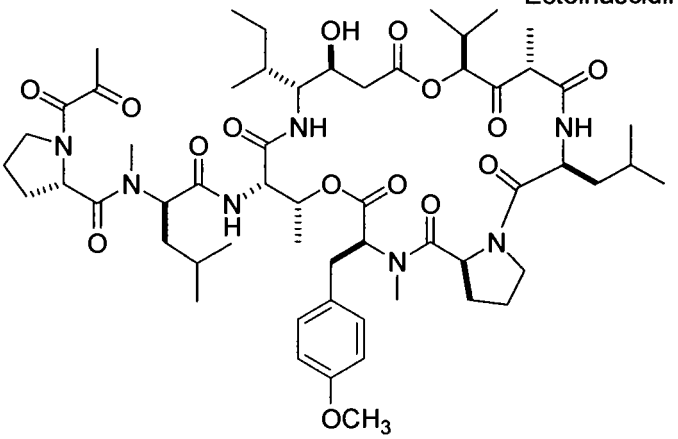

Dehydrodidemnin B (**12**) (= Aplidine)

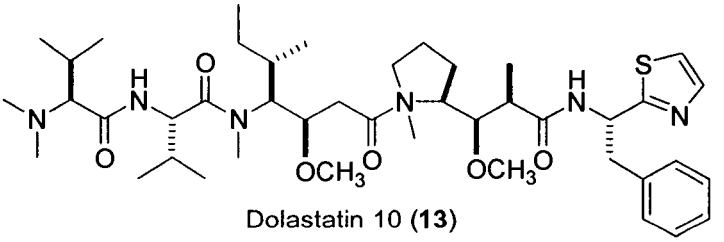

Dolastatin 10 (**13**)

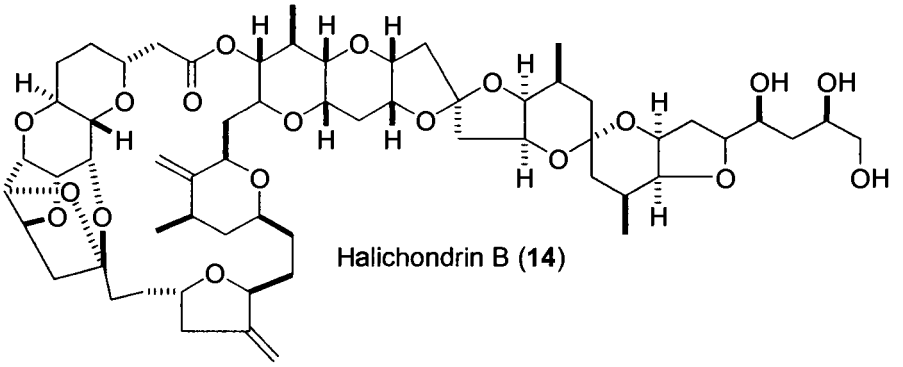

Halichondrin B (**14**)

Figure I.4 Anticancer marine natural products (I).

a symbiotic bacterial origin for bryostatin 1 (**10**) production.[20] This finding may open the way for genetic manipulation of the biosynthetic genes for increased production of this potent compound.

Another promising anticancer agent that is currently in phase II clinical trial is ecteinascidin 743 (**11**). This molecule is a complex alkaloid isolated from the Caribbean ascidian, *Ecteinascidia turbinata*, reported by two research groups in the United States.[21,22] It is currently being investigated for potential use in the treatment of small cell lung cancer and skin cancer. The present development of ecteinascidin 743 (**11**) as an anticancer drug is licensed to PharmaMar in Spain and the supply, like bryostatin 1 is met by aquaculture carried out by CalBioMarine.

Two other marine-derived compounds that are in clinical trial (phase I) are aplidine (= dehydrodidemnin B) (**12**) from the tunicate, *Aplidium albicans*[23] and dolastatin 10 (**13**), first isolated from the seahare, *Dolabella auricularia*[24] collected from the Indian Ocean. Didemnin B was the first marine metabolite to reach clinical testing as an anticancer agent. However, it was dropped due to a disappointing performance in phase II testing. The dehydro-derivative, dehydrodidemnin B (**12**) is ten times more effective than didemnin B, and is less toxic. Marine cyanobacteria are suggested to be the source of dolastatin 10 (**13**), and this will be discussed in the following section below. A synthetic compound, based on a class of sponge metabolites known as the bengamides, is also in phase I clinical trial.[56] Other noteworthy marine-derived metabolites undergoing intense investigation as anticancer agents in the United States are: halichondrin B (**14**)[25] and isohomohalichondrin B (**15**)[26] from the sponge *Axinella* sp.; aplyronine A (**16**) from the seahare, *Aplysia kurodai*;[27] discodermolide (**17**) from the sponge, *Discodermia dissolute*;[28] eleutherobin (**18**) from the soft coral, *Eleutherobia albifora*;[29] sarcodictyin A (**19**) from the stoloniferan coral, *Sarcodictyon roseum*;[30] curacin A (**20**) from the Curaçao cyanobacterium, *Lyngbya majuscula*;[31] and kahalalide F (**21**) from the Hawaiian mollusk, *Elysia rufescens* (Figures I.4 to I.6).[32] A new type of antitumor drug awaiting clinical trial in Japan is KRN7000 (**22**), which is a synthetic analog of a class of natural metabolites known as agelasphins isolated from the Okinawan sponge *Agelas mauritianus*.[33]

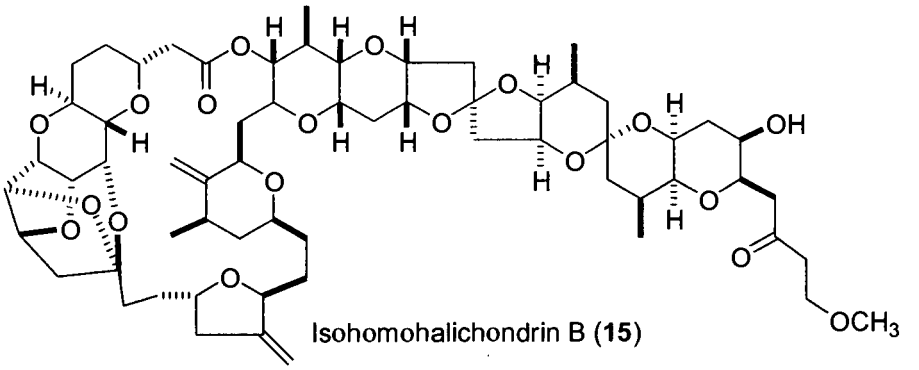

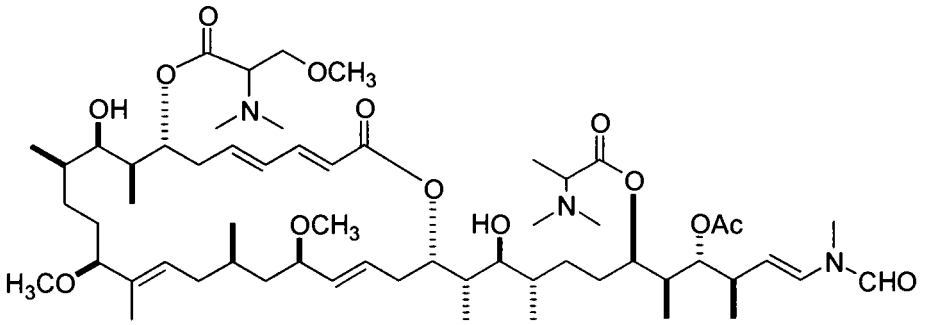

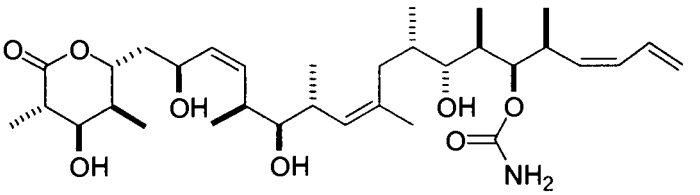

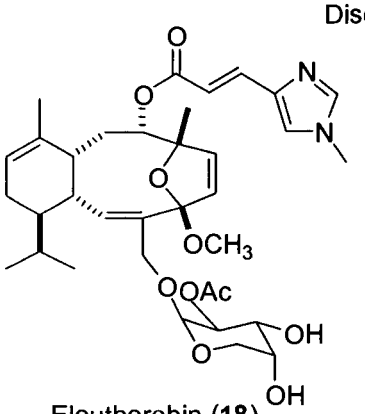

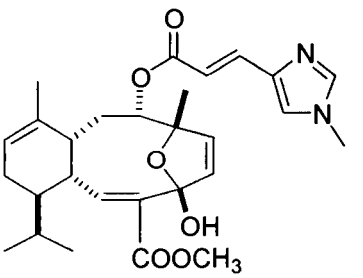

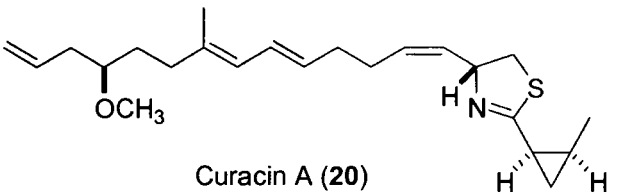

Figure I.5 Anticancer marine natural products (II).

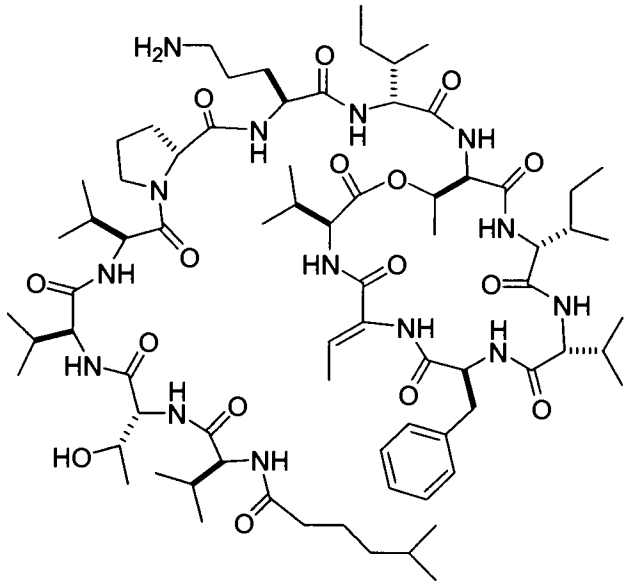

Kahalalide F (**21**)

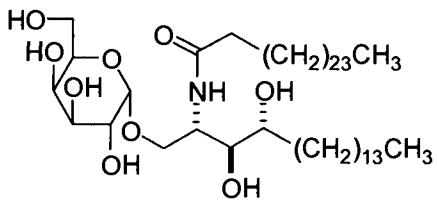

KRN7000 (**22**)

Figure I.6 Natural (**21**) and synthetic (**22**) anticancer molecules.

A common biological feature for most of these marine-derived anticancer agents is the antimitotic effect through interaction with tubulin structures in cancer cells. Antimitotic agents can be divided into four types depending on which step is being inhibited in the microtubule polymerization/depolymerization process. These include the type I colchicine site, type II vinca alkaloid binding site [halichondrin B (**14**), isohomohalichondrin B (**15**), and dolastatin 10 (**13**)], type III microtubule stabilization [eleutherobin (**18**) and discodermolide (**17**)], and type IV microtubule network disorganization [ecteinascidin 743 (**11**)]. Inhibition via tubulin interaction is therefore an important target for many anticancer agents.[34]

In addition to the discovery of marine natural products with anticancer properties, marine organisms have also yielded a number of important anti-inflammatory agents.

Most of these compounds act as phospholipase A_2 inhibitors, preventing release of arachidonic acid from the lipids of cell membranes.[35] Arachidonic acid is involved in the biosyntheses of many proinflammatory compounds via enzymes such as cyclooxygenase, lipoxygenase, or monooxygenase. A recent bioassay screening of marine natural products having such inhibitory activities includes; topsentin (**25**) from the sponge, *Spongosorites ruetzleri*,[36] scalaradial (**26**) from the sponge, *Cacospongia mollior*,[37] scytonemin (**27**), a pigment found in the extracellular sheaths of blue-green algae,[38] and manoalide (**28**) from the sponge, *Luffariella variabilis* (Figure I.7).[39] In addition, pseudopterosins A (**23**) and E (**24**), from the Caribbean gorgonian, *Pseudopterogorgia elisabethae*, are two diterpene glycosides showing promising *in vitro* and *in vivo* activities as anti-inflammatory agents.[40,41] These were found to be potential antagonists of lipoxygenases or other enzymes involved in the arachidonic cascade. The pseudopterosins and manoalide, the latter of which has become a standard drug in inflammation research, are currently being evaluated in clinical trials as topical anti-inflammatory agents.

The marine environment has also provided a number of useful compounds as molecular probes for understanding cellular processes. Molecules such as tetrodotoxin (**29**), saxitoxin (**30**), and the conotoxins are instrumental in detailing the functions and structures of the membrane channels involved in nerve transmission. The important neurotoxin, tetrodotoxin (**29**) represents a milestone in the recognition of the potential neuronal sodium channel blockers in CNS-related disorders.[42] Other marine secondary metabolites that are becoming important as molecular tools are okadaic acid (**8**), which is a potent inhibitor of phosphatases;[43] latrunculin A (**31**),[44] swinholide A (**32**),[45] and jaspamide (= jaspakinolide) (**33**),[46,47] which bind specifically to the intracellular actin network; ilimaquinone (**34**),[48] which affects vesiculation of the Golgi apparatus; and more recently an unique sponge compound, adociasulfate 2 (**35**),[49] which is an inhibitor of intracellular motor protein kinesin (Figure I.8).

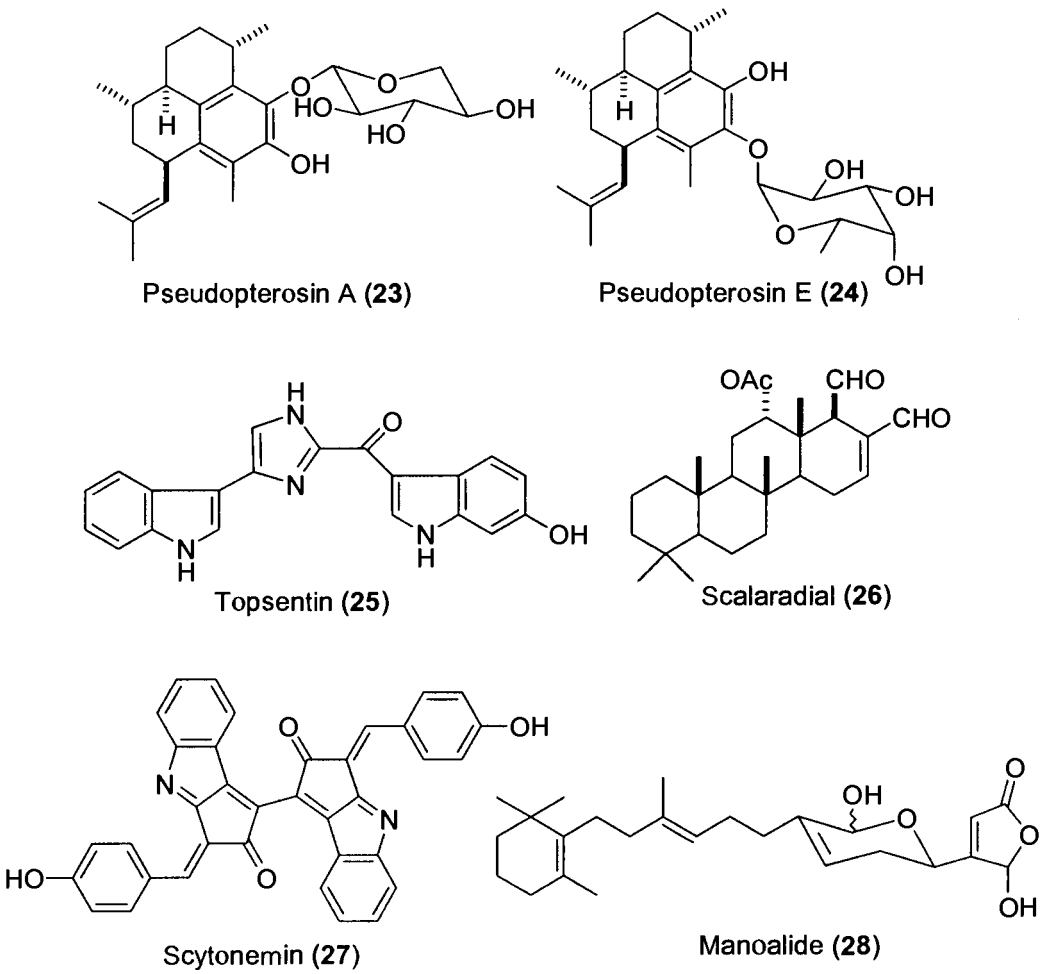

Figure I.7 Antiinflammatory marine natural products.

One of the emerging trends in many infectious organisms is the resistance to standard drugs that are currently being used for their treatment. This is especially so in malarial infections by the protozoan parasite, *Plasmodium* species. Many resistant strains of this parasite are being uncovered and treatments of such infections by traditional drugs are proving ineffective. However, recent research suggested that the next generation of new antimalarial chemotherapeutic agents might come from marine organisms. In an initial screening of extracts from marine sponges for antimalarial properties, *Acanthella klethra* yielded an active component, axisonitrile 3 (**36**), which is a bicyclic spiro-sesquiterpene with an isonitrile group.[50] This compound possessed potent

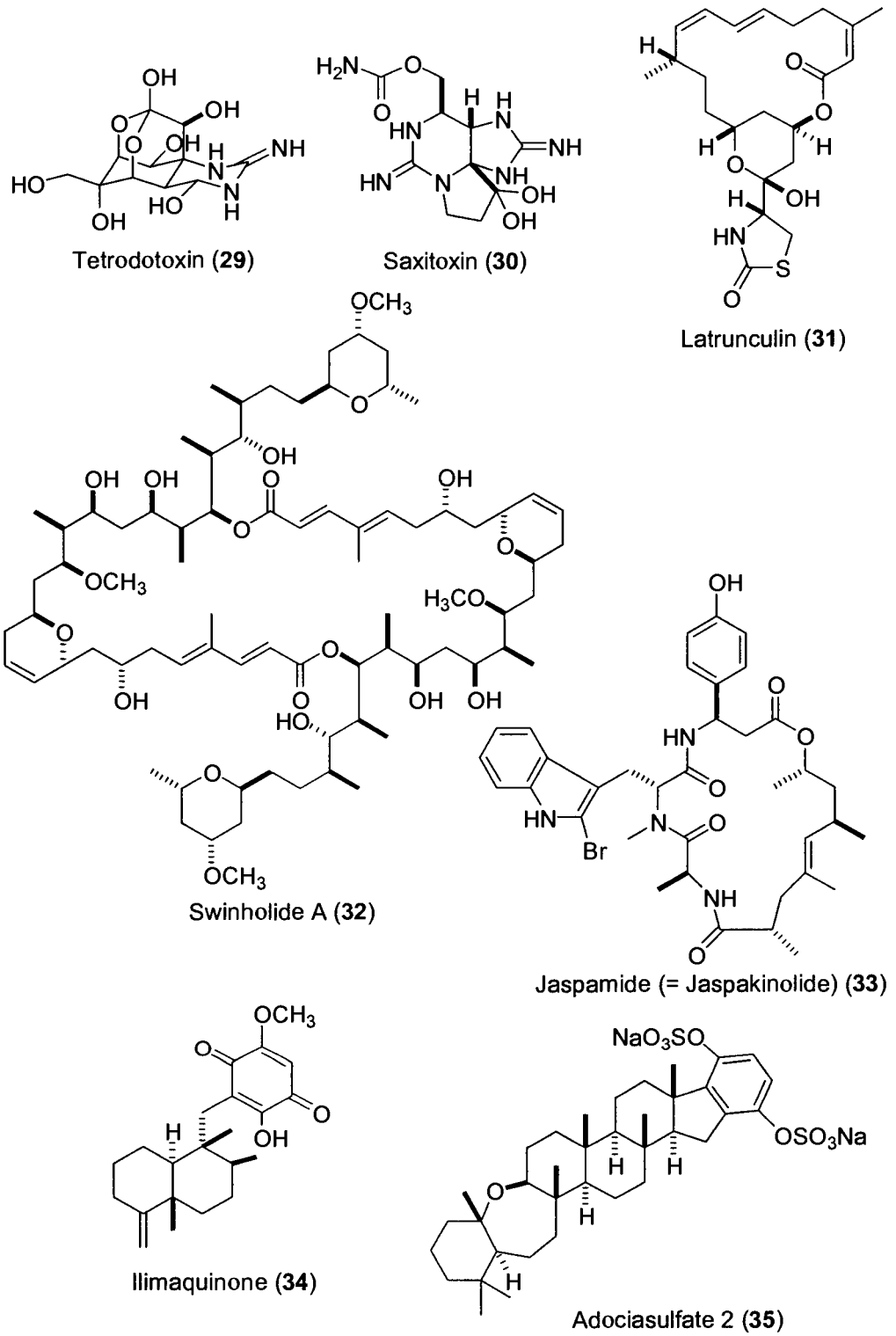

Figure I.8 Marine natural products as molecular probes.

in vitro antimalarial activity with no detectable cytotoxicity. It was further revealed that marine natural products containing –NC, –NCS, and –NCO functionalities exhibited antimalarial properties.[50] A new class of β-carboline alkaloids from marine sponges, known as the manzamines is gaining attention as potent antimalarial agents. Four

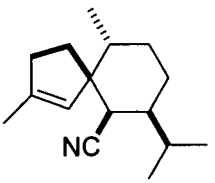

Axisonitrile 3 (**36**)

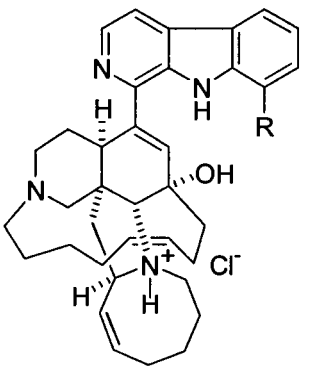

Manzamine A (**37**) R = H
8-Hydroxymanzamine A (**38**) R = OH

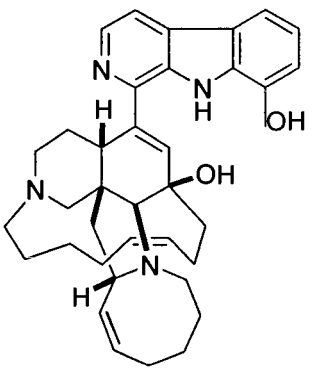

ent-8-Hydroxymanzamine A (**39**)

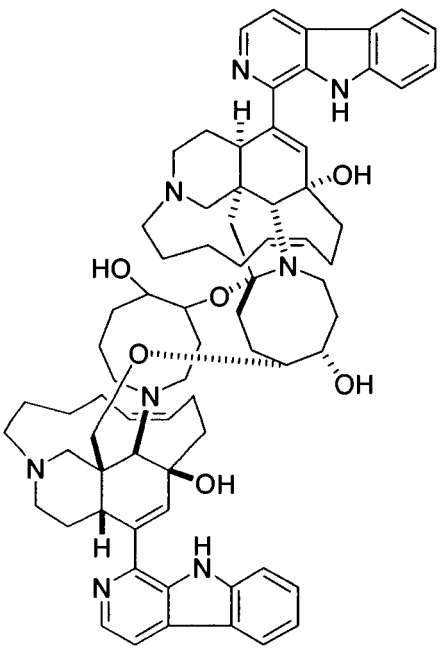

neo-Kauluamine (**40**)

Figure I.9 Antimalarial marine natural products.

members of this series, manzamine A (**37**), its enantiomer (**38**), 8-hydroxymanzamine A (**39**), and a manzamine dimer, *neo*-kauluamine (**40**) gave encouraging results in preliminary *in vivo* testing. These preliminary data also indicated that the manzamines are more active and less toxic than the current available drugs artemisinin and chloroquine.[51,52]

New structural classes of antimicrobial compounds have also been recently identified from marine organisms in the area of tuberculosis treatment. Like malarial infections, resistant forms of the causative agent *Mycobacterium tuberculosis*, a mycobacterium, are making treatment of tuberculosis a challenging task. In the process of discovering new antituberculosis agents, three new leads were generated from marine sources. These were the C-19 hydroxy steroids, scalarin sesquiterpenoids, and tetrabromospirocyclohexadienylisoxazolines.[53]

In the area of antiviral research, especially antiHIV (human immunodeficiency virus), two main leads have been found from marine sources. The natural marine compound ilimaquinone (**34**) is currently being investigated as a chemotherapeutic in HIV infection.[54] This compound acts by targeting at the RNase function of the reverse transcriptase enzyme encoded by HIV. The first natural product that inhibits HIV integrase enzyme was reported from a species of marine sponge belonging to the genus *Lamellaria*. The metabolite, lamellarin α 20-sulfate (**41**) was found to inhibit early steps of HIV replication.[55]

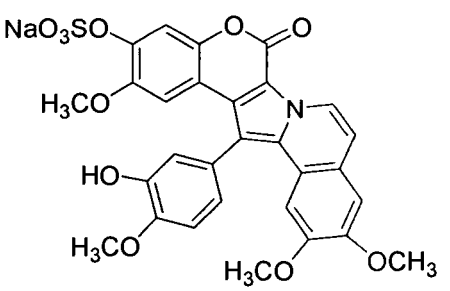

Lamellarin α 20-sulfate (**41**)

Figure I.10 AntiHIV marine natural product.

Apart from the biomedical potential of marine natural products, significant discoveries are also being made in the agrochemical front. This is especially so in the area of crop disease management where marine-derived secondary metabolites are being considered as possible insecticides for controlling crop pests, such as corn rootworm (*Diabrotica undecimpunctata howardi*) and tobacco budworm (*Heliothis virescens*).[57] Various structural classes with potent insecticidal properties have been identified, including cyclic depsipeptides [e.g. jaspamide (**33**)], diterpenes [e.g. juncin E (**42**) and gemmacolide A (**43**)], and macrolides [e.g. halichondramide (**44**) and swinholide A (**32**)] (Figure I.11).

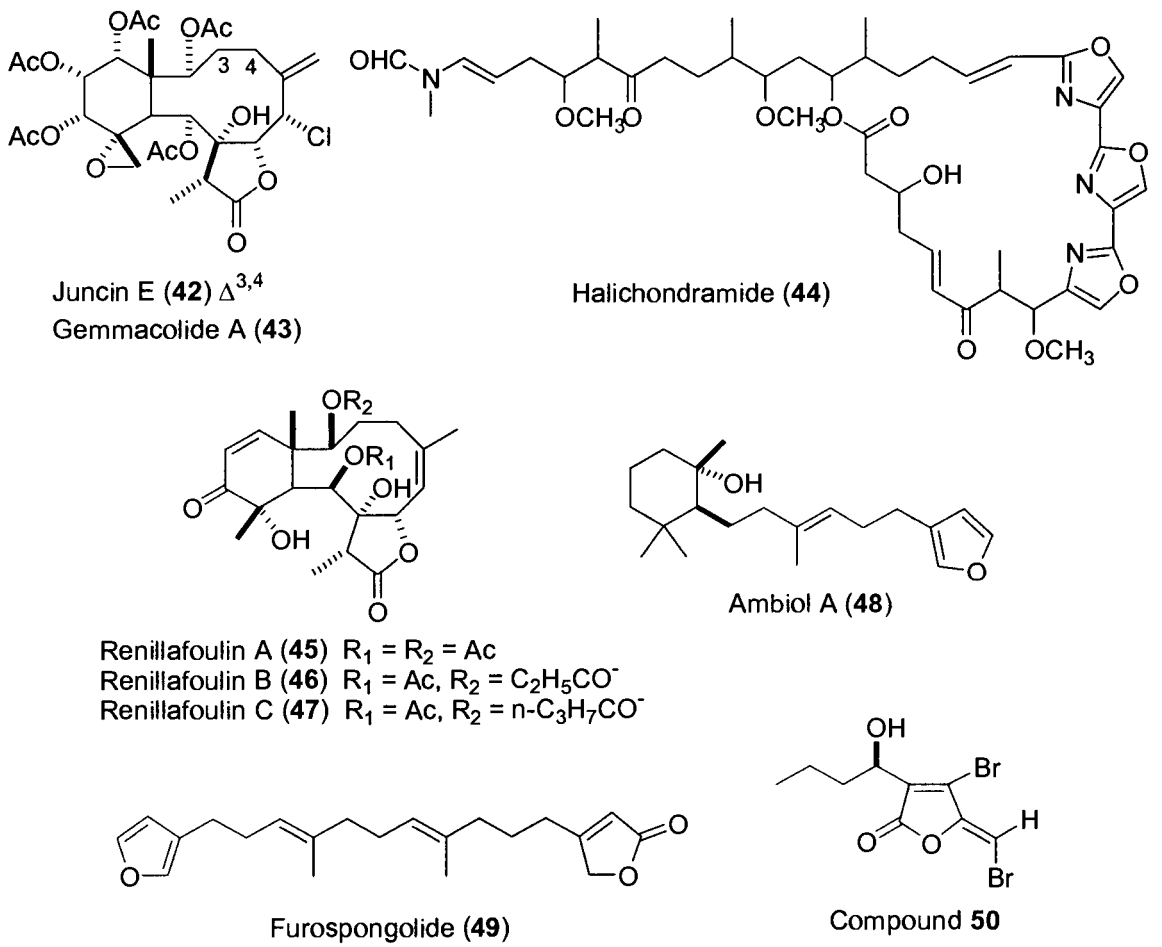

Figure I.11 Insecticidal and antifouling marine natural products.

Many marine sessile organisms produce chemicals to inhibit settling by fouling organisms. This has led chemists to search for nontoxic natural marine antifoulants that could be incorporated in paints to be applied on ships' hulls as well as offshore platforms. Over 90 marine antifoulants have now been characterized and they represent a high degree of structural diversity. In spite of the structural diversity, many have a striking similarity in possessing furan and/or lactone rings. Some examples are the renillafoulins (**45** to **47**)[58] from a octocoral, ambiol A (**48**)[59] and furospongolide (**49**)[60] from sponges, and halogenated furanones (e.g. compound **50**)[61] from the marine agla *Delisea pulchra*.

In just a short period of time research in marine natural products, as presented in the above examples, has made numerous significant discoveries in science, especially in the field of biomedicine. Marine natural products research in the early years was purely academic, focusing mainly on isolation and structural elucidation of novel metabolites. Within the past two decades, many spin-offs are being made in the areas of pharmacology, chemical ecology, as well as molecular biology. With the advent of high-end NMR instrumentation and development of sensitive NMR pulse sequences, it is now possible to solve the structures of minute quantities of natural products rapidly. Coupled with the development of high-throughput bioassay screening systems, it is only a matter of time before new marine-derived drugs are used widely in clinical settings. Without doubt, the marine realm is a tremendous bioresource, which translates to natural products that potentially are solutions to many human ailments.

Major concerns that need to be addressed in marine natural products drug development are the original source organisms and the supply issue of useful secondary metabolites. Since numerous marine microbes are associated symbiotically with invertebrates, such as sponges, new techniques are therefore needed to identify the true producers of secondary metabolites from complex microbial communities. Several fronts in aquaculture and in the area of molecular biology research, the latter involving manipulation of biosynthetic gene clusters to increase production of secondary metabolites, give new hopes and vigor in the field of marine natural products drug discovery.

BIOACTIVE SECONDARY METABOLITES FROM MARINE ALGAE

Marine algae are perhaps the most studied group of organisms by natural products chemists. Members of this group are well represented in coral reefs in terms of diversity and biomass. Marine algae are loosely divided into two groups, macroalgae, which include red (rhodophyta), brown (phaeophyta), and green algae (chlorophyta) and microalgae, including cyanobacteria (blue-green algae) as well as dinoflagellates. Secondary metabolites deriving from marine algae are also structurally diverse and possess different bioactivities. The most important of these are the marine toxins produced by dinoflagellates, which were highlighted in the preceding section. These toxins often accumulate in fish and shellfish through the food chain, resulting in human intoxication.

Of the various groups of marine algae, the red algae are the most predominant species comprising upwards of 5,000 members, and hence, well studied for their chemistry. For instance members of the red algal genus *Laurencia* contain an astounding myriad of complex terpenoids and acetogenins. It has been noted that over 500 different terpenes, represented by no less than 26 different structural classes with more than 16 novel types, reside in *Laurencia*, possibly making it as the world's most chemically complex genus (other than *Streptomyces*).[62]

One of the main themes in the secondary metabolites from marine algae is the high degree of halogenation. Although the concentration of chloride ion (19,000 mg/L) in the ocean is much higher than bromide ion (65 mg/L), marine algae are able to take up and incorporate bromine in their secondary metabolism. This has resulted in the frequent occurrence of organobromine metabolites, especially of the terpenoid class in marine algae.[63] For example, a novel antitumor agent, halomon (**51**), is a pentahalogenated monoterpene isolated from the red alga *Portieria hornemannii*.[64] This compound has been in preclinical trial in the United States. However, the development of halomon (**51**) as a usable antitumor drug has been hampered by the limited supply of the metabolite from natural sources as well as the lack of synthetic methods.[65] A favorite edible seaweed known in Hawaiian as 'limu kohu' (*Asparagopsis taxiformis*) is prized for its flavor and aroma and is also a source of more than 50 organobromine compounds.

Indeed, a very simple organobromine molecule, bromoform ($CHBr_3$) comprises 80% by weight of this seaweed.[63]

Two marine algal metabolites possessing important medicinal properties are kainic acid (**52**)[66] and domoic acid (**53**).[67] The former compound is associated with the red alga *Digenea simplex*, which has been used widely for centuries in Asia for the treatment of roundworm disease. Its medicinal use in crude drug form has been documented in a Japanese pharmacopeia published in the 9th century. Kainic acid (**52**) is now marketed as an antiparasitic compound with broad-spectrum antihelmintic properties against roundworm, whipworm, and tapeworm. A structurally related compound, domoic acid (**53**), a constituent of another red alga *Chondria armata*, is also used for the same purpose. However, the use of *Chondria armata* as folk medicine has only been recorded from Tokunoshima, a small island located northeast of Okinawa. In addition to the antiparasitic properties, these kainoids are potent neurotoxins and excitatory amino acids, and thus, are important tools in neurophysiology research. Domoic acid (**53**) is also produced by diatoms and is responsible for amnesic shellfish poisonings, first reported in Canada in 1987.[68]

One of the more surprising findings from marine algae is the presence of eicosanoids and related fatty acid natural products. Since the 1980s, there have been a large increase in the number of such compounds isolated from marine plants, especially from red algae. This has been a topic in a review by Gerwick.[69] In spite of their wide occurrence in marine algae, very little is known with regards to their ecological and physiological functions. Some of the more prolific producers of such metabolites are algae from the order Gracilariales (Rhodophyta), which have been studied mainly from Australia and Japan. A well-known example is prostaglandin E_2 (**54**), which was isolated from a Japanese species of *Gracilaria*, *Gracilaria verrucosa*, and is a proposed main culprit of "Ogonori" poisoning among humans in Japan.[70]

In addition to prostaglandin E_2 (**54**), there are a number of marine algal metabolites from the genus *Gracilaria* identified as causative agents in human poisonings. Polycavernoside A (**55**), a novel glycosidic macrolide from the red alga *Polycavernosa tsudai*, is a potent toxin, which resulted in human intoxication and three fatalities in Guam after ingestion of the alga.[71] Epiphytic blue-green algae have been

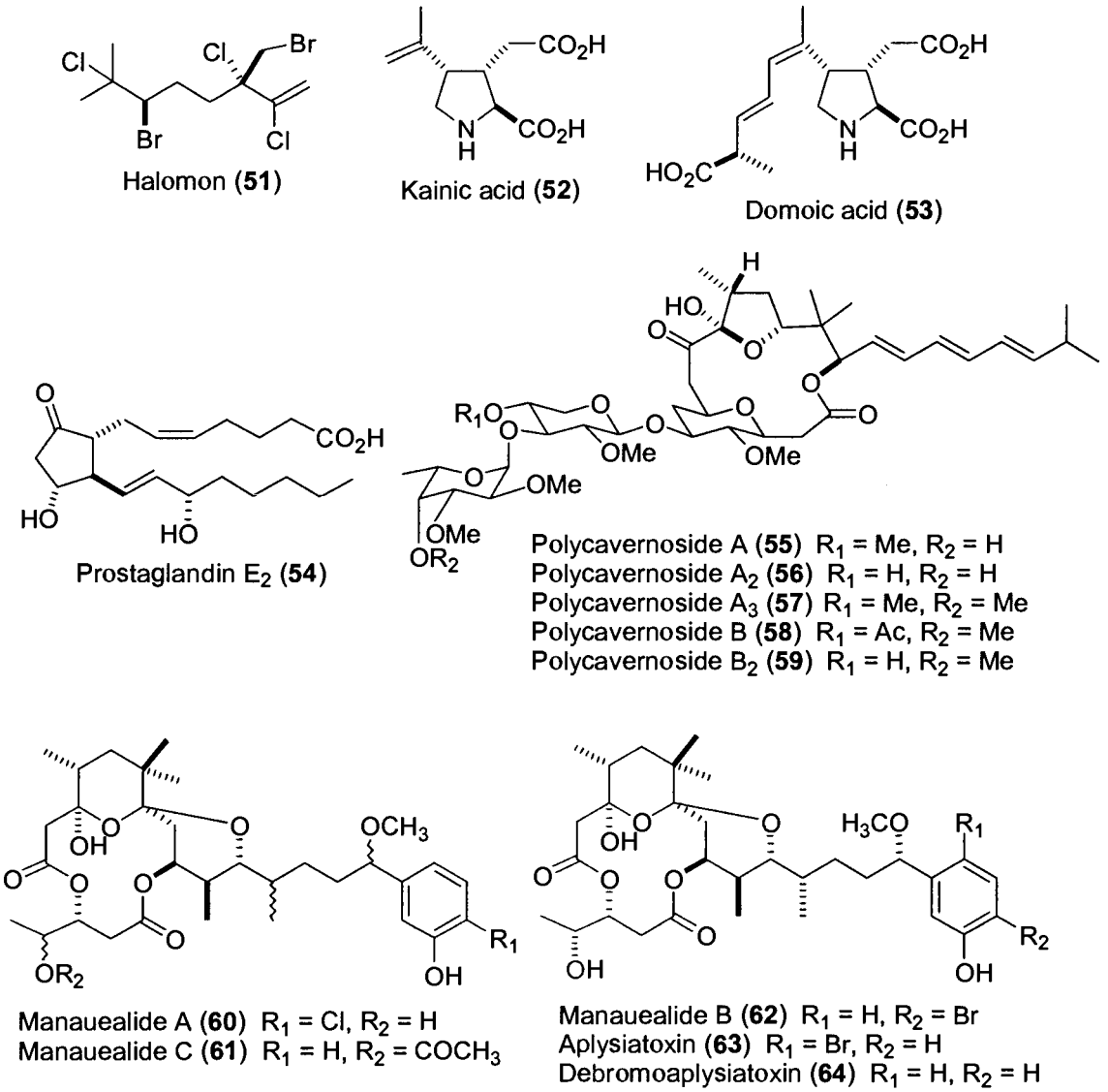

Figure I.12 Natural products from marine algae.

suggested to be the producers of this macrolide. Since the initial report of polycavernoside A (**55**), four new analogs (**56** to **59**) have been defined recently from the same alga using 2D NMR techniques and fragmentation patterns in the FABMS data.[72] In human poisoning cases in Hawaii, the manauealides (**60** to **62**) were reported to be the causative agents from the red alga *Gracilaria coronopifolia*.[73] Like the polycavernosides, the manauealides are almost certainly derived from an associated blue-green alga since they are structurally related to cyanobacterial (*Lyngbya majuscula*)

metabolites aplysiatoxin (**63**) and debromoaplysiatoxin (**64**).[74] Both aplysiatoxin (**63**) and debromoaplysiatoxin (**64**) are potent tumor-promoter agents and are also the causative agents of a contact dermatitis (swimmers' itch) that affects swimmers in Hawaiian waters.

The first example of eukaryotic interference with bacterial signaling processes comes from the control of bacterial fouling on the marine red alga, *Delisea pulchra*.[61] Investigation into the antifouling strategy employed by this red alga led to the discovery of a number of halogenated furanones with potent anti-bacterial properties. It was further demonstrated that these algal furanones (e.g. compound **50**) prevented bacterial fouling by interfering with the bacterial "quorum sensing" systems.[75] Currently, these natural furanones are being pursued for commercial use as potential antifoulants in paints.

Natural Products from Marine Cyanobacteria

Marine cyanobacteria or blue-green algae are emerging as an important source of pharmaceuticals. Since the pioneering work of Professor Richard Moore in Hawaii, many structurally diverse and biologically active natural products from cyanobacteria have been reported. To date, two metabolites of cyanobacterial source are in clinical trial for the treatment of human cancer. These are dolastatin 10 (**13**) (initially isolated from the sea-hare, *Dolabella auricularia*, but almost certainly of cyanobacterial origin)[24] and a synthetic derivative belonging to the cryptophycin series, cryptophycin 52 (**65**).[76] One of the appealing aspects of working with these microalgae is that they are amenable to culture in the laboratory for the production of secondary metabolites. This was demonstrated by the laboratory culture of a curacin A producing strain of cyanobacterium, *Lyngbya majuscula*.[77] Curacin A (**20**) is a potent anticancer agent currently in preclinical testing.

In contrast with the extensive survey of natural products from terrestrial blue-green algae, marine species are less well explored. However, in recent years natural products chemists are paying more attention to marine cyanobacteria as source of medicinally useful substances. This is attested to by the increasing number of

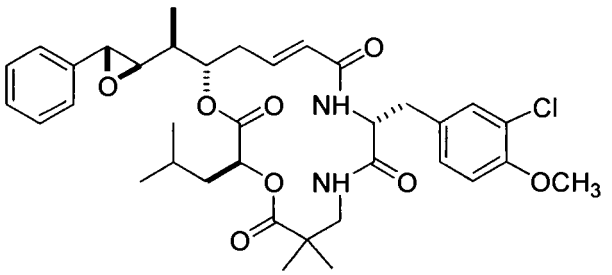

Crytophycin 52 (**65**)

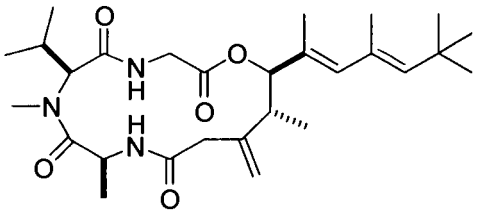

Antillatoxin (**66**)

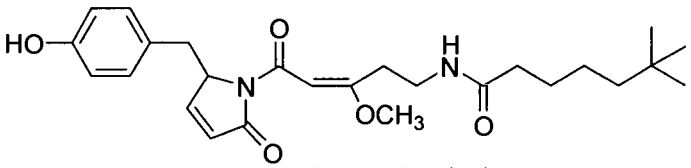

Ypaoamide (**67**)

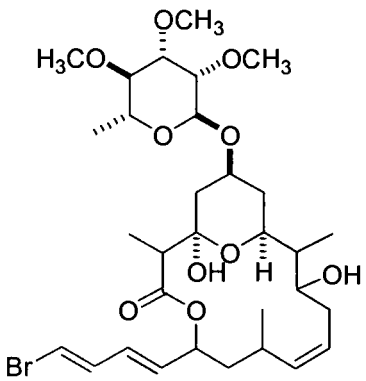

Lyngbyaloside (**68**)

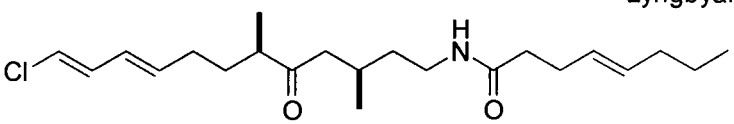

Pitiamide A (**69**)

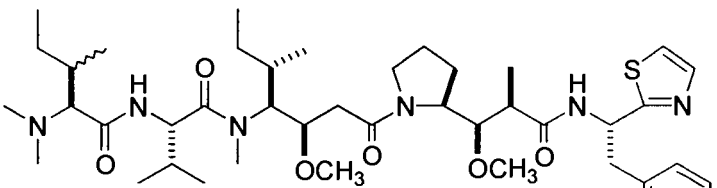

Symplostatin 1 (**70**)

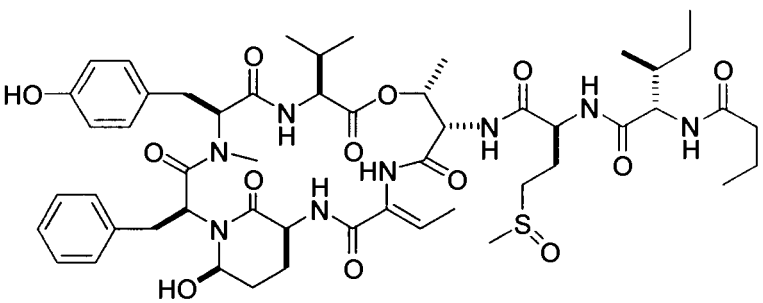

Symplostatin 2 (**71**)

Figure I.13 Natural products from marine cyanobacteria (I).

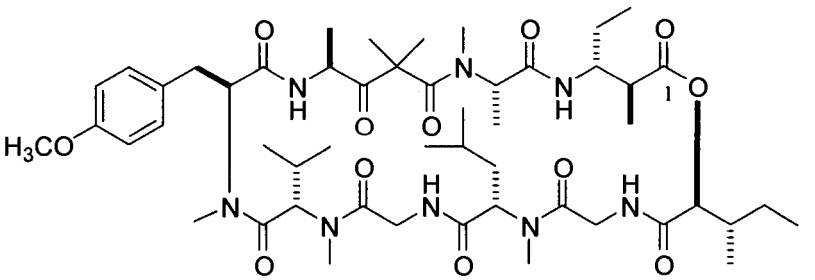

Lyngbyastatin 1 (**72**)

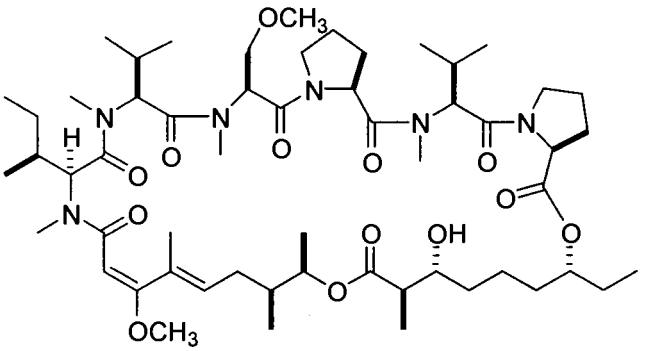

Lyngbyastatin 2 (**73**)

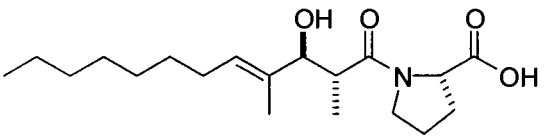

Tumonoic acid A (**74**)

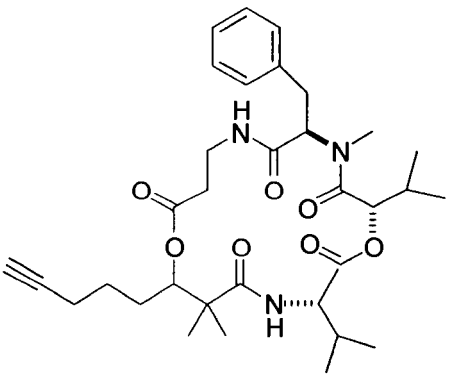

Yanucamide A (**75**)

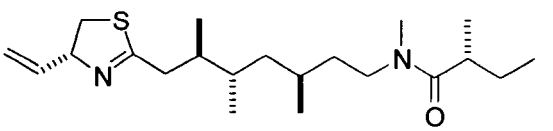

Kalkitoxin (**76**)

Figure 1.14 Natural products from marine cyanobacteria (II).

publications on metabolites from marine cyanobacteria, many of which showed potent bioactivities and are structurally intriguing. A majority of the secondary metabolites

from these microalgae are nitrogen-containing, belonging to the lipopeptide structural class. Recent examples of marine cyanobacterial compounds include antillatoxin (**66**, a

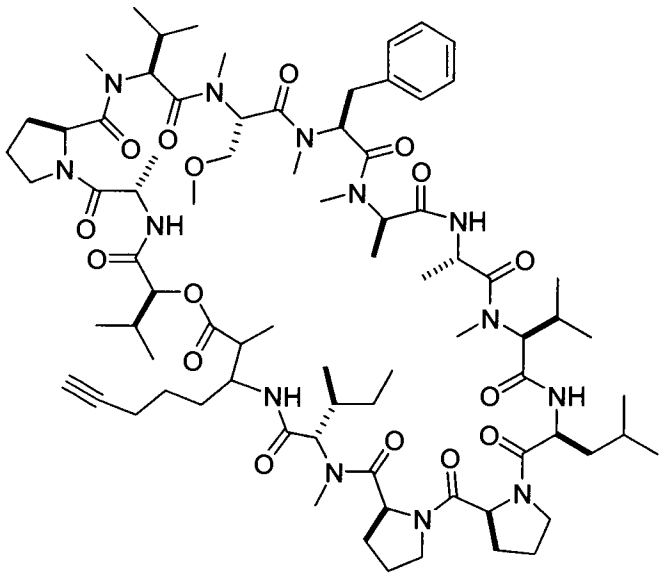

Malevamide C (**77**)

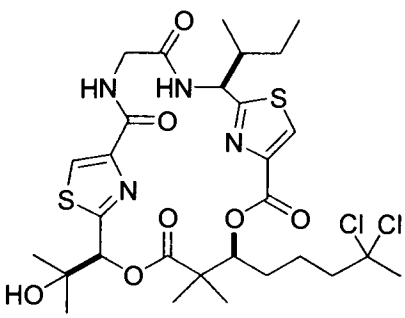

Lyngbyabellin A (**78**)

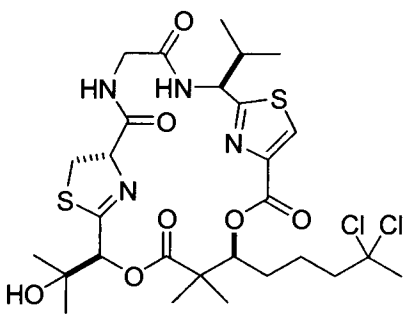

Lyngbyabellin B (**79**)

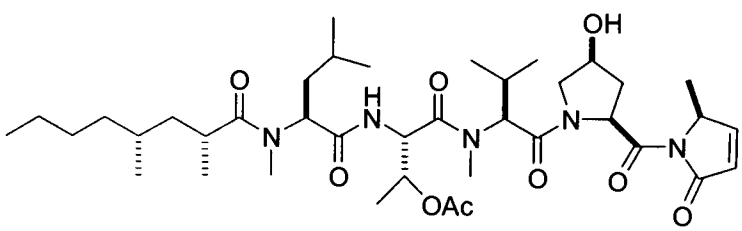

Microcolin A (**80**)

Figure I.15 Natural products from marine cyanobacteria (III).

potent neurotoxic agent),[78] ypaoamide (**67**, antifeedent),[79] lyngbyaloside (**68**),[80] pitiamide A, (**69**)[81] symplostatins (**70** and **71**) [symplostatin 1 (**70**) has antitubulin properties],[82,83] lyngbyastatins (**72** and **73**, cytotoxic),[84,85] tumonoic acids (e.g. **74**),[86] yanucamides (e.g. **75**),[87] kalkitoxin (**76**, potent neurotoxic agent),[88] malevamides (e.g. **77**),[89] lyngbyabellins (**78** and **79**, mild cytotoxicity),[90-92] and microcolin A (**80**).

Many of the above-mentioned metabolites are biosynthesized by the interplay of NRPS (non-ribosomal polypeptide synthetase) and PKS (polyketide synthase) pathways, resulting in a vast array of structural motifs. There is also a high degree of *N*-methylations as well as incorporation of unique β-amino/hydroxy acids among the cyanobacterial metabolites. In addition, the presence of heterocyclized amino acids and pyrrolidone moieties are common themes in these marine blue-green algal metabolites. Many of these structural themes are also seen in metabolites from marine invertebrates such as sponges, mollusks, and tunicates. Such structural similarities point to cyanobacteria as the true producers of these so-called invertebrate secondary metabolites.

INVERTEBRATE NATURAL PRODUCTS DERIVING FROM MARINE CYANOBACTERIA

Some species of marine sea-hares are able to sequester cyanobacterial metabolites by feeding on them. Examples of diet-derived metabolites are shown in the sea-hare *Stylocheilus longicauda*, where it feeds almost exclusively upon the cyanobacterium *Microcoleus* (= *Lyngbya*) species and concentrates its secondary metabolites, such as malyngamides A (**81**) and B (**82**).[93] The ecological function of these malyngamides in the mollusks appears to have a chemical defense role by deterring feedings from natural populations of carnivorous fishes. Further isolation of stylocheilamide (**83**), an acetate derivative of a cyanobacterial compound, malyngamide I, from the sea-hare, attests to the cyanobacterial source of these invertebrate molecules.[94]

The dolastatins are well known secondary metabolites isolated from the sea-hare *Dolabella auricularia*.[95] These are important metabolites due to their potent anticancer properties, as demonstrated by dolastatin 10 (**13**) which is currently in phase I clinical trial for the treatment of human cancer. There are growing speculations that the

dolastatins are produced by marine cyanobacteria due to reports of dolastatin and dolastatin-like compounds isolated from marine microalgae. The first of such reports was the isolation of symplostatin 1 (**70**), a dolastatin 10 analogue, from the cyanobacterium, *Symploca laete-viridis*.[82]

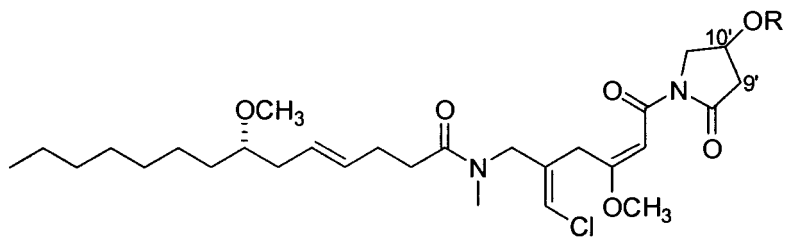

Malyngamide A (**81**) R = CH_3, $\Delta^{9',10'}$
Malyngamide B (**82**) R = H

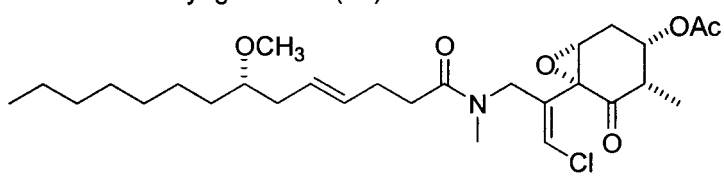

Stylocheilamide (**83**) (= Malyngamide I acetate)

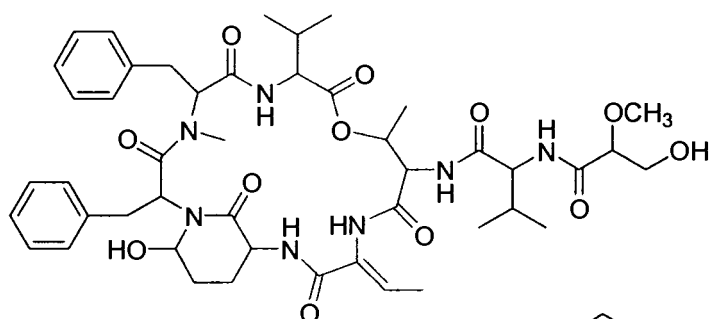

Dolastatin 13 (**84**)

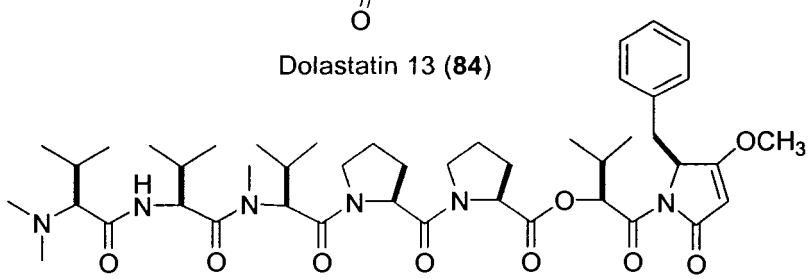

Dolastatin 15 (**85**)

Certain structural moieties present in the dolastatins are also seen in some cyanobacterial metabolites. A 19-membered depsipeptide, dolastatin 13 (**84**), from the

Indian Ocean sea-hare, possesses the unique Ahp unit (3-amino-6-hydroxy-2-piperidone) as well as a *L*-Thr unit as a lactone linkage.[96] Both of these moieties are also found in some terrestrial cyanobacterial depsipeptides, such as the micropeptins.[97] An analogue of dolastatin 13, symplostatin 2 (**71**) was later isolated from the same cyanobacterium that yielded symplostatin 1.[83] Incidently, a potent antitumor agent, kahalalide F (**21**), from the mollusk *Elysia rufescens*, has an *L*-Thr unit as a lactone linkage and a Abu (2-amino-2-butenoic acid) unit, both of which are also present in symplostatin 2 (**71**).[32] The presence of a pyrrolidone unit in dolastatin 15 (**85**) is another feature that is shared with cyanobacterial compounds such as the malyngamides (e.g. **81**), majusculamides, and microcolins.[98] Table I.2 is a comprehensive listing of dolastatins or dolastatin-like molecules isolated from marine cyanobacteria.

Table I.2 Isolation of identical/related dolastatins from marine cyanobacteria.

Dolastatins	Related/Identical Compounds	Species
3	Dolastatin 3	*Lyngbya majuscula*
	Homodolastatin 3	*L. majuscula*
10	Symplostatin 1	*Symploca hydnoides*
11 and 12	Dolastatin 12	*L. majuscula/Schizothrix calcola*
	Epidolastatin 12	*L. majuscula/S. calcola*
	Lyngbyastatin 1	*L. majuscula/S. calcola*
	Epilyngbyastatin 1	*L. majuscula/S. calcola*
	Majusculamide C	*L. majuscula*
	57-Normajusculamide C	*L. majuscula*
13	Symplostatin 2	*Symploca hydnoides*
G	Lyngbyastatin 2	*L. majuscula*
Nordolastatin G	Norlyngbyastatin 2	*L. majuscula*
Dolabellin	Lyngbyabellins	*L. majuscula*

The presence of identical β-amino/β-hydroxy acid units in compounds reported from both mollusks and cyanobacteria is also an indicator of the diet-derived nature of metabolites in the former organisms. In some cases the stereochemistries of these units in metabolites from mollusks and cyanobacteria were reported to be the same (Table I.3).

Table I.3 β-Amino and β-hydroxy acid units in molluscan and cyanobacterial compounds.

Units	Cyanobacterial Compounds	Molluscan Compounds
β-Amino acid units		
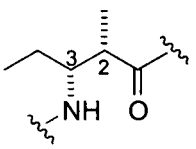	Majusculamide C & 57-Normajusculamide C *Lyngbya majuscula* Lyngbyastatin 1 & Epilyngbyastatin 1 *L. majuscula/Schizothrix calcicola*	Dolastatins 11 & 12 *Dolabella auricularia*
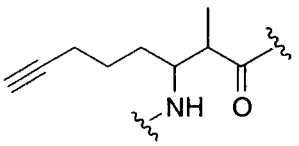	Malevamide C *Symploca laete-viridis*	Ochidin A (2*S*, 3*S*) *Onchidium sp.*
β-Hydroxy acid units		
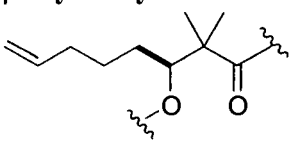	Pitipeptolide B (3*S*) *L. majuscula*	Kulolide-2 (3*S*) *Philinopsis speciosa*
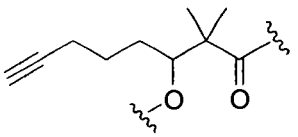	Yanucamides *L. majuscula* Pitipeptolide A *L. majuscula* Georgamide	Kulolide-1 (3*S*) & Kulokainalide-1 (3*S*) *P. speciosa*

Some marine cytotoxic macrolides isolated from mollusks and sponges have structures related to those obtained from cyanobacteria. Examples include swinholide A (**32**), a dimeric macrolide from a *Theonella* sponge and aplyronine A (**86**) from a sea-hare, both of which bear structural similarities to tolytoxin (**87**), a blue-green alga metabolite.[99] An acetate derivative of tolytoxin has also been reported from a mollusk

(*Philinopsis speciosa*) species.[100] In addition, two glycosidic macrolides known as the aurisides (e.g. auriside A, **88**) from *Dolabella auricularia* showed structural similarities to lyngbyaloside (**68**), a compound recently isolated from the cyanobacterium *Lyngbya bouillonii*.[101]

There are also a number of sponge-derived cyclic peptides which are structurally similar or identical to cyanobacterial compounds. These include arenastatin A (**89**), which is identical to a freshwater blue-green algal metabolite, cryptophycin-24;[102-103] and motuporin (**90**), which is an analog of nodularin (**91**), isolated from the brackish water cyanobacterium *Nodularia spumigena*.[104-105] Recent studies have unequivocally shown that the so-called sponge halogenated compounds such as dysidenin (**92**) and related molecules from *Dysidea herbacea* were indeed produced by the cyanobacterium, *Oscillatoria spongeliae*, which lives in symbiotic association with the sponge tissues.[106-107] This was demonstrated by two separate experiments using cell separation techniques coupled with HPLC analysis of the associated chemistries. This work concluded that the metabolite dysidenin (**92**) was found exclusively in the cyanobacterial cells. The presence of the trichloromethyl functional group in dysidenin (**92**) and other related compounds, was also reported in barbamide (**93**), a potent molluscicidal agent isolated from the marine cyanobacterium *Lyngbya majuscula*.[108]

Similar inference could also be made for secondary metabolites, especially cyclic peptides, from tunicates. Most species of tunicates contain symbiotic cyanobacteria living within their tissues in high biomass.[109] However, no experiments to date have proved that tunicate-associated compounds are produced by these symbiotic cyanobacteria. In spite of the lack of direct evidence, some structural features are shared in common by both tunicate and cyanobacterial metabolites. These include the previously mentioned Thr unit present as a lactone and an *N,O*-dimethyl-Tyr unit found for example in the didemnins (e.g. dehydrodidemnin B, **12**), a biomedically important class of tunicate cyclic depsipeptides.

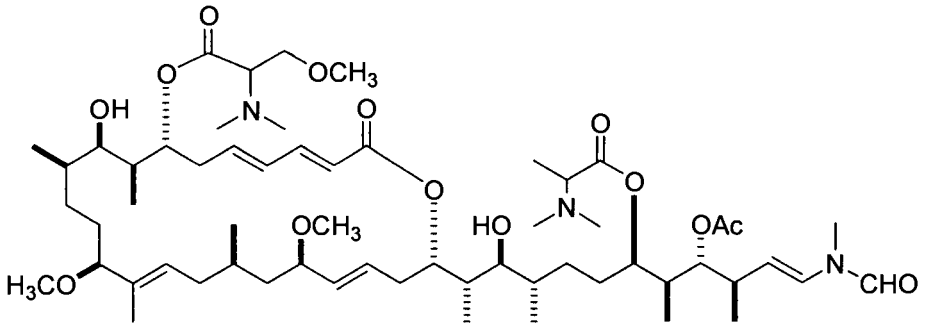

Aplyronine A (**86**)

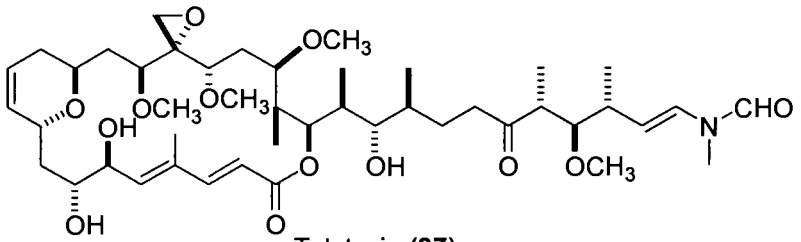

Tolytoxin (**87**)

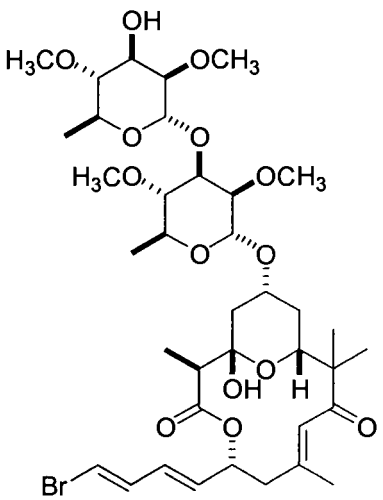

Auriside A (**88**)

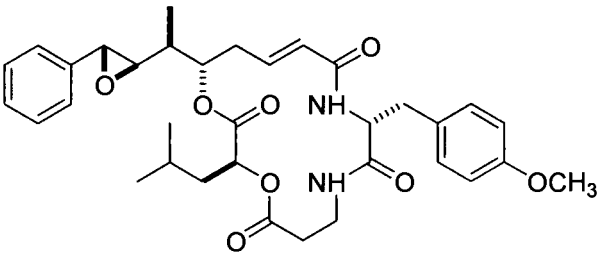

Arenastatin A (**89**) (= Crytophycin 24)

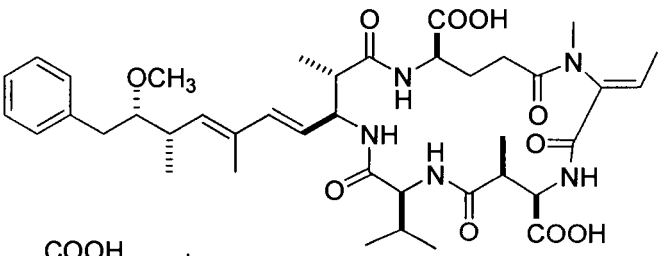

Motuporin (**90**)

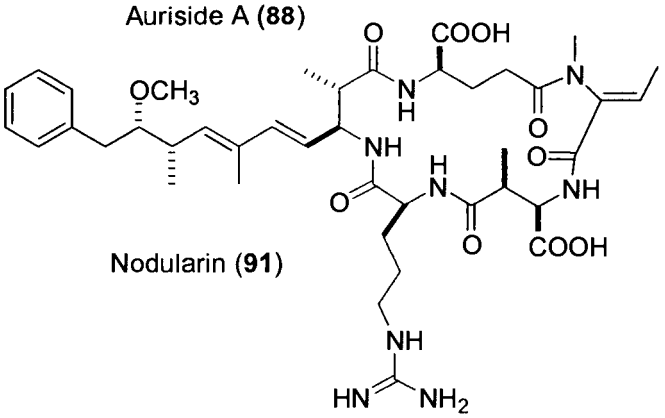

Nodularin (**91**)

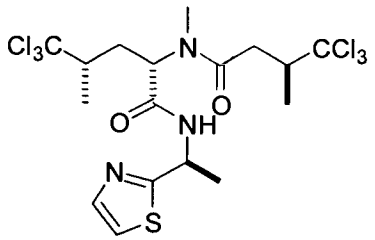

Dysidenin (**92**)

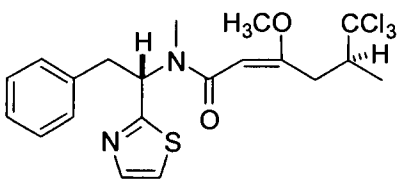

Barbamide (**93**)

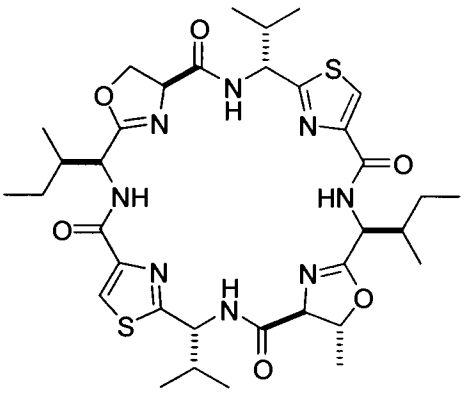

Patellamide A (**94**)

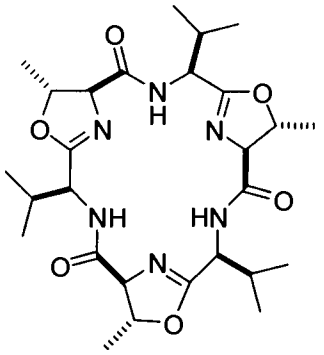

Cycloxazoline (**95**) (= westiellamide)

The modified amino acid, *N,O*-dimethyl-Tyr, is also found with high frequency in cyanobacterial metabolites, for example, lyngbyastatin 1 (**72**).[84] In addition, many tunicate cyclic peptides (e.g. patellamide A, **94**) contain heterocycle-amino acid moieties which are also featured in a number of cyanobacterial compounds.[109] In this regard, a tunicate cyclic peptide, cycloxazoline (**95**)[110] isolated from *Lissoclinum bistratum* is identical to westiellamide (**95**), a metabolite of a terrestrial cyanobacterium *Westiellopsis prolifica*.[111]

As illustrated in the above examples, marine cyanobacteria are a phenomenal source of many interesting and biologically active substances. Several of these metabolites possessed potent antimitotic properties [e.g. curacin A (**20**) and symplostatin 1 (**70**)], acting specifically on cellular protein polymerization processes, such as tubulin and actin. Such biological activities are desirable as agents for the treatment of cancer. It is also important to recognize that many important invertebrate metabolites have their true origin from cyanobacteria. These unique cyanobacterial lipopeptides are the products of the biosynthetic gene clusters, involving a hybrid of PKS and NRPS

pathways. Understanding the mechanisms and the eventual manipulation of these gene clusters represents an exciting research frontier in the field of natural products research.

General Thesis Contents

The search for new and useful natural products from marine algae has been the main focus of our laboratory. Our extensive collections of marine algae are the results of continual expeditions to different parts of the world, including the Caribbean, Indonesia, Japan, Papua New Guinea, Fiji, South Africa, and Madagascar. As such, the various chapters outlined in this thesis have unifying themes, which entail isolation, structure elucidation (both planar and stereochemical determinations), and biological characterization of novel secondary metabolites from marine algae (most notably marine cyanobacteria) collected from these different localities.

This thesis begins with an investigation of a species of red alga, *Ceratodictyon spongiosum* Zanardini (Rhodophyta), obtained from a coastal reef in Indonesia. The organic extract of this curious alga showed toxicity in the brine-shrimp assay, and following a bioassay-guided fractionation, yielded two new thiazole-containing cyclic heptapeptides, *cis,cis*- and *trans,trans*-ceratospongamide. These are stable conformational isomers of the two proline amide bonds in each compound. It was later shown that the *trans*-form is a potent inhibitor of secreted phospholipase A_2 ($sPLA_2$) expression in a cell-based model. Structure elucidations of these cyclopeptides were based on extensive 1D and 2D NMR spectroscopy.

Chapter three presents two new cytotoxic metabolites given the trivial names hermitamides A and B, isolated from the marine cyanobacterium, *Lyngbya majuscula* Gomont (Oscillatoriaceae) collected from reefs off Hermit Village Island, Papua New Guinea in 1998. These metabolites are new additions to a growing class of cyanobacterial metabolites collectively known as the malyngamides. In addition to the structure determination of the hermitamides, semi-syntheses of these compounds based on three different methods will be presented. These syntheses utilized the co-occurring C-14 acid, "lyngbic acid", and commercially obtained free amines. Data on their

biological activities, such as ichthyotoxicity and brine shrimp toxicity, will also be discussed.

A total of six novel cyclic depsipeptides from an organic extract of another Papua New Guinean collection of *Lyngbya majuscula* will be presented in chapter four. These were initially pursued due to significant antifungal properties associated with the organic extract of this *L. majuscula* collection. These intriguing secondary metabolites contained unique β-amino and β-hydroxy acid moieties, which are becoming a structural trend in many marine cyanobacterial metabolites. Two units, Maba (2-methyl-3-amino-butanoic acid) and Dmhha (2,2-dimethyl-3-hydroxy-hexanoic acids), present in clairamide B and the guinamides, respectively, have not been reported in any cyanobacterial compounds. The structure determination and stereochemistries of these cyclopeptides will be presented. Of special interest is the use of *L*- and *D*-Marfey reagents in the stereochemical determination of modified amino acids in these metabolites, especially the Mapa (2-methyl-3-amino-pentanoic acid) unit in clairamide A and the *N,O*-diMe-Tyr units in carliamide and wewakamide.

In the penultimate chapter, the structural and stereochemical analyses of three novel cytotoxic natural products (two cyclic depsipeptides, bouillonamides A and B, and one glycosidic macrolide, lyngbouilloside) from *Lyngbya bouillonii* Hoffmann and Demoulin will be discussed. The source of this cyanobacterium came from two collection trips to Papua New Guinea. This species of marine cyanobacterium was described in the early 1990's from Papua New Guinea and is a rich source of many unique secondary metabolites. Initial investigation of this cyanobacterium was based on ecological observation of the microalga in nature, a point that will be highlighted in chapter five.

The thesis will end with a concluding chapter, summarizing the results presented in the preceding chapters as well as comments on structural trends that are emerging in cyanobacterial secondary metabolites.

CHAPTER TWO

CIS,CIS- AND *TRANS,TRANS*-CERATOSPONGAMIDE, NEW BIOACTIVE CYCLIC HEPTAPEPTIDES FROM THE INDONESIAN RED ALGA *CERATODICTYON SPONGIOSUM* AND SYMBIOTIC SPONGE *SIGMADOCIA SYMBIOTICA*

ABSTRACT

Chemical investigation of the marine red alga (Rhodophyta) *Ceratodictyon spongiosum* containing the symbiotic sponge *Sigmadocia symbiotica* collected from Biaro Island, Indonesia yielded two isomers of a new and bioactive thiazole-containing cyclic heptapeptide, *cis,cis*-ceratospongamide (**96**) and *trans,trans*-ceratospongamide (**97**). Isolation of these peptides was assisted by bioassay-guided fractionation using a brine shrimp toxicity assay (*Artemia salina*). The structures of the ceratospongamides, which each consist of two *L*-phenylalanine residues, one (*L*-isoleucine)-*L*-methyl-oxazoline residue, one *L*-proline residue, and one (*L*-proline)-thiazole residue, were established through extensive NMR spectroscopy, including ^{1}H-^{13}C HMQC-TOCSY and ^{1}H-^{15}N HMBC experiments, as well as chemical degradation and chiral analysis. *Cis,cis*- and *trans,trans*-ceratospongamide are stable isomers differing only in the conformation of the two proline amide bonds. Molecular modeling of these two ceratospongamide isomers showed the *trans,trans* isomer to be quite planar whereas the *cis,cis* isomer has a more puckered overall conformation. *Trans,trans*-ceratospongamide exhibits potent inhibition of $sPLA_2$ expression in a cell-based model for anti-inflammation (ED_{50} 32 nM), whereas the *cis,cis* isomer is inactive. *Trans,trans*-ceratospongamide was also shown to inhibit the expression of a human-$sPLA_2$ promoter-based reporter by 90%.

INTRODUCTION

The marine red macroalga, *Ceratodictyon spongiosum* Zanardini (Rhodophyta), is a widely distributed tropical Indo-Pacific species occurring between southern Japan and eastern Australia. It is an intriguing organism in that the alga grows in nature with a sponge symbiont, *Sigmadocia symbiotica*.[112] The thallus of this algal species consists of a reticular meshwork of algal filaments which is surrounded and covered by the sponge symbiont. Despite its wide occurrence, information on its chemical constituents is lacking with the only report being a series of sphingosine-derived ceramides isolated from a Taiwanese collection of *C. spongiosum*.[113] As part of our continued search for bioactive secondary metabolites from marine sources, we have examined the organic extract of an Indonesian collection of this species and were able to isolate two stable conformers of a bioactive cyclic heptapeptide, *cis,cis*- (**96**) and *trans,trans*-ceratospongamide (**97**). These isolation efforts were guided by a brine shrimp toxicity assay.

Further evaluation of the bioactivity of these metabolites revealed the minor component, *trans,trans*-ceratospongamide (**97**) to be a potent inhibitor of the expression of a key enzyme, the secreted phospholipase A_2 ($sPLA_2$), in the inflammatory cascade with an ED_{50} of 32 nM. The *cis,cis* conformer (**96**) was inactive. Additionally the anti-$sPLA_2$ activity of *trans,trans*-ceratospongamide was observed in a $sPLA_2$ promoter-based reporter based assay.[114] During the inflammation process, the pro-inflammatory cytokine interleukin, IL-1β induces the increased expression of $sPLA_2$ in various cell types, such as rheumatoid synoviocytes and hepatocytes.[115-118] The increased expression of $sPLA_2$ by IL-1β involves a complex signal transduction pathway involving proteins such as TRAF, MAP kinases, NFκ-β, and the *fos/jun* family of transcription factors.[119,120] Released $sPLA_2$ catalyzes the hydrolysis of arachidonic acid from the *sn*-2 position of membrane phospholipids, thus providing substrate for eicosanoid biosynthesis, including leukotrienes, prostaglandins, and thromboxanes, which are potent down-stream mediators of inflammation implicated in several disease states including arthritis and sepsis. $sPLA_2$ has therefore become an important target for therapeutic agents in the control of inflammation.[121] Herein, we report the isolation,

structural characterization, and biological profile of these unique cyclic peptides obtained from the Indonesian red alga *Ceratodictyon spongiosum* and its symbiotic sponge *Sigmadocia symbiotica*.

RESULTS AND DISCUSSION

Fresh samples of the symbiotic red alga *C. spongiosum* and sponge *S. symbiotica* were collected by hand in shallow reefs off the coast of Biaro Island, Indonesia. Upon collection, the specimens were steeped in isopropyl alcohol and stored at –20 °C. The sample was subsequently thawed and repetitively extracted using CH_2Cl_2/MeOH to yield about 2 g of organic extract. A brine shrimp toxicity bioassay was used to direct the fractionation of the extract using a combination of normal-phase silica vacuum flash chromatography and repeated reversed-phase HPLC. This process afforded two stable conformers of a cyclic heptapeptide, *cis,cis*-ceratospongamide (**96**) as the major form and *trans,trans*-ceratospongamide (**97**) as the minor (Figure II.1). Structural characterization of these metabolites were carried out using a battery of 2D NMR experiments including ^{1}H-^{13}C HMQC-TOCSY and ^{1}H-^{15}N HMBC.

Cis,cis-ceratospongamide (**96**) was obtained as a white amorphous solid of molecular formula $C_{41}H_{49}N_7O_6S$ by HR FABMS [positive ion, 3-nitrobenzyl alcohol, *m/z* 768.3545 $(M + H)^+$, (Δ +0.2 mmu)], yielding 21 degrees of unsaturation. Several features of the ^{1}H and ^{13}C NMR spectra suggested the peptidic nature of compound **96**; three amide-type protons were observed at δ 6.51, δ 6.58, and δ 8.12 and several ^{13}C NMR signals attributable to amide or ester carbonyls were located between δ 169-171 (Figure II.2 and II.3). Moreover, the IR spectrum contained bands at 3295 and 1647 cm^{-1}, characteristic of peptide bonds. The cyclic nature of the compound was suggested from a positive ninhydrin test only following acidification (6 N HCl) and heating (100 °C) of the developed TLC plate. Confirmation of the peptidic nature of compound **96** came from routine amino acid analysis of the hydrolysate, which showed the presence of one molar equivalent each of proline and isoleucine, and two molar equivalents of phenylalanine. However, further analysis by ^{13}C NMR and HMQC spectra revealed two units of proline and phenylalanine; the decreased molar equivalency of proline from amino acid analysis is likely due to this residue's acid lability.

The structure of **96** was determined by careful analysis of both one and two dimensional NMR spectral measurements, such as ^{1}H-^{1}H COSY, ^{1}H-^{13}C HMQC, ^{1}H-^{13}C HMQC-TOCSY, and HMBC, which revealed six independent spin systems. Particularly

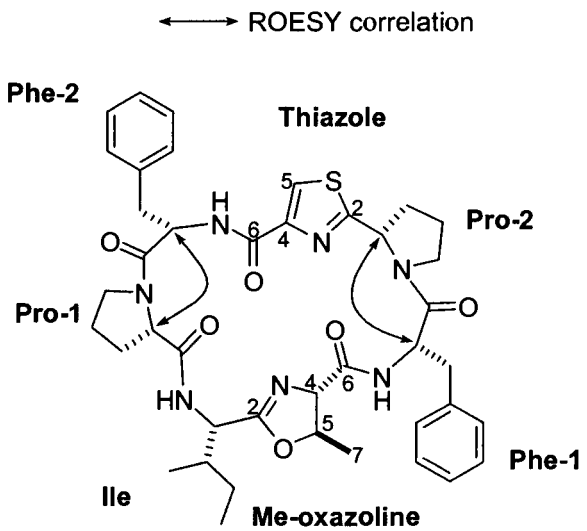

Cis,cis-ceratospongamide (**96**)

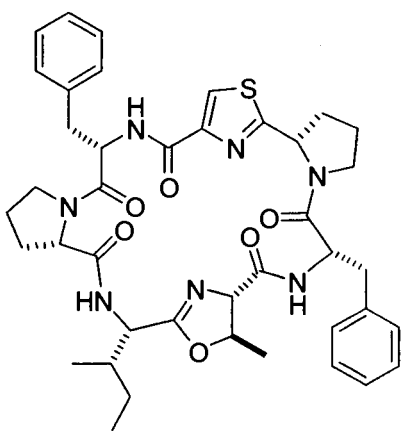

Trans,trans-ceratospongamide (**97**)

Figure II.1 New cyclic heptapeptides (**96** and **97**) from *Ceratodictyon spongiosum* Zanardini (IBI-4/Nov/94-15).

useful was HMQC-TOCSY which unambiguously defined the spin system of individual amino acid units as well as resolved many overlapping proton signals. For instance, the α-protons of Pro-1 (δ 3.42) and Pro-2 (δ 5.14) showed correlations to carbon signals within the proton spin systems: δ 61.1 (C^{α}), δ 30.9 (C^{β}), δ 21.8 (C^{γ}), and δ 46.6 (C^{δ}) for Pro-1 and δ 59.5 (C^{α}), δ 35.0 (C^{β}), δ 21.4 (C^{γ}), and δ 46.4 (C^{δ}) for Pro-2. Likewise, both α-protons of Phe-1 (δ 4.73) and Phe-2 (δ 4.74) have correlations to their respective C^{α} and C^{β} signals: δ 52.1 (C^{α}) and δ 39.0 (C^{β}) for Phe-1 and δ 53.7 (C^{α}) and δ 40.5 (C^{β}) for Phe-2. The β-protons in Phe-1 and Phe-2 in turn showed long-range HMBC correlations to carbon signals belonging to their respective phenyl groups. The presence of an Ile-like unit was confirmed from HMQC-TOCSY data which showed correlations between $C^{\gamma 2}H_3$-protons (δ 0.82) and carbon signals δ 11.6 ($C^{\delta 1}$), δ 24.6 ($C^{\gamma 1}$), δ 38.1 (C^{β}), and δ 51.4 (C^{α}).

Another spin system in **96** belonged to a cyclic unit, a methyl oxazoline ring, which was inferred from two characteristic mid-field carbon signals at δ 73.6 and δ 81.4 as well as an up-field methyl signal at δ 21.2. In addition, the HMQC-TOCSY showed correlations from the H-7 methyl protons to these mid-field carbon signals. Together with the observation of H-4 (δ 3.17) and H-5 proton (δ 3.94) correlations to a carbon signal at δ 168.7 (C-2) by HMBC, a methyl oxazoline moiety was firmly established to be part of compound **96**.

The final residue in **96** consisted of a broad singlet proton resonance at δ 8.01 with an associated carbon atom at δ 124.2, indicative of a thiazole ring. HMBC correlation of this proton signal to carbon signals δ 148.6 (C-4), δ 159.4 (C-6), and δ 169.8 (C-2) further supported the thiazole unit, and correlated well with other marine derived thiazole-containing cyclic peptides in the literature.[122]

Determination of the sequence and connection of amino acid residues and other units (thiazole, methyl oxazoline) in **96** was achieved primarily by long range ^{13}C-^{1}H correlation experiments (HMBC) with different mixing times and a ROESY experiment. Characterization of a (proline)-thiazole unit was established by the following HMBC correlations: H^{α} (Pro-2), $H^{\beta 1}$ (Pro-2), $H^{\beta 2}$ (Pro-2), and H-5 (Thiazole) to C-2 (Thiazole); H-5 (Thiazole) to C-4 (Thiazole). The (isoleucine)-methyl oxazoline segment was

deduced in a similar manner by observing the following correlations: H^{α} (Ile), H^{β} (Ile), H-4 (Me-oxazoline), and H-5 (Me-oxazoline) to C-2 (Me-oxazoline). Two overlapping carbonyl signals at δ 169.6 (Me-oxazoline C-6 and Phe-1 C′) were assigned by the following HMBC correlations: H-4 (Me-oxazoline) and H^{N} (Phe-1) to C-6 (Me-oxazoline); H^{α} (Pro-2), $H^{\delta 1}$ (Pro-2), $H^{\delta 2}$ (Pro-2), and H^{α} (Phe-1) to C′ (Phe-1). Additional information from ROESY data confirmed the Phe-1-Pro-2 unit with a strong correlation between H^{α} (Pro-2) and H^{α} (Phe-1). Similarly, other residue connections were assigned from HMBC correlations: H^{α} (Pro-1) and H^{N} (Ile) to C′ (Pro-1); H-5 (Thiazole) and H^{N} (Phe-2) to C-6 (Thiazole); H^{α} (Phe-2), H^{α} (Pro-1), and H^{δ} (Pro-1) to C′ (Phe-2) (Table II.1).

Information from a ^{1}H-^{15}N HMBC was used to confirm the sequence developed from the above HMBC data.[123-125] Such long-range ^{1}H-^{15}N coupling data is particularly useful since ^{15}N chemical shifts are more widely dispersed than those of ^{13}C or ^{1}H.[126] One of the two main residue sequences, Pro-2-thiazole-Phe-2, was confirmed from the following ^{1}H-^{15}N HMBC cross peaks data: N (Thiazole)/H^{α} (Pro-2) and H^{N} (Phe-2); N (Phe-2)/H^{α} (Phe-2), $H^{\beta 1}$ (Phe-2), and $H^{\beta 2}$ (Phe-2). The second sequence, Pro-1-Ile-Me-oxazoline-Phe-1, was deduced as follows: N (Ile)/H^{α} (Pro-1) and H^{α} (Ile); N (Me-oxazoline)/H^{α} (Ile), H-4 (Me-oxazoline); N (Phe-1)/H-4 (Me-oxazoline) and H^{α} (Phe-1). Selected ^{1}H-^{15}N HMBC correlations are depicted in Figure II.4. In addition, positive ion FABMS of **96** gave fragmentation patterns supportive of the proposed amino acid sequence (Figure II.5).

Absolute stereochemistry of *cis,cis*-ceratospongamide (**96**) was characterized by ozonolysis followed by acid hydrolysis and analysis by Marfey's method[127] as well as chiral GC-MS. Ozonolysis avoided racemization of Pro-2 by destroying the aromaticity of the thiazole.[128] Acid hydrolysis and derivatization with Marfey's reagent was followed by comparative HPLC analysis with derivatized standard *D*- and *L*-amino acids and established an *L*-configuration for each (*L*-isoleucine, *L*-phenylalanine, *L*-proline, and *L*-threonine). The all *L*-configuration for residues in **96** was also supported by chiral GC-MS analysis of the pentafluoropropyl isopropyl ester derivatives of the acid hydrolysate (see Experimental).

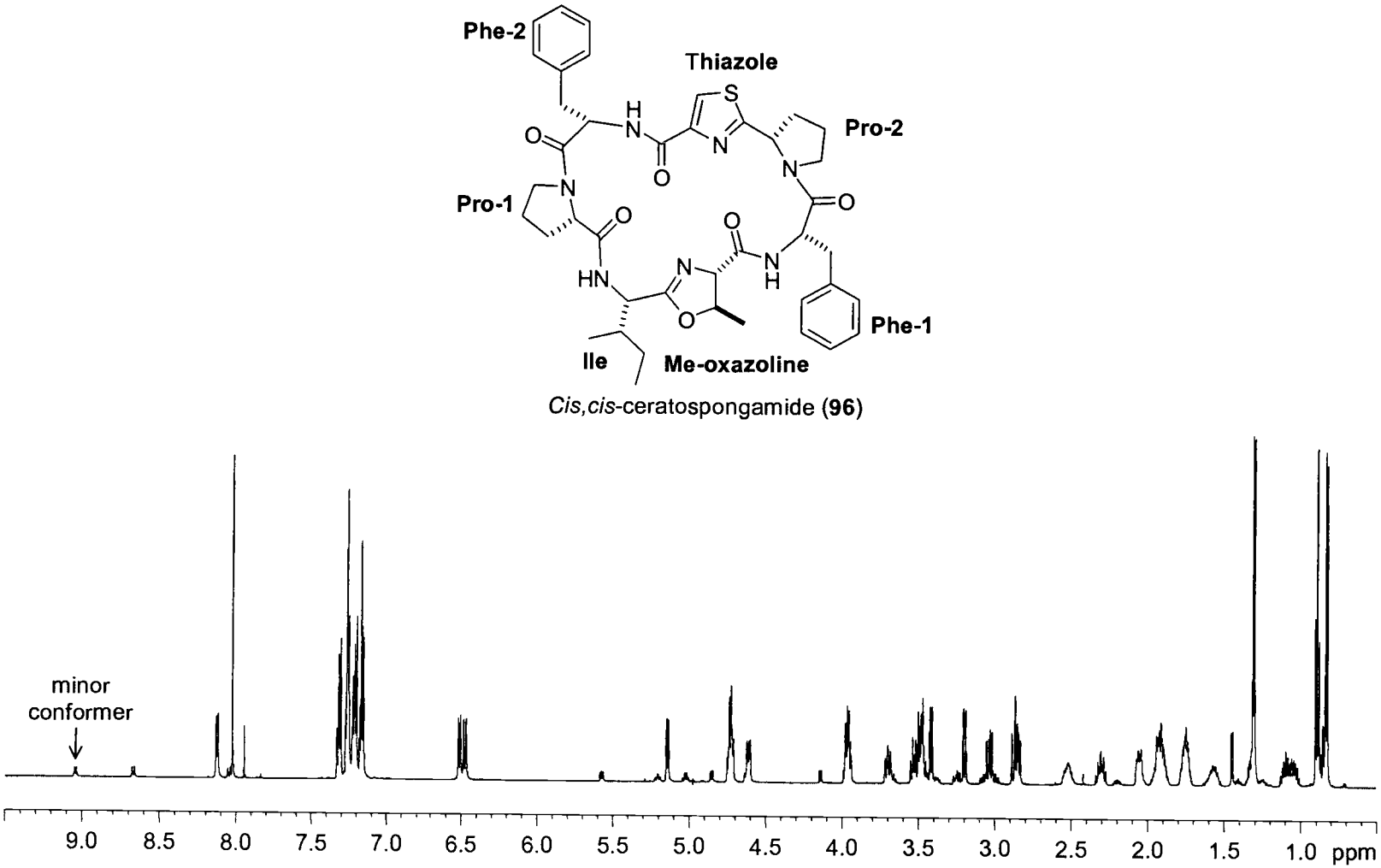

Figure II.2 ^{1}H NMR spectrum of *cis,cis*-ceratospongamide (**96**) in $CDCl_3$.

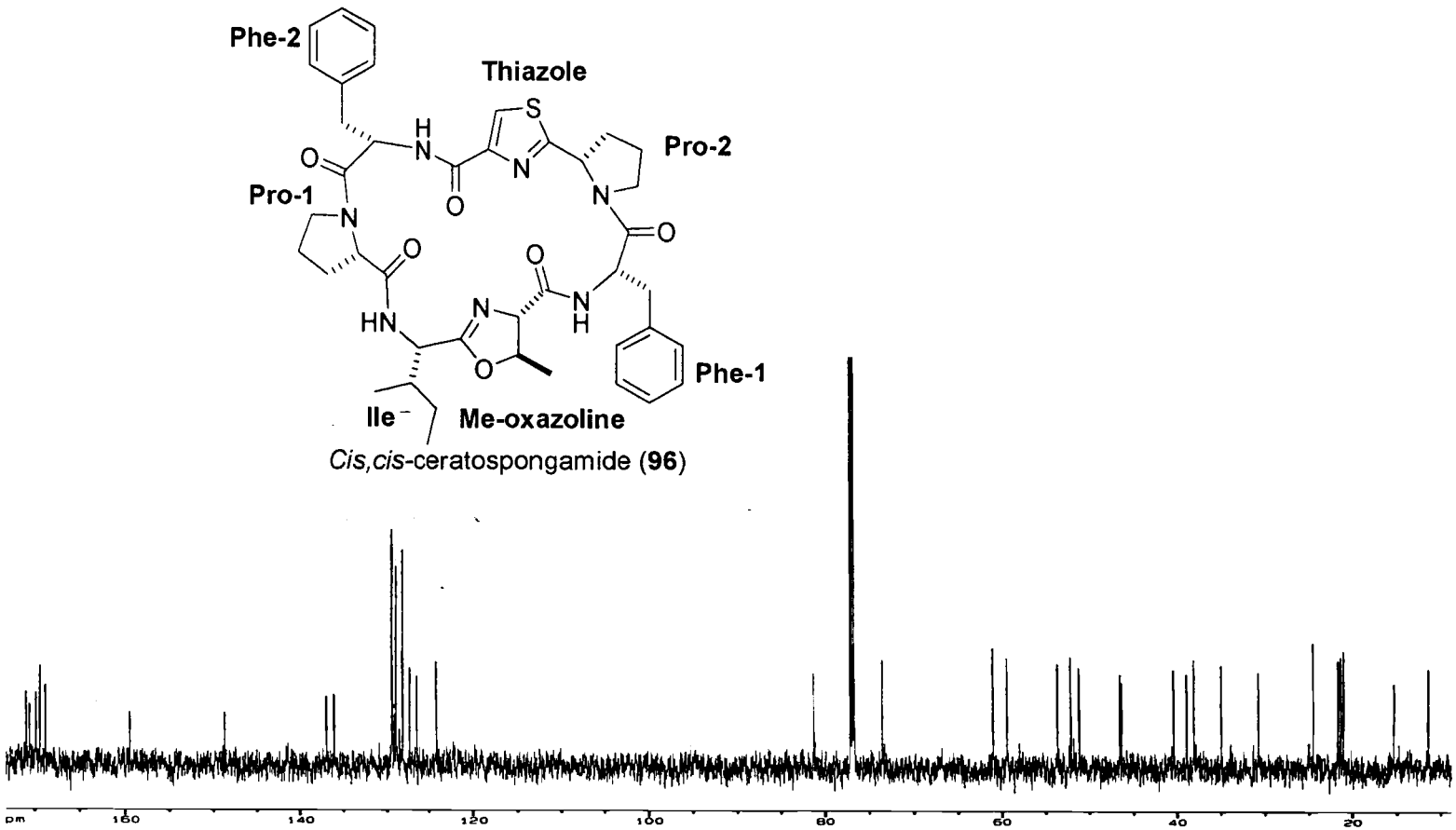

Figure II.3 ^{13}C NMR spectrum of *cis,cis*-ceratospongamide (**96**) in $CDCl_3$.

Table II.1 ^{1}H and ^{13}C NMR spectral data (in ppm) for *cis,cis*-ceratospongamide (**96**)[a] with HMBC and ROESY correlations.

amino acid	Position[b]	^{1}H	*m*	*J* (Hz)	^{13}C	HMBC	ROESY
Proline-1	H^{α}	3.42	d	7.9	61.1	21.8, 30.9, 169.7, 170.4	4.60, 4.74, 6.51
	H^{β}	1.09	m		30.9	21.8, 46.6, 61.1, 169.7	
	H^{β}	1.89	m			21.8, 46.6, 61.1, 169.7	
	H^{γ}	1.55	m		21.8	30.9, 46.6	1.89, 3.68
	H^{γ}	1.75	m			30.9, 61.1	
	H^{δ}	3.46	m		46.6	30.9, 61.1, 170.4	
	H^{δ}	3.68	m			30.9, 61.1	1.55, 1.75, 6.51
	C'				169.7		
Isoleucine	H^{α}	4.60	dd	9.7, 1.7	51.4	15.5, 24.6, 38.1, 168.7, 169.7	0.82, 0.87, 1.73, 3.42, 6.51
	H^{β}	1.73	m		38.1	11.6, 15.5, 24.6, 51.4, 168.7	1.28
	$H^{\gamma 1}$	1.04	m		24.6	11.6, 15.5, 38.1, 51.4	
	$H^{\gamma 1}$	1.28	m			11.6, 15.5, 38.1, 51.4	4.60
	$(H^{\gamma 2})_3$	0.82	d	6.8	15.5		
	$(H^{\delta 1})_3$	0.87	t	7.4	11.6	24.6	
	H^{N}	6.51	d	9.7		51.4, 169.7	
Me-oxazoline	2				168.7		
	4	3.17	d	9.5	73.6	21.2, 81.4, 168.7, 169.6	1.28, 3.94, 4.74, 6.58
	5	3.94	m		81.4	73.6, 168.7, 169.6	
	6				169.6		
	7	1.24	d	6.2	21.2	73.6, 81.4	
Phenylalanine-1	H^{α}	4.73	dt	8.4, 8.2, 7.3	52.1	39.0, 169.6	
	H^{β}	2.81	dd	13.2, 6.8	39.0	52.1, 136.9, 169.6	
	H^{β}	3.01	dd	13.2, 8.3		52.1, 136.9, 169.6	
	C^{γ}				136.9		
	$H^{\delta 1}$, $H^{\delta 2}$	7.23	m		129.4	128.1, 136.9	

(**Table II.1** *continued*)

	$H^{\varepsilon1}$, $H^{\varepsilon2}$	7.19 m		128.1	126.5, 129.4	
	H^{ζ}	7.19 m		126.5	128.1	
	C'			169.6		
	H^{N}	6.58 d	8.7		52.1, 169.6	2.81, 3.01, 4.73
Proline-2	H^{α}	5.14 dd	7.4, 1.6	59.5	21.4, 46.4, 35.0, 169.8	2.04, 2.31, 3.95, 4.73
	H^{β}	2.04 m		35.0	21.4, 46.4, 169.8	1.89
	H^{β}	2.31 ddt	12.3, 7.6, 7.5		21.4, 59.5, 46.4, 169.8	
	H^{γ}	1.89 m		21.4	35.0, 46.4, 59.5	
	H^{γ}	1.89 m			35.0, 46.4, 59.5	
	H^{δ}	3.46 m		46.4	35.0, 59.5, 169.6	
	H^{δ}	3.95 m			59.5	
Thiazole	2			169.8		
	4			148.6		
	5	8.01 s		124.2	59.5, 148.6, 159.4, 169.8	
	6			159.4		
Phenylalanine-2	H^{α}	4.74 dt	10.7, 6.4, 4.9	53.7	40.5, 170.4	
	H^{β}	2.85 dd	12.8, 10.6	40.5	53.7, 136.0, 170.4	
	H^{β}	3.50 m				
	C^{γ}			136.0		
	$H^{\delta1}$, $H^{\delta2}$	7.34 m		129.4	128.9, 136.0	
	$H^{\varepsilon1}$, $H^{\varepsilon2}$	7.28 m		128.9	127.4, 129.4	
	H^{ζ}	7.34 m		127.4	128.9	
	C'			170.4		
	H^{N}	8.12 d	6.5		53.7, 159.4, 170.4	

[a] All spectra measured in $CDCl_3$ and referenced to residual solvent signal at δ_H 7.26 and δ_C 77.4.

[b] Nomenclature in identifying amino acid residues in accordance with reference 135.

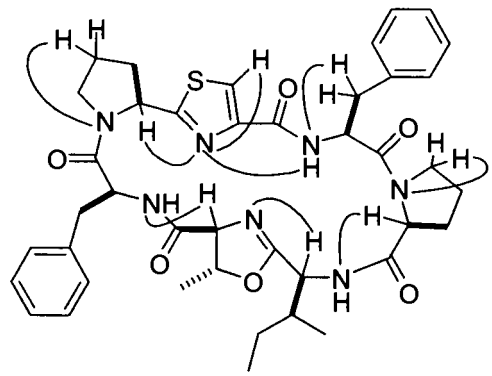

Figure II.4 Selected correlations observed by ^{1}H-^{15}N HMBC of *cis,cis*-ceratospongamide (**96**).

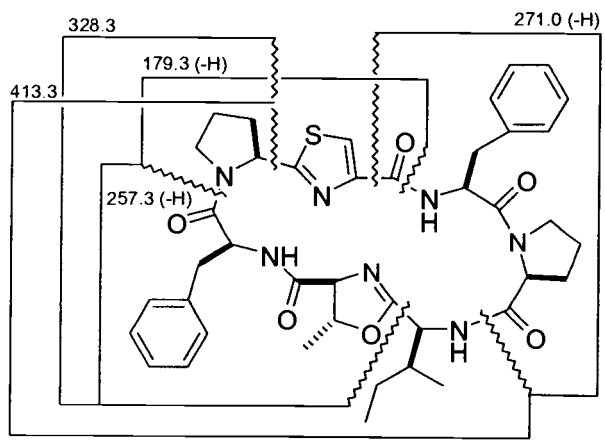

Figure II.5 FAB mass spectral fragmentations observed for *cis,cis*-ceratospongamide (**96**) and *trans,trans*-ceratospongamide (**97**).

The minor component, *trans,trans*-ceratospongamide (**97**), was also obtained as a white amorphous solid with IR and UV spectra identical to that of **96**. While metabolite **97** had an identical molecular formula as compound **96** as deduced by HR FABMS [positive ion, 3-nitrobenzyl alcohol, *m/z* 768.3542 $(M + H)^+$ (Δ –0.1 mmu)], the magnitude of its optical rotation was different $[\alpha]_D$ –39° (c = 0.52). Analysis of COSY, HMQC, HMQC-TOCSY, and HMBC data showed that the planar structures of **96** and **97** were identical. Moreover, stereochemical analysis of **97** using Marfey's method[127] indicated that all amino acids were of the *L*-configuration. By NMR chemical shift analysis, the differences between **96** and **97** were confined to signals associated with the two proline units, and to some degree, the amino acids adjacent to these two proline units.

It is well documented that *cis/trans* conformational differences of proline amide bonds correlates with differential values between proline β and γ carbons ($\Delta\delta_{\beta\gamma}$).[129] In compound **2**, $\Delta\delta_{\beta\gamma}$ of Pro-1 and Pro-2 were 4.4 ppm and 7.0 ppm, respectively. This is markedly different than the $\Delta\delta_{\beta\gamma}$ of Pro-1 and Pro-2 of **96** (9.1 ppm and 13.6 ppm, respectively). Hence, both proline amide bonds in **96** are *cis* while those in **97** are *trans*. These conformational assignments are further supported from ROESY data which showed a strong correlation between the α-protons of Pro-2/Phe-1 as well as Pro-1/Phe-2 in the *cis* conformation (**96**), but no such correlations in the *trans* form (**97**). Therefore, the relationship of these two peptides is that of two stable proline peptide bond conformers.

Variable temperature NMR experiments were performed on *cis,cis*- (**96**) and *trans,trans*-ceratospongamide (**97**) in order to probe 1) the interconvertability of these two proline amide conformers, and 2) the degree and nature of intramolecular hydrogen bonding within these two molecules.[130] ^{1}H NMR spectra of the *cis,cis* isomer (**96**) in DMSO over the range 25 °C to 90 °C showed no detectable conversion to the *trans,trans* isomer (**97**). However, when the *cis,cis* isomer (**96**) was heated to 175 °C in DMSO, the conversion to the *trans,trans* isomer (**97**) was detected using gradient HPLC under two different reverse-phase HPLC conditions [Phenomenex Phenosphere 10 C_8 90A and Phenomenex Sphereclone 5μ ODS (2)] and was confirmed by co-injection with

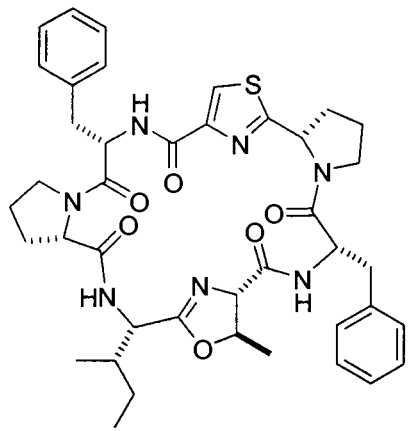

Trans,trans-ceratospongamide (**97**)

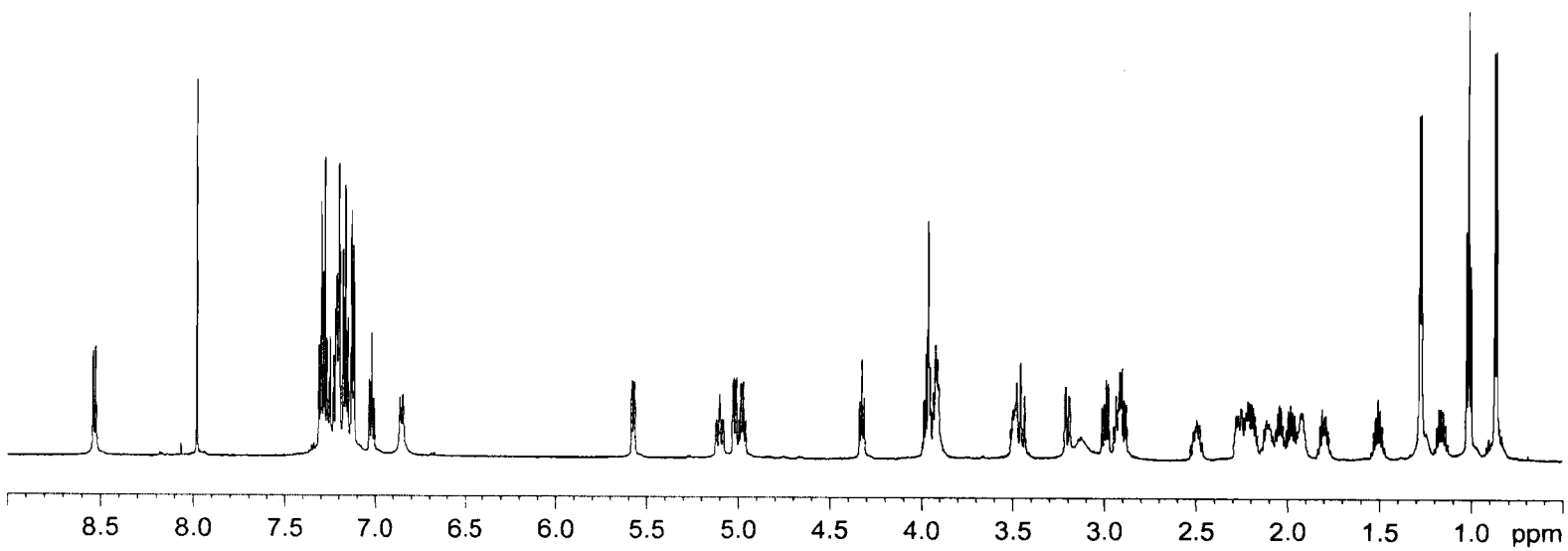

Figure II.6 ^{1}H NMR spectrum of *trans,trans*-ceratospongamide (**97**) in $CDCl_3$.

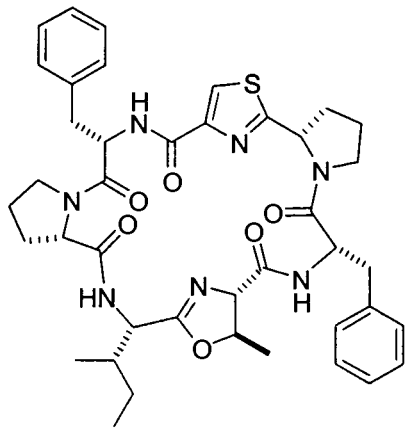

Trans,trans-ceratospongamide (**97**)

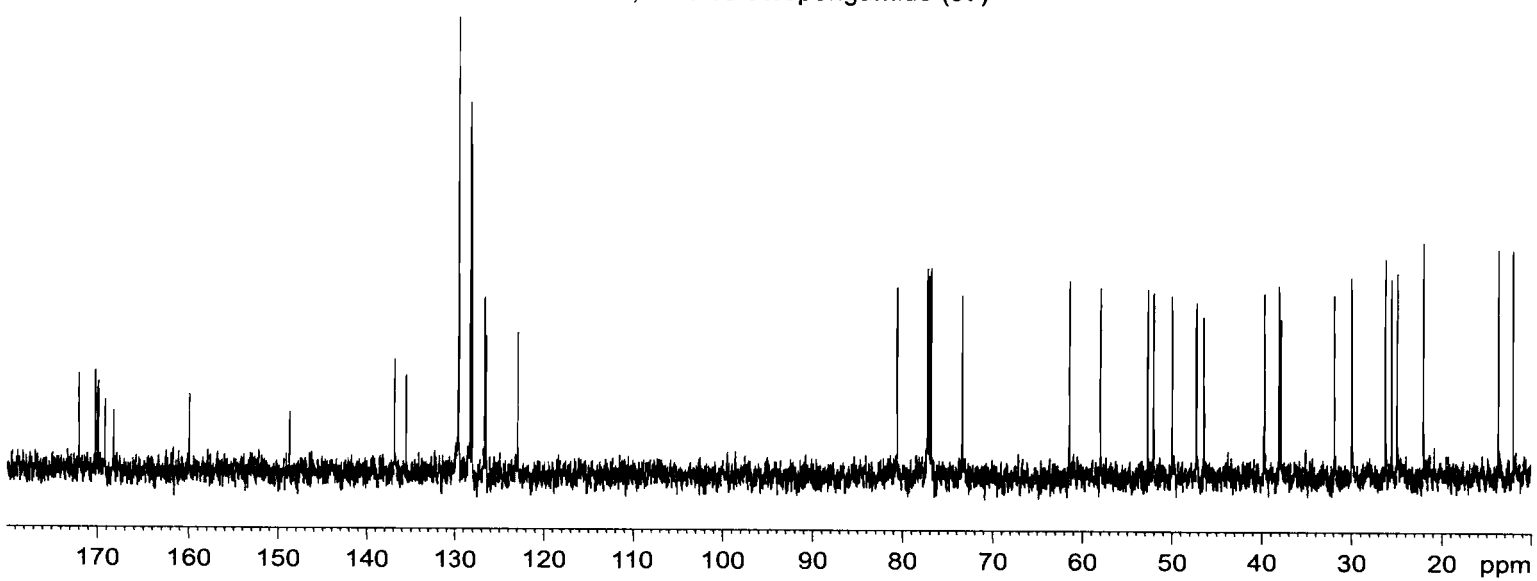

Figure II.7 ^{13}C NMR spectrum of *trans,trans*-ceratospongamide (**97**) in $CDCl_3$.

Table II.2 ^{1}H and ^{13}C NMR spectral data (in ppm) for *trans,trans*-ceratospongamide (**97**)[a] with HMBC and ROESY correlations.

amino acid	Position[b]	^{1}H	*m*	*J* (Hz)	^{13}C	HMBC	ROESY
Proline-1	H^{α}	4.32	t	7.3	61.4	25.5, 29.9, 169.9, 172.0	1.79, 3.49, 6.85
	H^{β}	1.98	m		29.9	25.5, 47.2, 61.4	
	H^{β}	2.19	m			61.4, 172.0	
	H^{γ}	1.79	ddq	14.3, 12.2, 7.4	25.5	29.9, 47.2, 61.4	4.32
	H^{γ}	2.04	m			29.9, 47.2, 61.4	
	H^{δ}	2.92	m		47.2	25.5, 29.9	4.98
	H^{δ}	3.49	m			25.5, 29.9, 61.4	2.89, 4.32, 4.98
	C'				172.0		
Isoleucine	H^{α}	5.02	dd	8.8, 3.0	49.9	13.7, 26.2, 38.0, 168.2, 172.0	0.86, 1.01, 1.50, 8.53
	H^{β}	1.92	m		38.0	26.2	0.86, 1.01
	$H^{\gamma 1}$	1.16	ddq	13.7, 13.5, 7.3	26.2	11.9, 13.7, 38.0, 49.9	
	$H^{\gamma 1}$	1.50	ddq	13.7, 13.8, 7.6		11.9, 13.7, 38.0, 49.9	
	$(H^{\gamma 2})_3$	0.86	d	6.9	13.7	26.2, 38.0, 49.9	
	$(H^{\delta 1})_3$	1.01	t	7.3	11.9	26.2, 38.0	
	H^{N}	6.85	d	8.9		168.2, 172.0	4.32
Me-oxazoline	2				168.2		
	4	3.94	d	6.5	73.3	168.2, 170.2	1.27
	5	3.99	ddd	6.4, 6.2	80.5	21.9, 73.3	
	6				170.2		
	7	1.27	d	5.8	21.9	73.3, 80.5	
Phenylalanine-1	H^{α}	5.09	dt	10.3, 3.2	52.6	37.8, 170.0	3.92
	H^{β}	3.20	dd	13.2, 3.0	37.8	52.6, 129.5, 136.8	3.92
	H^{β}	3.45	t	13.0		52.6, 129.5, 136.8	3.92
	C^{γ}				136.8		
	$H^{\delta 1}$, $H^{\delta 2}$	7.21	m		129.5	136.8, 126.6	

(**Table II.2** *continued*)

	$H^{\varepsilon1}$, $H^{\varepsilon2}$	7.30	t	7.4	128.0	129.5, 136.8	
	H^{ζ}	7.02	t	7.3	126.6	128.0, 129.5	C'
	170.0						
	H^{N}	7.27	d	10.4		52.6, 170.2	
Proline-2	H^{α}	5.57	dd	7.9, 2.6	57.9	24.8, 31.8, 46.4, 169.1	
	H^{β}	2.27	m		31.8	57.9	
	H^{β}	2.49	m			24.8, 57.9, 169.1	3.92
	H^{γ}	2.10	m		24.8	31.8, 46.4	
	H^{γ}	2.22	m			31.8, 46.4	
	H^{δ}	3.92	m		46.4	24.8	
	H^{δ}	3.92	m			24.8	
Thiazole	2				169.1		
	4				148.7		
	5	7.98	s		122.9	148.7, 159.9, 169.1	
	6				159.9		
Phenylalanine-2	H^{α}	4.98	dd	7.4, 7.3	51.9	39.6, 135.5, 159.9, 169.9	
	H^{β}	2.89	dd	13.8, 7.3	39.6	51.9, 129.5, 135.5, 169.9	
	H^{β}	2.99	dd	13.7, 6.2		51.9, 129.5, 135.5, 169.9	
	C^{γ}				135.5		
	$H^{\delta1}$, $H^{\delta2}$	7.13	d	7.1	129.5	126.5	
	$H^{\varepsilon1}$, $H^{\varepsilon2}$	7.16	t	7.5	128.2	129.5, 135.5	
	H^{ζ}	7.22	m		126.5	129.5	
	C'				169.9		
	H^{N}	8.53	d	8.4		51.9, 159.9, 169.9	

[a] All spectra measured in $CDCl_3$ and referenced to residual solvent signal at δ_H 7.26 and δ_C 77.4.

[b] Nomenclature in identifying amino acid residues in accordance with reference 135.

trans,trans-ceratospongamide (**97**). Because of the very small quantity of isolated *trans,trans* isomer (**97**), high temperature interconversion experiments beginning with **97** were not conducted. Metabolites **96** and **97** are not the first stable cyclic peptide conformers to be reported from a marine source. Theopalauamide and isotheopalauamide are a pair of conformationally-stable cyclic peptides which were recently reported from a sponge.[131] The major difference between these latter two peptides is the rotation of the bond between the α-carbon and the adjacent carbonyl group in the Phe residue.

Additional ^{1}H NMR spectra of compounds **96** and **97** were acquired at 5 °C, 15 °C, and 25 °C in $CDCl_3$. For **96**, $\Delta\delta/\Delta T$ (ppb/K) values for H^N-Ile, H^N-Phe-1, and H^N-Phe-2 were 4.05, 6.50, and 0.70, respectively. These suggest that the amide proton of Phe-2 participates in an intramolecular hydrogen bond while that of Ile and Phe-1 do not. A similar data set was obtained for compound **97** yielding values of 7.60 and 1.30 ppb/K for H^N-Ile and H^N-Phe-2, respectively. No data was obtained for H^N-Phe-1 as the amide proton was hidden within the envelope of aromatic protons.

The degree of anti-inflammatory activity of compounds **96** and **97** was measured as the inhibition of secreted phospholipase A_2 by hepatocellular carcinoma cells stimulated with IL-1β. The *trans,trans*-form (**97**) is a potent inhibitor of $sPLA_2$ expression with an ED_{50} of 32 nM. No inhibitory activity was recorded for the *cis,cis*-form (**96**) up to a maximal concentration of 32 μM. Both compounds **96** and **97** showed only moderate potency in the brine shrimp toxicity assay (LD_{50} = *ca.* 13-19 μM). In IL-1β stimulated, reporter-transfected HepG2 cells pretreated with *trans,trans*-ceratospongamide (**97**) (50 ng/mL), the expression of the reporter (–326 to +20) was reduced by 50% relative to control and 90% in the (–159 to +20) plasmid construct. These results taken together with the ELISA data suggest that *trans,trans*-ceratospongamide (**97**) inhibits $sPLA_2$ at the level of intracellular signaling by acting on cytoplasmic activation or transcription factor binding of specific IL-1β stimulated mediators.

Models of the 3-dimensional structures of *cis,cis*- (**96**) and *trans,trans*-ceratospongamide (**97**) were determined by molecular mechanics minimization. The 3-D models were constructed from distance geometry energy minimization calculations

using additional distance restraints observed from proton ROESY correlations (Tables II.1 and II.2) (Figure II.8). The most striking difference between the two forms of ceratospongamide is the conformation of the macrocyclic ring. In the *trans,trans* isomer (**97**) the overall conformation of this ring is planar with amino acid side-chains above and below the ring. Puckering of the macrocycle occurs in the *cis,cis* isomer (**96**), and the thiazole and Pro-2 rings are approximately orthogonal to their position in *trans,trans*-ceratospongamide (**97**). Moreover, Phe-1 as well as other amino acid residue side-chains lie more in the plane of the macrocycle in the *cis,cis* isomer (**96**). As could be implied from the observed dramatic differences in biological activity of these two proline-amide isomers, the overall 3-dimensional structures of these two substances are quite distinct (Figure II.8).

Given the biological nature of this algal-sponge symbiotic pair, the true metabolic origin of these cyclic peptides is uncertain. However, recognizing the frequency of isolation of cyclic peptides from marine sponges, it would be logical that these two new cyclic peptides derive from the sponge symbiont. Further complication of this point is given by recent work by Bewley and Faulkner which provides evidence that similar cyclic peptides found in "sponges" actually derive from microorganisms living in association with their invertebrate hosts.[132] Therefore, it is uncertain if the sponge, one of the associated microorganisms, or the alga is the true source of metabolites **96** and **97**.

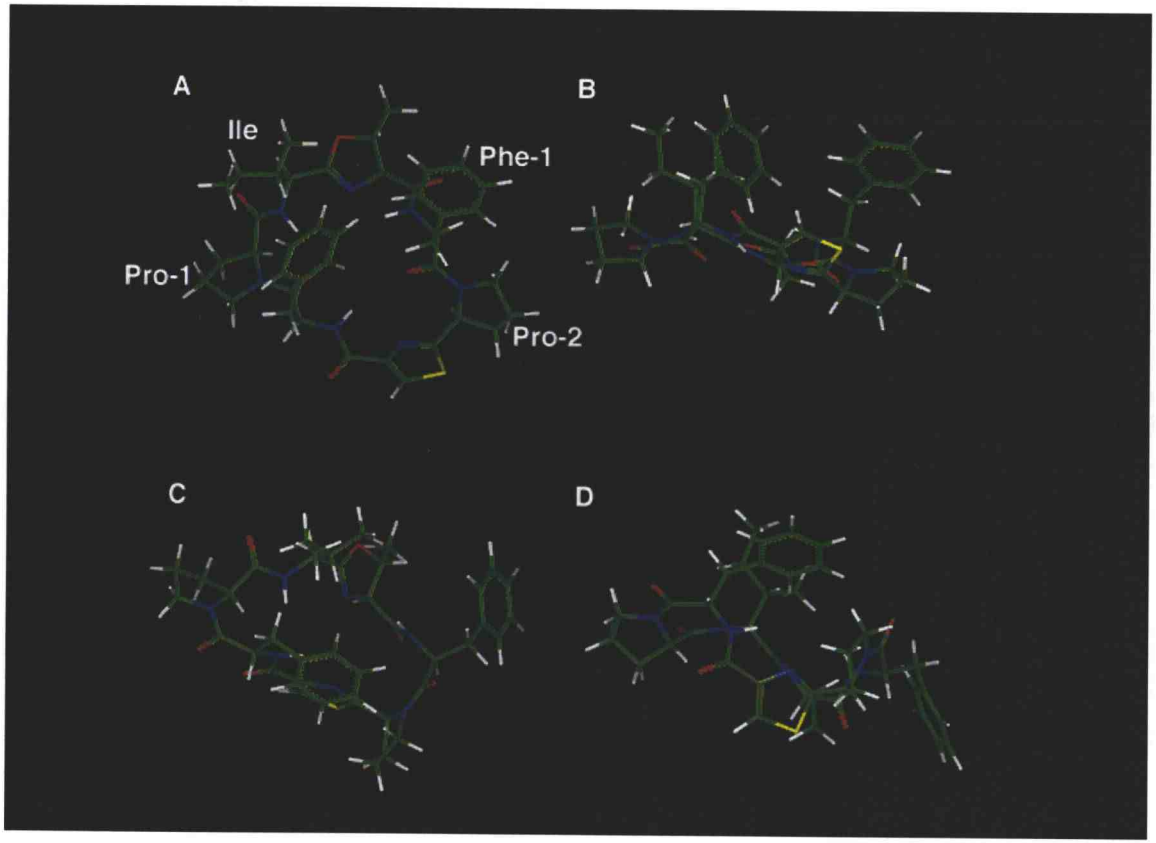

Figure II.8 Molecular modeling of the ceratospongamides: (A) view of **97** looking down on macrocycle, (B) orthogonal view of **97**, (C) view of **96** looking down on macrocycle, (D) orthogonal view of **96**.

EXPERIMENTAL

Extraction and Isolation. *Ceratodictyon spongiosum* Zanardini containing symbiotic sponge *Sigmadocia symbiotica* was collected on November 4, 1994 (IBI-4/Nov/94-15) in shallow waters by snorkeling at Biaro Island, Indonesia. The alga appeared as irregular clumps with multiple branching, commonly 10 cm or more in diameter and about 5 cm high.

The specimens were preserved in isopropanol and maintained at –20 °C. After thawing, the sample was extracted three times using CH_2Cl_2/MeOH (2:1) and the crude extract (2 g) was initially fractionated using normal-phase Si vacuum flash chromatography (VLC) employing gradient solvent systems of hexanes/EtOAc/MeOH. Fractions eluted with EtOAc:MeOH (9:1) and EtOAc:MeOH (1:1) were combined based on their TLC profiles and refractionated over normal-phase Si VLC (gradient of $CHCl_3$/MeOH). Fractions eluting with 100% $CHCl_3$ to $CHCl_3$:MeOH (19:1) were enriched with peptides; they were combined and purified with repeated reversed-phase HPLC [Phenomenex Sphereclone 5μ ODS (2); MeOH/H_2O (78:22)] to yield pure *cis,cis*-ceratospongamide (**96**, 15.0 mg, 0.02%) and *trans,trans*-ceratospongamides (**97**, 4.0 mg, 0.005%).

***Cis,cis*-ceratospongamide (96):** white amorphous solid; $[\alpha]_D$ –190° (c = 0.13, $CHCl_3$); UV ($CHCl_3$) λ_{max} 246 nm (ϵ 11 800); IR (neat) 3385, 3295, 2967, 1647, 1534, 1444, 1200 cm^{-1}; LR FABMS *m/z* 768 (100), 413 (7.8), 328 (5), 271 (7.1), 257 (5.7), 231 (12.8), 179 (11.5); ^1H NMR (600 MHz, $CDCl_3$) see Table II.1; ^{13}C NMR (150 MHz, $CDCl_3$) see Table II.1.

***Trans,trans*-ceratospongamide (97):** white amorphous solid; $[\alpha]_D$ –39.2° (c = 0.52, $CHCl_3$); UV ($CHCl_3$) λ_{max} 246 nm (ϵ 11 200); IR (neat) 3385, 3295, 2967, 1647, 1534, 1444, 1200 cm^{-1}; LR FABMS *m/z* 768 (100), 413 (15), 328 (7.1), 271 (7.8), 257 (8.1), 231 (20), 179 (19.5); ^1H NMR (600 MHz, $CDCl_3$) see Table II.2; ^{13}C NMR (150 MHz, $CDCl_3$) see Table II.2.

Ozonolysis of 96 and 97. A stream of O_3 was carefully bubbled into a vial containing 1 mL of CH_2Cl_2 solution of **96** or **97** (200 μg; 0.260 μmol) at 25 °C for about

10 min. Solvent was removed under a stream of N_2 and the resulting residue was subjected to hydrolysis and derivatization as described below.

Stereochemical Determination of 96 and 97. Hydrolysis of **96** or **97** (400 μg; 0.520 μmol) was achieved in 1 mL of 6 N HCl in a sealed vial at 110 °C for 20 h. Traces of HCl were removed *in vacuo*. The resulting hydrolysate was resuspended in 30 μL of H_2O and derivatized with *N*α-(2,4-dinitro-5-fluoro-phenyl)-*L*-alaninamide (FDAA).[127] HPLC analyses of the FDAA-derivatized hydrolysate of **96** or **97** and standard FDAA-derivatized amino acids were carried out using Waters NOVAPAK C_{18} (3.9 × 150 mm column) with a linear gradient of triethylammonium phosphate (50 mM, pH 3.0)/MeCN 90:10 to 60:40 in 40 min at 1 mL/min (UV detection at λ 340 nm). The analysis established the presence of *L*-Thr (7.07 min) [*D*-Thr (11.97 min), *L*-allo-Thr (7.81 min), *D*-allo-Thr (8.50 min)], *L*-Pro (9.35 min), *L*-Ile (13.51 min) [*D*-Ile (15.49 min), *L*-allo-Ile (12.77 min), *D*-allo-Thr (14.77 min)], and *L*-Phe (13.94 min).

Amino Acid Analysis by Chiral GC. Compound **96** (200 μg) was hydrolyzed with 6 N HCl (1 mL) at 110 °C for 24 h. After drying the reaction mixture under a stream of N_2, the amino acid hydrolysate was heated with acetyl chloride (150 μL) and *i*PrOH (500 μL) at 100 °C for 45 min. The mixture was dried under N_2 and the residue was treated with pentafluoropropionic anhydride (1 mL) in CH_2Cl_2 (2 mL) at 100 °C for 15 min. After 15 min the excess reagent was evaporated with N_2 and the mixture of derivatized amino acids in CH_2Cl_2 was analyzed by GC-MS using an Alltech Capillary Chirasil-Val column (25 m × 0.25 mm; the program rate: 70-180 °C at 4 °C/min). The retention times for the *N*-pentafluoropropionyl isopropyl ester derivatives of the amino acids from compound **96** were at 6.26 min (*L*-Thr), 8.15 min (*L*-Ile), 11.02 min (*L*-Pro), 19.34 min (*L*-Phe).

Interconversion of *Cis,cis*-ceratospongamide (96) to *Trans,trans*-ceratospongamide (97). Compound **96** (1.5 mg, 1.95 μmole) was dissolved in 1.5 mL of DMSO in a vial and heated to 175 °C. After 30 min, the DMSO was removed *in vacuo* and the residue dissolved in MeOH. This was analyzed for the presence of the *trans,trans* isomer (**97**) using gradient HPLC under two different reversed-phase HPLC conditions with a photodiode array detector: a) Phenomenex Phenosphere 10 C_8 90A, 40% MeOH in water to 100% MeOH over 60 min, 1.5 mL/min [standard *cis,cis*-

ceratospongamide (16.93 min), standard *trans,trans*-ceratospongamide (18.01 min), detected *trans,trans*-ceratospongamide (17.98 min)]; b) Phenomenex Sphereclone 5μ ODS (2), 30% MeOH in water to 100% MeOH over 40 min, 2.4 mL/min [standard *cis,cis*-ceratospongamide (6.12 min), standard *trans,trans*-ceratospongamide (8.56 min), detected *trans,trans*-ceratospongamide (8.55 min)].

Drug Screening. Hepatocellular carcinoma cells (ATCC HB-8065) were prepared for drug screening by plating at 2×10^5/mL into 24-well tissue culture plates. After 24 h, the medium in each of the 24 wells was replaced with 1 mL of serum free media. After a 1 h drug incubation (1% DMSO), the media in each of the drug treatment wells was replaced with minimal essential media containing 10% FBS , earle's salts, non-essential amino acids, and 400 pg/mL IL-1β (Genzyme, #80-3542-01). The cells were then incubated for 24 h. At the end of the IL-1β treatment, the cells were examined by light microscopy for signs of cytotoxicity. The conditioned media was frozen at –20 °C for further analysis by $sPLA_2$ ELISA.

Cellular Transfection. Cells and reporter plasmids were prepared as described elsewhere[114] (Reporter plasmids graciously provided by Dr. Jean Luc Olivier, *Laboratoire de Biochimie, Université Pierre et Marie Curie, Paris, France*). IL-1β was used as the proinflammatory cytokine for these studies rather than IL-6.

CAT and $sPLA_2$ ELISA. Human secreted-PLA_2 ELISA was completed as described elsewhere[133] (PLA_2 antibodies graciously provided by Dr. Lisa Marshall, SmithKline Beecham Pharmaceuticals, Department of Immunopharmacology, King of Prussia, PA). The expression level of reporter plasmids containing the chloramphenical acetyl transferase gene were quantified using a commercially available ELISA (Boehringer Mannheim, #1363727). Color development was measured at 490 nm on a Molecular Devices Vmax plate reader. The data were analyzed using Softmax™ software.

Computer Modeling. *Cis,cis*- (**96**) and *trans,trans*-ceratospongamide (**97**) were refined by geometry optimization using the CVFF forcefield for peptides and proteins[134] as implemented in the Discover subroutine of Insight II (MSI/Biosym, San Diego, CA) molecular modeling package. The models were initially refined with 100 rounds of steepest gradient and then further refined with conjugate gradient. ROESY correlations

between protons on separate residues (Tables II.1 and II.2) were used in energy minimization calculations by limiting their interatomic distances to within 5 Å. A Silicon Graphics Iris platform (OS Irix 6.3) was used to perform these calculations.

CHAPTER THREE

HERMITAMIDES A AND B, TOXIC MALYNGAMIDE-TYPE NATURAL PRODUCTS FROM THE MARINE CYANOBACTERIUM *LYNGBYA MAJUSCULA* GOMONT

ABSTRACT

A Papua New Guinea collection of the marine cyanobacterium *Lyngbya majuscula* yielded two new and toxic natural products, hermitamides A (**123**) and B (**124**). The hermitamides were isolated using a brine shrimp (*Artemia salina*) toxicity assay. Planar chemical structures of **123** and **124** were established through 1D and 2D NMR, as well as FABMS data. Three different coupling methods for the semi-syntheses of the hermitamides were explored. Good yields of **123** and **124** were achieved by coupling the acid chloride derivative of 7(*S*)-methoxytetradec-4(*E*)-enoic acid (**98b**), obtained from the same cyanobacterium collection, and the respective free amines, phenethylamine and tryptamine. The *N*-methylated analogs of the hermitamides (**125** and **126**) were also synthesized using similar methods and their biological activities evaluated using the brine-shrimp toxicity assay. Structure elucidations of these new analogs were determined mainly from FABMS data. Hermitamides A (**123**) and B (**124**) exhibited LD_{50}'s of 5 μM and 18 μM in the brine shrimp bioassay, and IC_{50}'s of 2.2 μM and 5.5 μM to neuro-2a neuroblastoma cells in tissue culture, respectively. Hermitamide A (**123**) was mildly ichthyotoxic to goldfish with an LD_{50} 19 μM while hermitamide B (**124**) was inactive at 25 μM.

INTRODUCTION

Many tropical and sub-tropical shallow-water collections of marine cyanobacteria produce a class of metabolites known as the 'malyngamides'.[136-141] Although there are reports of malyngamides isolated from sea-hares and a red alga, these are considered to be deriving from cyanobacteria, either through diet (e.g. sea-hare grazing on marine microalgae) or from blue-green algae growing epiphytically on the macroalga. To date, more than two-dozen members belonged to this growing class of cyanobacterial metabolites (Figure III.2 and compounds **81** to **83** in chapter one), and they are isolated mainly from *Lyngbya majuscula*. There are two distinct portions present in the malyngamides; a methoxy fatty acid (known trivially as "lyngbic acid') and a variety of functionalized amines, linked through an amide bond. The different lyngbic acids present in the malyngamides are shown in Figure III.1. These lyngbic acids have varying chain lengths, ranging from C-12 to C-20, with a methoxy group at C-7 as well as a *trans* double bond at C-4. A majority of the reported malyngamides contain the C-14 lyngbic acid. The C-16 analog is present in malyngamides D (**105**) and E (**106**), while the C-12 and C-20 analogs are present in malyngamide G (**109**) and the serinol-derived malyngamides (**119** and **120**), respectively. Only the C-12 and C-14 lyngbic acids have been detected in free form from marine cyanobacteria. These lyngbic acids, such as the C-12 and C-14 analogs, were the subject of at least three total syntheses.[142-144]

The biological activities reported for these intriguing malyngamides are at best modest (1-50 μM range) and these are summarized in Table III.1. Given the relative abundance and high frequencies of these metabolites in nature, it is uncertain if the true biological target of these molecules has yet been defined. The types of biological activities reported for the malyngamides include antifeedant activity (malyngamide A, **81**),[155] ichthyotoxicity (malyngamide H, **110**),[144] brine shrimp toxicity (malyngamides J, **112** and L, **104**),[146] cytotoxicity to mouse neuroblastoma cells (malyngamides I acetate, **83** and N, **114**),[145,147] and immunosuppressant activity (malyngamide G, **109**)[143] (Table III.1).

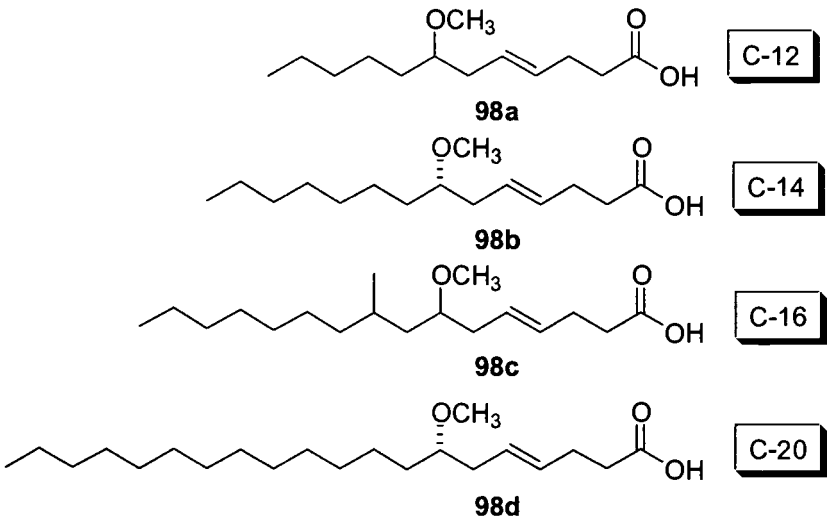

Figure III.1 Lyngbic acids.

Chemical Ecology of the Malyngamides

Of the malyngamides, only malyngamides A (**81**) and B (**82**) have been investigated for their chemical ecology in nature. The first of such studies indicated that malyngamide A (**81**), isolated from the cyanobacterium *Microcoleus lyngbyaceus* (= *Lyngbya majuscula*) has feeding deterrence property when fed to the surgeonfish, *Zebrasoma flavescens*.[155] This study was one of the few experiments showing secondary metabolites as major factors in food preferences of an herbivorous fish. Further studies by Paul and Pennings revealed that malyngamides A (**81**) and B (**82**) were concentrated in the sea-hare, *Stylocheilus longicauda*, by feeding exclusively on *Microcoleus lyngbyaceus*.[93] In addition, the sequestered malyngamide B (**82**) was converted to its acetate derivative in the animal.[93] An acetate derivative of malyngamide I (= stylocheilamide) (**83**) has also been reported in collections of *S. longicauda*.[94] Such diet-derived metabolites have been suggested to play chemical defense roles in the sea-hare. However, the location of the malyngamides within the sea-hare was found to be almost exclusively in the internal organs, e.g. the digestive gland, rather than exterior parts of the animal which are the optimal location for chemical defense.[156]

Additional dietary preference studies on the sea-hare, *S. longicauda*, showed increased feeding when malyngamides A (**81**) and B (**82**) were present in low concentrations and inhibited feeding at higher concentrations in collections of *Lyngbya majuscula* from Guam.[157] This study concluded that dietary selection of blue-green algae by the sea-hare is regulated by the concentration of specific chemical signals produced by *L. majuscula*. Post-ingestive consequences of consumed malyngamides in sea-hares were also investigated and showed that malyngamide B (**82**) has significant effects in reducing growth of *Aplysia juliana* by over 70% as compared with control animals.[158]

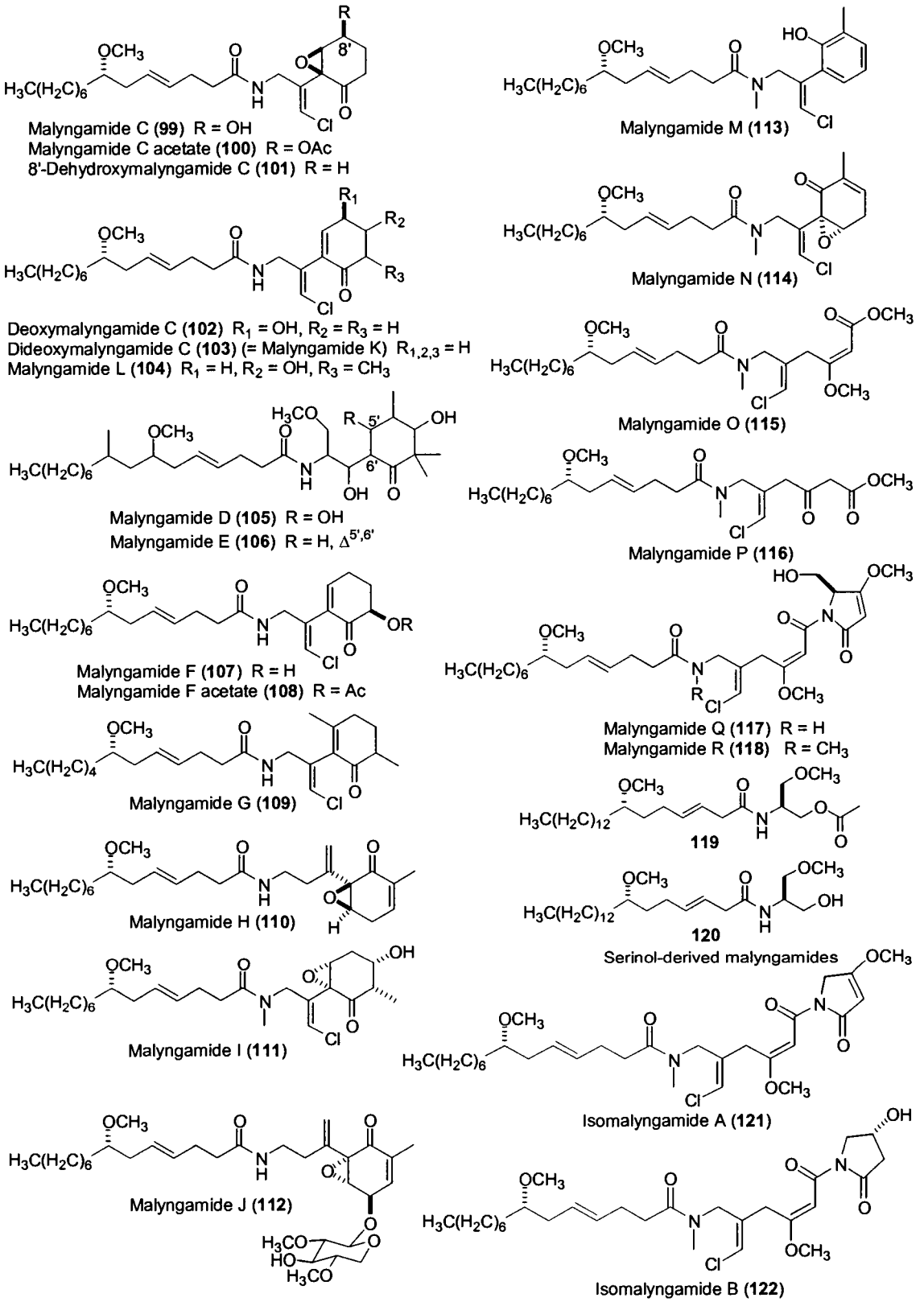

Figure III.2 Malyngamides from marine cyanobacteria.

Table III.1 Biological activities of the malyngamides.

Malyngamides	Biological Activities	Species
A (**81**)	Antifeedant	*L. majuscula*
B (**82**)	Growth reduction of *Aplysia juliana*	*L. majuscula*
F (**107**)	Mild cytotoxic to KB cells (ID_{50} < 30 μg/ml)	*L. majuscula*
F acetate (**108**)	slight activity to *Staphylococcus aureus*	*L. majuscula*
G (**109**)	Immunosuppressive activity (ED_{50} = 6 μg/mL on culture cells with concanavaline K and LPS)	*L. majuscula*
H (**110**)	Ichthyotoxic to goldfish (LC_{50} = 5 μg /mL, EC_{50} = 2 μg /mL)	*L. majuscula*
I (**111**)	Toxic to brine shrimp (LD_{50} = 35 μg /mL) Ichthyotoxic to goldfish (LD_{50} < 10 μg /mL)	*L. majuscula*
I acetate (**83**)	Moderate cytotoxic to NB cells (IC_{50} = 12 μM)	*Gracilaria coronopifolia*
J (**112**)	Toxic to brine shrimp (LD_{50} = 18 μg /mL) Ichthyotoxic to goldfish (LD_{50} = 40 μg /mL)	*L. majuscula*
K (**103**)	Toxic to brine shrimp (LD_{50} = 6 μg /mL) Ichthyotoxic to goldfish (LD_{50} = 7 μg /mL)	*L. majuscula*
L (**104**)	Toxic to brine shrimp (LD_{50} = 8 μg /mL) Ichthyotoxic to goldfish (LD_{50} = 15 μg /mL)	*L. majuscula*
M (**113**)	Weak cytotoxic to NB cells (IC_{50} > 20 μM)	*G. coronopifolia*
N (**114**)	Moderate cytotoxic to NB cells (IC_{50} = 12 μM)	*G. coronopifolia*
O (**115**)	Cytotoxic to mouse lymphoma (P388), human lung carcinoma (A-549), human colon carcinoma (HT-29) (IC_{50} = 2 μg/mL)	*Stylocheilus longicauda*
R (**118**)	Toxic to brine shrimp (LD_{50} = 18 ppm)	*L. majuscula*
Isomalyngamide A (**121**)	lethal to crayfish (*Procambarus clarkii*) (IC_{50} = 250 μg/kg)	*L. majuscula*
Isomalyngamide B (**122**)	lethal to crayfish (*Procambarus clarkii*) (IC_{50} = 500 μg/kg)	*L. majuscula*
Serinols (**119** & **120**)	weak antiHIV activity	*L. majuscula*

RESULTS AND DISCUSSION

In our continued search for pharmaceutically-useful agents from marine cyanobacteria, we have isolated two new malyngamide-type secondary metabolites, hermitamides A (**123**) and B (**124**), from *Lyngbya majuscula* collected from coral reefs at Hermit Island Village, Papua New Guinea. Preliminary bioassay of the organic extract showed activity in the brine shrimp and the mouse neuroblastoma cell toxicity assays at 10 ppm. Guided by the brine shrimp toxicity assay, the natural products **123** and **124** were isolated as pale yellow oils using vacuum liquid chromatography and HPLC.

Hermitamide A (**123**) showed a $[M + H]^+$ peak at *m/z* 360.2910 for a molecular formula of $C_{23}H_{37}NO_2$ by high resolution FABMS of **123** (6° unsaturation). The presence of a methoxy group in **123** was revealed by a diagnostic loss in the LR FABMS ($[M–OCH_3]^+$ peak at *m/z* 328). Structure elucidation of **123** was established mainly from analysis of 1D [^{1}H NMR, ^{13}C NMR, and DEPT] and 2D NMR spectra [COSY, HSQC, and HMBC]. The ^{1}H NMR spectrum of **123** was indicative of a malyngamide-type metabolite, especially in its presence of proton signals attributable to the "fatty acid" portion. These included an $–OCH_3$ singlet signal at δ 3.18 (H_3-15), olefinic signals at δ 5.47 (H-4) and δ 5.51 (H-5), an α-methoxy methine multiplet at δ 3.08 (H-7), protons of a long aliphatic chain in the δ 1.20–δ 1.60 envelope, and a terminal $–CH_3$ triplet signal at δ 0.90 (Table III.2).

In addition, a phenyl moiety could be deduced from five low-field proton signals between δ 6.90 and δ 7.20 in the ^{1}H NMR spectrum. This grouping was confirmed by ^{13}C NMR in which carbon signals at δ 140.1 (C-3'), δ 129.5 (C-4'/8'), δ 129.1 (C-5'/7'), and δ 126.9 (C-6') were observed. The remaining degrees of unsaturation were accounted for by an amide carbonyl (δ 171.4; IR absorption at 1644 cm^{-1}) and an olefin (δ 131.9 and 128.1), both present in the methoxy fatty acid portion of **123**. Placement of the methoxy group at C-7 was in part confirmed by an HMBC correlation between the $–OCH_3$ proton signal (δ 3.18) and the C-7 (δ 81.2) carbon signal. The geometry of the

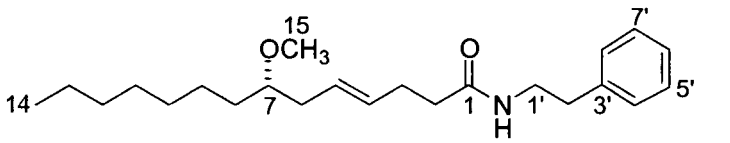

Hermitamide A (**123**)

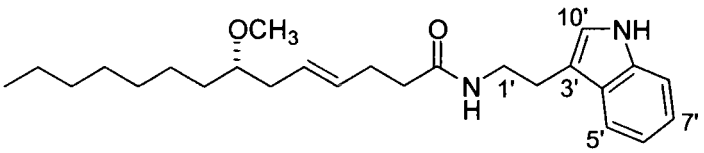

Hermitamide B (**124**)

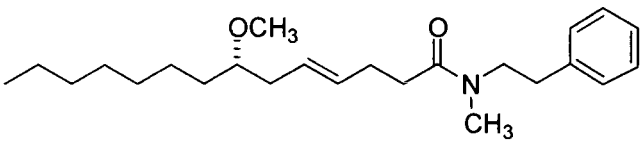

N-Methyl-hermitamide A (**125**)

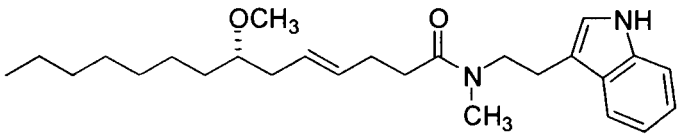

N-Methyl-hermitamide B (**126**)

Figure III.3 New and semi-synthetic hermitamides.

olefin group at C-4 and C-5 was determined as *E* based on a $^3J_{H4\text{-}H5}$ = 15.3 Hz when the ^{1}H NMR of **123** was measured in C_6D_6.

The phenethylamine moiety of **123** was established by analysis of COSY and HMBC spectral data. In the COSY spectrum, the methylene protons at δ 3.29 (H_2-1') showed only two proton correlations, one to an amide proton at δ 4.58 and the second to a high field methylene proton band at δ 2.56 (H_2-2'). The placement of the phenyl group at C-2' (δ 36.5) was revealed by an HMBC correlation from H_2-2' (δ 2.56) to C-3' (δ 140.1). Finally, a correlation from H_2-1' to the amide carbonyl signal at δ 171.4 (C-1) established the placement of the phenethylamine moiety as shown in **123**.

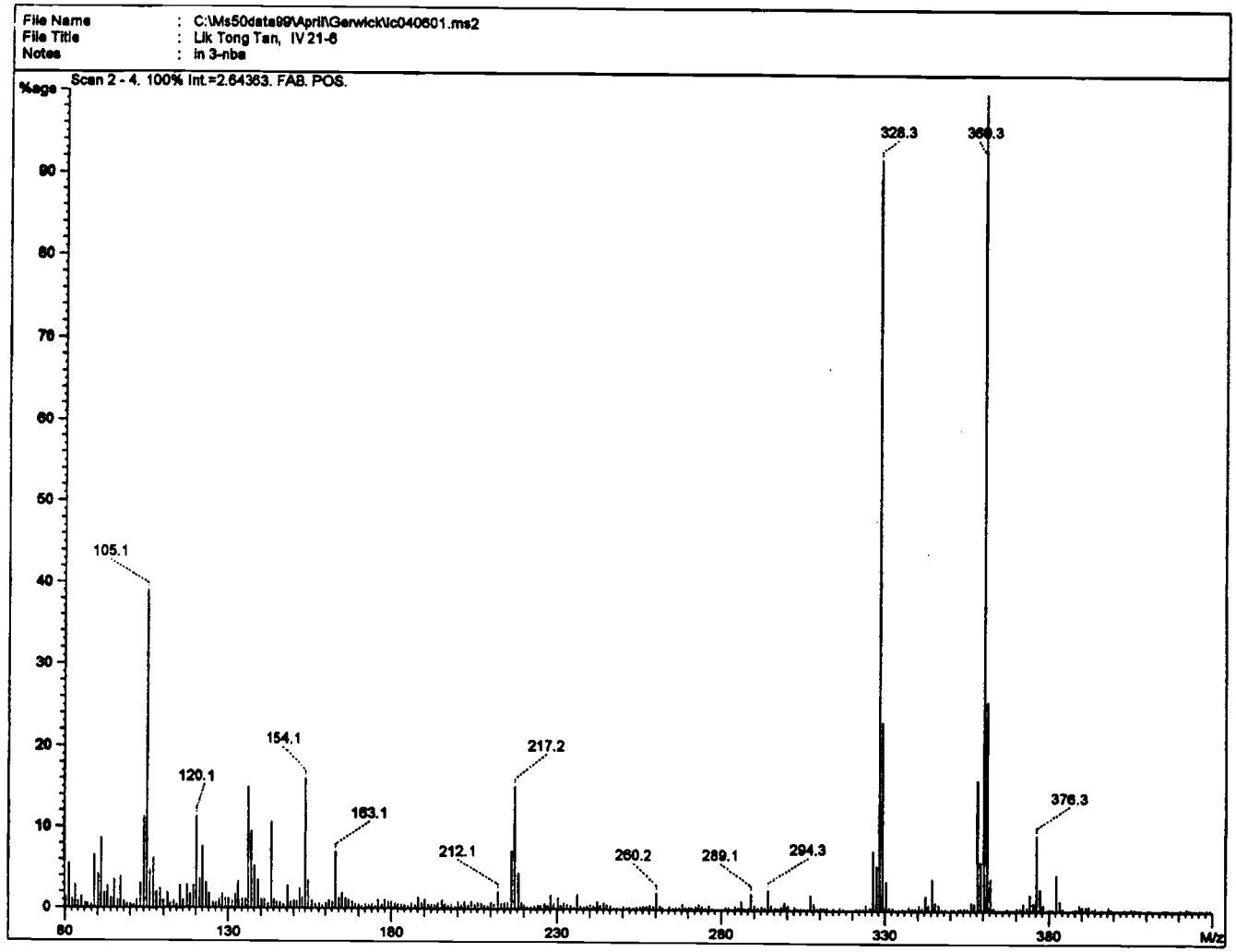

Figure III.4 LR FABMS spectrum of hermitamide A (**123**).

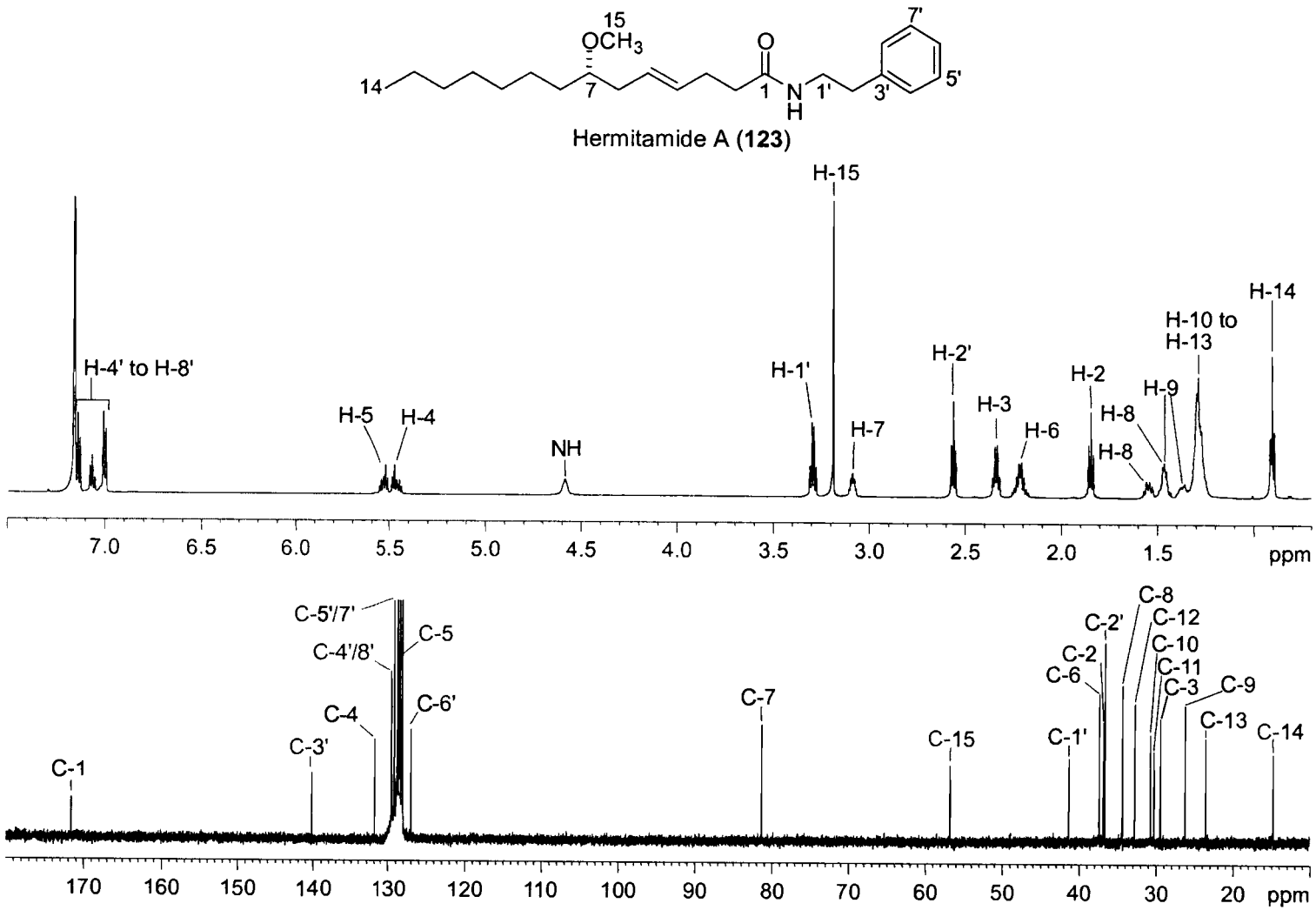

Figure III.5 1D NMR spectra of hermitamide A (**123**) in C_6D_6.

Table III.2 ^{1}H and ^{13}C NMR data for hermitamide A (**123**) in C_6D_6.[a]

Position	^{1}H mult	*J* (Hz)	^{13}C mult	HMBC[b]
1			171.4 s	
2	1.83 t	7.2	36.7 t	C-1, C-3, C-4
3	2.33 dt	7.4, 7.2	29.3 t	C-1, C-2, C-4, C-5
4	5.47 brdt	15.3, 6.4	131.9 d	C-3, C-6
5	5.51 brdt	15.3, 6.9	128.1 d	C-3, C-6
6	2.21 m		37.2 t	C-4, C-5, C-7
7	3.08 m		81.2 d	C-5, C-8, C-9, C-15
8	1.46 m		34.2 t	C-7, C-9, C-10
	1.54 m			C-6, C-7, C-9, C-10
9	1.36 m		26.1 t	C-10
	1.46 m			
10	1.28 m		30.6 t	
11	1.28 m		30.1 t	
12	1.28 m		32.6 t	
13	1.28 m		23.4 t	
14	0.90 t	7.2	14.7 q	C-12, C-13
15 ($-OCH_3$)	3.18 s		56.6 q	C-7
*N*H	4.58 m			
1'	3.29 dd	13.3, 7.0	41.2 t	C-1, C-2', C-3'
2'	2.56 t	7.0	36.5 t	C-1', C-3', C-4'/8'
3'			140.1 s	
4'/8'	6.99 m		129.5 d	C-2', C-6'
5'/7'	7.14 m		129.1 d	C-3'
6'	7.06 m		126.9 d	C-4'/8'

[a] Spectral data reported in ppm (600 MHz). [b] Optimized for 6 Hz.

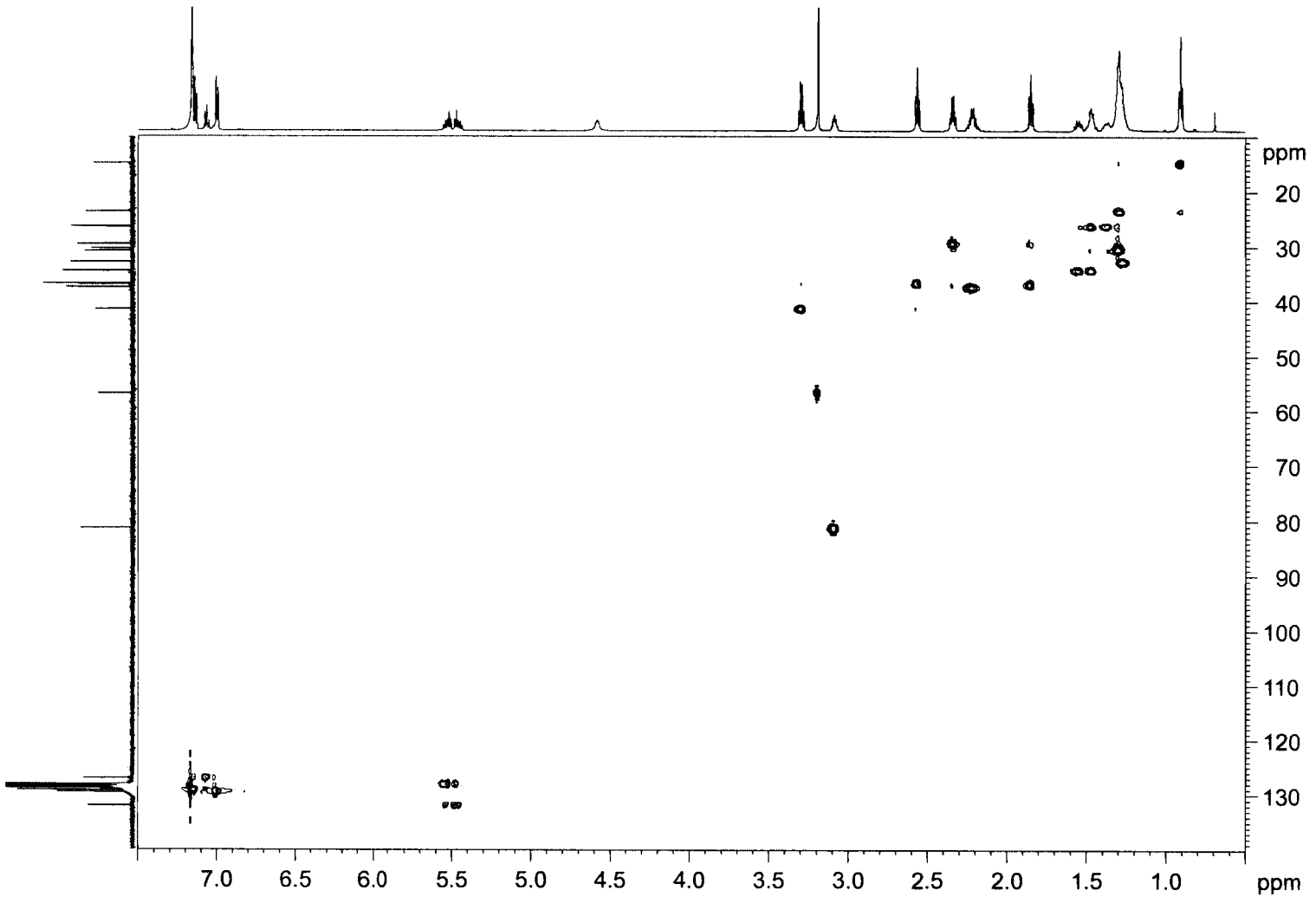

Figure III.6 HSQC spectrum of hermitamide A (**123**) in C_6D_6.

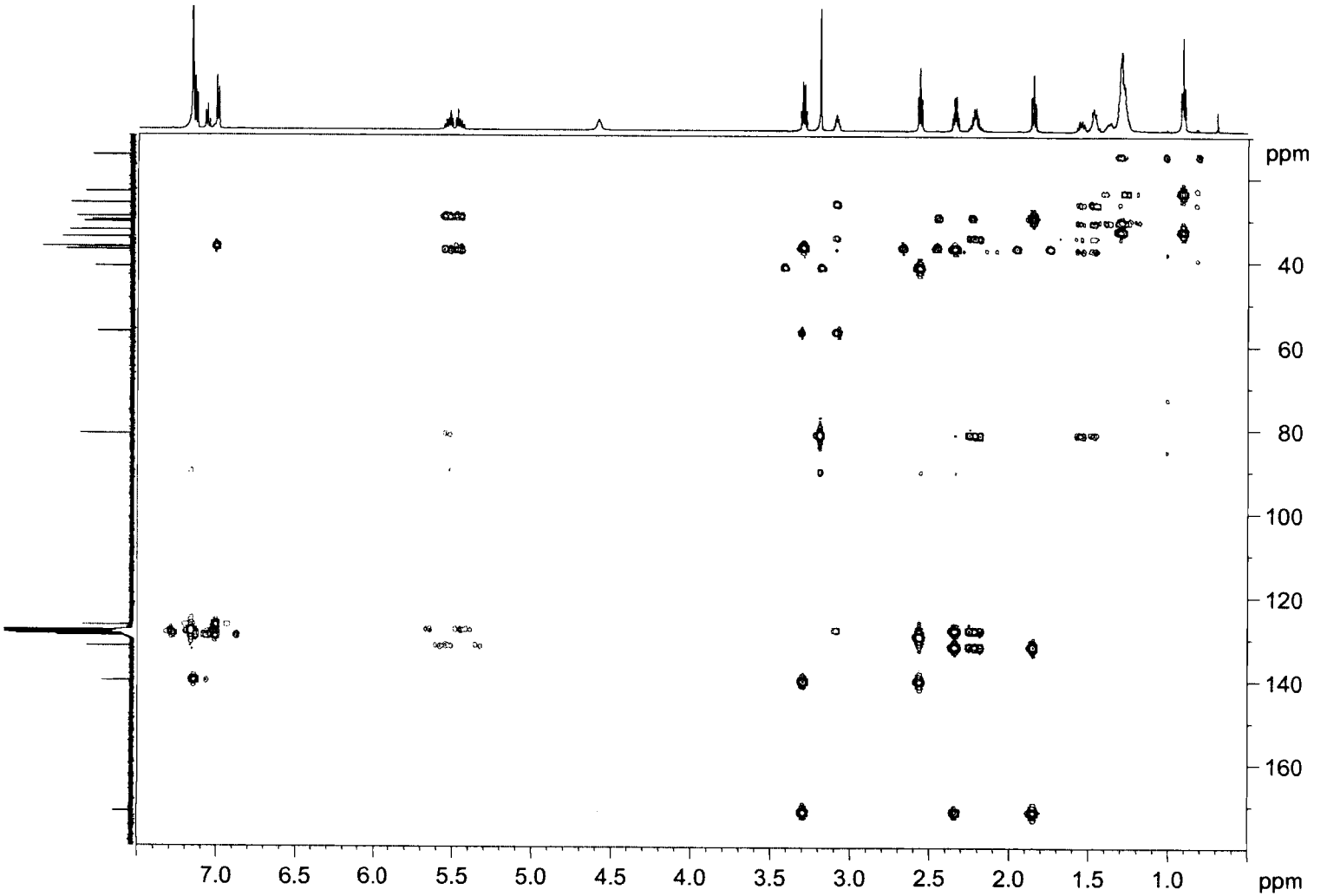

Figure III.7 HMBC spectrum of hermitamide A (**123**) in C_6D_6.

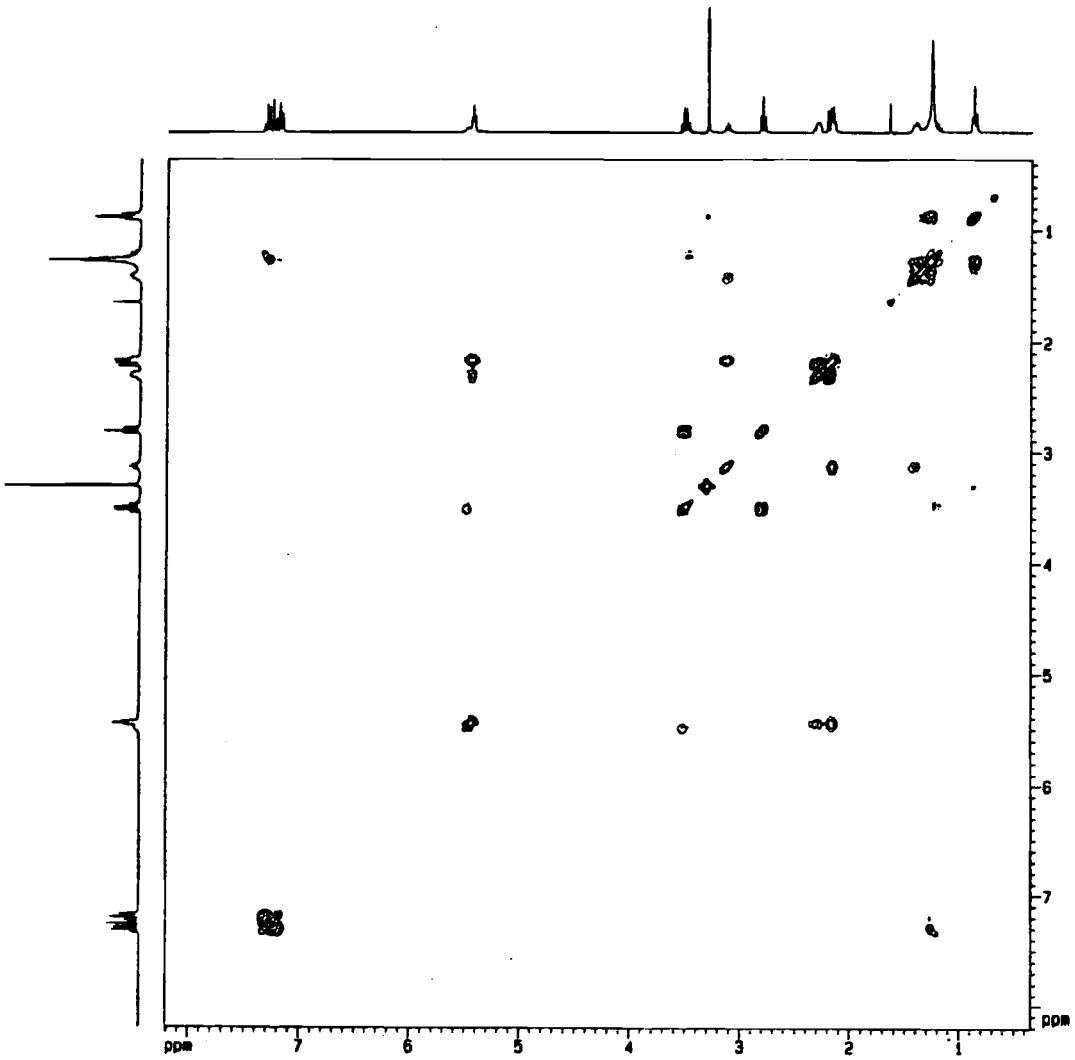

Figure III.8 COSY spectrum of hermitamide A (**123**) in C_6D_6.

High resolution FABMS of hermitamide B (**124**) gave an $[M + H]^+$ peak at 399.3013, yielding a molecular formula of $C_{25}H_{38}N_2O_2$ with eight degrees of unsaturation. In addition, an $[M-OCH_3]^+$ peak at *m/z* 367 was again present in the LR FABMS. As for **123**, the planar chemical structure of **124** was elucidated using an assemblage of 1D and 2D NMR [COSY, TOCSY, HSQC, and HMBC] experiments. The ^{1}H NMR spectrum of compound **124** had several features strikingly similar to that of **123**, mainly in the proton signals attributable to the methoxy fatty acid portion of the molecule.

The main differences between compounds **123** and **124** were in the low field aromatic proton signals between δ 7.00 and δ 8.20. The indolic moiety of **124** was confirmed through analysis of the low field multiplicity patterns in the ^{1}H NMR [δ 7.60 bd (H-5'), δ 7.37 bd (H-8'), δ 7.02 brd (H-10'), δ 7.20 td (H-7'), and δ 7.12 td (H-6')] as well as correlations in the COSY and TOCSY spectra (Table III.3). For example, the H-5' to H-8' spin system could be traced from ^{1}H-^{1}H correlations in the TOCSY spectrum of **124**. The COSY spectrum of **124** showed cross peaks between H-5' (δ 7.60)/H-6' (δ 7.12) and H-7' (δ 7.20)/H-8' (δ 7.37). In addition, a cross peak was observed between H-10' (δ 7.02) and the indole NH at δ 8.22 in the TOCSY spectrum. The location of the tryptamine functionality in **124** was deduced mainly from HMBC data, which showed correlations from H_2-1' (δ 3.60) and H_2-2' (δ 2.96) to C-3' (δ 113.2) of the indole. Finally, a cross peak between H_2-1' (δ 3.60) and the amide proton (δ 5.55) observed in both the COSY and TOCSY spectra, taken together with a correlation from H_2-1' to the amide carbonyl signal at C-1 (δ 172.6) in the HMBC spectrum, confirmed the location of the tryptamine moiety in **124**.

The absolute stereochemistry at C-7 for hermitamides A (**123**) and B (**124**) was suggested through the isolation of the co-occurring free methoxy acid from the organic extract. The optical rotation value of the isolated 7(*S*)-methoxytetradec-4(*E*)-enoic acid (**3b**) had a close match to the reported value in the literature ($[\alpha]^{26}_D$ −12.5° (*c* = 1.91, $CHCl_3$); lit. $[\alpha]^{26}_D$ −11.1° (*c* = 3.9, $CHCl_3$),[136] suggesting a 7*S* stereochemistry in **123** and **124**. This was confirmed through semi-syntheses of both hermitamides.

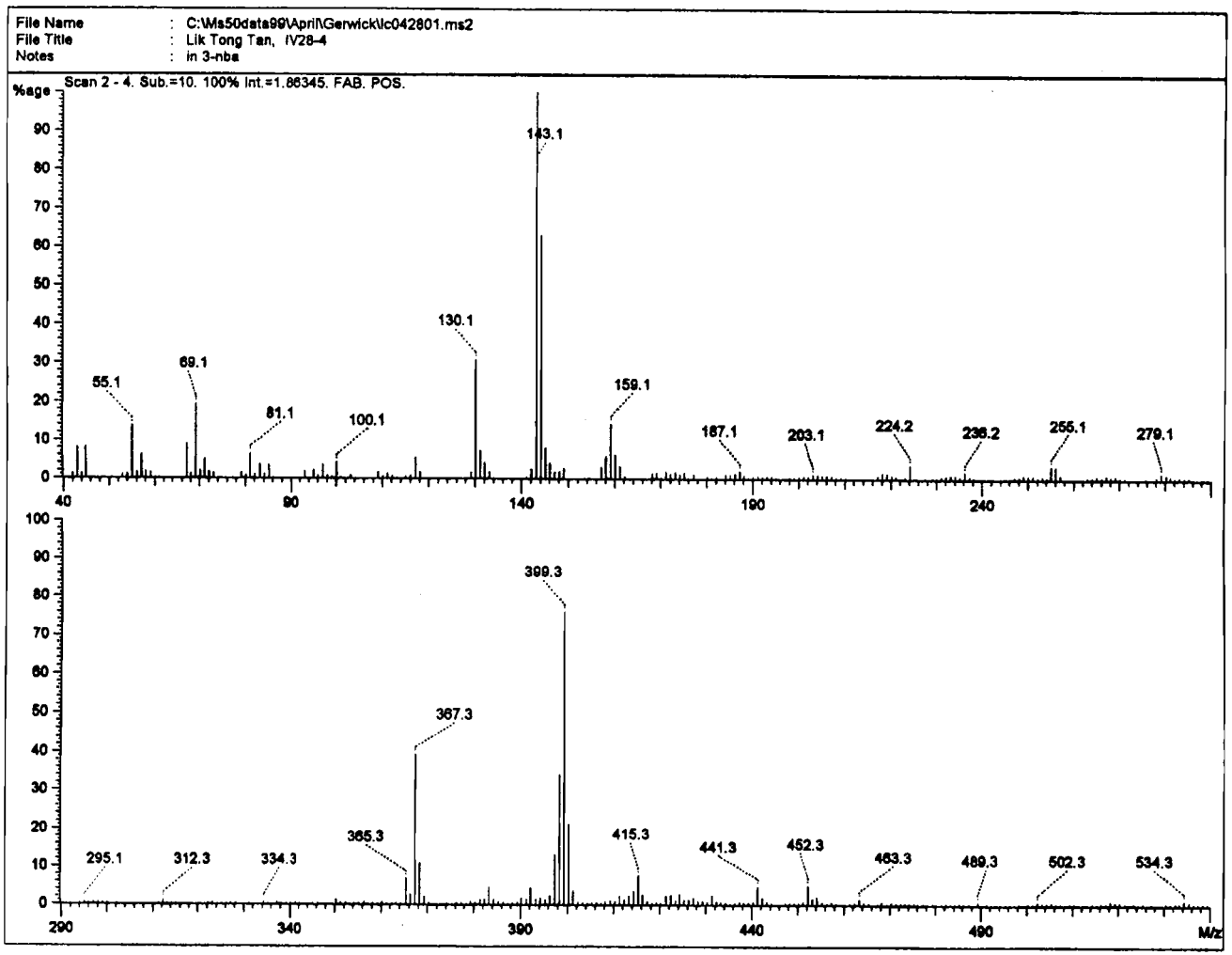

Figure III.9 LR FABMS spectrum of hermitamide B (**124**).

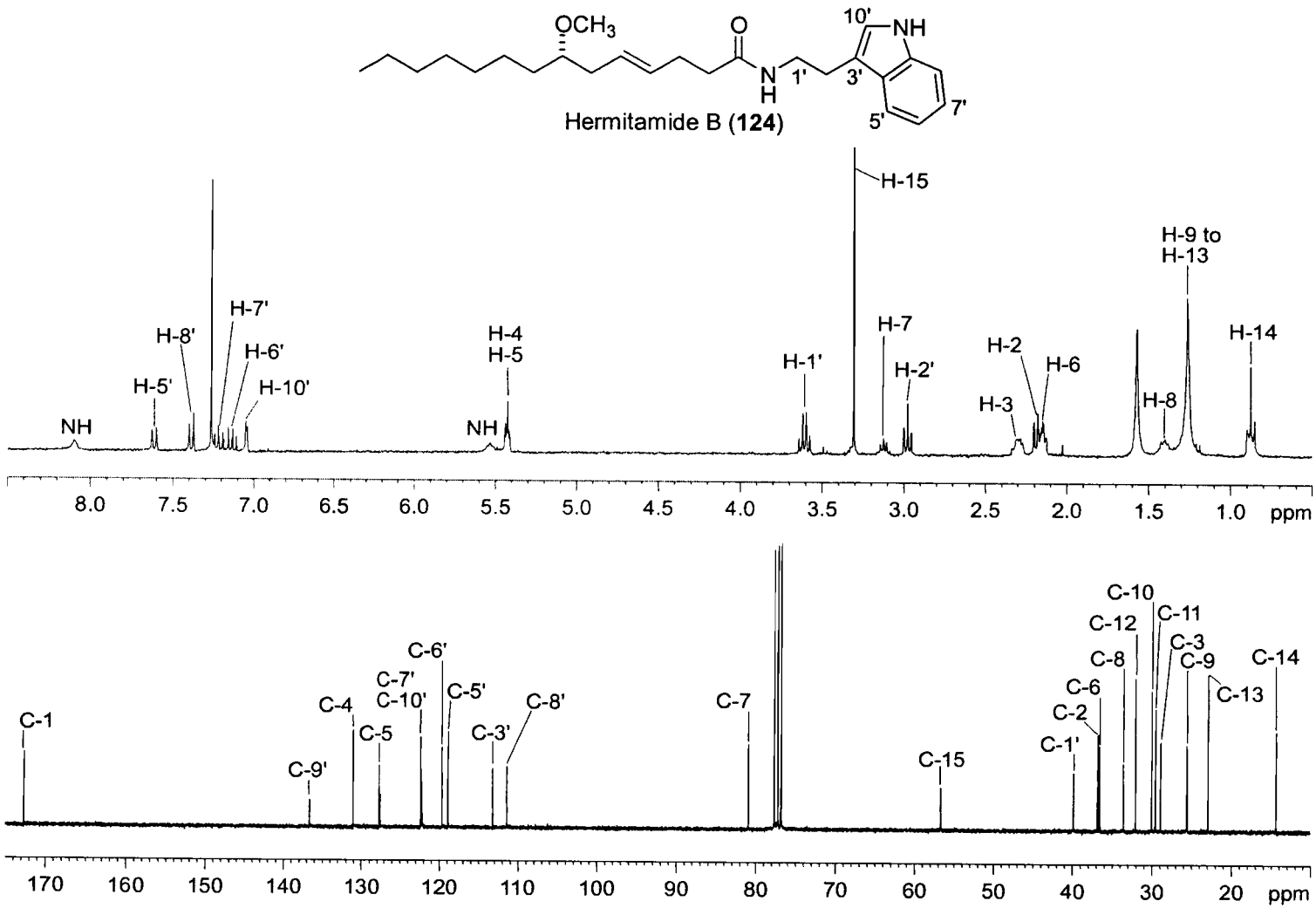

Figure III.10 1D NMR spectra of hermitamide B (**124**) in $CDCl_3$.

Table III.3 ^{1}H and ^{13}C NMR data for hermitamide B **(124)** in $CDCl_3$.[a]

Position	^{1}H mult	*J* (Hz)	^{13}C mult	HMBC[b]
1			172.6 s	
2	2.17 m		36.7 t	C-1, C-3, C-4
3	2.29 m		28.8 t	C-1, C-2, C-4, C-5
4	5.42 m		131.0 d	C-3, C-6
5	5.42 m		127.7 d	C-3, C-6
6	2.14 m		36.5 t	C-4, C-5, C-7
7	3.12 ddd	5.8, 5.6, 5.3	80.9 d	C-5, C-8, C-9, C-15
8	1.40 m		33.5 t	C-7, C-9, C-10
9	1.26 m		25.4 t	
10	1.26 m		29.9 t	
11	1.26 m		29.5 t	
12	1.26 m		32.0 t	
13	1.26 m		22.8 t	
14	0.87 t	6.4	14.3 q	C-12, C-13
15 ($-OCH_3$)	3.30 s		56.6 q	C-7
*N*H	5.55 m			
1'	3.60 dd	12.8, 6.6	39.8 t	C-1, C-2', C-3'
2'	2.96 t	6.6	25.5 t	C-1', C-3', C-4', C-10'
3'			113.2 s	
4'			127.5 s	
5'	7.60 bd	7.9	118.9 d	C-3', C-4', C-6', C-9'
6'	7.12 td	8.0, 1.3	119.4 d	C-4', C-8', C-9'
7'	7.20 td	8.0, 1.3	122.3 d	C-5', C-9'
8'	7.37 bd	8.0	111.4 d	C-4', C-7'
9'			136.6 s	
10'	7.02 brd	2.1	122.2 d	C-2', C-3', C-4'
*N*H	8.22 brs			

[a] Spectral data reported in ppm (600 MHz). [b] Optimized for 6 Hz.

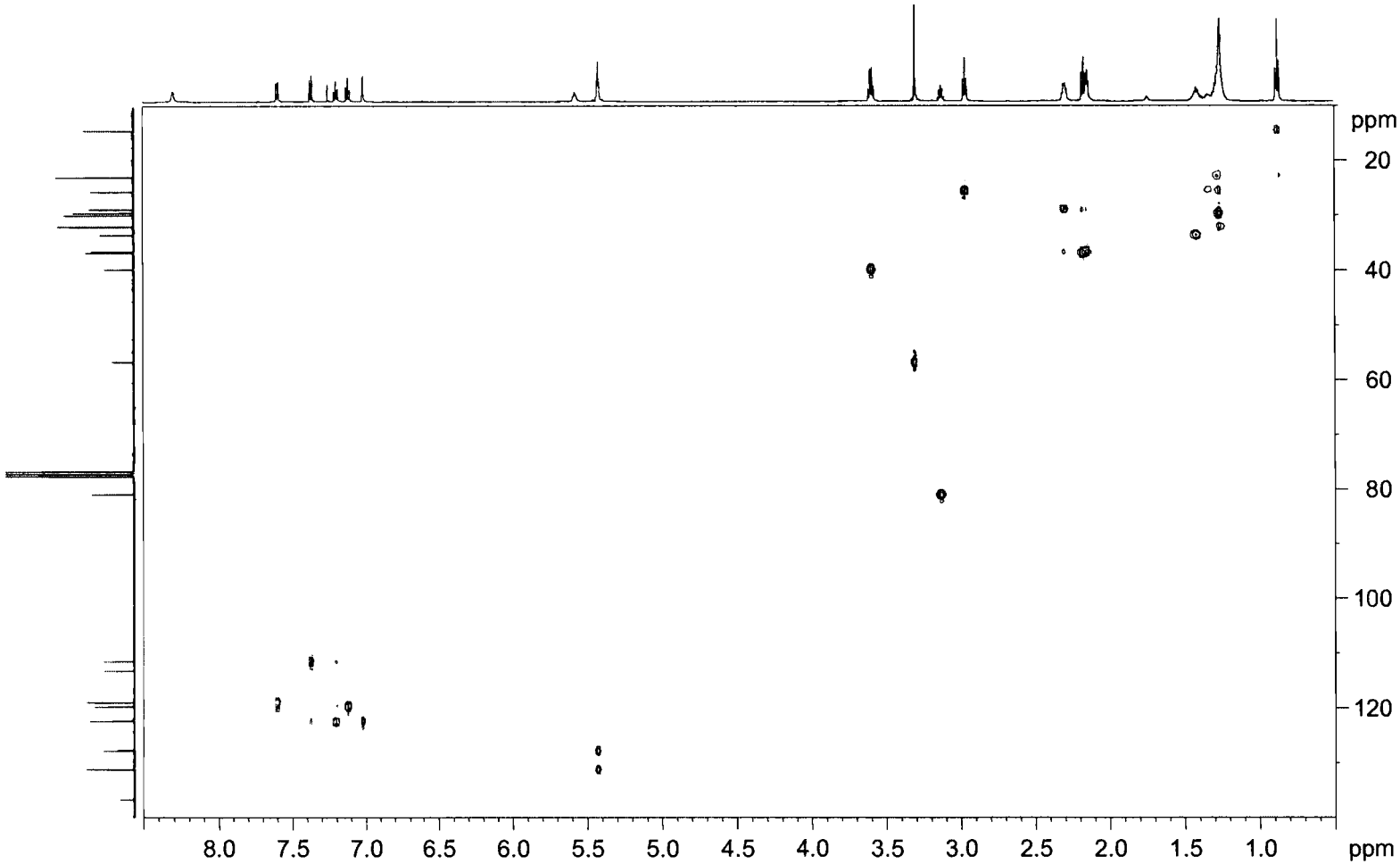

Figure III.11 HSQC spectrum of hermitamide B (**124**) in $CDCl_3$.

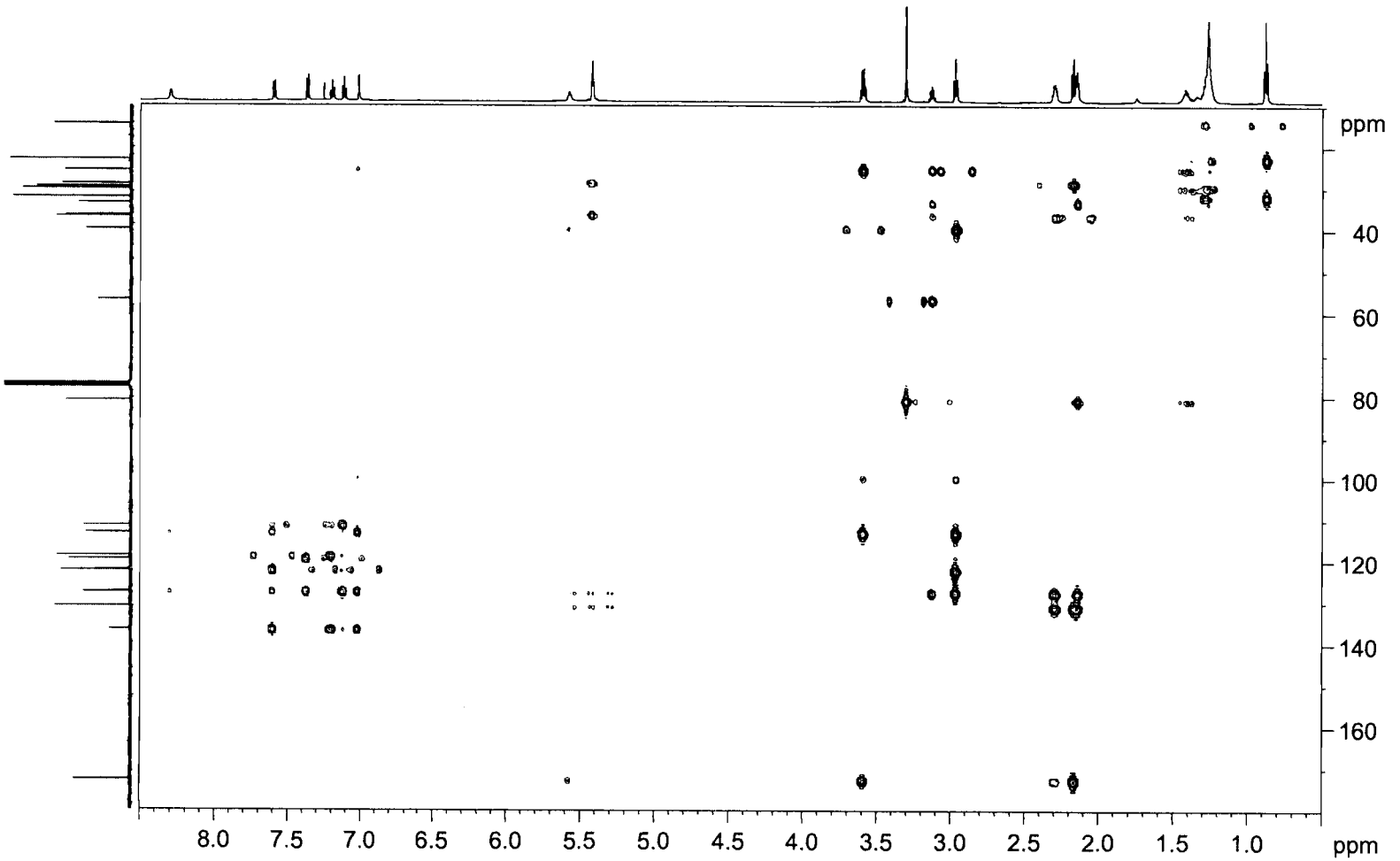

Figure III.12 HMBC spectrum of hermitamide B (**124**) in $CDCl_3$.

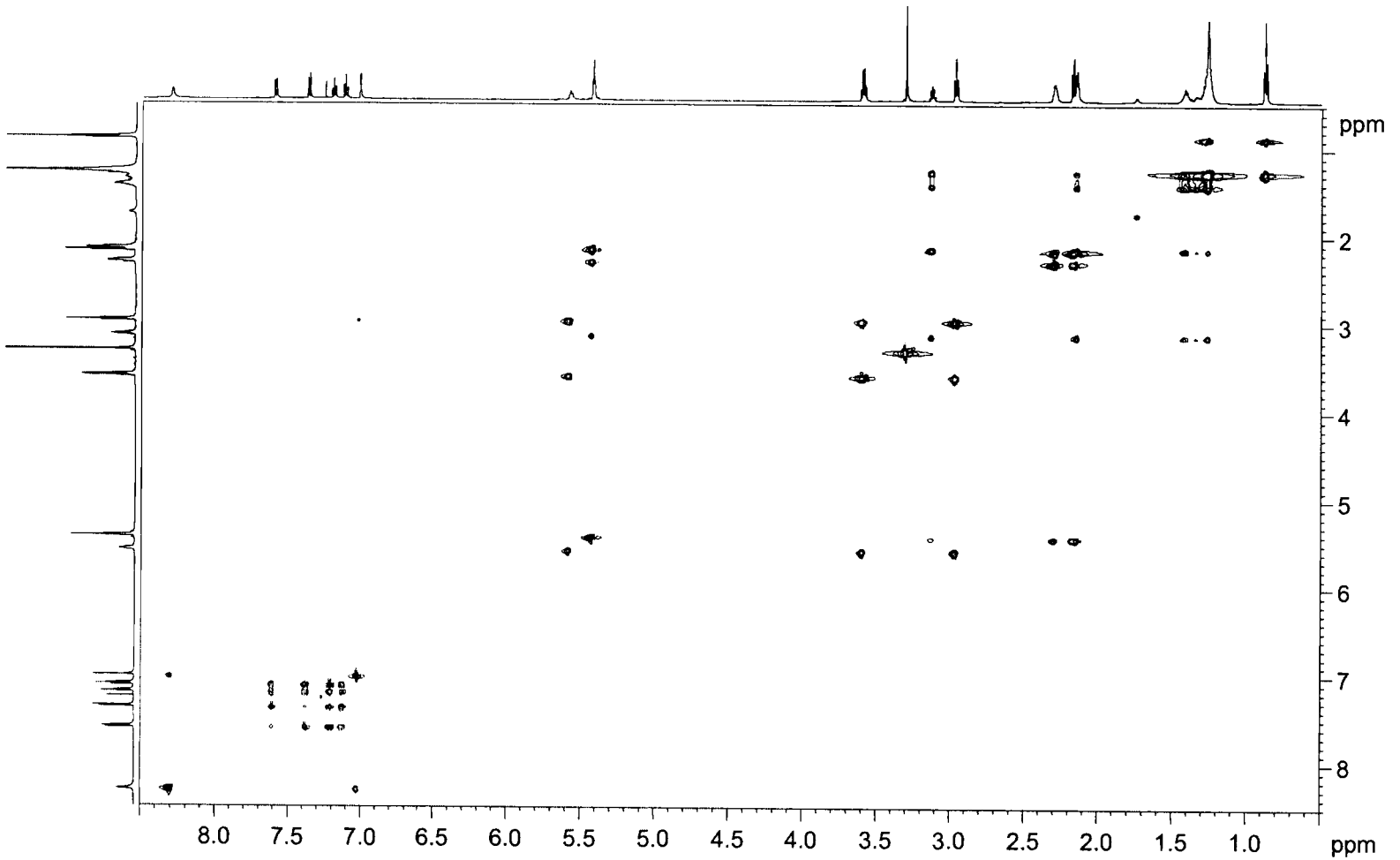

Figure III.13 TOCSY spectrum of hermitamide B (**124**) in $CDCl_3$.

Semi-Syntheses of the Hermitamides and Analogs

7(*S*)-Methoxy fatty acid (**98b**) from *L. majuscula* (PNHV-11 Sep 98-04) was used in the semi-synthesis of hermitamides A (**123**) and B (**124**). Three coupling reaction methods were employed. The first used dicyclohexylcarbodiimide (DCC) to couple 7(*S*)-methoxytetradec-4(*E*)-enoic acid and phenethylamine; however, the yield of product **123** was poor (22%) due to the formation of side products.[159] Improvement of the coupling yield was achieved through conversion of the free acid to the corresponding acid chloride, generated by thionyl chloride, and reacting this with either phenethylamine or tryptamine. A recent report, involving the use of trichloroacetonitrile (TCA) and triphenylphosphine in generating acid chlorides, was also used as a one-pot reaction in the synthesis of hermitamide A (**123**).[160] The reaction of TCA with triphenylphosphine readily generates triarylphosphonium chloride, which can then react with the methoxy acid to produce the acid chloride derivative. The yield from this method is comparable to using thionyl chloride. One dimensional NMR spectra and FABMS of the semi-synthetic compounds produced by these synthetic routes were identical with the natural products **123** and **124**. The optical rotation values were –9.8° (c = 0.50, $CHCl_3$) [natural –6.9° (c = 0.43, $CHCl_3$)] for hermitamide A (**123**) and –8.6° (c = 0.28, $CHCl_3$) [natural –4.5° (c = 0.11, $CHCl_3$)] for hermitamide B (**124**).

The *N*-methyl analogs of the hermitamides were also synthesized through the coupling of the methoxy fatty acid chloride derivative with the respective amines, *N*-Me-tryptamine and *N*-Me-phenethylamine. The ^{1}H NMR spectra of these new analogs were complicated due the existence of conformers imparted by the presence of *N*-methyl amides. High resolution FABMS data were therefore important for structural confirmations of *N*-Me-hermitamides A (**125**) and B (**126**), which gave $[M + H]^+$ peaks at 374.3065 ($C_{24}H_{40}NO_2$) and 413.3171 ($C_{26}H_{41}N_2O_2$), respectively. The $[M–OCH_3]^+$ peaks were also evident in the LR FABMS spectra for *N*-Me-hermitamides A (*m/z* 342) and B (*m/z* 381).

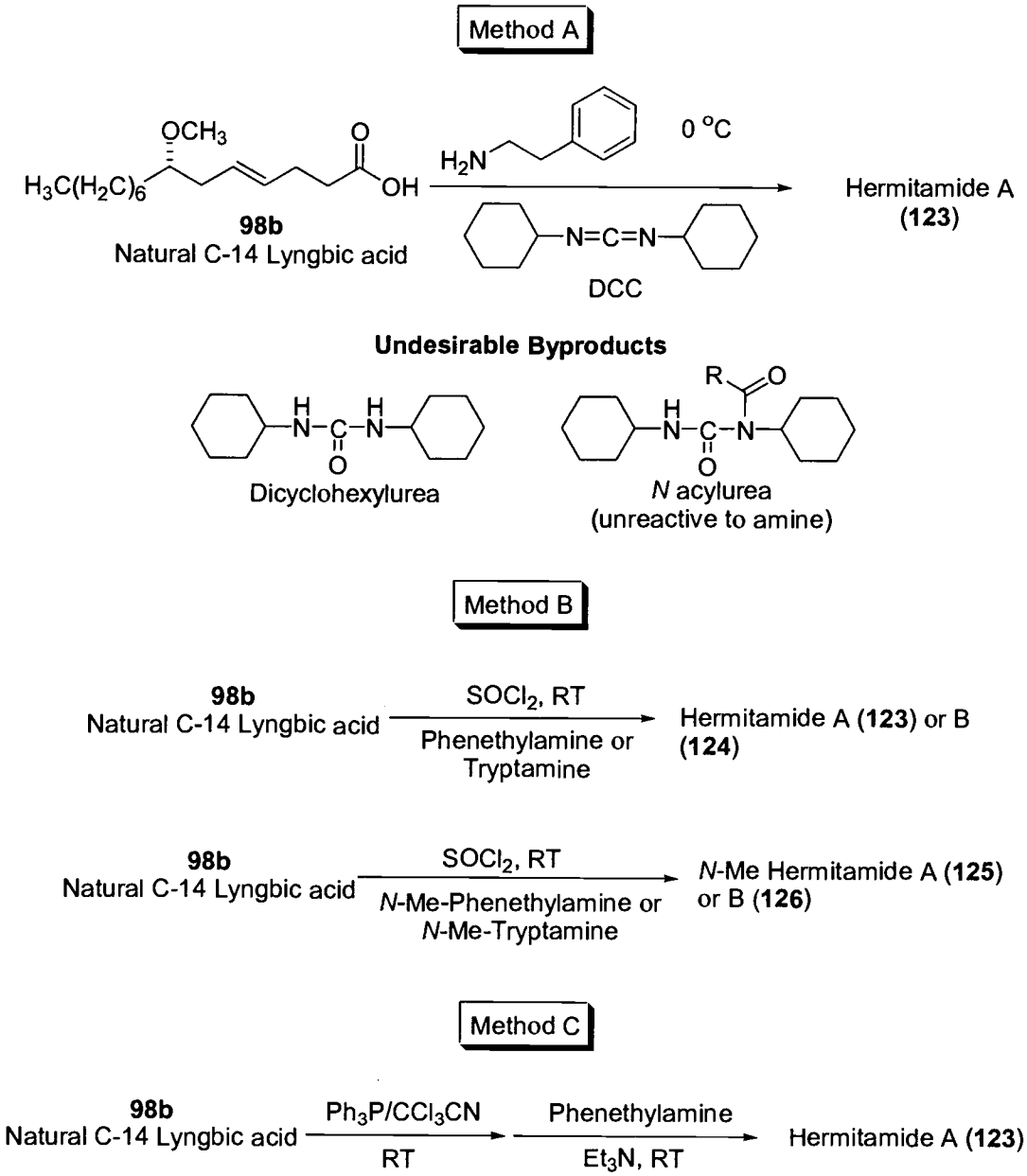

Figure III.14 Methods utilized in the syntheses of the hermitamides (**123** and **124**) and derivatives (**125** and **126**).

Hermitamides A (**123**) and B (**124**) represent interesting examples of aromatized malyngamide-type compounds from the marine cyanobacterium *Lyngbya majuscula*. The first example of an aromatic-ring containing malyngamide, malyngamide M (**113**),

was recently reported by Kan *et al.* from the Hawaiian red alga *Gracilaria coronopifolia*.[147] Since the malyngamides are well known secondary metabolites of marine cyanobacteria, it has been suggested that the true producer of malyngamide M (**113**) is a cyanobacterium growing epiphytically on *Gracilaria coronopifolia*. This is supported by reports of cyanobacteria growing epiphytically on other species of *Gracilaria*.[161]

The hermitamides were evaluated for their biological activity in several systems. In the brine shrimp (*Artemia salina*) toxicity assay, hermitamides A (**123**) and B (**124**) showed LD_{50}'s of 5 μM and 18 μM, respectively. The *N*-methylated analogs (**125** and **126**) also showed comparable LD_{50} values in the brine shrimp toxicity assay (6 and 18 μM, respectively). Hermitamide A (**123**) exhibited modest ichthyotoxicity to goldfish with an LD_{50} of 19 μM, while compound **124** was inactive at 25 μM. Both **123** and **124** were inactive at 10 ppm in a molluscicidal (*Biomphalaria glabrata*) bioassay. The hermitamides were also found to be cytotoxic to neuro-2a neuroblastoma cells in tissue culture with IC_{50}'s of 2.2 μM (A, **123**) and 5.5 μM (B, **124**). By comparison, malyngamide M (**113**) was reported to have only weak cytotoxicity to neuroblastoma cells ($IC_{50} > 20$ μM) while both malyngamides I acetate (**83**) and N (**114**) showed moderate cytotoxicity with IC_{50}'s at 12 μM.[147]

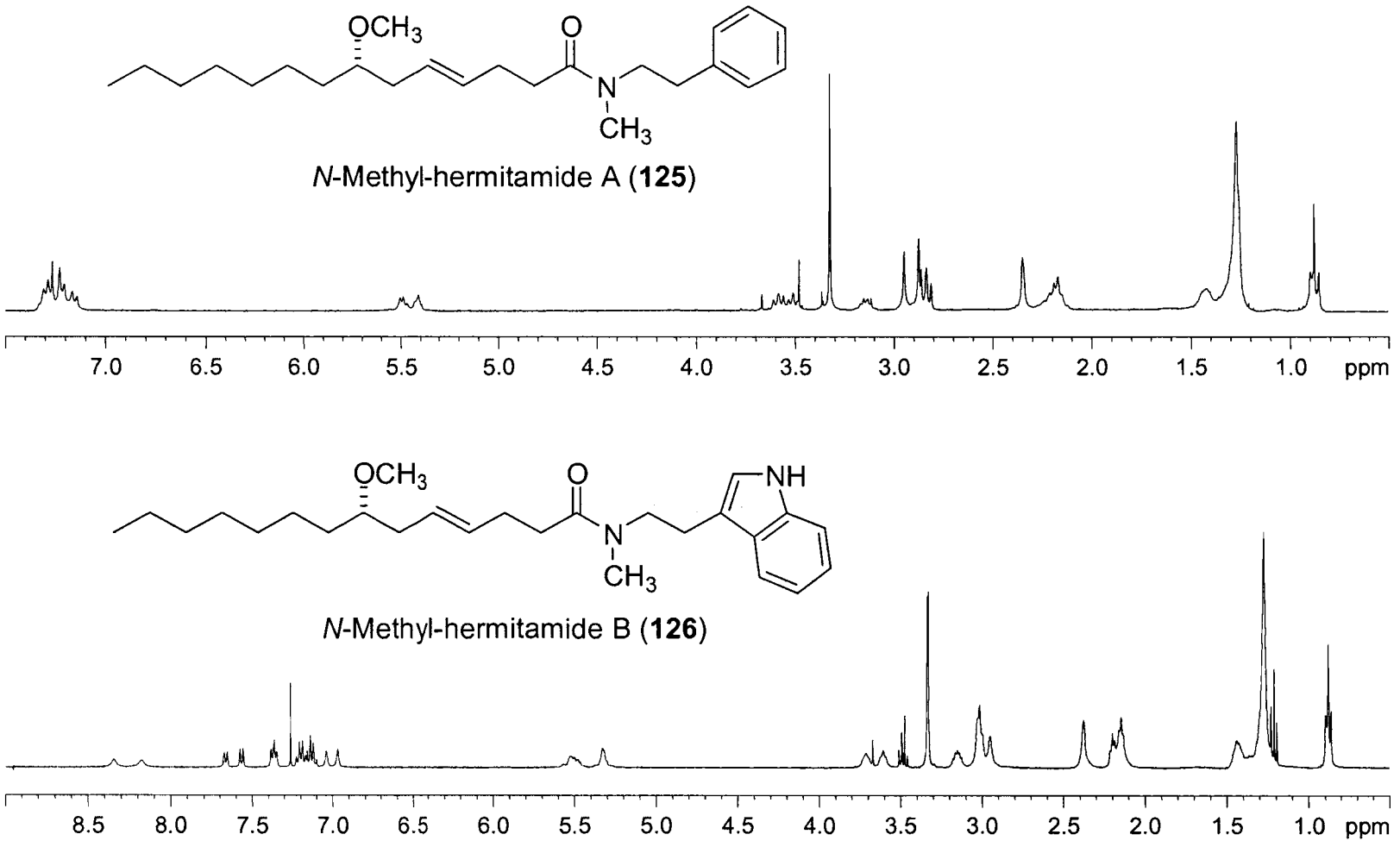

Figure III.15 ^{1}H NMR spectra of *N*-Me-hermitamides A (**125**) and B (**126**) in $CDCl_3$.

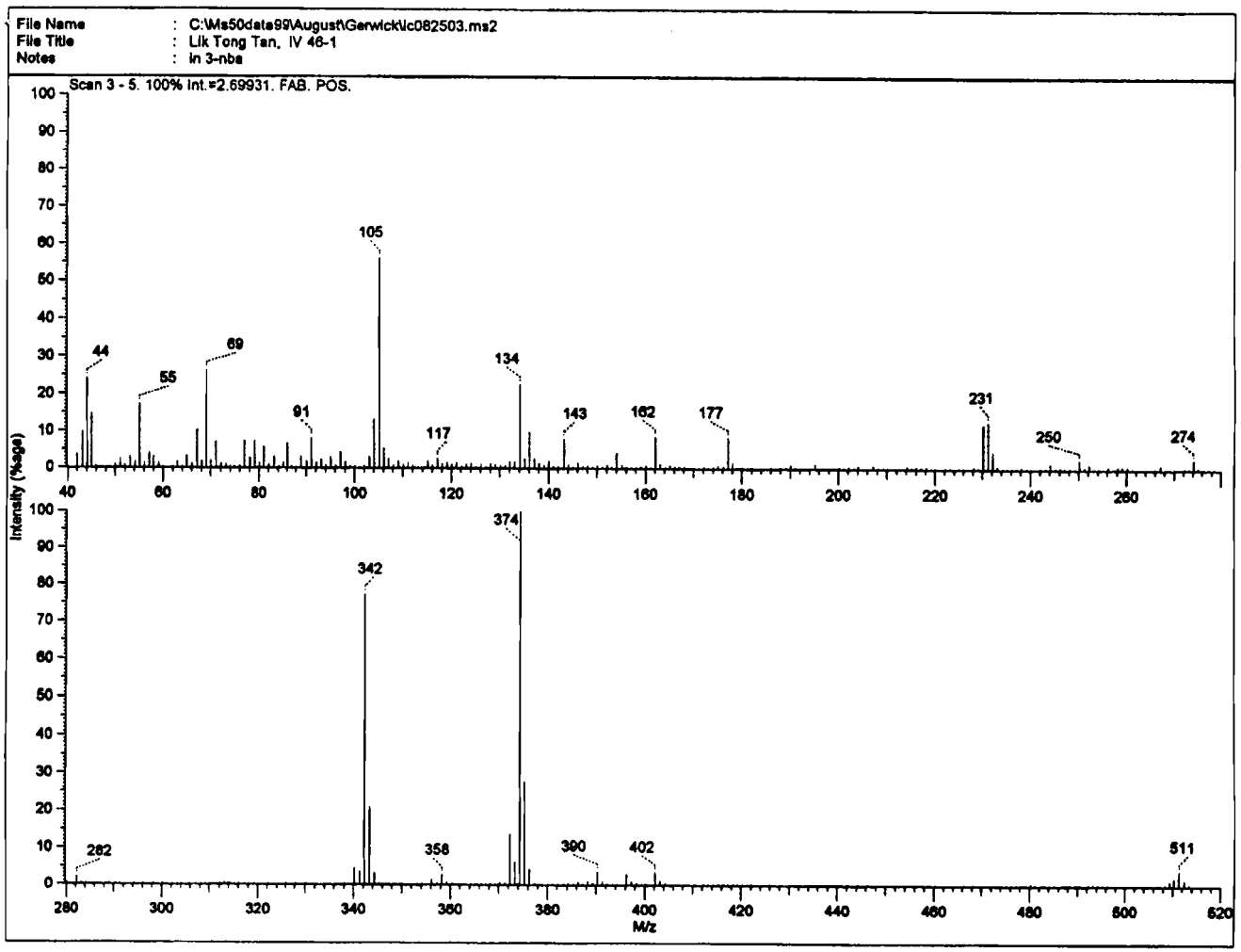

Figure III.16 LR FABMS spectrum of *N*-Me-hermitamide A (**125**).

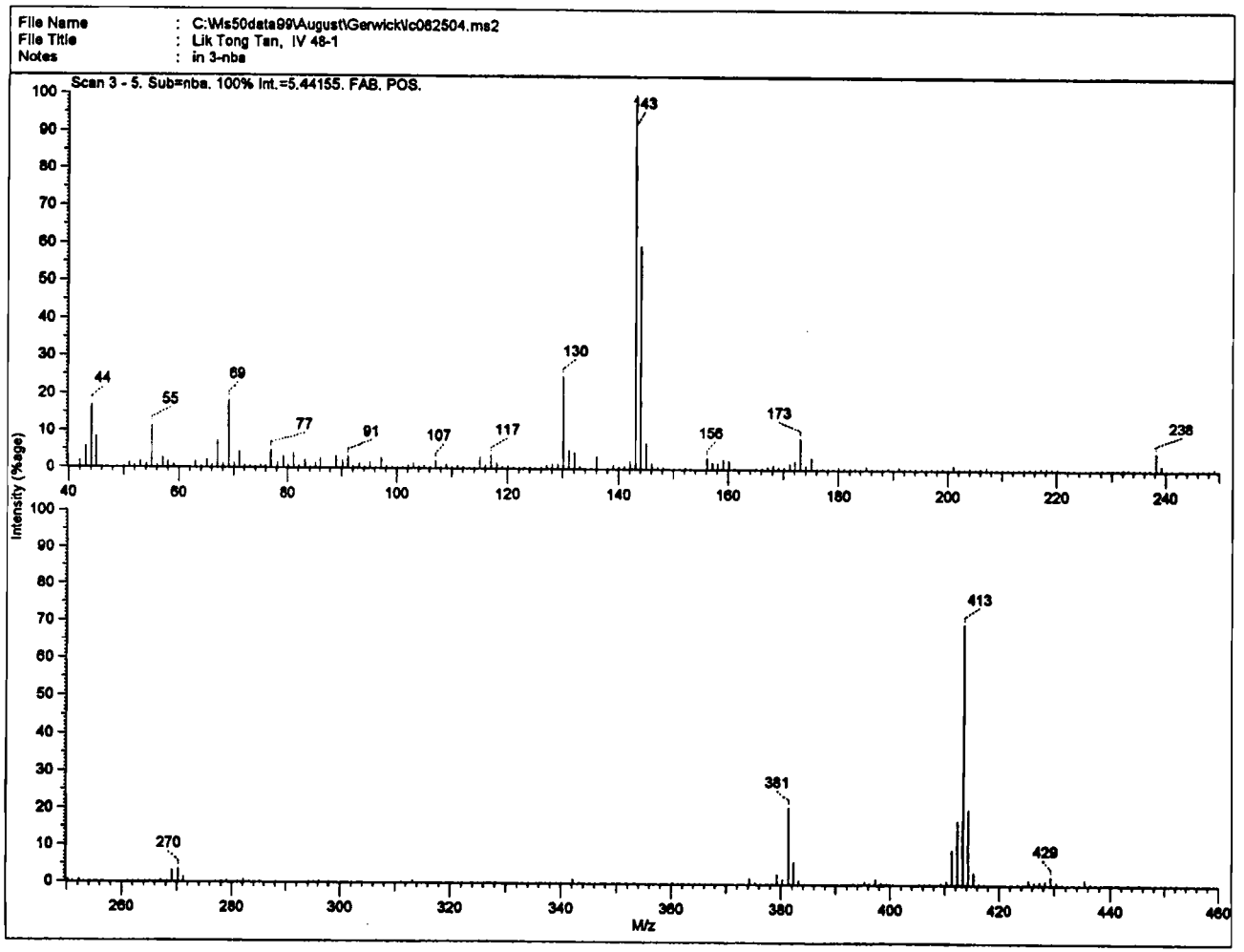

Figure III.17 LR FABMS spectrum of *N*-Me-hermitamide B (**126**).

EXPERIMENTAL

General Experimental Procedures. ^{1}H and ^{13}C NMR spectra were measured on a Bruker DRX 600 MHz NMR spectrometer with the solvent, C_6D_6 or $CDCl_3$, used as an internal standard. High resolution mass spectra were recorded on a Kratos MS50TC mass spectrometer. Optical rotations were measured on a Perkin-Elmer 141 polarimeter. UV and IR spectra were recorded on Hewlett-Packard 8452A UV-VIS and Nicolet 510 spectrophotometers, respectively. Isolation of compounds **123** and **124** were performed using a Waters Millipore® Model 590 Pump and detected with a Waters Millipore® Lambda-Max Model 480 LC spectrophotometer.

Algal Collection. The marine cyanobacterium, *Lyngbya majuscula* (PNHV-11 Sep 98-04), was hand-collected at 8 m water depth using SCUBA from reefs near the Hermit Village Islands (*S* 1° 28.621′, *E* 145° 2.632′), Papua New Guinea on 11 September 1998. The specimens were preserved in isopropyl alcohol upon collection and stored at low temperature until work-up.

Extraction and Isolation of Hermitamides A (123) and B (124) and Free Acid (98b). The thawed algal material was homogenized in CH_2Cl_2/MeOH (2:1, v/v), filtered, and the solvents removed *in vacuo* to yield a residue which was partitioned between CH_2Cl_2 and H_2O. The marc was extracted repeatedly with CH_2Cl_2/MeOH (2:1, v/v) and the combined CH_2Cl_2 layers reduced *in vacuo* to yield about 3.0 g of a dark green extract. The crude extract was fractionated using normal phase silica gel vacuum liquid chromatography (VLC) through a step-wise gradient solvent system of increasing polarity starting from EtOAc in hexanes to EtOAc in MeOH. Fractions eluting with hexanes:EtOAc 3:7, 100% EtOAc, and EtOAc:MeOH 49:1 were combined and found to be the most active at 10 ppm in the brine shrimp toxicity assay. This recombined fraction was refractionated using Mega Bond RP-18 SEP PAK. The most active material (85% toxicity at 1 ppm to brine shrimp) was eluted with 20% H_2O in MeOH and was further purified by HPLC [Phenomenex Sphereclone 5μ ODS (2), MeOH/H_2O (82:18); detection at 254 nm] giving both hermitamides A (**123**, 5.0 mg) and B (**124**, 1.1 mg). 7(*S*)-Methoxytetradec-4(*E*)-enoic acid (**98b**), showing $[\alpha]^{26}_{D}$ –12.5° (c = 1.91, $CHCl_3$) was isolated from fractions eluting from VLC with hexanes:EtOAc (4:1), Mega

Bond RP-18 SEP PAK (10% H_2O in MeOH), and HPLC [Phenomenex Sphereclone 5μ ODS (2), MeOH/H_2O (89:11); detection at 210 nm].

Hermitamide A (123): pale yellow oil; $[\alpha]^{26}_{D}$ –6.9° (c = 0.43, $CHCl_3$); UV (EtOH) λ_{max} 216 nm (ϵ 5700); IR (neat) 3293, 2934, 2855, 1644, 1551, 1453, 1097, 970, 748, 699 cm^{-1}; LR FABMS *m/z* 360 (100), 328 (92), 217 (15), 163 (70), 154 (16), 120 (11), 105 (39); HR FABMS (positive ion, 3-nitrobenzyl alcohol) *m/z* obs. $[M + H]^+$ 360.2910 ($C_{23}H_{38}NO_2$, 0.8 mmu dev.); ^1H NMR (600 MHz, C_6D_6) and ^{13}C NMR (150 MHz, C_6D_6) see Table III.2.

Hermitamide B (124): pale yellow oil; $[\alpha]^{26}_{D}$ –4.5° (c = 0.11, $CHCl_3$); UV (EtOH) λ_{max} 224 nm (ϵ 13600), 282 nm (ϵ 3600), 292 nm (ϵ 3000); IR (neat) 3301, 2930, 2854, 1646, 1549, 1455, 1095, 970, 740 cm^{-1}; LR FABMS *m/z* 399 (77), 367 (39), 255 (3), 224 (5), 187 (2), 143 (100), 130 (31); HR FABMS (positive ion, 3-nitrobenzyl alcohol) *m/z* obs. $[M + H]^+$ 399.3013 ($C_{25}H_{39}N_2O_2$, 0.2 mmu dev.); ^1H NMR (600 MHz, $CDCl_3$) and ^{13}C NMR (150 MHz, $CDCl_3$) see Table III.3.

Semi-Synthesis of Hermitamide A (123). Method A. A solution of CH_2Cl_2 (1 mL) containing the free acid (**98b**, 0.07 mmol) and phenethylamine (14 μL, 0.11 mmol) was cooled to 0 °C. This was followed by addition of dicyclohexylcarbodiimide (DCC, 14.4 mg, 0.07 mmol), dissolved in 1 mL of CH_2Cl_2. After stirring for 30 min at 0 °C, the reaction was allowed to proceed overnight under N_2 at RT. The crude mixture was filtered and washed successively with 5% HCl, 5% $NaHCO_3$, and H_2O and then extracted 3 × with CH_2Cl_2. Semi-synthetic hermitamide A (**1**, 5.0 mg, 22%) was purified using HPLC [Phenomenex Sphereclone 5μ ODS (2), CH_3CN/H_2O (91:9); detection at 254 nm].

Semi-Synthesis of Hermitamide A (123). Method B. The acid chloride 7(*S*)-methoxytetradec-4(*E*)-enoic acid was prepared by adding 5 μL of pyridine to 11.7 mg of 7(*S*)-methoxytetradec-4(*E*)-enoic acid (**98b**, 0.046 mmol) and then 200 μL of $SOCl_2$ (2.74 mmol, 59 molar equivalent) and heating to 60 °C for 1 h under argon. Excess $SOCl_2$ was removed *in vacuo*. This was followed by addition of 3 molar equivalents of phenethylamine (17 μL, 0.13 mmol) and stirred for 1 h at RT. The crude mixture was successively washed with 5% HCl, 5% $NaHCO_3$, and H_2O and then extracted 3 × with

CH_2Cl_2. Semi-synthetic hermitamide A (**123**, 10.0 mg, 60%) was purified using the method described above and showed $[\alpha]^{26}_D$ –9.8° (c = 0.50, $CHCl_3$).

Semi-Synthesis of Hermitamide B (124). Method B. The acid chloride of 7(*S*)-methoxytetradec-4(*E*)-enoic acid was prepared identically as described above for hermitamide A (**123**). However, in this case, 3 molar equivalents of tryptamine (22 mg, 0.12 mmol) in THF (300 μL) were added to the acid chloride and stirred for 1 h at RT. Work-up was carried out as above for hermitamide A (**123**). Semi-synthetic hermitamide B (**124**, 9.0 mg, 50%) was purified using HPLC [Phenomenex Sphereclone 5μ ODS (2), MeOH/H_2O (84:16); detection at 254 nm] and showed $[\alpha]^{26}_D$ –8.6° (c = 0.28, $CHCl_3$).

Semi-Synthesis of Hermitamide A (123). Method C. To a mixture of 7(*S*)-methoxytetradec-4(*E*)-enoic acid (**98b**, 17.0 mg, 0.06 mmol) and trichloroacetonitrile (28.7 mg, 0.20 mmol) in CH_2Cl_2 (0.5 mL) under argon was added Ph_3P (52.2 mg, 0.19 mmol) in CH_2Cl_2 (0.5 mL) dropwise at RT. After the reaction mixture was stirred for 3.5 hr, it was treated with phenethylamine (17 μL, 0.13 mmol), followed by triethylamine (46 μL). The reaction mixture was allowed to react for 30 min at RT. The mixture was washed with water and the organic layer was dried over anhydrous $MgSO_4$. After filtration, the solvent was removed and the residue purified using the same method described above to give hermitamide A (**123**, 15.7 mg, 65%).

Semi-Syntheses of *N*-Methyl-Hermitamides A (125) and B (126) Using Method B. The semi-syntheses of *N*-CH_3-hermitamides A (**125**) and B (**126**) was accomplished using the same method outlined above in Method B for hermitamides A and B, respectively. About 5.0 mg of the lyngbic acid (**98b**, 0.02 mmol) was used in each of the synthesis for conversion to the acid chloride derivative by adding 45 μL (0.61 mmol) of $SOCl_2$. Three equivalents (0.06 mmol) of the *N*-Me-phenethylamine and *N*-Me-tryptamine were used in each of the synthesis. The yield of *N*-CH_3-hermitamides A (**125**) and B (**126**) were 4.4 mg (59%) and 4.5 mg (55%), respectively.

***N*-Methyl-Hermitamide A (125):** pale yellow oil; $[\alpha]^{26}_D$ –5.0° (c = 0.15, $CHCl_3$); UV (EtOH) λ_{max} 216 nm (ϵ 5600); LR FABMS *m/z* 374 (100), 342 (76), 231 (12), 162 (8), 143 (8), 134 (21), 105 (56); HR FABMS (positive ion, 3-nitrobenzyl alcohol) *m/z* obs. $[M + H]^+$ 374.3065 ($C_{24}H_{40}NO_2$, 0.6 mmu dev.); ^1H NMR ($CDCl_3$): δ

7.10–7.35 (m), 5.48 (m), 5.41 (m), 3.58 (m), 3.51 (m), 3.32 (s), 3.13 (m), 2.94 (s), 2.87 (s), 2.83 (m), 2.34 (m), 2.19 (m), 1.42 (m), 1.26 (m), 0.87 (t, J = 6.4).

***N*-Methyl-Hermitamide B (126):** pale yellow oil; $[\alpha]^{26}_{D}$ –5.5° (c = 0.18, $CHCl_3$); UV (EtOH) λ_{max} 224 nm (ϵ 13000); LR FABMS *m/z* 413 (70), 381 (21), 143 (100), 130 (25), 69 (17), 44 (17); HR FABMS (positive ion, 3-nitrobenzyl alcohol) *m/z* obs. $[M + H]^+$ 413.3171 ($C_{26}H_{41}N_2O_2$, 0.4 mmu dev.); ^{1}H NMR ($CDCl_3$): δ 8.34 (brs), 8.17 (brs), 7.66 (d, J = 7.7), 7.56 (d, J = 7.8), 7.36 (t, J = 7.7), 7.26–7.09 (m), 7.03 (brs), 6.96 (brs), 5.52 (m), 5.32 (m), 3.71 (m), 3.60 (m), 3.33 (s), 3.32 (s), 3.15 (m), 3.01 (m), 2.94 (m), 2.37 (m), 2.19 (m), 2.15 (m), 1.43 (m), 1.27 (m), 0.88 (t, J = 6.4).

Brine Shrimp Toxicity, Ichthyotoxicity, and Molluscicidal Bioassays. Evaluation of the crude extract, chromatography fractions, and pure compounds for brine shrimp (*Artemia salina*) toxicity was determined as detailed previously.[162] Ichthyotoxicity of pure compounds using goldfish (*Carassius auratus*) was also measured as detailed previously.[163] Molluscicidal bioassays used the aquatic snail *Biomphalaria glabrata* in protocols previously described.[164]

Cytotoxicity Assay.[165] Neuro 2a mouse neuroblastoma cells (ATCC CCL-131) were grown in RPMI 1640 medium supplemented with 10% heat-inactivated fetal bovine serum, 1 mM sodium pyruvate, 50 μg/mL streptomycin, and 50 units/mL penicillin in an atmosphere of 5% CO_2 at 37 °C. Growth medium (200 μL) containing the cell suspension (1×10^5 cells/mL) was placed in 96-well culture plates. After 24 h, 30 μL of the samples were added to the cells. The sample was dissolved in EtOH and serially diluted with medium to make the final concentration of EtOH less than 1%. Cultures were incubated for 24 h, and cytotoxicity determined by the MTT (3-[4,5-dimethylthiazol-2-yl]-2,5-diphenyltetrazolium bromide) assay with colorimetric measurement at 570 nm.

CHAPTER FOUR

NOVEL BIOACTIVE CYCLIC DEPSIPEPTIDES FROM A PAPUA NEW GUINEA COLLECTION OF *LYNGBYA MAJUSCULA* GOMONT

ABSTRACT

A total of six novel cyclic depsipeptides were isolated and characterized from a marine cyanobacterium, *Lyngbya majuscula* Gomont, collected from Papua New Guinea. These are unique cyclic metabolites consisting of β-amino or β-hydroxy acid units which are becoming common structural features in marine cyanobacterial compounds. The planar structures of these molecules were established using an extensive array of 1D and 2D NMR experiments, including HSQC, TOCSY, and HMBC. Clairamides A (**151**) and B (**152**) are thiazole-containing molecules having the Mapa (2-methyl-3-amino-pentanoic acid) unit and the Maba (2-methyl-3-amino-butanoic acid) unit, respectively. Clairamide B (**152**) is the first report of a marine cyanobacterial metabolite that consists of the Maba unit. Two other unique β-amino acid units are present in wewakamide (**153**) and carliamide (**154**). The Maha (2-methyl-3-amino-hexanoic acid) moiety is present in the former compound while the Amoa (3-amino-2-methyl-oct-7-ynoic acid) unit is featured in the latter molecule. The guinamides A (**155**) and B (**156**) contained a new β-hydroxy acid; 2,2-dimethyl-3-hydroxy-hexanoic acid (Dmhha). Absolute stereochemical analyses of these cyclodepsipeptides were carried out using a combination of chemical degradation and Marfey analyses. *D*-Marfey reagent was used extensively in these analyses, especially in the absolute stereochemical determination of the Mapa unit in clairamide A (**151**). Antifungal and cytotoxic activities of these molecules are also presented.

INTRODUCTION

In recent years, marine cyanobacteria, especially members belonging to the genus *Lyngbya*, are proving to be a prolific source of secondary metabolites with potential as new pharmaceuticals. For instance, the pantropical species, *Lyngbya majuscula* Gomont has yielded no less than 150 compounds as reported in the literature. It has also been reported that different structural classes of bioactive metabolites have been described from a single source of marine cyanobacterium. A high percentage of these marine cyanobacterial secondary metabolites are nitrogen-containing, belonging to the lipopeptide structural class. These lipopeptides occur as either linear or cyclic forms with a variety of associated bioactivities, including antitubulin activity (lyngbyastatin 1, **72**),[84] ichthyotoxicity (antillatoxin, **66**),[78] and antifungal activity (lyngbyabellin B, **79**).[90]

In addition to the preponderance of *N*-methylated α-amino acids, other structural motifs such as α-hydroxy acids, β-amino acids, and β-hydroxy acids are commonly found in these cyanobacterial lipopeptides. These structural features are also present in metabolites reported from mollusks, leading to speculations that such invertebrate compounds are sequestered from the diet by feeding on cyanobacteria. In addition to the dolastatins[95] (Table I.2), which are a series of highly important lipopeptides isolated from the sea-hare, *Dolabella auricularia*, a host of other molluscan metabolites (**127** to **134**), especially from *Onchidium* sp. and *Philinopsis speciosa*, are also considered to be derived from marine cyanobacteria.[166-169]

A wide variety of β-amino and β-hydroxy acid residues of different carbon chain length, usually branching from C-3, have been identified from both molluscan and cyanobacterial metabolites (Table IV.1 and IV.2). The C-2s' of these acid moieties usually occur either as methylenes, with attachment of mono or dimethyl functionalities. It was also noted that the absolute stereochemistries of the same β-amino and β-hydroxy acid residues found in both molluscan and cyanobacterial metabolites were identical. For example, the stereochemistry at C-3 of the 2,2-dimethyl-oct-7-ynoic acid moiety in pitipeptolide A (**140**)[177], a cyanobacterial metabolite, as well as the mollusk compounds, kulolide-1 (**127**)[100] and kulokainalide-1 (**130**),[100] were all of the *S* configuration.

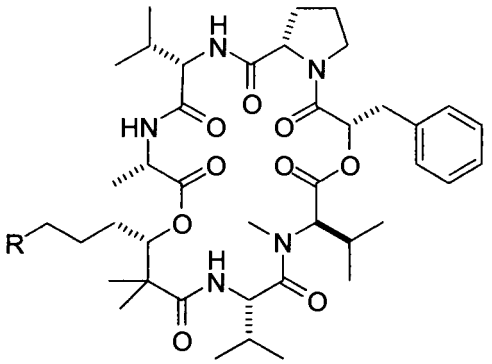

Kulolide-1 (**127**) 

Kulolide-2 (**128**) 

Kulolide-3 (**129**) 

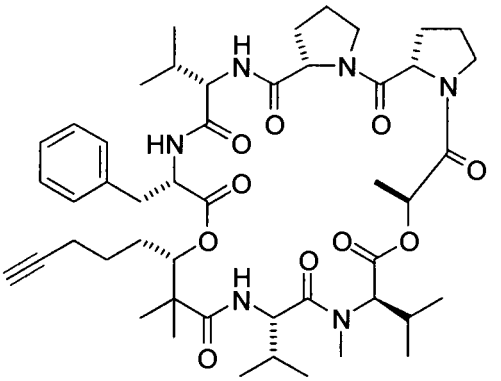

Kulokainalide-1 (**130**)

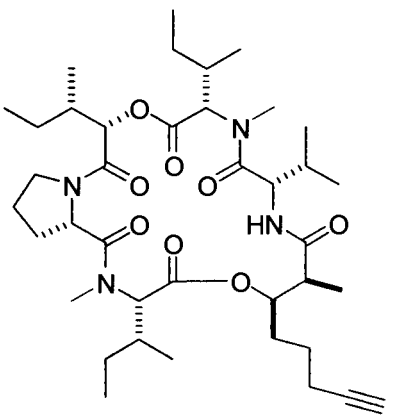

Kulomo'opunalide-1 (**131**)

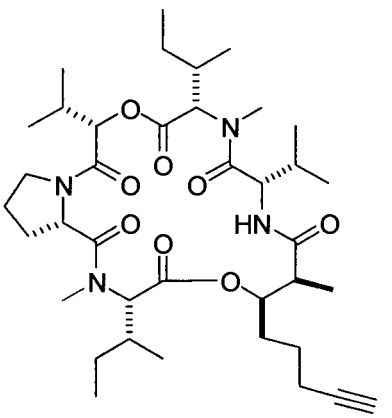

Kulomo'opunalide-2 (**132**)

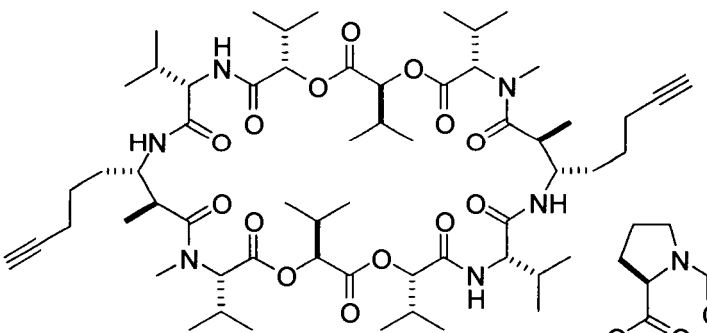

Onchidin A (**133**)

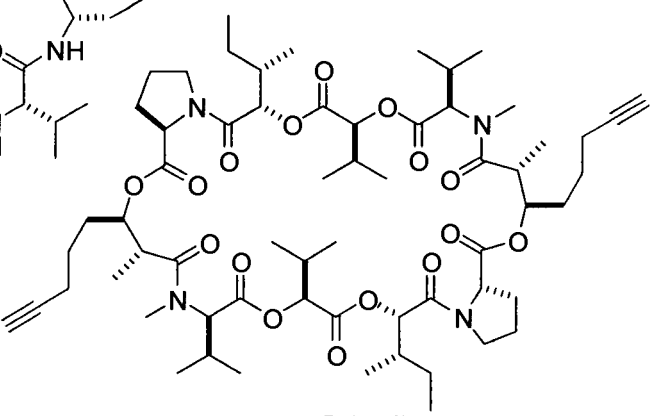

Onchidin B (**134**)

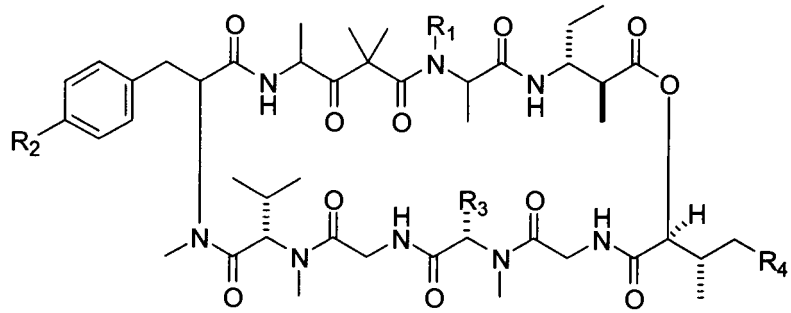

Majusculamide C (**135**) R_1 = H, R_2 = OMe, R_3 = CH(Me)CH_2Me, R_4 = Me
57-Normajusculamide C (**136**) R_1 = H, R_2 = OMe, R_3 = CH(Me)CH_2Me, R_4 = H
Dolastatin 11 (**137**) R_1 = H, R_2 = OMe, R_3 = $CH_2CH(Me)_2$, R_4 = Me
Dolastatin 12 (**138**) R_1 = Me, R_2 = H, R_3 = $CH_2CH(Me)_2$, R_4 = Me

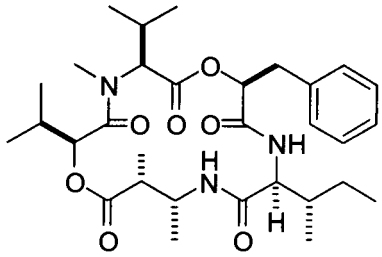

Dolastatin D (**139**)

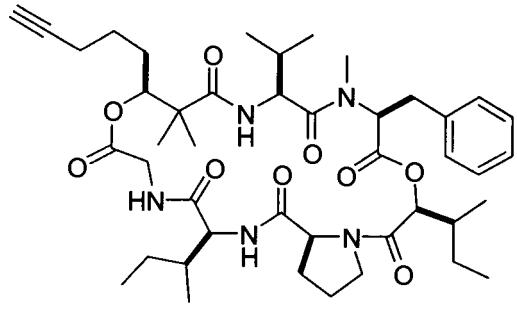

Pitipeptolide A (**140**)

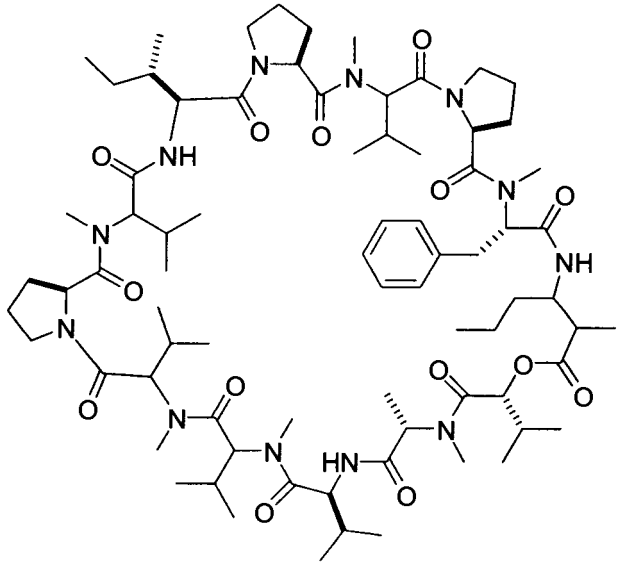

Malevamide B (**141**)

In most cases, the presence of these β-amino and β-hydroxy acid units in cyanobacterial and molluscan metabolites makes their absolute stereochemical analysis

difficult and challenging. For instance, two methods have been presented for the absolute stereochemical analysis of the Mapa unit (**143**, 2-methyl-3-amino-pentanoic acid) present in dolastatins 11 (**137**) and 12 (**138**), majusculamide C (**135**), and 57-normajusculamide C (**136**).[170-173] The first of these was achieved by synthetic means reported by Andersen *et al.* for the purpose of stereochemical determination of the Mapa unit in majusculamide C (**135**).[171] This method involved the generation of a mixture of all four stereoisomers of Mapa (**143**) using ethyl propionate as the starting material. The final stereochemical analysis was carried out using a combination of chemical degradation, Marfey derivatization, and subsequent HPLC analysis of the derivatized Mapa stereoisomers, as well as the natural Mapa from majusculamide C (**135**) on RP-18 column as 2*S*,3*R*-Mapa. Further confirmation of these assignments was provided by X-ray data, obtained on crystals of a Mapa derivative (**144**). A second method, reported by Bates and Gangwar, involved the syntheses of pure stereoisomers of Mapa.[174] They confirmed the absolute configuration of the Mapa units in majusculamide C, 57-normajusculamide C, and dolastatins 11 and 12 to be the same as those reported by the Andersen group.[174]

The truncated β-amino acid, Maba (**142**, 2-methyl-3-amino-butanoic acid) is a moiety in the cytotoxic cyclic depsipeptide, dolastatin D (**139**). The absolute configuration of Maba (**142**) was determined to be 2*R*,3*R* through syntheses of two of the stereoisomers, epimerization of each stereoisomer, and Marfey analysis.[175]

A rather elaborate method was used for the stereochemical determination of the β-hydroxy acid, Hymo (**145**, 3-hydroxy-2-methyl-oct-7-ynoic acid) present in a pulmonate metabolite, onchidin B (**134**). All four possible stereoisomers of this unit were generated in a diastereoselective way. These stereoisomers were then derivatized as 3-*O*-[(-)-(*R*)-α-methoxy- α-(9-anthryl)acetyl]-2-methyloct-7-ynoic methyl esters (**146**) and analyzed by HPLC-MS, which gave four distinct peaks with clean CIMS fragmentation patterns. The final assignments of 2*R*,3*R* in Hymo (**145**) were determined by coinjection of standard derivatized β-hydroxy acids, such as **146**, and the natural Hymo, derived from onchidin B (**134**), by HPLC-MS.[169,176]

An epimer at C-2 of the Hymo unit (**145**) is present in kulomo'opunalides 1 (**131**) and 2 (**132**), isolated from the marine mollusk, *Philinopsis speciosa*. The 2*S*,3*R*

configurations of this Hymo unit were determined by the analysis of authentic *p*-bromobenzoyl Hmoaa methyl esters (**147**, synthesized by hydrogenation of Hymo stereoisomers, converting to the methyl esters, and derivatization with *p*-bromobenzoyl chloride) on chiral HPLC, and coinjection of standards with the natural hydrogenated and derivatized Hymo from the kulomo'opunamides. Proton NMR comparisons of the four stereoisomers of Hymo with that of natural Hymo were also made as further evidence of the assignments.[100]

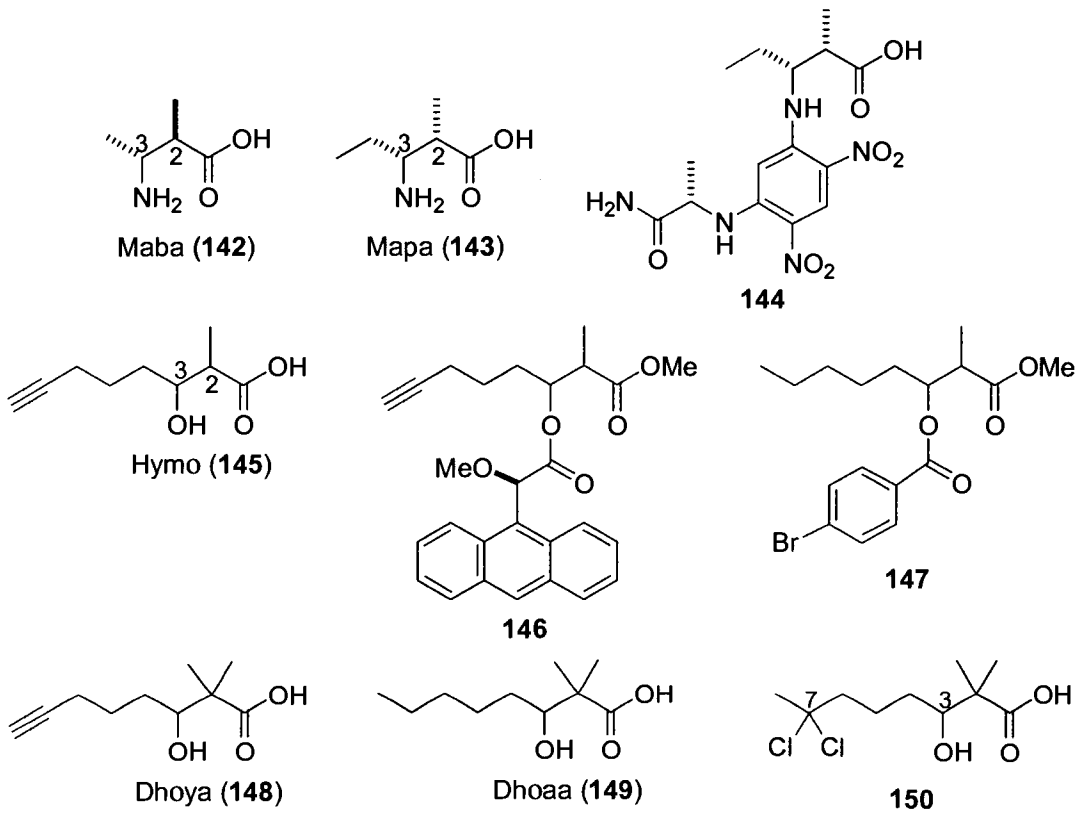

Mosher method was used in the stereochemical assignment of another β-hydroxy acid residue, Dhoya (**148**, 2,2-dimethyl-3-hydroxy-7-octynoic acid), in kulolide-1 (**127**) as 2*S*. Like the kulomo'opinamides, kulolide-1 (**127**) was also a constituent of *P. speciosa*.[166] Subsequently, the optical rotation value of the pure tetrahydro-derivative of Dhoya (Dhoaa, **149**) was used to assign the stereochemistry of identical units found in

Table IV.1 β-Amino acid moieties found in marine cyanobacterial and molluscan metabolites.

β-Amino acid units	Marine Cyanobacteria	Mollusks
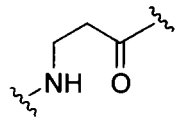	Yanucamides *Lyngbya majuscula*	
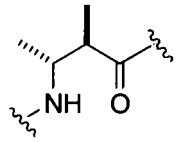		Dolastatin D *Dolabella auricularia*
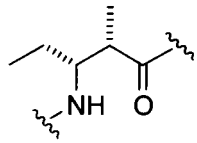	Majusculamide C & derivatives *L. majuscula* Lyngbyastatin 1 *L. majuscula/S. calcicola*	Dolastatins 11 and 12 *D. auricularia*
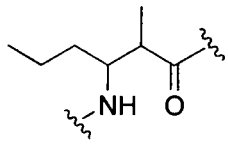	Malevamide B *Symploca laete-viridis*	
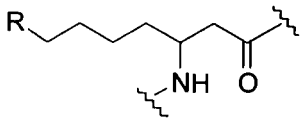	Laxaphycin A (R = CH_3) Laxaphycin B (R = C_3H_7) *L. majuscula* Hormothamnin A (R = CH_3) *Hormothamnion* sp.	
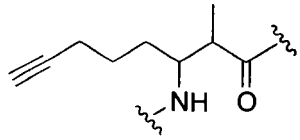	Malevamide C *S. laete-viridis*	Ochidin A (2S, 3S) *Onchidium sp.*
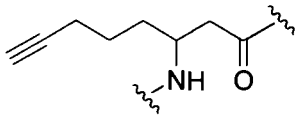		Dolastatin 17 *D. auricularia*
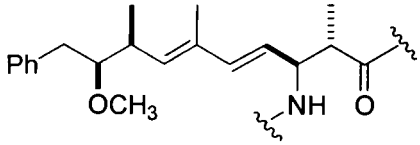	Nodularin *Nodularia spumigena*	

four other metabolites, kulokainalide-1 (**130** from *P. speciosa*), lyngbyabellins (**74** and **79** from *L. majuscula*), and pitipeptolide A (**140** from *L. majuscula*).[177] The Dhoaa units in the lyngbyabellins (**74** and **79**) contained two chlorine atoms at C-7 (**150**). However, these halogens were far from the stereocenter at C-3 and were not expected to influence the magnitude of optical rotation significantly, thereby allowing direct optical rotation comparison with that of pure Dhoaa (**149**).

Table IV.2 β-Hydroxy acid moieties found in marine cyanobacterial and molluscan metabolites.

β-Hydroxy acid units	Marine Cyanobacteria	Mollusks
		Kulolide-3 *Philinopsis speciosa*
	Pitipeptolide B *Lyngbya majuscula*	Kulolide-2 *P. speciosa*
	Yanucamides *L. majuscula* Pitipeptolide A *L. majuscula*	Kulolide-1 and Kulokainalide-1 *P. speciosa*
		Kulomo'opunalides (2S, 3R) *P. speciosa* Ochidin B (2R, 3R) *Ochidium sp.*
	Lyngbyabellins *L. majuscula*	
		Dolabellin *Dolabella auricularia*

RESULTS AND DISCUSSION

In addition to our search for anticancer agents from marine algae, we are also interested in marine natural products that possess other useful properties such as antifungal and neurotoxic activities. A preliminary screening by our industrial collaborator of our bank of marine algal extracts indicated significant antifungal activities in an organic extract from the cyanobacterium, *Lyngbya majuscula* Gomont. This marine cyanobacterium (PNSM-4/Sep/98-01) was collected from the northern coast of Papua New Guinea on an expedition in 1998. Based on these preliminary bioassay results, the organic extract was further pursued in order to identify the bioactive constituents. A bioassay-guided fractionation (Figure IV.2) of the organic extract, using a combination of VLC, RP-SepPak, and HPLC on RP-8 and phenyl-hexyl columns, led to the isolation of six novel cyclic depsipeptides (**151** to **156** in Figure VI.1). These cyclic metabolites contained a high degree of *N*-methylated amino acids, α-hydroxy acids, β-amino, and β-hydroxy acids and they were given the trivial names of clairamides A (**151**) and B (**152**), wewakamide (**153**), carliamide (**154**) and guinamides A (**155**) and B (**156**). The planar structures of these cyanobacterial metabolites were established mainly through detailed analyses of 1D and 2D NMR data. The planar structures of two compounds, clairamide A (**151**) and carliamide (**154**) were previously disclosed and will not be included in this discussion.[167] However, the absolute stereochemical determination of the Mapa unit in clairamide A (**151**) will be presented.

A molecular formula of $C_{32}H_{45}N_5O_6S$ (13 degrees of unsaturation) was determined for clairamide B (**152**) by HR FABMS. Preliminary inspection of the ^{1}H NMR spectrum suggested the peptide nature of **152** by having signals for exchangeable protons at δ 8.85 and δ 8.07, and two *N*-Me singlets at δ 3.07 and δ 3.22, attributable to secondary and tertiary amide functionalities, respectively (Figure IV.3). The ^{1}H NMR spectrum also revealed the presence of a mono-substituted phenyl group as well as a thiazole moiety, consistent with the diagnostic singlet proton signal at δ 7.95. At least five proton signals were discernable between 4-6 ppm in the ^{1}H NMR spectrum and these were due to protons adjacent to heteroatoms such as oxygen and nitrogen. Five ester/amide carbonyl resonances were observed in the ^{13}C NMR spectrum of **152** (Figure

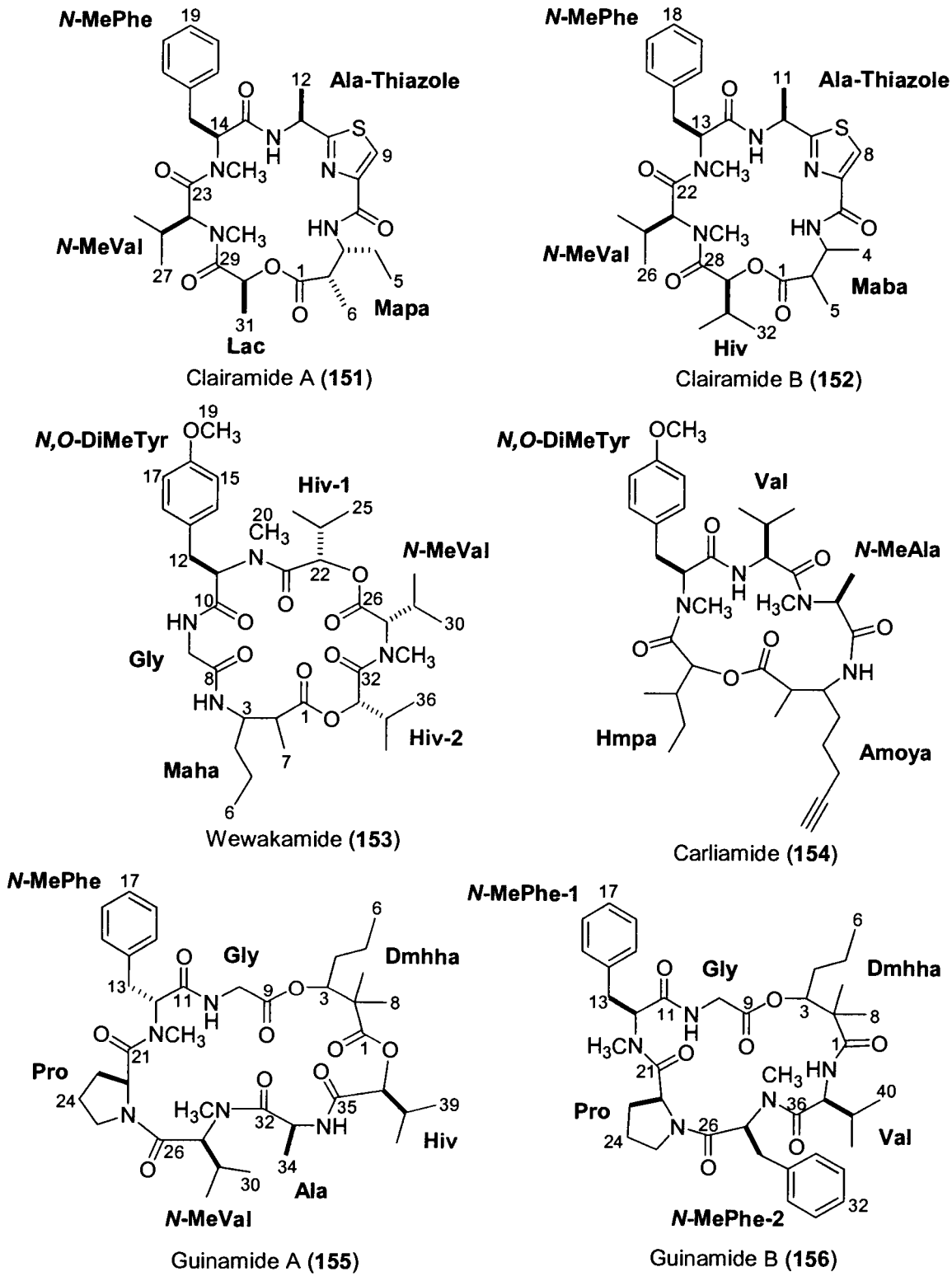

Figure IV.1 Novel cyclic depsipeptides isolated from *Lyngbya majuscula* (PNSM-4/Sep/98-01).

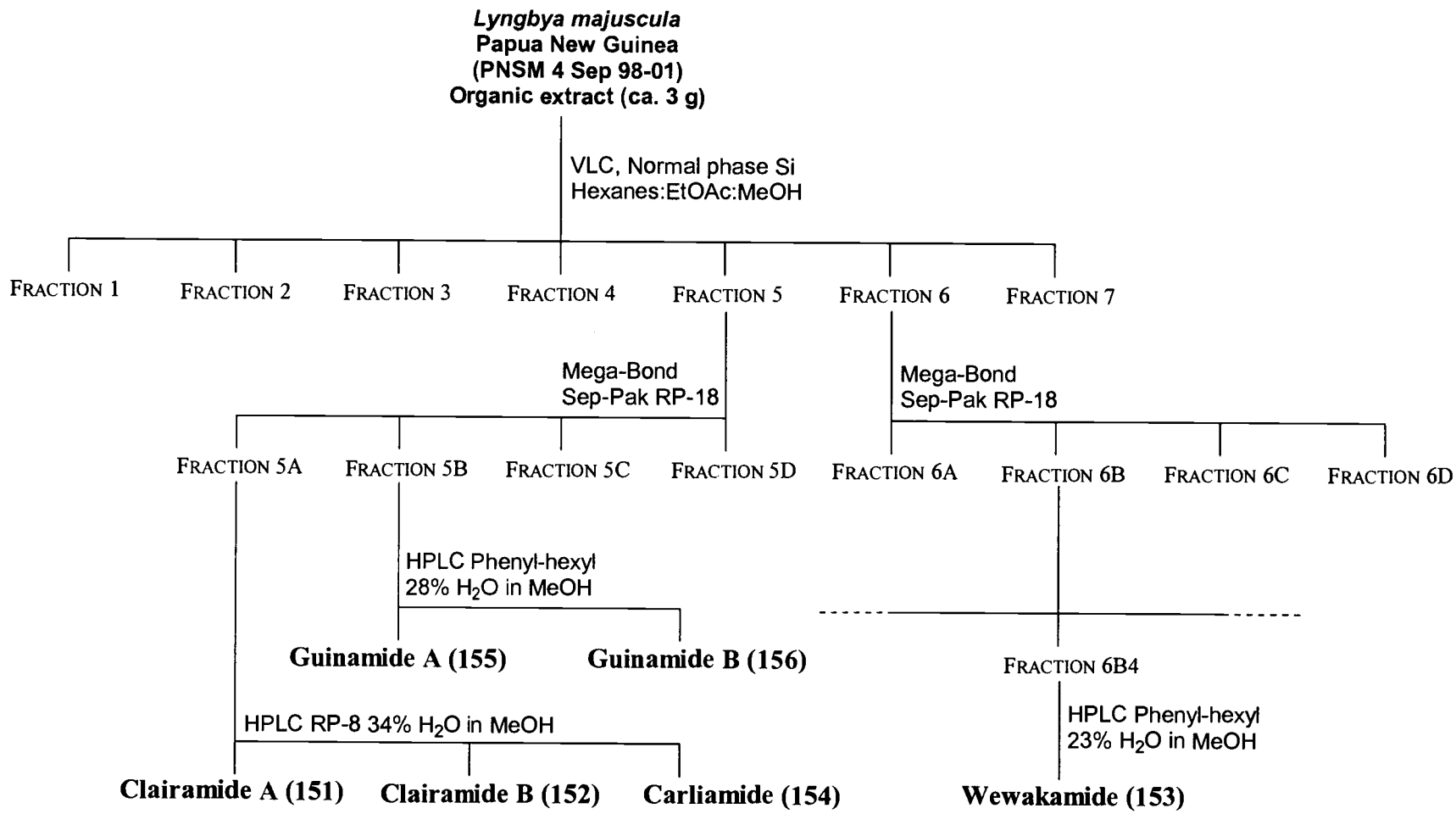

Figure IV.2 Isolation and purification of compounds **151** to **156**.

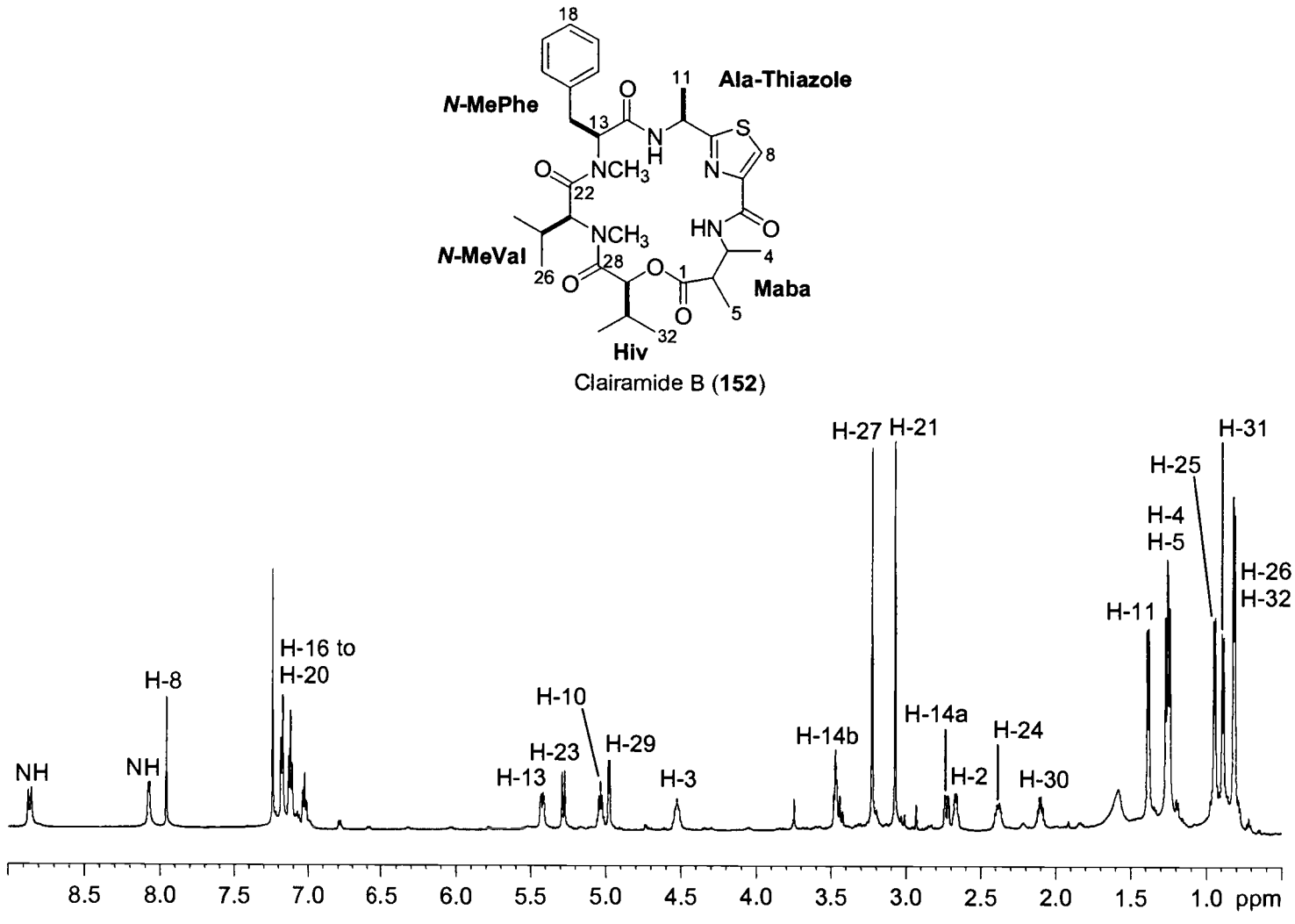

Figure IV.3 ^{1}H NMR spectrum of clairamide B (**152**) in $CDCl_3$.

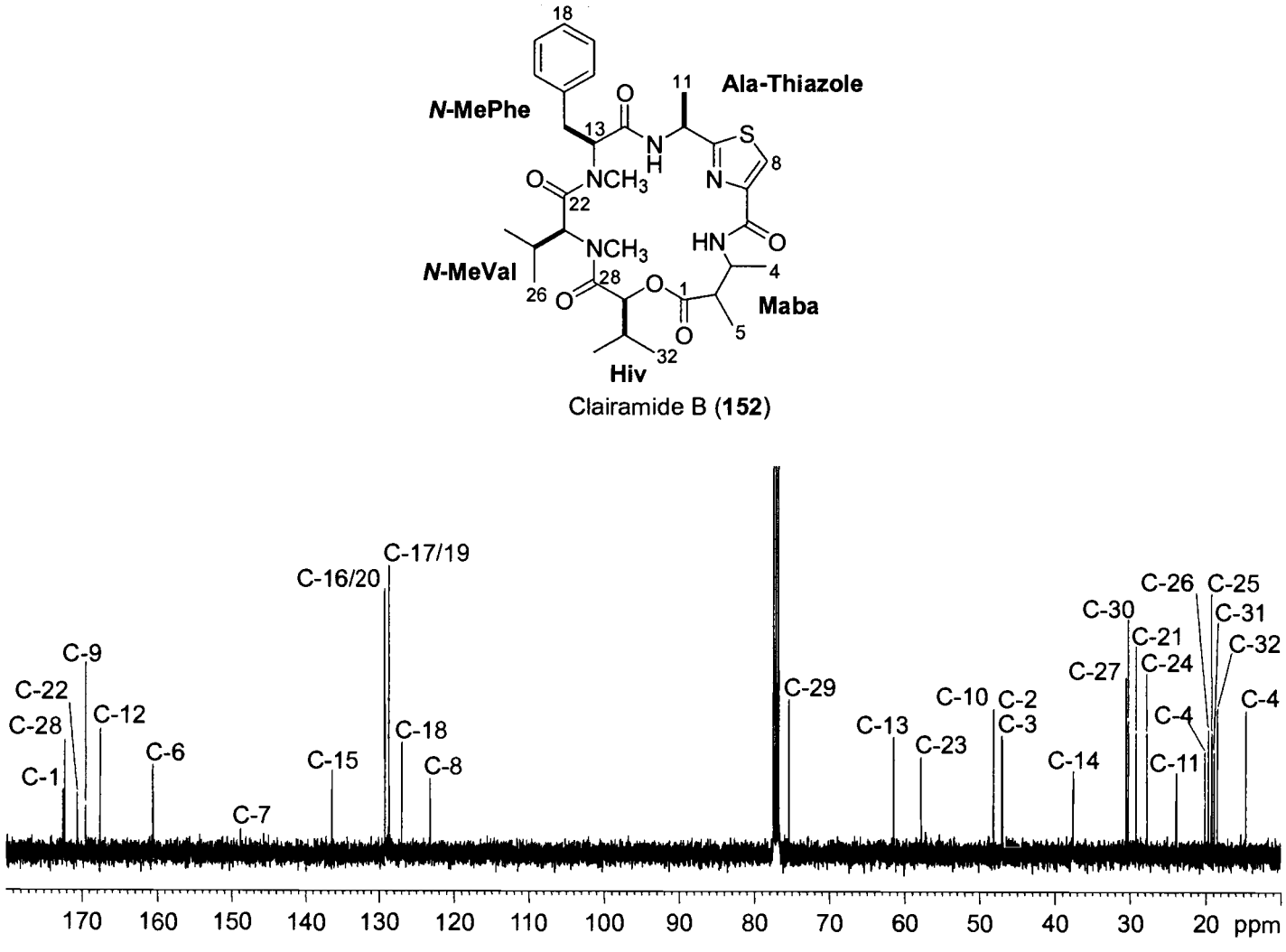

Figure IV.4 ^{13}C NMR spectrum of clairamide B (**152**) in $CDCl_3$.

Table IV.3 NMR spectral data for clairamide B (**152**) at 600 MHz (^{1}H) and 100 MHz (^{13}C) in $CDCl_3$.

Position	^{1}H	mult	J (Hz)	^{13}C	HMBC
			2-methyl-3-amino-butanoic acid (Maba)		
1				172.5	
2	2.66	dt	6.7, 2.4	46.9	14.6, 47.0, 172.5
3	4.52	m		47.0	172.5
4	1.24	d	7.3	20.0	172.5
5	1.25	d	7.2	14.6	172.5
*N*H	8.85	d	10.4		47.0, 160.7
				Ala-Thiazole	
6				160.7	
7				148.8	
8	7.95	s		123.2	148.8, 160.7, 169.5
9				169.5	
10	5.03	m		48.1	23.8, 167.7, 169.5
11	1.37	d	6.8	23.8	169.5
*N*H	8.07	d	6.1		48.1, 167.7, 169.5
				***N*-MePhe**	
12				167.7	
13	5.41	dd	10.4, 4.0	61.1	29.1, 37.5, 136.5, 167.7, 170.6
14a	2.72	dd	13.4, 3.7	37.5	61.1, 129.3, 136.5, 167.7
14b	3.45	m			61.1, 129.3, 136.5, 167.7
15				136.5	
16/20	7.17	brd	7.4	129.3	37.5, 127.0
17/19	7.12	brt	7.5	128.7	136.5
18	7.02	t	7.2	127.0	129.3
21 (*N*-CH_3)	3.07	s		29.1	61.1, 170.6
				***N*-MeVal**	
22				170.6	
23	5.27	d	10.6	57.8	19.1, 27.7, 30.5, 170.6, 172.2
24	2.38	m		27.7	19.6, 57.8
25	0.94	d	6.5	19.1	19.6, 27.7, 57.8
26	0.82	d	6.5	19.6	19.1, 27.7, 57.8
27 (*N*-CH_3)	3.22	s		30.5	57.8, 172.2
			2-hydroxyisovaleric acid (Hiv)		
28				172.2	
29	4.97	d	5.7	75.4	18.4, 30.2, 172.2, 172.5
30	2.09	m		30.2	18.4, 75.4
31	0.88	d	6.9	18.8	18.4, 30.2, 75.4
32	0.82	d	6.5	18.4	18.8, 30.2, 75.4

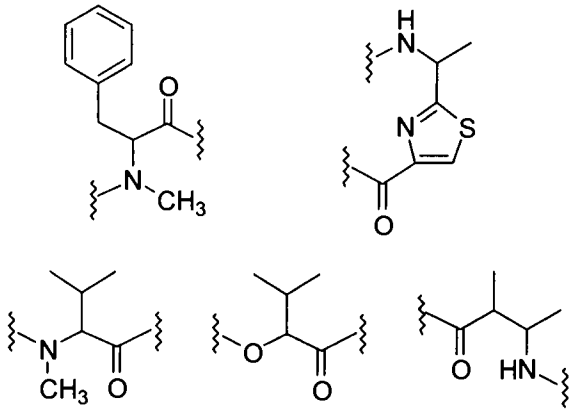

Figure IV.5 Partial structures of clairamide B (**152**).

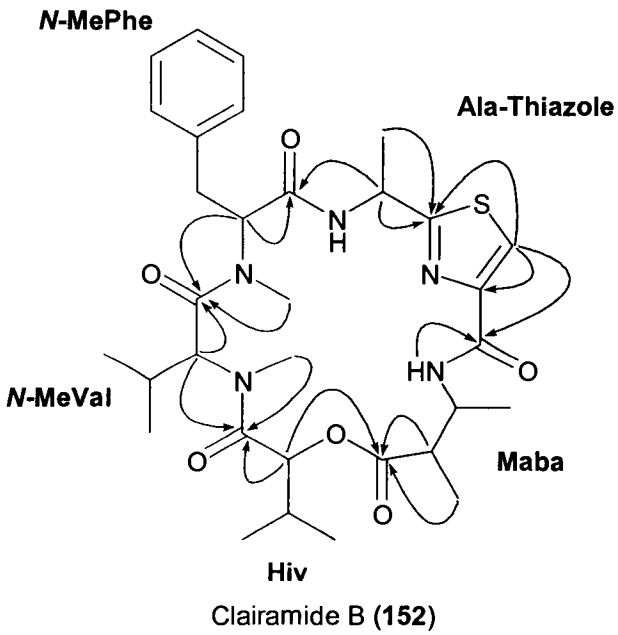

Figure IV.6 HMBC correlations in clairamide B (**152**).

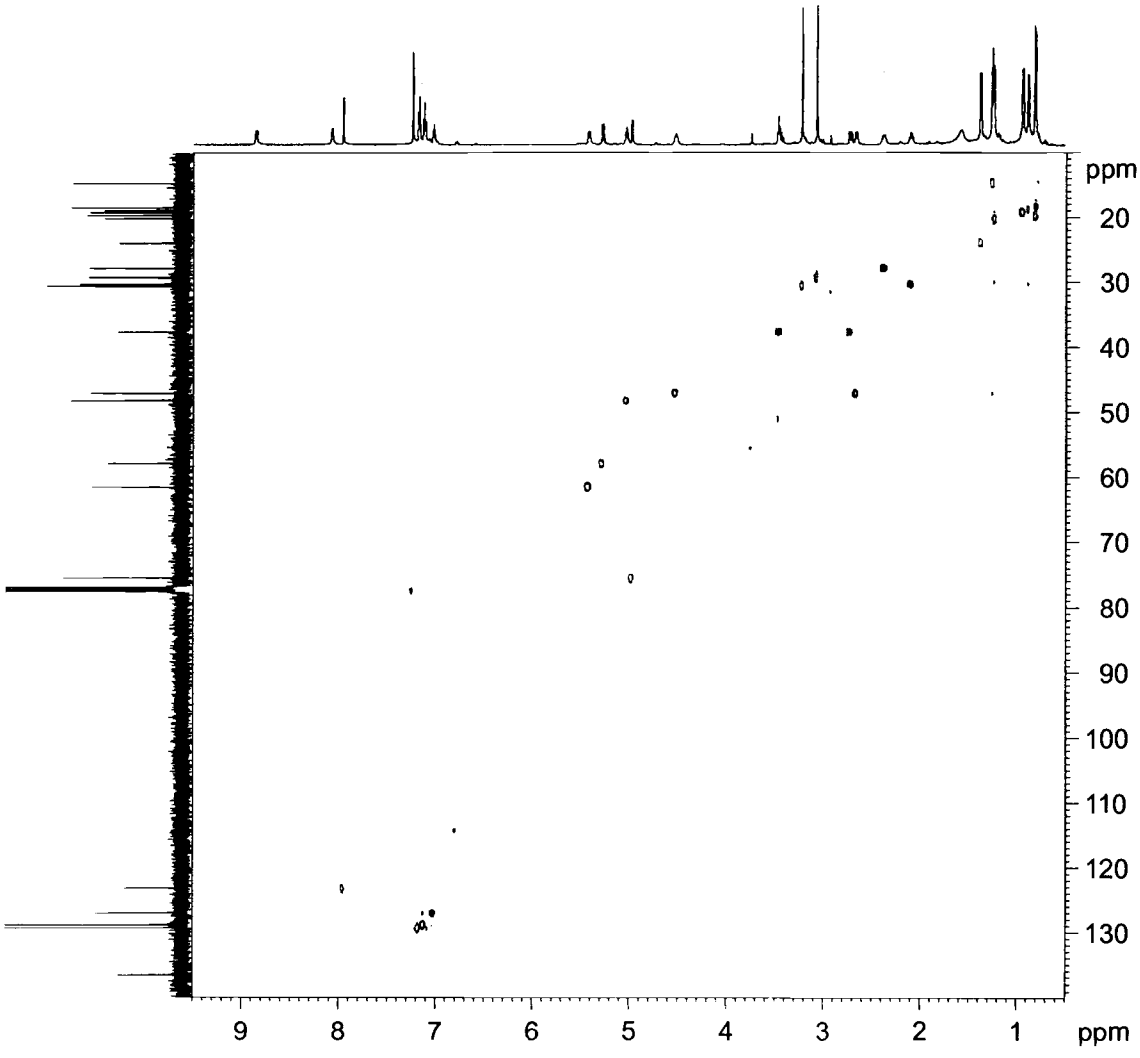

Figure IV.7 HSQC spectrum of clairamide B (**152**) in $CDCl_3$.

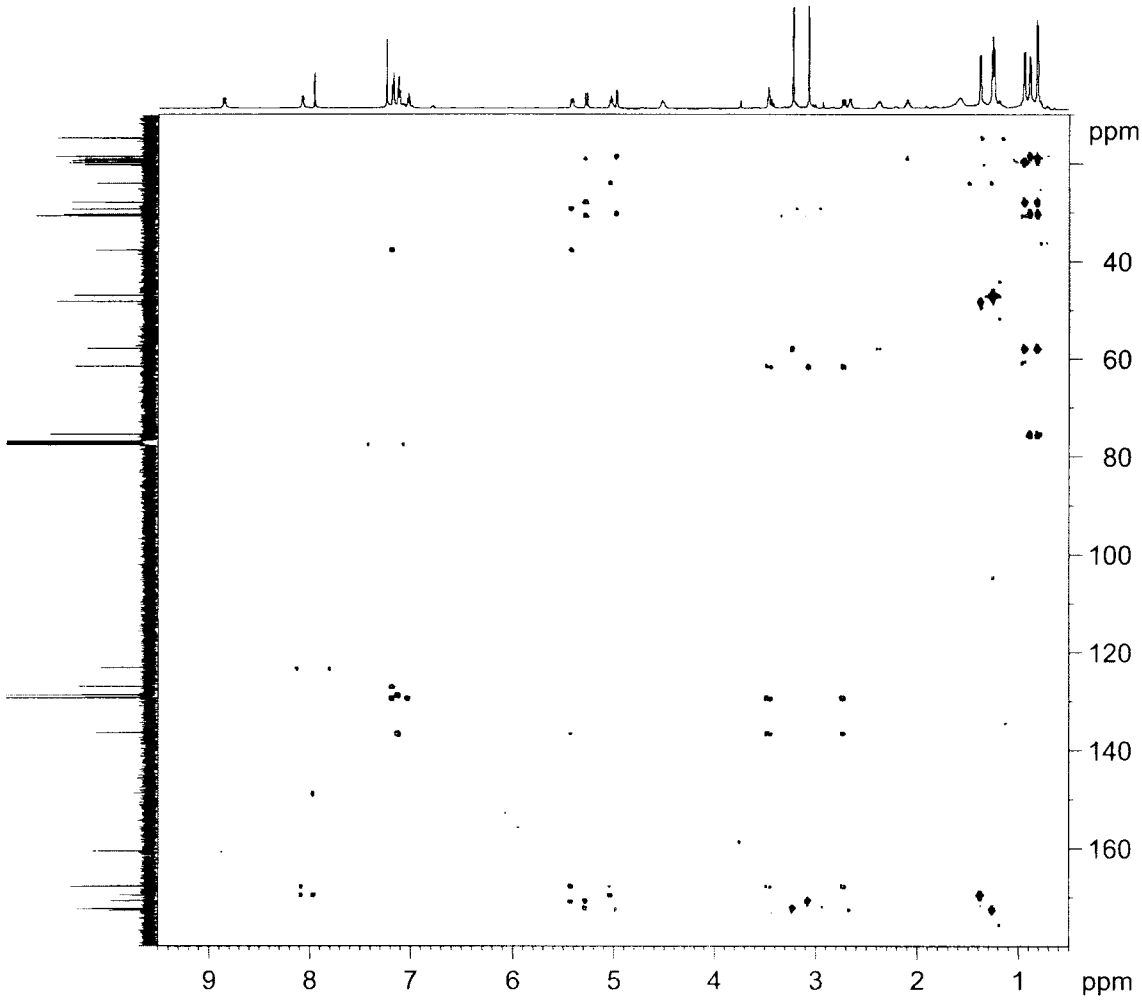

Figure IV.8 HMBC spectrum of clairamide B (**152**) in $CDCl_3$.

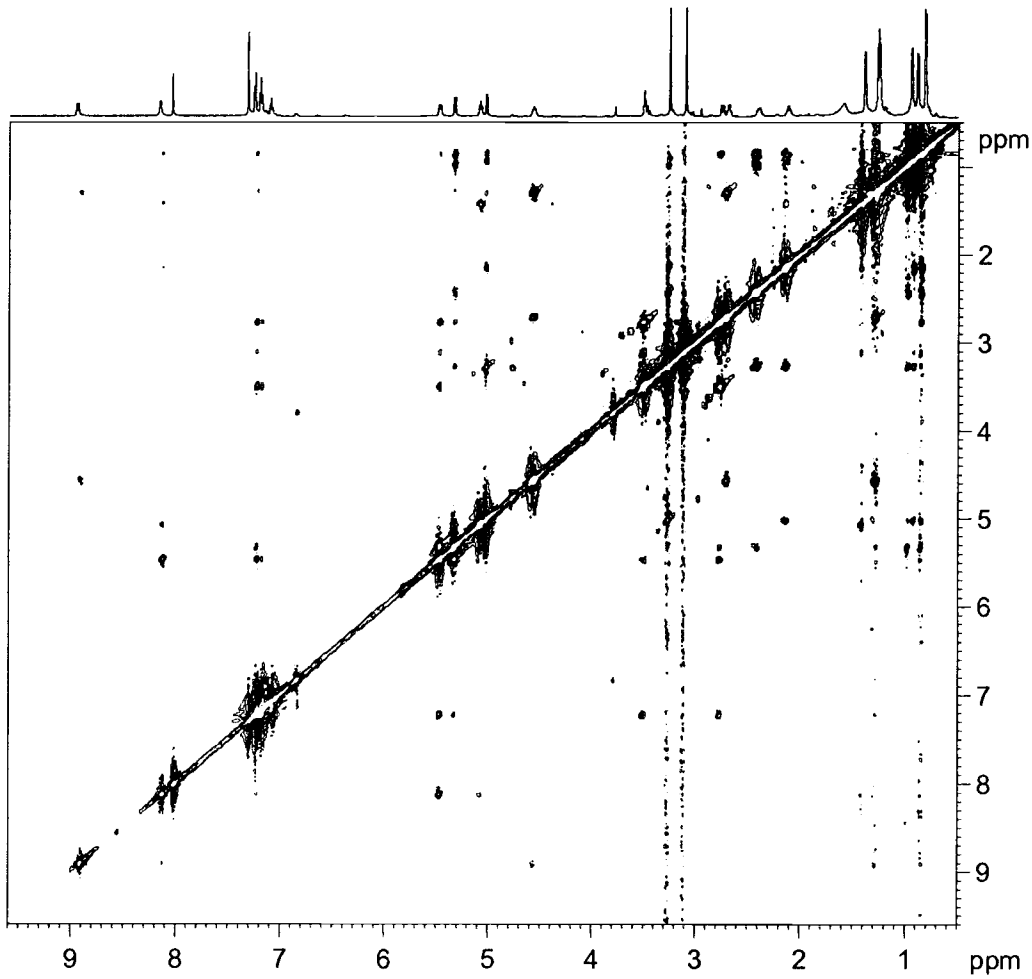

Figure IV.9 TOCSY spectrum of clairamide B (**152**) in $CDCl_3$.

IV.4). One of the signals at δ 160.7 was diagnostic for a carbonyl carbon adjacent to an aromatic heterocycle, such as a thiazole group. The presence of ester/amide carbonyl functionalities could be inferred from the IR spectrum, displaying strong absorption bands centered at 1730 and 1628 cm^{-1}. One oxygenated sp^3 carbon was suspected due to a signal resonating at δ 75.4 in the ^{13}C NMR spectrum, suggesting the presence of a hydroxy acid unit in **152**.

Five partial structures could be assembled by the analyses of 1D and 2D NMR data. These include *N*-methylphenylalanine (*N*-MePhe), *N*-methylvaline (*N*-MeVal), 2-hydroxyisovaleric acid (Hiv), 2-methyl-3-amino-butanoic acid (Maba), and a thiazole-alanine residue (Figure IV.5). A search of the chemical literature indicated that the Maba unit has only been identified in the sea-hare metabolite, dolastatin D (**139**).

The sequential relationship of the different residues in clairamide B could be established from the HMBC experiment, leading to the planar structure as shown in **152**. For instance, sequential HMBC correlations were observed between *N*H (δ 8.85)/C-6; H-7, H-8/C-6; H-10, *N*H (δ 8.07)/C-12; H-13, H-21/C-22; H-23, H-27/C-28; and H-29/C-1 revealing the sequence of Maba/Ala-Thiazole/*N*-MePhe/*N*-MeVal/Hiv (Figure IV.6). The final ring closure between Hiv and Maba was obtained from an HMBC correlation of the α-H of Hiv unit to the carbonyl carbon of Maba unit. The partial sequence of Ala-Thiazole/*N*-MePhe/*N*-MeVal was also present in clairamide A (**151**). However, the present compound deviates from clairamide A (**151**) in having a Hiv and Maba unit, instead of a Lac and Mapa unit in the latter compound.

Absolute configurations of the α-amino acids and the Hiv unit in **152** were determined by Marfey analysis and chiral GC-MS, respectively. Clairamide B (**152**) was subjected to ozonolysis to prevent epimerization at the α-carbon of Ala of the Ala-Thiazole unit during acid hydrolysis. The aqueous layer of the acid hydrolysate of **152** was divided in two portions and one half was subjected to Marfey analysis to yield *L*-Ala, *L*-*N*-MePhe, and *L*-*N*-MeVal. The other half was subjected to chiral GC-MS analysis, which determined the stereochemistry of Hiv in **152** as *L*.

The molecular formula of wewakamide (**153**) was determined as $C_{36}H_{56}N_4O_9$ (11 degrees of unsaturation) by HR FABMS. The ^1H NMR spectra of wewakamide taken in three different deuterated solvents, $CDCl_3$, CD_3OD, and C_6D_6, were complicated due to

the presence *N*-methyls in the molecule, giving rise to different conformers in solution. Fortunately, a single conformer predominated when the molecule was measured in DMSO-d_6 and all NMR experiments were therefore measured in this solvent. Like clairamide B (**152**), several spectral features of **153** were indicative of its peptidic nature. These include the presence of two low field *N*H protons at δ 8.55 and δ 7.00 in the ^{1}H NMR data (Figure IV.10). IR spectrum suggested the presence of ester/amide carbonyl functionalities from strong absorption bands at 1731 and 1663 cm^{-1}. In addition, a para di-substituted phenyl functionality could be deduced from the ^{1}H NMR spectrum due to two low field aromatic doublet proton signals at δ 7.14 (2H) and δ 6.79 (2H). Three distinct singlet protons signals could be observed from the ^{1}H NMR data, attributable to one *O*Me (δ 3.67) and two *N*Me (δ 3.07 and δ 2.88) protons. Of a total of 36 carbon resonances in the ^{13}C NMR spectrum of wewakamide (**153**), six low field signals in the 165-175 ppm range were due to ester/amide carbonyls (Figure IV.11). The presence of two hydroxy acids in the molecule was also inferred from two carbon resonances at δ 74.7 and δ 75.0.

Six substructures in wewakamide (**153**) were generated from detailed analyses of 1D and 2D NMR data. These were two units of α-hydroxy acids, Hiv-1 and Hiv-2 (2-hydroxy-isovaleric acid); three α-amino acids, *N,O*-dimethyl-tyrosine (*N,O*-diMeTyr), *N*-methylvaline (*N*-MeVal), and glycine (Gly); and a unique β-amino acid unit, 2-methyl-3-amino-hexanoic acid (Maha) (Figure IV.12). The presence of an *N,O*-diMeTyr unit was confirmed from the observation of an HMBC correlation from the *O*CH$_3$ proton signal at δ 3.67 to C-16 (δ 158.8). The Maha unit in **153** was deduced mainly from HMBC and TOCSY data. In the latter spectral data, two proton spin-systems, H-7/H-2/H-3 and *N*H(δ 7.00)/H-3/H-4, could be deduced in the Maha moiety. Key proton correlations from HMBC data gave further structural evidence of this β-amino acid: H-7 to C-1 and C-3; H-4 to C-3, C-5, and C-6; and H-5 to C-3 and C-4. This β-amino acid moiety has only been reported in one other cyanobacterial metabolite, malevamide B (**141**), recently isolated from *Symploca laete-viridis*.[89]

The sequential connectivity of the above substructures in wewakamide was achieved mainly through HMBC correlations (Figure IV.13). These correlations include

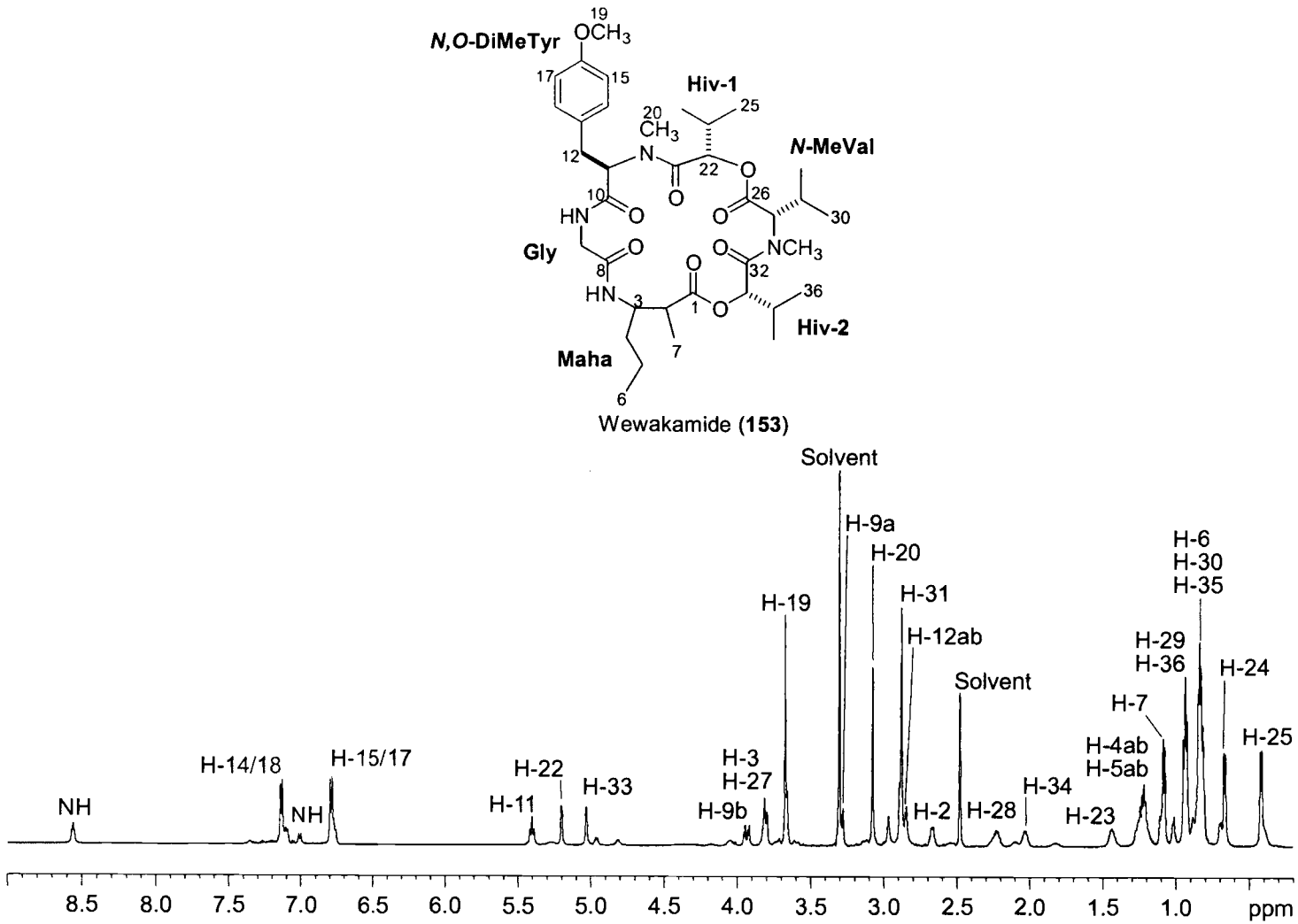

Figure IV.10 ^{1}H NMR spectrum of wewakamide (**153**) in DMSO-d_6.

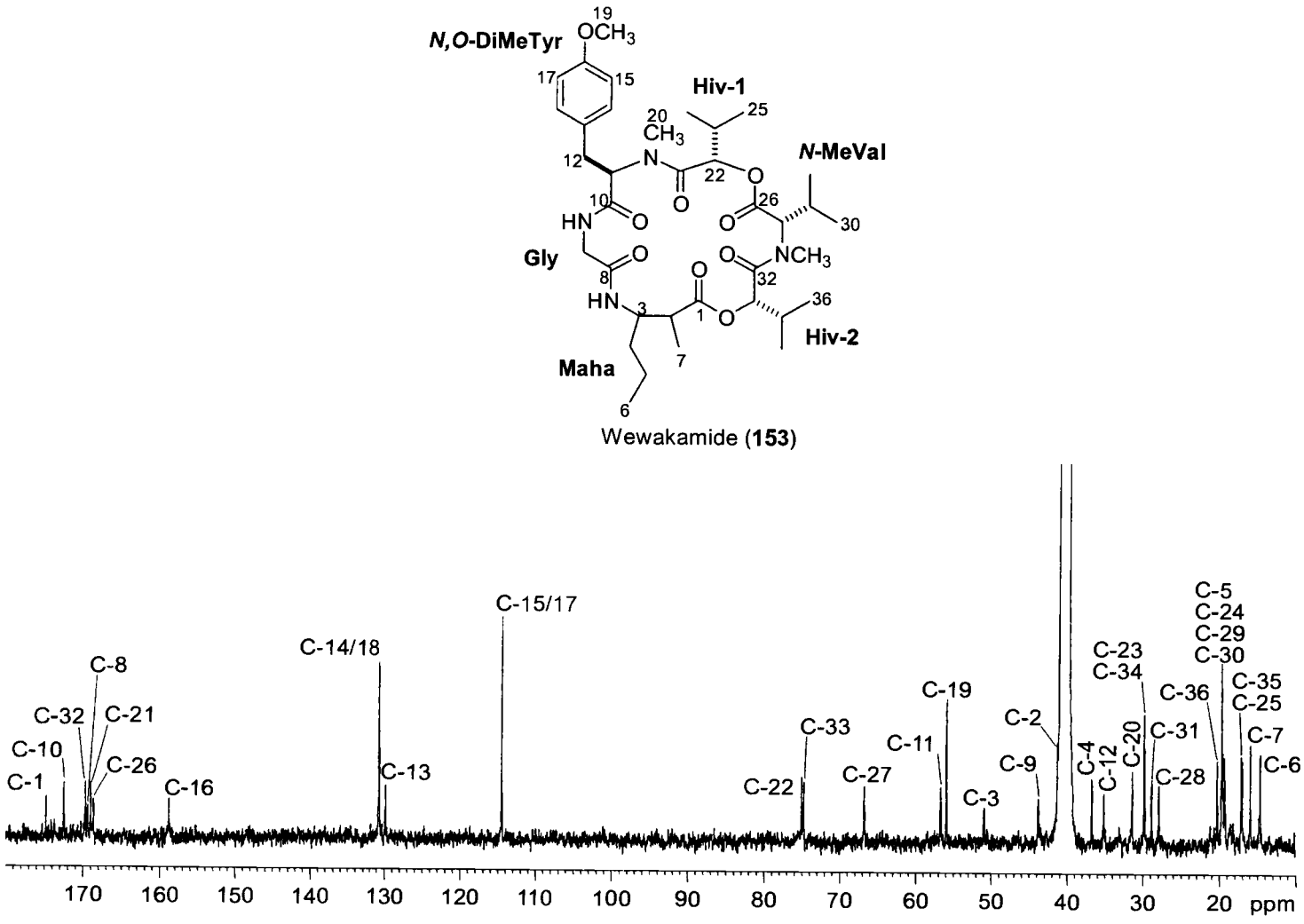

Figure IV.11 ^{13}C NMR spectrum of wewakamide (**153**) in DMSO-d_6.

Table IV.4 NMR spectral data for wewakamide (**153**) at 600 MHz (^{1}H) and 100 MHz (^{13}C) in DMSO-d_6.

Position	^{1}H	mult	J (Hz)	^{13}C	HMBC
			2-methyl-3-amino-hexanoic acid (Maha)		
1				174.7	
2	2.67	m		41.2	15.9, 174.7
3	3.79	m		50.8	
4ab	1.25	m		36.7	14.6, 19.5, 36.7, 50.8
5ab	1.24	m		19.5	36.7, 50.8
6	0.85	m		14.6	19.5, 36.7
7	1.08	d	7.0	15.9	41.2, 50.8, 174.7
*N*H	7.00	d	9.1		169.3
				Gly	
8				169.3	
9a	3.30	m		43.7	169.3, 172.4
9b	3.93	dd	16.8, 6.3		169.3, 172.4
*N*H	8.55	m			43.7, 172.4
				***N,O*-DiMeTyr**	
10				172.4	
11	5.40	brt	8.1	56.6	31.3, 35.1, 129.8, 169.0, 172.4
12ab	2.89	m		35.1	56.6, 129.8, 172.4
13				129.8	
14/18	7.14	d	8.1	130.6	35.1, 114.5, 130.6, 158.8
15/17	6.79	d	8.1	114.5	114.5, 129.8, 158.8
16				158.8	
19 (*O*-CH_3)	3.67	s		55.9	
20 (*N*-CH_3)	3.07	s		31.3	56.6, 169.0
			2-hydroxy-isovaleric acid (Hiv-1)		
21				169.0	
22	5.20	brd	2.7	75.0	16.9, 19.3, 29.8, 168.6, 169.0
23	1.45	m		29.8	16.9, 19.3
24	0.67	d	6.8	19.3	16.9, 29.8, 75.0
25	0.43	d	6.5	16.9	19.3, 29.8, 75.0
				***N*-MeVal**	
26				168.6	
27	3.79	m		66.7	27.9, 28.8, 168.6, 169.6
28	2.25	m		27.9	19.5, 66.7, 168.6
29	0.94	m		19.5	19.2, 27.9, 66.7
30	0.85	m		19.2	19.5, 27.9, 66.7
31 (*N*-CH_3)	2.88	s		28.8	66.7, 169.6
			2-hydroxy-isovaleric acid (Hiv-2)		
32				169.6	
33	5.03	brd	2.8	74.7	17.1, 20.2, 29.9, 169.6, 174.7
34	2.04	m		29.9	17.1, 20.2
35	0.85	m		17.1	20.2, 29.9, 74.7
36	0.94	m		20.2	17.1, 29.9, 74.7

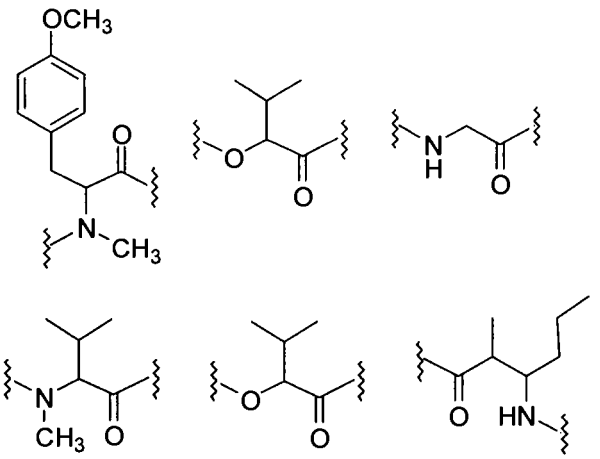

Figure IV.12 Partial structures of wewakamide (**153**).

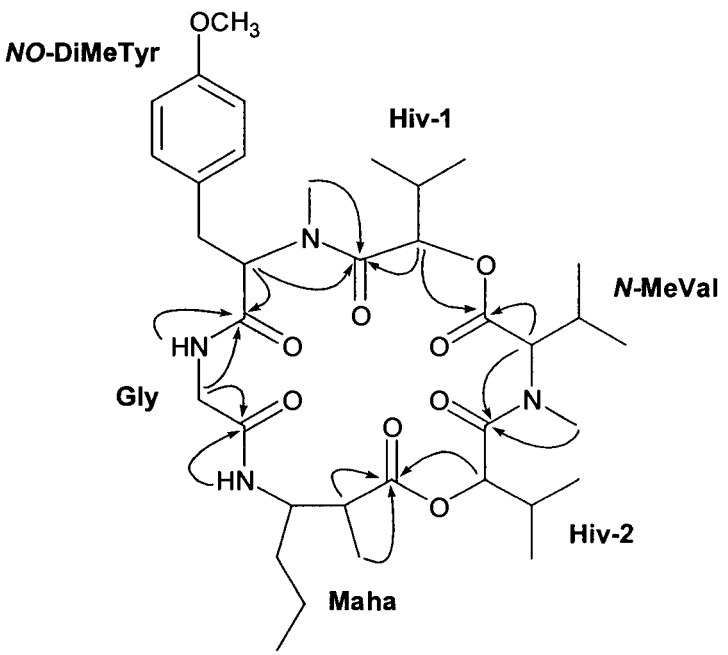

Wewakamide (**153**)

Figure IV.13 HMBC correlations in wewakamide (**153**).

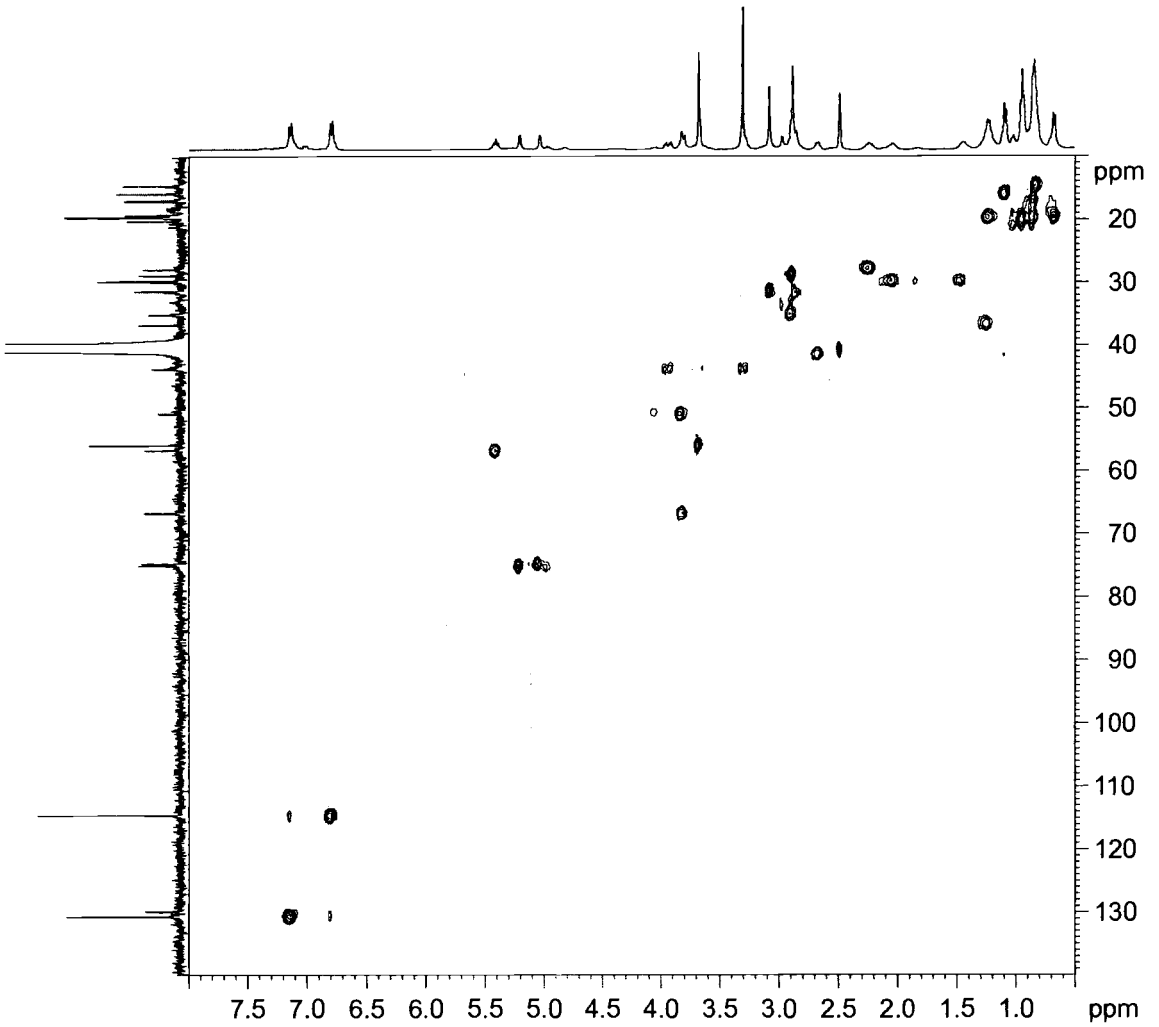

Figure IV.14 HSQC spectrum of wewakamide (**153**) in DMSO-d_6.

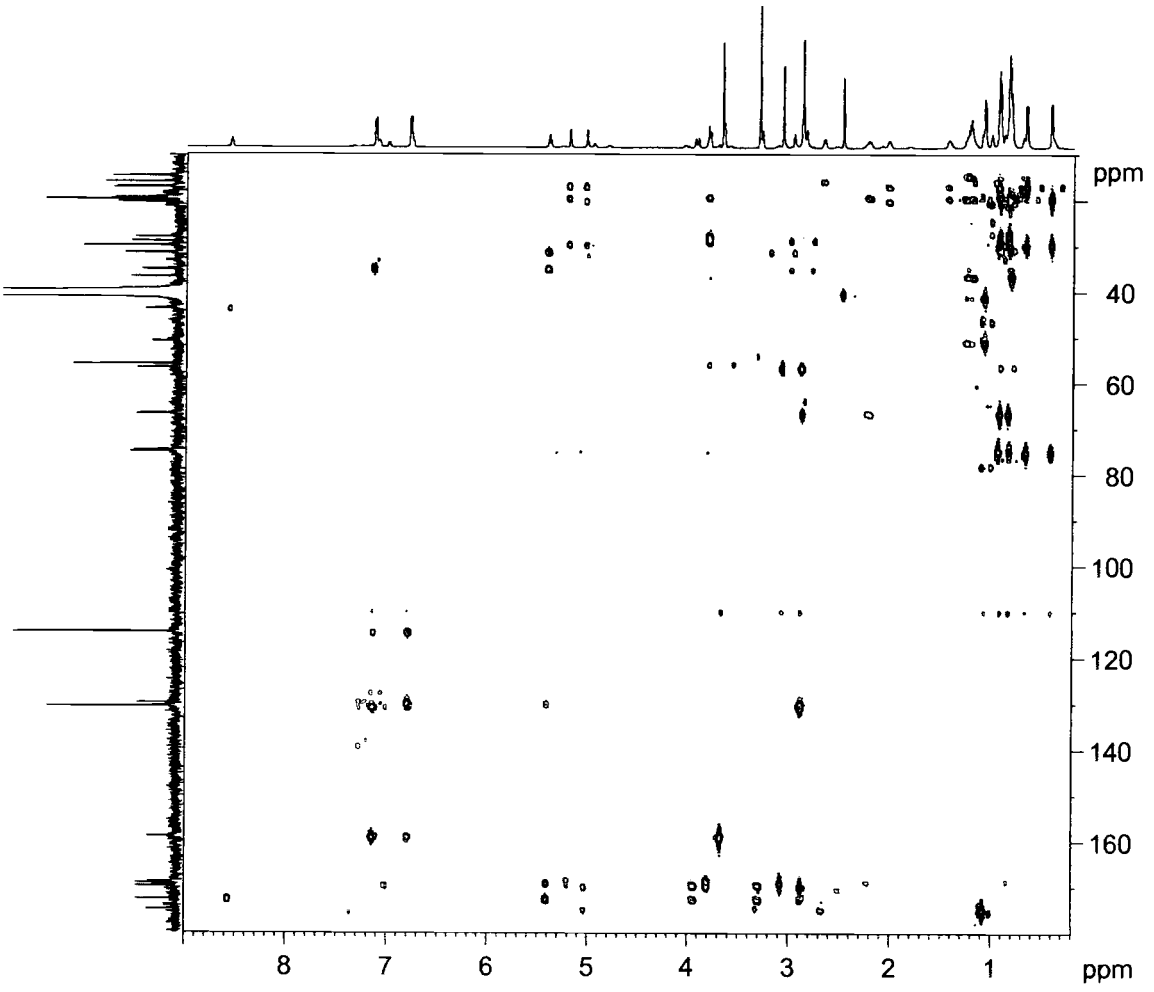

Figure IV.15 HMBC spectrum of wewakamide (**153**) in DMSO-d_6.

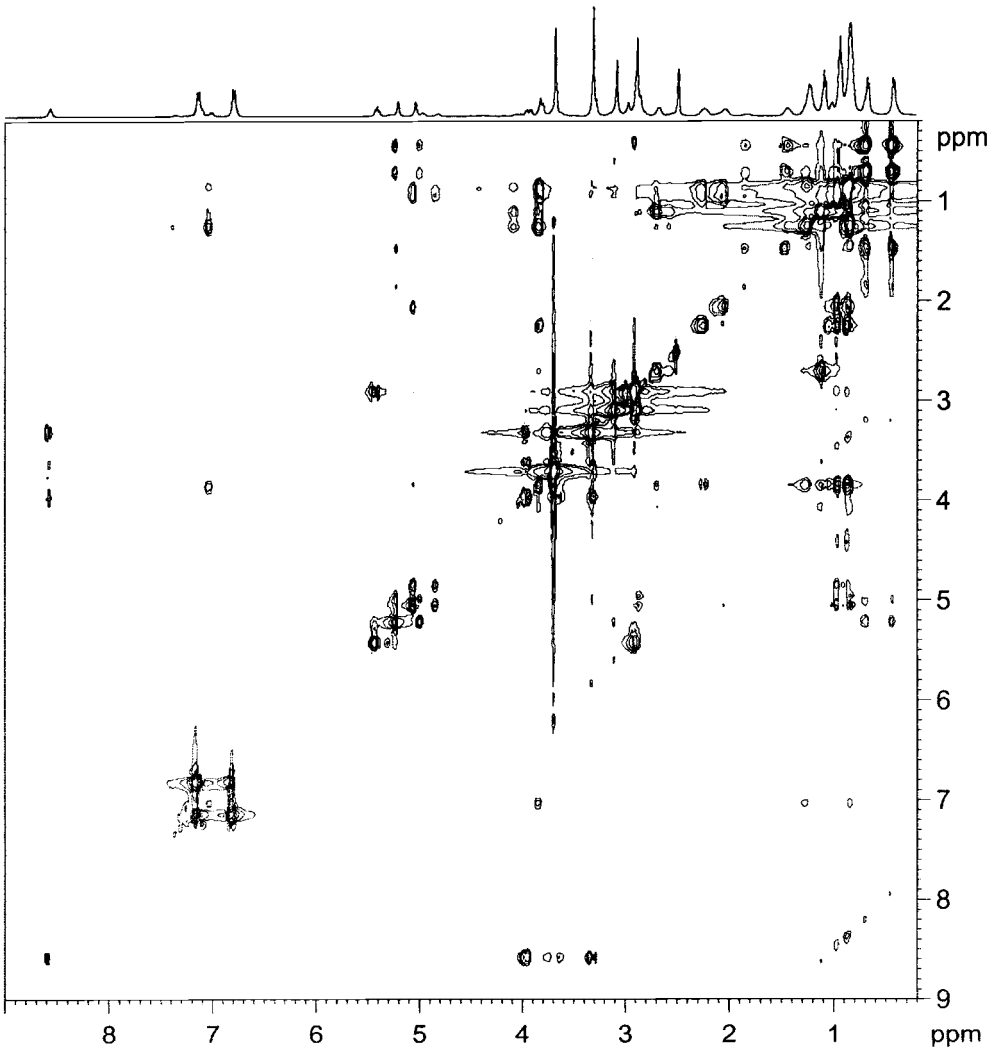

Figure IV.16 TOCSY spectrum of wewakamide (**153**) in DMSO-d_6.

H-2, H-7, and H-33/C-1; *N*H (δ 7.00), H-9/C-8; *N*H (δ 8.84), H-9, H-11/C-10; H-11, H-20, H-22/C-21; H-22, H-27, and H-28/C-26; and H-27, H-31, and H-33/C-32, giving rise to the sequence of Hiv-2/Maha/Gly/*N,O*-diMeTyr/Hiv-1/*N*-MeVal as indicated in **153**. Evidence for the linkage between *N*-MeVal and Hiv-2 were provided from HMBC data which showed correlations of *N*-CH_3 and α-H of Hiv-2 to carbonyl carbon of Hiv-2.

The absolute configurations of the α-hydroxy and α-amino acids in wewakamide (**153**) were determined by Marfey analysis and GC-MS method. Derivatization of the acid hydrolysate of **153** with Marfey reagent, followed by HPLC analyses with amino acid standards yielded *L-N*-MeVal and *D-N,O*-diMeTyr. Since standard *D-N,O*-diMeTyr could not be obtained commercially, the *L*-form was derivatized with the *D*-Marfey reagent. HPLC analysis of this derivative (*D*-Marfey-*L-N,O*-diMeTyr) has retention time identical to the enantiomeric *L*-Marfey-*D-N,O*-diMeTyr. By chiral GC-MS analysis, only *L*-Hiv was observed from the acid hydrolysate of wewakamide (**153**).

Guinamide A (**155**) has a molecular formula of $C_{39}H_{59}N_5O_9$ calculated from the HR FABMS which gave a strong $[M + H]^+$ peak. Similar to the previously discussed metabolites, clairamide B (**152**) and wewakamide (**153**), the IR spectrum of guinamide A (**155**) gave characteristic absorption bands at 1742 and 1666 cm^{-1}, indicative of ester/amide carbonyl functionalities. Of the 13 degrees of unsaturation inherent to the molecular formula, four could be accounted for by a phenyl group as suggested in the ^1H NMR spectrum (Figure IV.17). In addition, the peptidic nature of **155** was indicated by exchangeable *N*H protons resonating at δ 8.94 and δ 6.66. Two distinct *N*CH_3 proton singlets were also observed in the ^1H NMR data at δ 3.27 and δ 2.87. Two other high field CH_3 proton singlets were also observed at δ 1.28 and δ 1.29. Thirty-nine carbon signals were observed in the ^{13}C NMR data (Figure IV.18) of guinamide A (**155**), which include characteristic low field aromatic carbon signals suggesting a mono-substituted phenyl group as well as signals belonging to amide/ester carbonyls in the 165-180 ppm range. Two oxygenated sp^3 carbons resonating at δ 78.2 and δ 77.9 were also detected in the ^{13}C NMR spectrum.

From 1D and 2D NMR data, including HMBC and TOCSY, seven substructures were assembled for guinamide A (**155**), including five α-amino acids, *N*-MePhe, Pro, *N*-MeVal, Ala, and Gly; and two hydroxy acids, 2-hydroxy-isovaleric acid (Hiv) and 2,2-

dimethyl-3-hydroxy-hexanoic acid (Dmhha) (Figure IV.19). The latter hydroxy acid, Dmhha, is a new β-hydroxy acid unit to be reported from a cyanobacterial metabolite and was deduced solely from HMBC and TOCSY data. For instance, the proton spin system from H-3 to H-6 in the Dmhha unit was revealed in the TOCSY data. Extensive proton correlations were also observed from the HMBC data, confirming the planar structure of this unique β-hydroxy acid. Key HMBC correlations were: H-7 and H-8 to C-1, C-2, C-3; H-3 to C-1, C-2, C-4, and C-5; H-4 to C-3, C-5, and C-6; and H-6 to C-4 and C-5.

The sequence of these seven moieties in guinamide A (**155**) was established mainly from HMBC correlations (Figure IV.20). Sequential HMBC correlations were observed between H-22, H-20, H-12/C-21; H-12, H-10, *N*H (δ 8.94)/C-11; H-10, H-3/C-9; H-3, H-7, H-8, H-36/C-1; H-36, *N*H (δ 6.66)/C-35; and H-31, H-27/C-32, which gave rise to the Pro/*N*-MePhe/Gly/Dmhha/Hiv/Ala/*N*-MeVal sequence. A connection between *N*-MeVal and Pro was not observed in the HMBC spectrum. However, this was the only possibility to connect these residues and satisfy the degrees of unsaturation dictated by the molecular formula. The conformation of the Pro amide bond in **155** was depicted as *cis* due to $\Delta\delta_{\beta\gamma}$ (differential value of C_β and C_γ in Pro) value of 9.6 (see chapter 2 for further discussion).

Absolute stereochemistries of the α-amino/hydroxy acid units in guinamide A (**155**) were determined by either Marfey or chiral GC-MS analysis, which indicated the presence of *L*-Pro, *L*-*N*-MeVal, *L*-Ala, *D*-*N*-MePhe, and *L*-Hiv.

An $[M + H]^+$ peak observed in HR FABMS for guinamide B (**156**) suggested a molecular formula of $C_{40}H_{55}N_5O_7$, accounting for 16 degrees of unsaturation. The peptidic nature of this molecule was again established from tell-tale exchangeable *N*H protons resonating at δ 8.84 and δ 5.86 in the ^{1}H NMR data (Figure IV.24). Similarly to guinamide A (**155**), four singlet CH_3 proton signals (δ 3.02, δ 3.44, δ 1.23, and δ 1.20) were present in the ^{1}H NMR data. The two low field singlet proton signals at δ 3.02 and δ 3.44 suggested *N*-methylations. Six distinct low field carbon signals, due to ester/amide carbonyls, were observed in the ^{13}C NMR data of guinamide B (**156**) (Figure

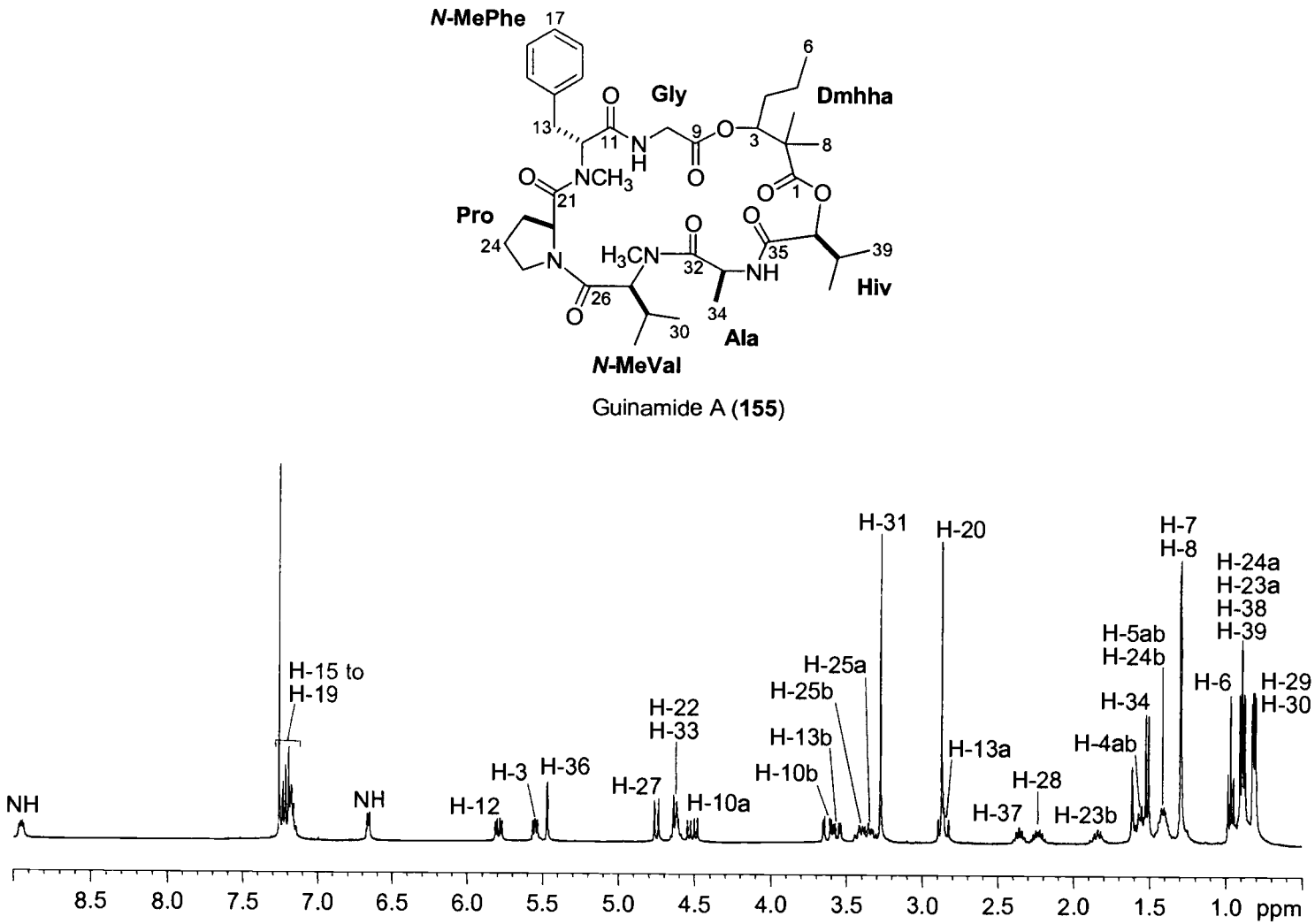

Figure IV.17 ^{1}H NMR spectrum of guinamide A (**155**) in $CDCl_3$.

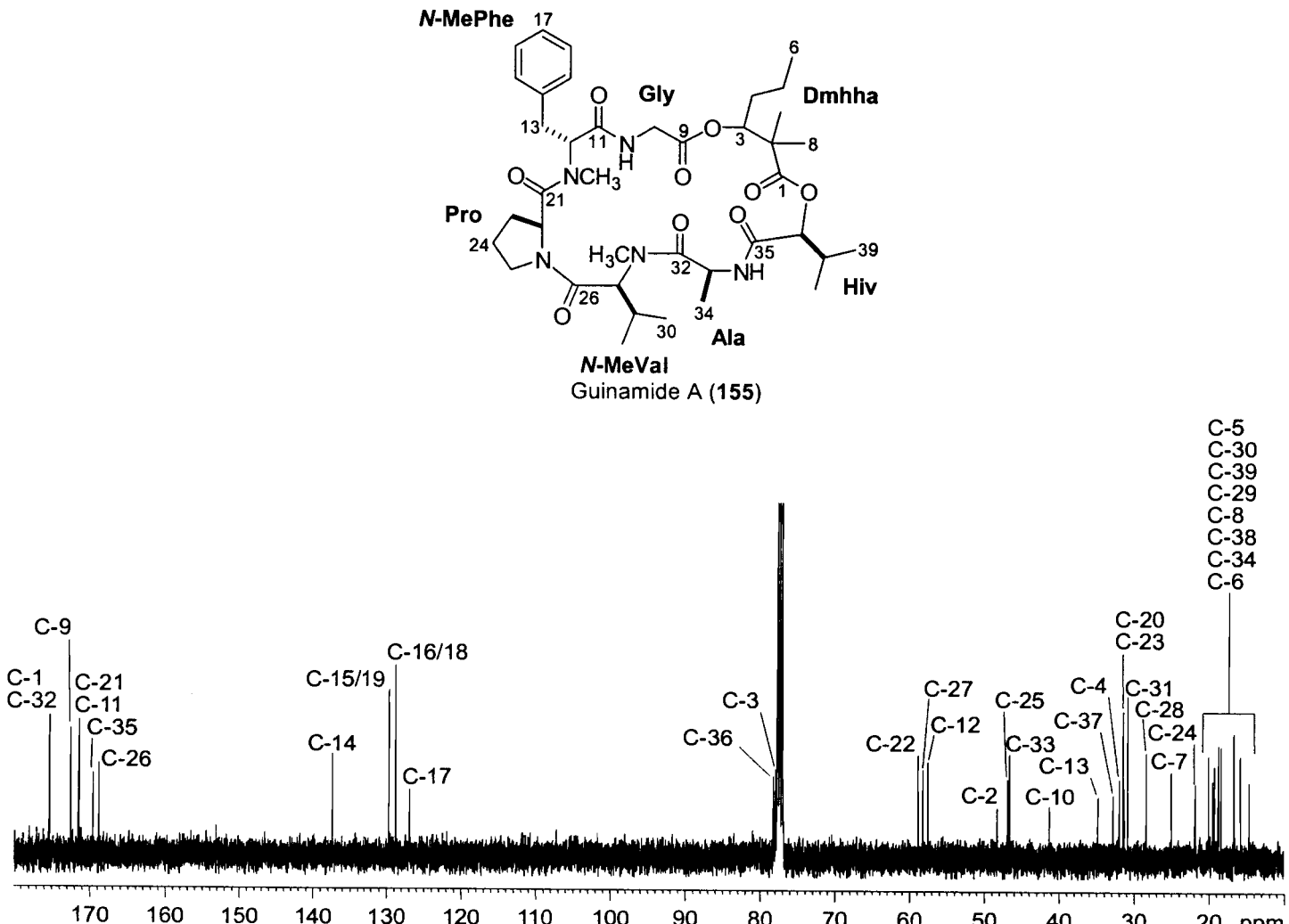

Figure IV.18 ^{13}C NMR spectrum of guinamide A (**155**) in $CDCl_3$.

Table IV.5 NMR spectral data for guinamide A (**155**) at 400 MHz (^{1}H) and 100 MHz (^{13}C) in $CDCl_3$.

Position	^{1}H	mult	*J* (Hz)	^{13}C	HMBC
			2,2-dimethyl-3-hydroxy-hexanoic acid (Dmhha)		
1				175.2	
2				48.2	
3	5.54	dd	7.1, 5.3	77.9	18.3, 20.0, 25.0, 31.9, 48.2, 172.5, 175.2
4ab	1.56	m		31.9	14.6, 20.0, 77.9
5ab	1.40	m		20.0	
6	0.96	t	7.2	14.6	20.0, 31.9
7	1.29	s		25.0	18.3, 48.2, 77.9, 175.2
8	1.28	s		18.3	25.0, 48.2, 77.9, 175.2
				Gly	
9				172.5	
10a	4.51	dd	18.0, 8.2	41.2	171.5, 172.5
10b	3.62	dd	18.0, 4.1		171.5, 172.5
*N*H	8.94	brdd	8.0, 4.0		171.5
				***N*-MePhe**	
11				171.5	
12	5.79	dd	12.1, 4.8	57.5	31.4, 34.7, 137.5, 171.5, 175.6
13a	2.86	m		34.7	57.5, 129.7, 137.5, 171.5
13b	3.55	dd	15.0, 4.8		57.5, 129.7, 137.5, 171.5
14				137.5	
15/19	7.19	m		129.7	
16/18	7.21	m		128.8	
17	7.17	m		127.0	
20 (*N*-CH_3)	2.87	s		31.4	57.5, 171.6
				Pro	
21				171.6	
22	4.61	m		58.8	21.7, 31.3, 46.8, 171.6
23a	0.89	m		31.3	21.7
23b	1.84	m			21.7, 58.8, 171.6
24a	0.90	m		21.7	
24b	1.40	m			
25a	3.35	m		46.8	21.7, 31.3
25b	3.40	m			
				***N*-MeVal**	
26				168.8	
27	4.74	d	10.9	58.1	18.7, 19.4, 28.3, 30.8, 168.8, 175.2
28	2.23	m		28.3	18.7, 19.4, 58.1, 168.8
29	0.81	d	6.7	18.7	19.4, 28.3, 58.1
30	0.79	d	6.4	19.4	18.7, 28.3, 58.1
31 (*N*-CH_3)	3.27	s		30.8	58.1, 175.2
				Ala	
32				175.2	
33	4.63	m		46.6	15.8, 175.2
34	1.51	d	7.2	15.8	46.6, 175.2
*N*H	6.66	brd	5.1		15.8, 46.6, 169.8

Table IV.5 (*continued*)

			2-hydroxy-isovaleric acid (Hiv)		
35				169.6	
36	5.46	d	2.2	78.2	16.6, 19.2, 32.7, 169.6, 175.2
37	2.35	m		32.7	16.6, 19.2
38	0.89	d	5.5	16.6	19.2, 32.7, 78.2
39	0.88	d	5.6	19.2	16.6, 32.7, 78.2

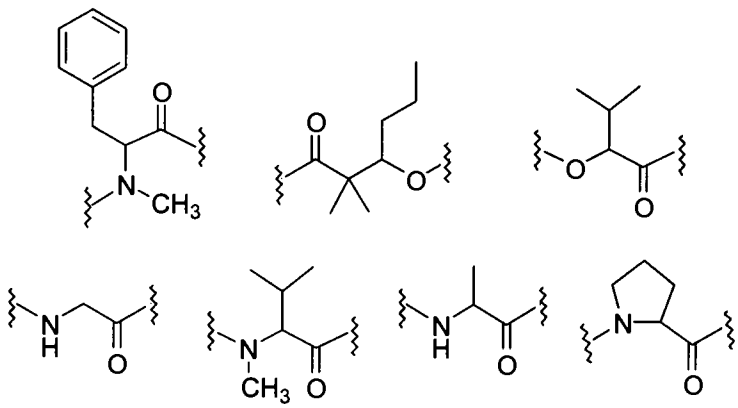

Figure IV.19 Partial structures of guinamide A (**155**).

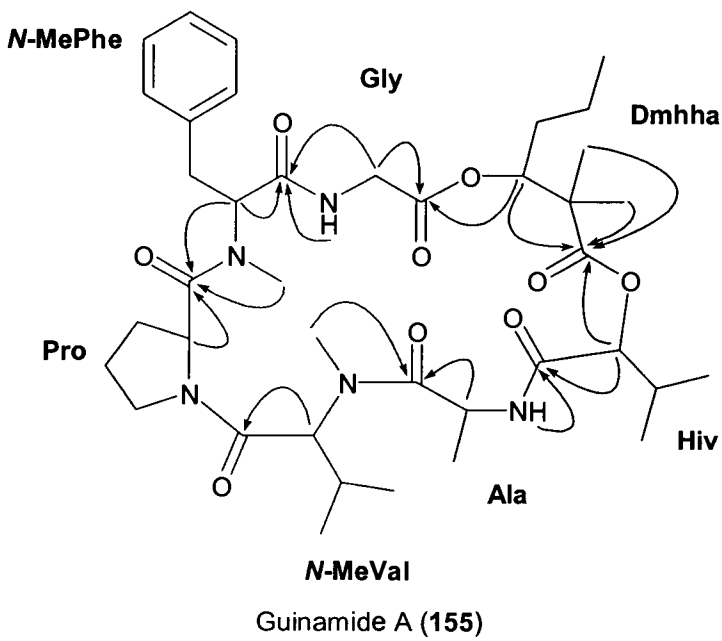

Figure IV.20 HMBC correlations in guinamide A (**155**).

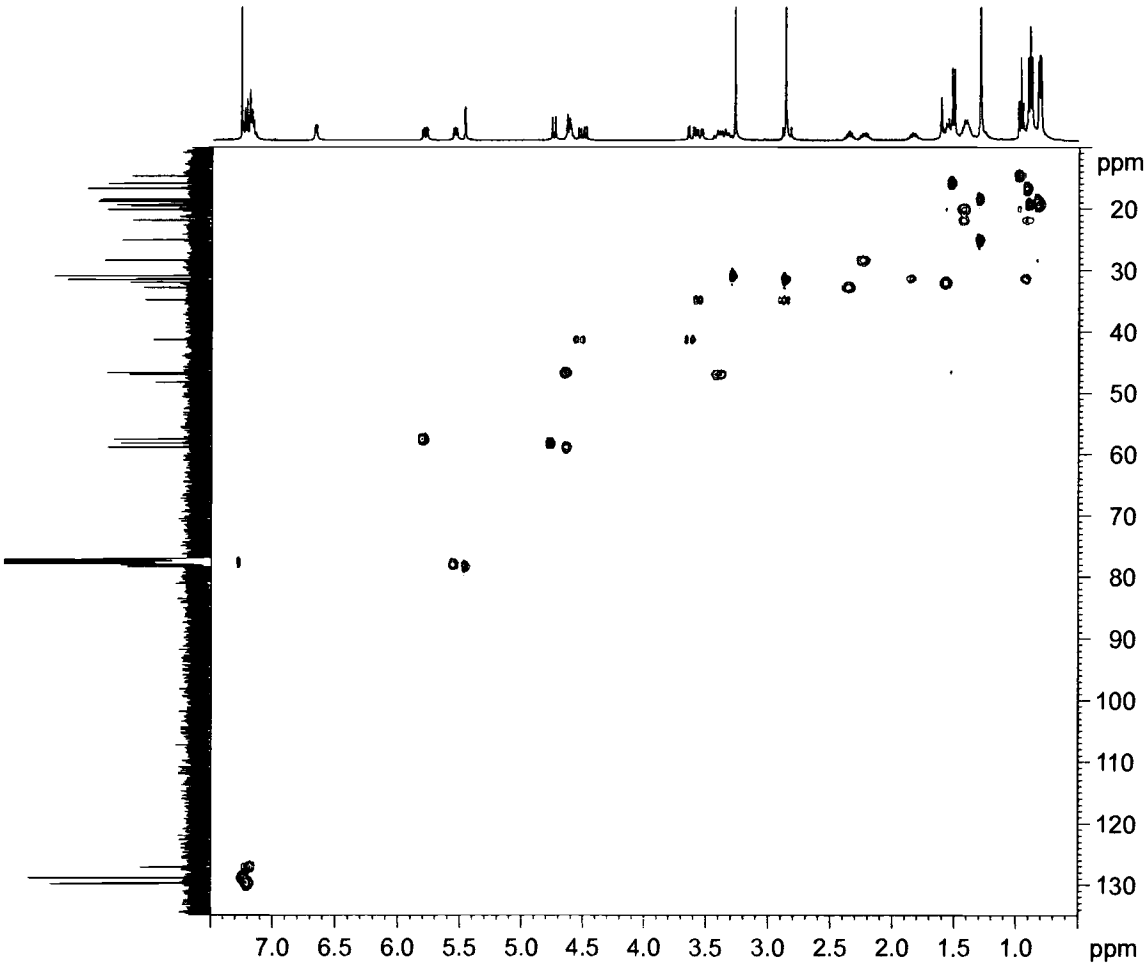

Figure IV.21 HSQC spectrum of guinamide A (**155**) in $CDCl_3$.

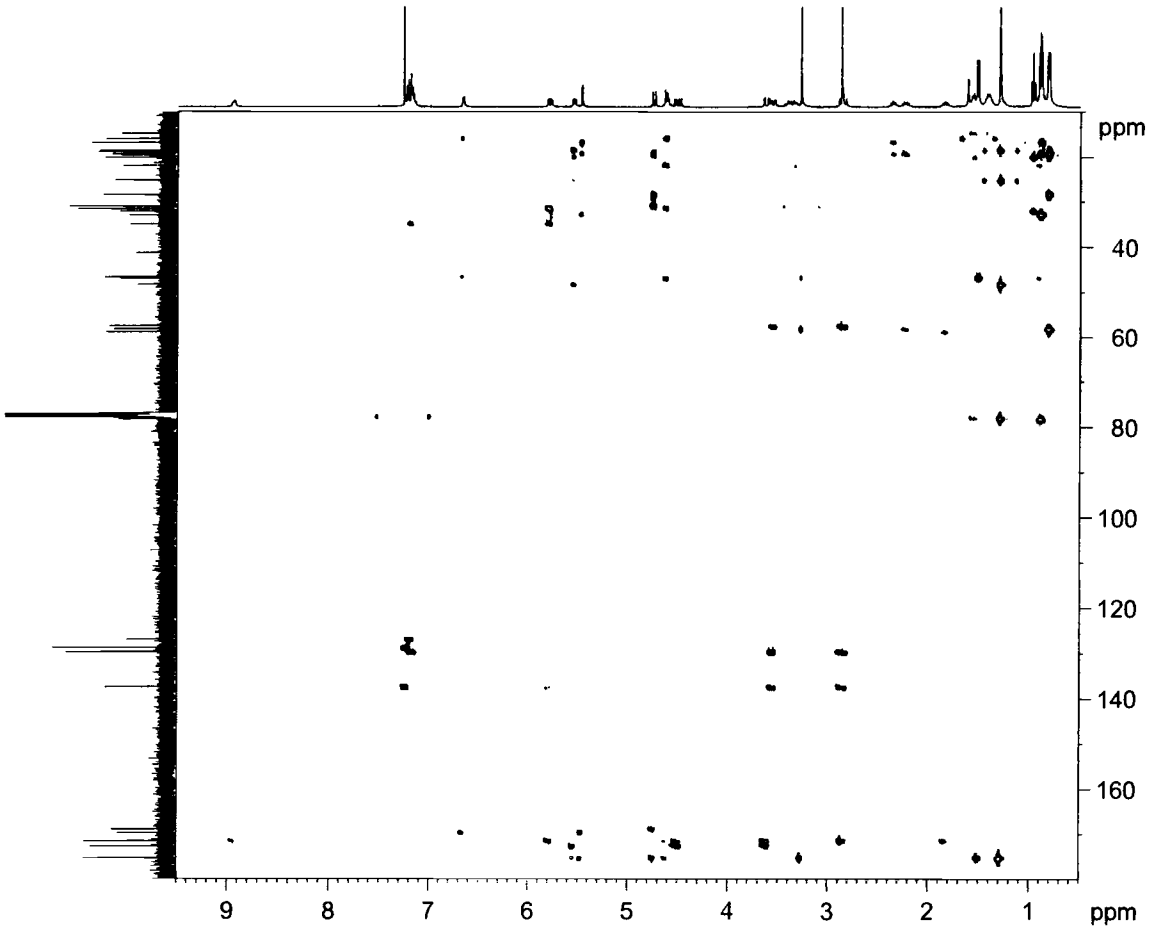

Figure IV.22 HMBC spectrum of guinamide A (**155**) in $CDCl_3$.

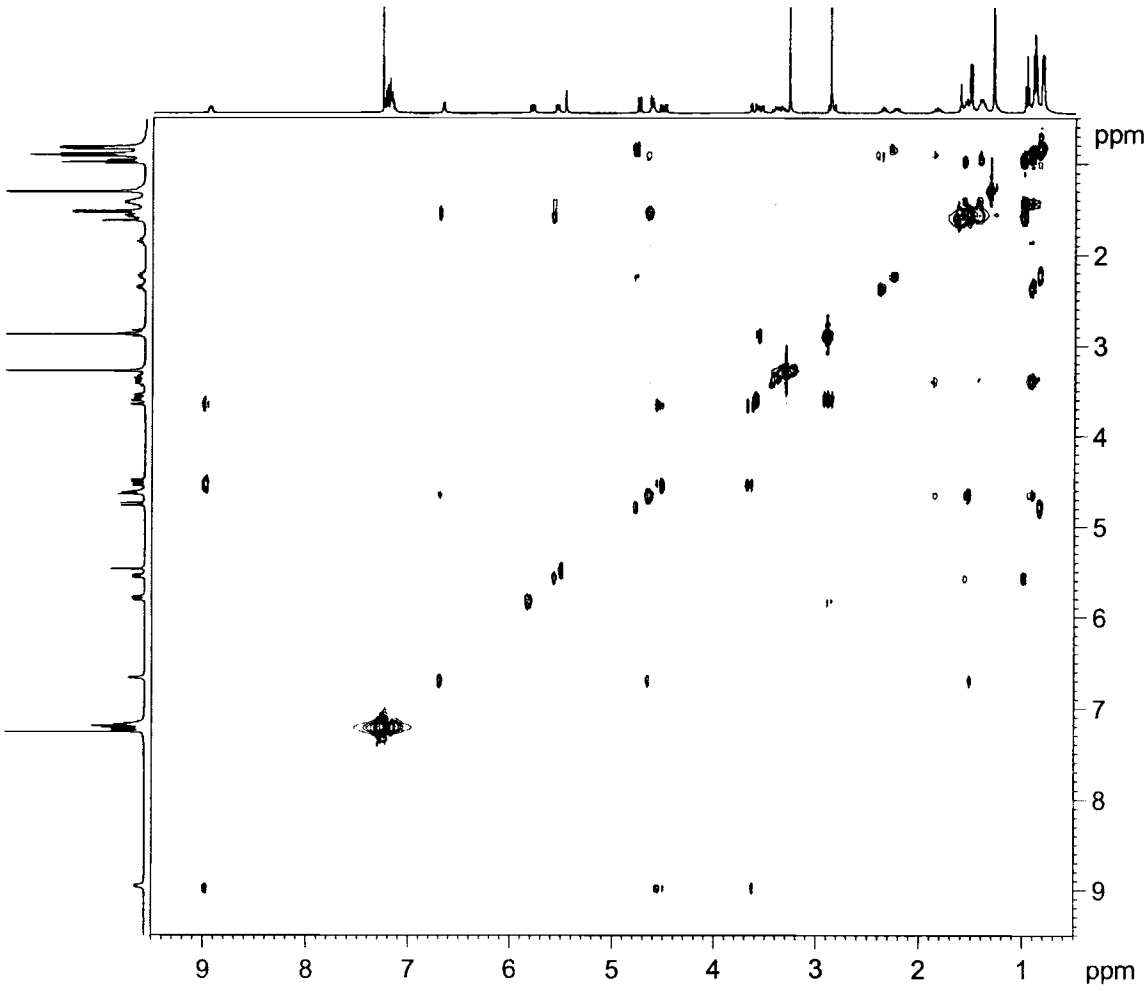

Figure IV.23 TOCSY spectrum of guinamide A (**155**) in $CDCl_3$.

IV.25). At least 12 olefinic carbon signals, with four peaks having two overlapping carbon signals, were present in the 128-132 ppm range. Taken together with low field aromatic proton signals (6.8–7.4 ppm) in the ^{1}H NMR data, two mono-substituted phenyl groups in **156** were suggested. In contrast to guinamide A (**155**), only one oxygenated sp^3 carbon signal was observed at δ 77.6. An interesting feature of the ^{1}H NMR spectrum of guinamide B was the presence of a shielded diastereotopic proton resonance at δ –0.03.

Careful analyses of TOCSY and HMBC data of guinamide B (**156**) revealed one residue less than in A (**155**). These six residues comprised of two units of *N*-MePhe, one Pro, one Val, one Gly and the unique Dmhha, which was also present in guinamide A (**155**) (Figure IV.26). The placement of the shielded proton signal at δ –0.03 was assigned as one of the methylene protons on β-C of the Pro unit. Such a shielding effect could arise from the influence of nearby aromatic amino acids, such as *N*-MePhe-1 and *N*-MePhe-2 in the molecule. In addition, as in guinamide A, the Pro amide bond in guinamide B was deduced to be in the *cis* conformation due to $\Delta\delta_{\beta\gamma}$ value of 8.0. The structure elucidation of the Dmhha unit in guinamide B (**156**) was based on a similar rationale to that used in A (**155**).

The final planar structure of guinamide B as depicted in **156** was determined from key proton correlations observed in the HMBC data (Figure IV.27). These correlations were: H-23, H-20, H-12/C-21; H-12, H-13, H-10, *N*H (δ 8.84), H-10/C-11; H-10, H-3/C-9; H-3, H-7, H-8, H-37, *N*H (δ 5.86)/C-1; and H-27, H-28, H-35/C-36. This gave the sequence of Pro/*N*-MePhe-1/Gly/Dmhha/Val/ *N*-MePhe-2. The sequence of Pro/*N*-MePhe-1/Gly/Dmhha was also present in guinamide A (**155**). Although no HMBC correlations were detected for the *N*-MePhe-2-Pro sequence, it is the remaining linkage needed to account for the degrees of unsaturation calculated from the molecular formula.

Marfey analysis was used for the absolute stereochemical assignment of the α-amino acids in guinamide B (**156**). HPLC analyses of the Marfey-derivatized hydrolysate of **156** as well as amino acid standards gave peaks corresponding to *L*-Pro, *L*-*N*-MePhe-1/2, and *L*-Val.

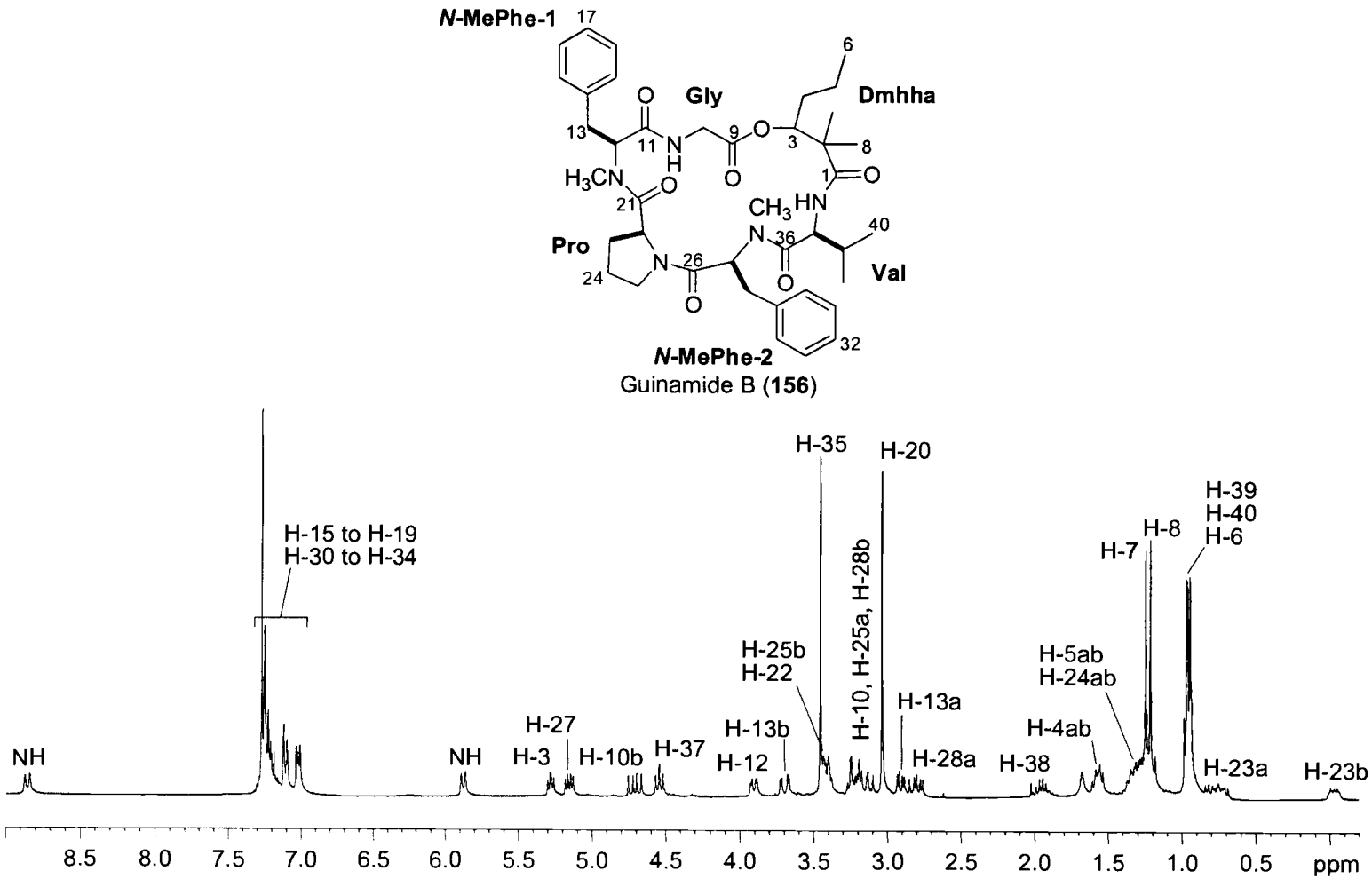

Figure IV.24 ^{1}H NMR spectrum of guinamide B (**156**) in $CDCl_3$.

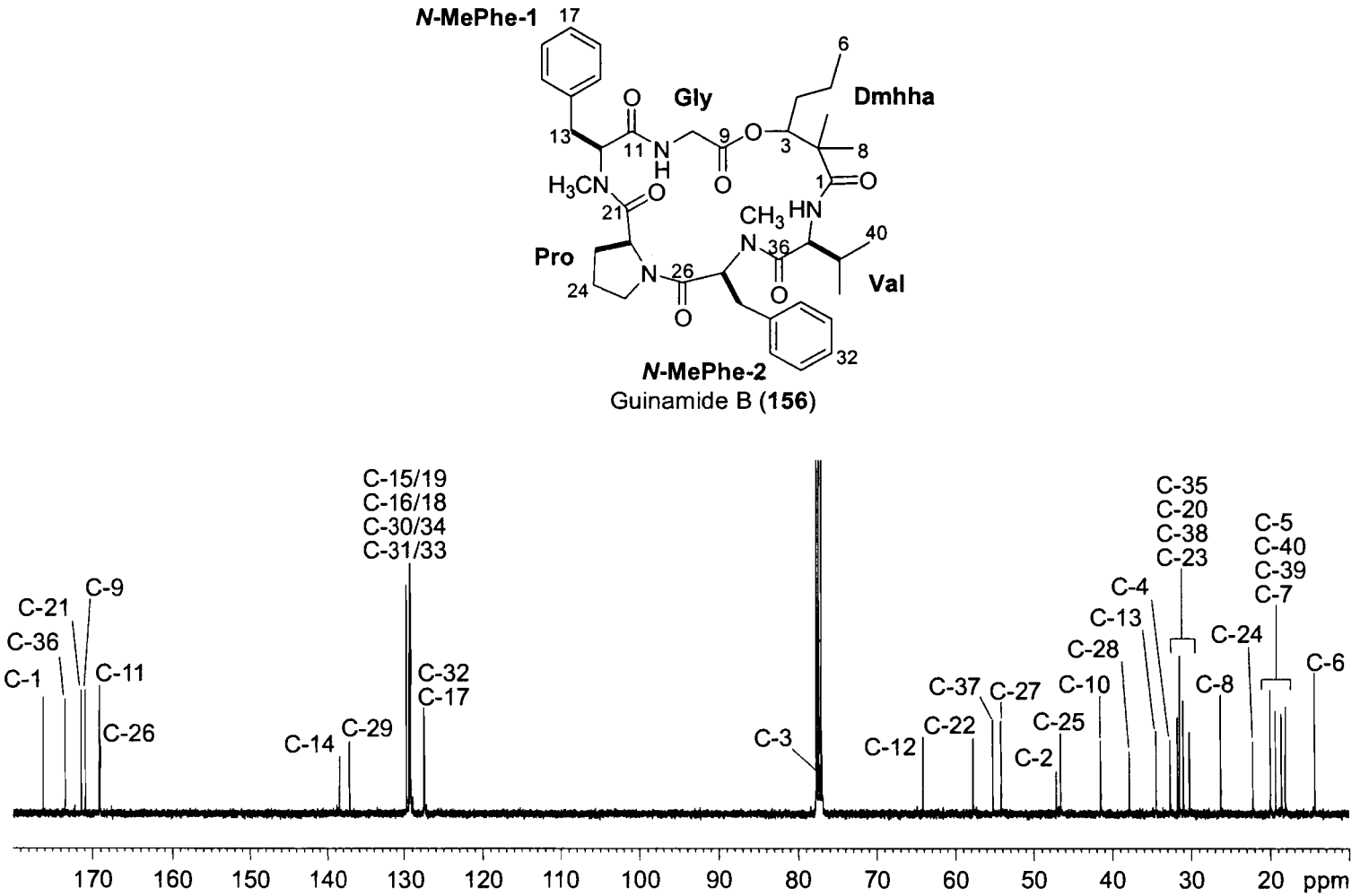

Figure IV.25 ^{13}C NMR spectrum of guinamide B (**156**) in $CDCl_3$.

Table IV.6 NMR spectral data for guinamide B (**156**) at 400 MHz (^{1}H) and 100 MHz (^{13}C) in $CDCl_3$.

Position	^{1}H	mult	J (Hz)	^{13}C	HMBC
			2,2-dimethyl-3-hydroxy-hexanoic acid (Dmhha)		
1				176.1	
2				47.1	
3	5.27	brt	6.0	77.6	18.0, 20.0, 26.2, 32.6, 47.1, 171.0, 176.1
4a	1.55	m		32.6	14.4, 20.0, 47.1, 77.6
4b	1.55	m		32.6	14.4, 20.0, 47.1, 77.6
5a	1.31	m		20.0	
5b	1.31	m		20.0	
6	0.95	m		14.4	
7	1.23	s		18.0	26.2, 47.1, 77.6, 176.1
8	1.20	s		26.2	18.0, 47.1, 77.6, 176.1
					Gly
9				171.0	
10a	3.20	m		41.5	169.2, 171.0
10b	4.69	dd	16.9, 9.6		169.2, 171.0
*N*H	8.84	d	9.4		169.2
					***N*-MePhe-1**
11				169.2	
12	3.89	dd	10.2, 3.1	64.2	31.4, 34.5, 138.5, 169.2, 171.5
13a	2.87	dd	13.7, 10.2	34.5	64.2, 129.7, 138.5, 169.2
13b	3.68	dd	14.5, 3.1		64.2, 129.7, 138.5, 169.2
14				138.5	
15/19	7.10	m		129.7	34.5, 127.4
16/18	7.23	m		127.2	
17	7.23	m		127.4	
20 (*N*-CH_3)	3.02	s		31.4	64.2, 171.5
					Pro
21				171.5	
22	3.41	m		57.8	22.2, 30.2, 46.5
23a	0.74	m		30.2	22.2, 46.5, 171.5
23b	-0.03	m			22.2, 46.5, 171.5
24a	1.27	m		22.2	
24b	1.27	m			
25a	3.20	m		46.5	
25b	3.39	m			
					***N*-MePhe-2**
26				169.1	
27	5.14	dd	10.2, 4.9	54.2	31.7, 37.9, 137.2, 169.1, 173.4
28a	2.78	dd	12.6, 4.9	37.9	54.2, 129.3, 137.2, 169.1
28b	3.12	dd	12.6, 10.3		54.2, 129.3, 137.2, 169.1
29				137.2	
30/34	7.00	m		129.3	37.9, 127.5, 129.2
31/33	7.23	m		129.2	137.2
32	7.19	m		127.5	
35 (*N*-CH_3)	3.44	s		31.7	54.2, 173.4

Table IV.6 (*continued*)

					Val
36				173.4	
37	4.53	brt	7.4	55.2	18.5, 19.3, 31.0, 173.4, 176.1
38	1.93	m		31.0	18.519.355.2173.4
39	0.95	m		18.5	31.0, 19.3, 55.2
40	0.95	m		19.3	31.0, 18.5, 55.2
*N*H	5.86	d	7.9		176.1

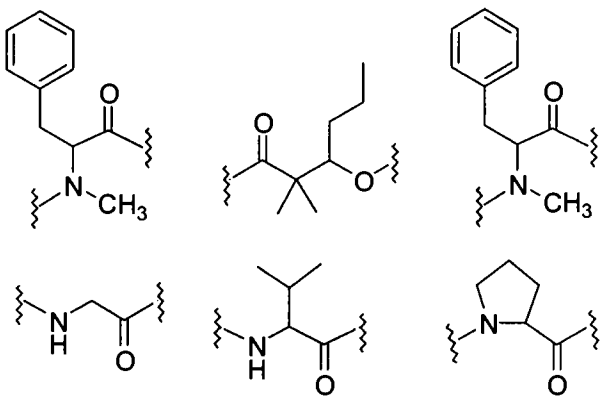

Figure IV.26 Partial structures of guinamide B (**156**).

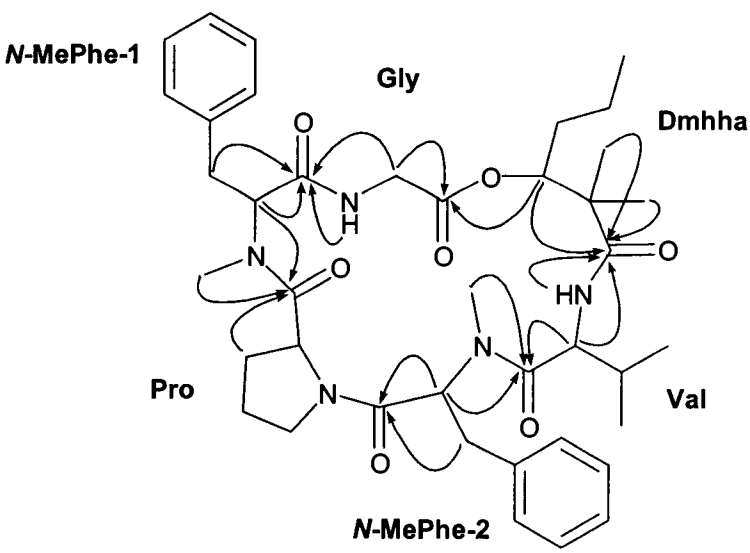

Guinamide B (**156**)

Figure IV.27 HMBC correlations in guinamide B (**156**).

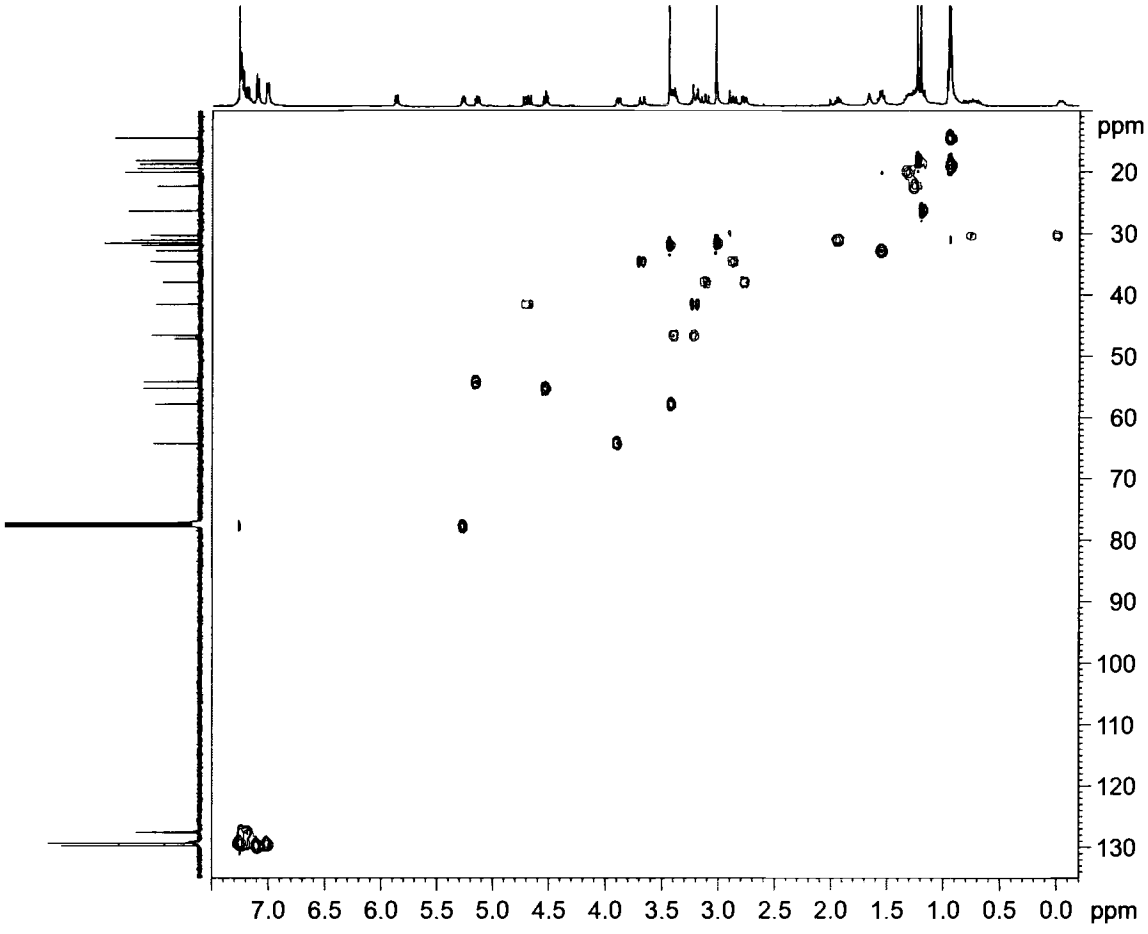

Figure IV.28 HSQC spectrum of guinamide B (**156**) in $CDCl_3$.

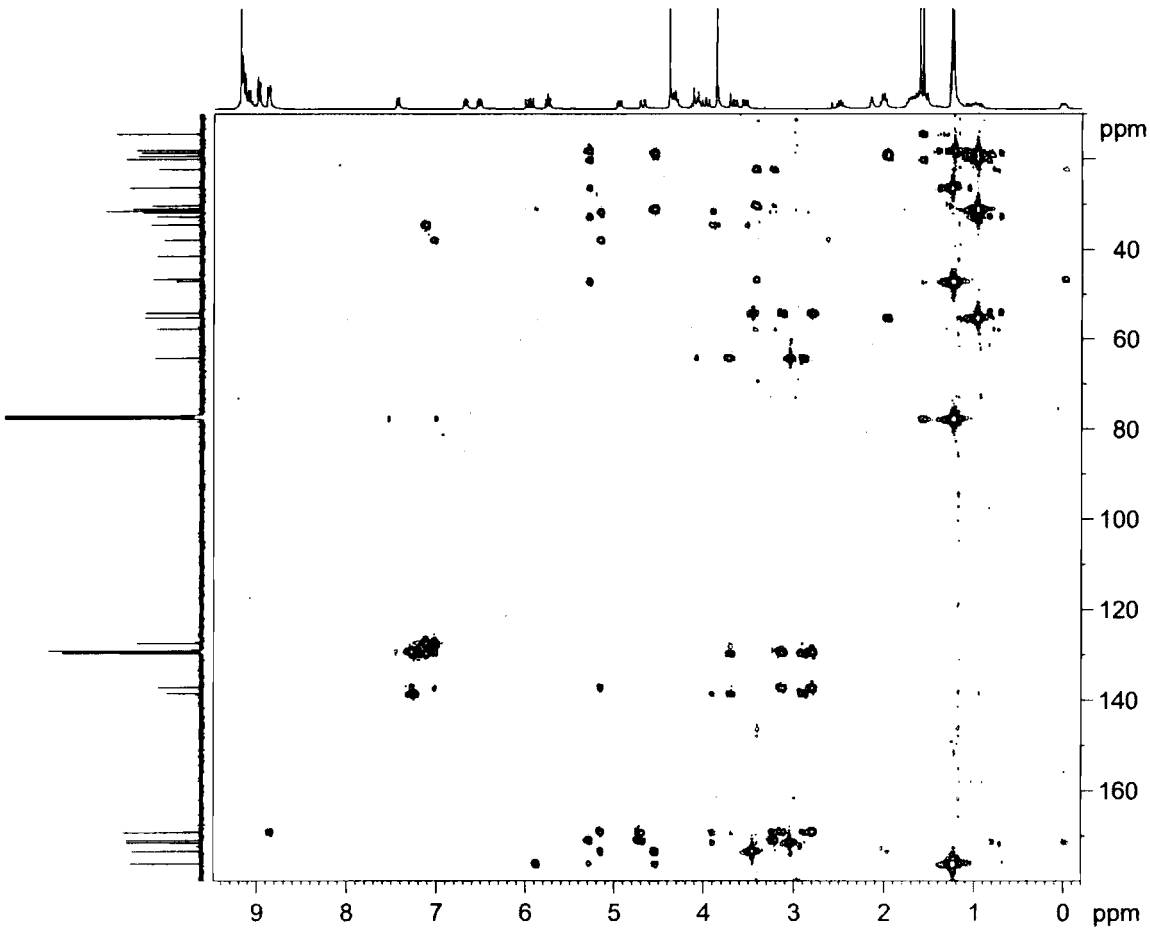

Figure IV.29 HMBC spectrum of guinamide B (**156**) in $CDCl_3$.

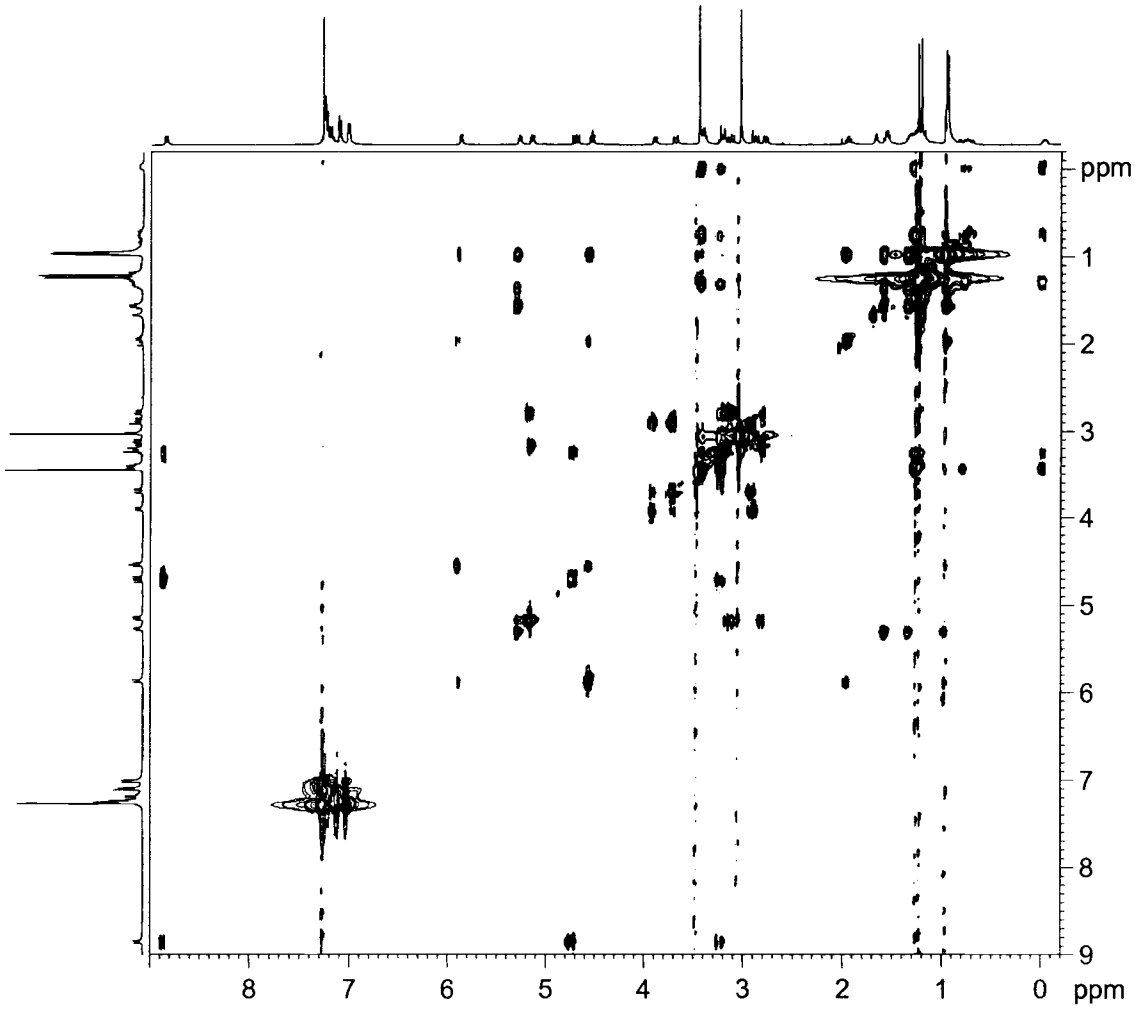

Figure IV.30 TOCSY spectrum of guinamide B (**156**) in $CDCl_3$.

Absolute Stereochemistry of the Mapa unit in Clairamide A (151)

Along with the above-mentioned novel cyclic depsipeptides, clairamide A (**151**) was also isolated from this collection of *Lyngbya majuscula* in high quantity relative to metabolites **152** to **156**. The planar structure and partial stereochemistry of clairamide A (**151**) were recently disclosed.[167] However, there remained two stereocenters yet to be determined, C-2 and C-3 of the Mapa (2-methyl-3-amino-pentanoic acid) unit in clairamide A (**151**). Several efforts involving NMR (e.g. HSQMBC experiments) as well as synthetic methods were utilized to determine the stereochemistry of this Mapa unit. Unfortunately, these efforts appeared to be fruitless. It was only through a fortuitous gift of a pure sample of 2*S*,3*R*-Mapa (**143**) from Professor Bates (University of Arizona) that allowed the unequivocal complete absolute stereochemical determination of clairamide A (**151**).

The approach used to determine the absolute stereochemistry of the Mapa unit in clairamide A (**151**) involved a combination of synthetic manipulation and the use of both *L*- and *D*-Marfey reagents. A summary of this approach is outlined in Figure IV.32. Through these methods, four distinct peaks, equating to the four stereoisomers of Mapa, were observed from HPLC analysis. These peaks were attributable to *L*-Marfey-2*S*,3*R*-Mapa (40.7 min), *D*-Marfey-2*S*,3*R*-Mapa (35.9 min; identical retention time as the enantiomer, *L*-Marfey-2*R*,3*S*-Mapa), *L*-Marfey-2*R*,3*R*-Mapa (39.3 min; 2*R*,3*R*-Mapa was obtained from epimerization of 2*S*,3*R*-Mapa), and *D*-Marfey-2*R*,3*R*-Mapa (36.4 min; identical retention time as the enantiomer, *L*-Marfey-2*S*,3*S*-Mapa). From careful analysis and co-injections with the Marfey derivatized natural Mapa unit from clairamide A, the absolute configurations were determined to be 2*S*,3*R* as indicated in **151**. The Mapa unit has also been reported in other marine metabolites such as majusculamide C (**135**), dolastatin 11 (**137**) and 12 (**138**), and the stereochemistries are identical.

These cyclic depsipeptides (**151** to **156**) represent novel compounds from the marine cyanobacterium, *Lyngbya majuscula* collected from Papua New Guinea. Table IV.7 is a summary of the constituents of these metabolites and it revealed a high occurrence of *N*-methylated amino acids, such as *N*-MeVal and *N*-MePhe. As for the α-

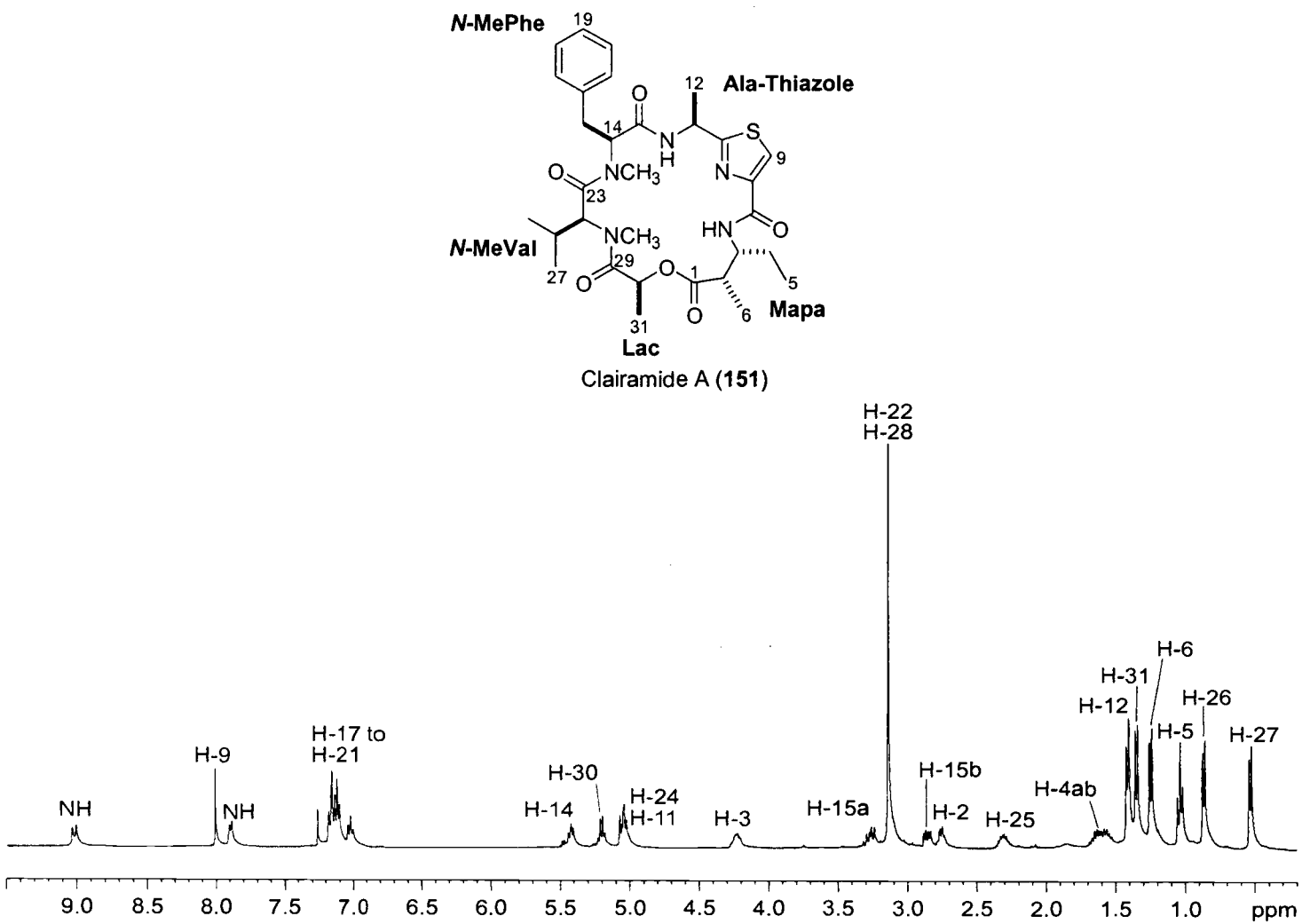

Figure IV.31 ^{1}H NMR spectrum of clairamide A (**151**) in $CDCl_3$.

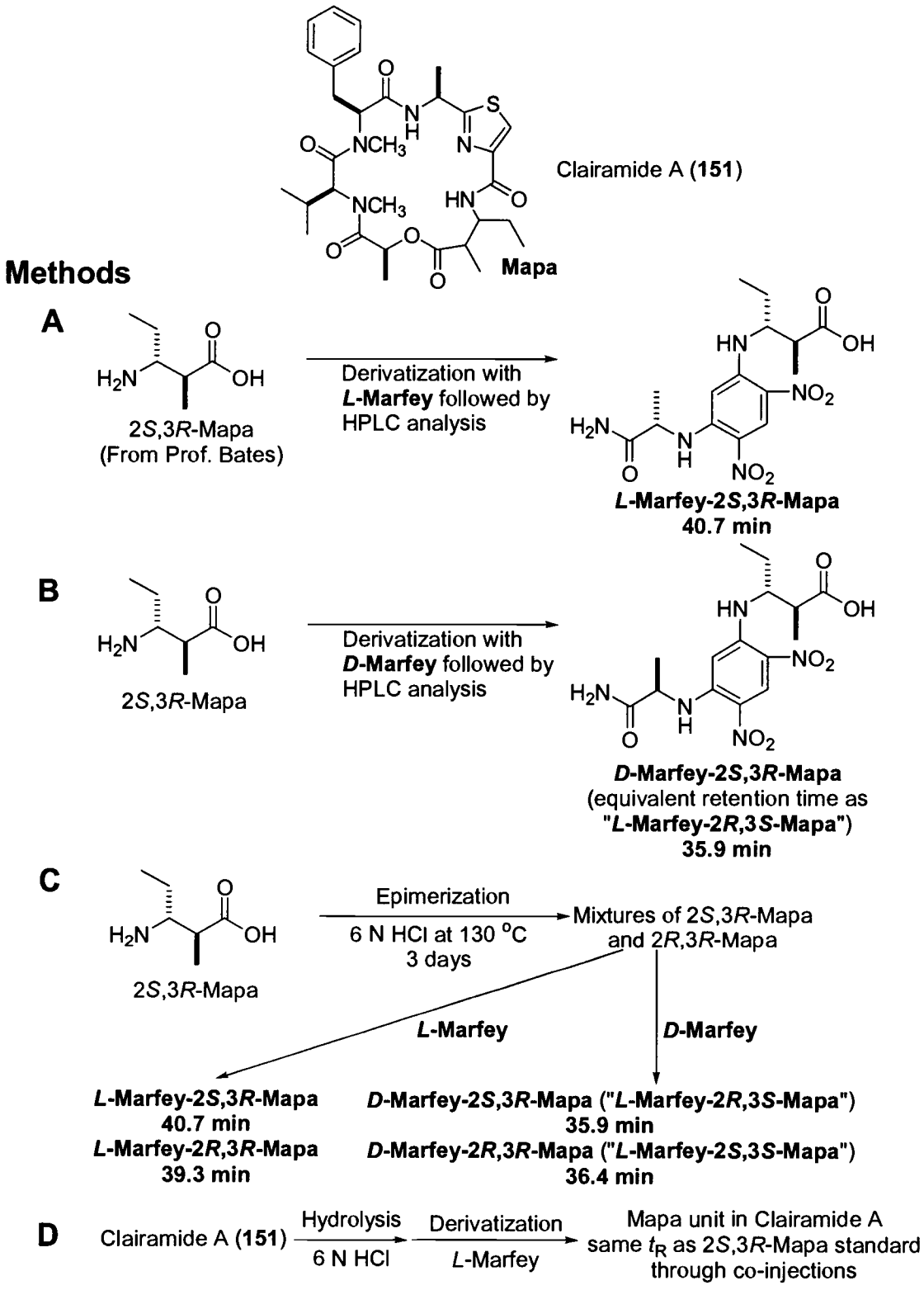

Figure IV.32 Absolute stereochemical analysis of the Mapa unit in clairamide A (**151**).

hydroxy acids, there was a preponderance of 2-hydroxy-isovaleric acid (Hiv). Together with the unique β-hydroxy/amino acids, these represent structural hallmarks of cyanobacterial metabolites, which are products of mixed PKS (polyketide synthase) and NRPS (non-ribosomal polypeptide synthetase) biosynthetic pathways.

The Maba unit in clairamide B (**152**) is also a moiety in a mollusk (*Dolabella auricularia*) metabolite, dolastatin D (**139**), thus, supporting the diet-derived hypothesis of compounds reported from sea-hares. In addition, the Dmhha unit present in the guinamides (**155** and **156**) is a new β-hydroxy acid residue to be reported from marine natural products.

Antifungal properties of these new cyclodepsipeptides were evaluated in a series of proprietary bioassays by our industrial collaborator and they exhibited biological activities against several fungal strains. Our in-house cytotoxicity bioassay using the neuro 2a mouse neuroblastoma cell line was also used to evaluate these compounds. Clairamide A (**151**) had no activity at 10 μg/mL while carliamide (**154**) and clairamide B (**152**) had only moderate activities with IC_{50} values of 16 μM and 15 μM, respectively.

Table IV.7 Constituents of the *Lyngbya majuscula* cyclic depsipeptides (**151** to **156**).

Compounds	α/β-Hydroxy/β-Amino acids	α-Amino acids	Heterocycle
Clairamide A (**151**)	lactic acid (Lac) 2-methyl-3-amino-pentanoic acid (Mapa)	*N*-MePhe, *N*-MeVal, Ala	Thiazole
Clairamide B (**152**)	2-hydroxy-isovaleric acid (Hiv) 2-hydroxy-3-amino-butanoic acid (Maba)	*N*-MePhe, *N*-MeVal, Ala	Thiazole
Carliamide (**154**)	2-hydroxy-3-methyl-pentanoic acid (Hmpa) 3-amino-2-methyl-oct-7-ynoic acid (Amoya)	*N,O*-diMeTyr, Val, *N*-MeAla,	
Wewakamide (**153**)	Two 2-hydroxy-isovaleric acid (Hiv) 2-methyl-3-amino-hexanoic acid (Maha)	*N,O*-diMeTyr, *N*-MeVal, Gly	
Guinamide A (**155**)	2-hydroxy-isovaleric acid (Hiv) 2,2-dimethyl-3-hydroxy-hexanoic acid (Dmhha)	*N*-MePhe, *N*-MeVal, Ala, Gly, Pro	
Guinamide B (**156**)	2,2-dimethyl-3-hydroxy-hexanoic acid (Dmhha)	Two *N*-MePhe, Val, Gly, Pro	

EXPERIMENTAL

General Experimental Procedures. 1D and 2D NMR experiments were measured on either a Bruker AM 400 MHz NMR spectrometer or a Bruker DRX600 spectrometer with the solvents, $CDCl_3$ or DMSO-d_6, used as an internal standards. Chemical shifts are reported in ppm and coupling constants (J) are reported in Hz. Mass spectra were recorded on a Kratos MS50TC mass spectrometer. Optical rotations were measured on either Perkin-Elmer 141 polarimeter or Perkin Elmer 243 polarimeter. GC-MS data were obtained on a Hewlett-Packard 5890 Series II GC connected to a Hewlett-Packard 5971 mass spectrometer. UV and IR spectra were recorded on Beckman DU® 640B and Nicolet 510 spectrophotometers, respectively. The isolation of **151** to **156** was performed on Waters Millipore® Model 590 and detected with Waters Millipore® Lambda-Max Model 480 LC spectrophotometer. All Marfey derivatized products were analyzed using Waters 515 HPLC Pump and Waters 996 Photodiode Array Detector.

Algal Collection. The marine cyanobacterium, *Lyngbya majuscula* Gomont (voucher specimen available as collection number PNSM-4/Sep/98-01) was collected by hand from reefs off Sea mountain (S 3° 33.237' E 143° 39.845', 2 miles north of Wewak) Papua New Guinea, at depth of 54 ft using SCUBA. Upon collection, the microalga was stored in 2-propanol at reduced temperature until workup.

Extraction and Isolation of the Clairamides (151 and 152), Carliamide (154), Wewakamide (153), and the Guinamides (155 and 156). Approximately 0.5 L wet weight of preserved alga was extracted with CH_2Cl_2-MeOH (2:1) three times to give ca. 3.0 g of crude organic extract. The organic extract was subjected to Si gel VLC using a stepped gradient elution from 100% hexanes to 50% EtOAc in MeOH, giving seven distinct fractions. Fraction 5, which showed antifungal activities, was purified further by Mega-Bond Sep-Pak RP-18 and HPLC on Phenomenex 10 C8 90A (250 × 4.6 mm), 34% H_2O in MeOH, to yield clairamides A (**151**, 10.0 mg), B (**152**, 1.7 mg), and carliamide (**154**, 2.0 mg). The second subfraction obtained from Mega-Bond Sep-Pak RP-18 was also subjected through further purification using HPLC on Phenomenex Luna 5μ Phenyl-hexyl (250 × 4.60 mm), 28% H_2O in MeOH to give guinamides A (**155**, 1.8 mg) and B (**156**, 3.7 mg). Fraction 6, obtained from Si VLC of the organic extract, was

subjected through similar purification steps involving Mega-Bond Sep-Pak RP-18 and HPLC on Phenomenex Phenyl-hexyl column, 23% H_2O in MeOH, yielding wewakamide (**153**, 9.5 mg).

Clairamide B (152): white amorphous solid $[\alpha]^{26}_D$ –5° (*c* = 0.17, $CHCl_3$); UV (EtOH) λ_{max} 213 nm (ϵ 24900); IR (neat) 3308, 2967, 2934, 1730, 1628, 1549, 1520, 1255, 1084, 752 cm^{-1}; LR FABMS *m/z* 628 (48), 244 (14), 196 (100), 134 (51), 86 (61); HR FABMS (positive ion, 3-nitrobenzyl alcohol) *m/z* obs. $[M + H]^+$ 628.3161 ($C_{32}H_{46}N_5O_6S$, 0.8 mmu dev.); ^1H NMR (600 MHz, $CDCl_3$) and ^{13}C NMR (100 MHz, $CDCl_3$) see Table IV.3.

Wewakamide (153): white amorphous solid $[\alpha]^{26}_D$ +55° (*c* = 0.95, $CHCl_3$); UV (EtOH) λ_{max} 210 nm (ϵ 21200); IR (neat) 2965, 2935, 1731, 1663, 1514, 1248, 1182 cm^{-1}; LR FABMS *m/z* 689 (100), 274 (46), 164 (38), 121 (19), 86 (24); HR FABMS (positive ion, 3-nitrobenzyl alcohol) *m/z* obs. $[M + H]^+$ 689.4130 ($C_{36}H_{57}N_4O_9$, 0.4 mmu dev.); ^1H NMR (600 MHz, DMSO-d_6) and ^{13}C NMR (100 MHz, DMSO-d_6) see Table IV.4.

Guinamide A (155): white amorphous solid $[\alpha]^{26}_D$ –2.7° (*c* = 0.18, $CHCl_3$); UV (EtOH) λ_{max} 215 nm (ϵ 38300); IR (neat) 3259, 2966, 2937, 1742, 1666, 1631, 1203, 753 cm^{-1}; LR FABMS *m/z* 742 (100), 267 (10), 217 (10), 134 (25), 107 (24); HR FABMS (positive ion, 3-nitrobenzyl alcohol) *m/z* obs. $[M + H]^+$ 742.4383 ($C_{39}H_{60}N_5O_9$, 0.8 mmu dev.); ^1H NMR (400 MHz, $CDCl_3$) and ^{13}C NMR (100 MHz, $CDCl_3$) see Table IV.5.

Guinamide B (156): white amorphous solid $[\alpha]^{26}_D$ –49° (*c* = 0.37, $CHCl_3$); UV (EtOH) λ_{max} 215 nm (ϵ 28700); IR (neat) 3301, 2962, 1745, 1661, 1640, 1524, 1198, 752 cm^{-1}; LR FABMS *m/z* 718 (100), 196 (12), 134 (83), 107 (11), 97 (14); HR FABMS (positive ion, 3-nitrobenzyl alcohol) *m/z* obs. $[M + H]^+$ 718.4197 ($C_{40}H_{56}N_5O_7$, 1.8 mmu dev.); ^1H NMR (400 MHz, $CDCl_3$) and ^{13}C NMR (100 MHz, $CDCl_3$) see Table IV.6.

Ozonolysis of Clairamide B (152). A stream of O_3 was carefully bubbled into a vial containing 1 mL of CH_2Cl_2 solution of **152** (200 μg) at 25 °C for about 10 min. Solvent was removed under a stream of N_2 and the resulting residue was subjected to acid hydrolysis and derivatization as described below.

Stereochemical Determination of Clairamide B (152). Hydrolysis of the ozonolyzed clairamide B (**152**) was achieved in 1 mL of 6 N HCl placed a sealed ampoule at 120 °C for 20 h. Traces of HCl were removed *in vacuo*. The resulting hydrolysate was resuspended in 100 μL of H_2O. A portion of the aqueous acid hydrolysate (50 μL) was derivatized with *N*α-(2,4-dinitro-5-fluoro-phenyl)-*L*-alaninamide (FDAA). HPLC analyses of the FDAA-derivatized hydrolysate of **152** and standard FDAA-derivatized amino acids were carried out on Waters NOVAPAK C_{18} (3.9 × 150 mm column) with a linear gradient of triethylammonium phosphate (50 mM, pH 3.0)/MeCN 90:10 to 60:40 in 60 min at 1 mL/min (UV detection at λ 340 nm). The analyses established the presence of *L*-*N*-MePhe (36.79 min; *D*-*N*-MePhe, 37.01 min), *L*-*N*-MeVal (25.67 min; *D*-*N*-MeVal, 28.01 min), and *L*-Ala (11.21 min; *D*-Ala, 14.80 min).

Absolute Stereochemistry of the 2-Hydroxyisovaleric Acid (Hiv) Moiety in Clairamide B (152). Aqueous layer of the acid hydrolysate of **152** (50 μL) was dried under a stream of N_2 gas. The hydrolysate was diluted in 0.4 mL of diethyl ether and treated with diazomethane for 10 min. Excess CH_2N_2 was removed under a stream of N_2. Capillary GC-MS analyses were carried out on a Chiralsil-Val column (Alltech, 25 × 0.25 mm) and the conditions were: a 11 psi initial head pressure and a column temperature held at 40 °C for 10 min after injection of the sample, then from 100 °C to 150 °C at a rate of 15 °C/min, and finally held at 150 °C for 5 min. The retention time found for the clairamide B-derived Hiv was found at 8.30 min. Standards of *D*- and *L*-Hiv were also converted to the corresponding methyl ester derivatives by the same procedure and analyzed on chiral GC-MS (*D*-Hiv, 9.10 min; *L*-Hiv, 8.30 min).

Synthesis of the *D*-Marfey reagent (1-Fluoro-2,4-Dinitrophenyl-5-*D*-Alanine amide). A sample of *D*-Ala-NH_2.HCl (236.0 mg) was dissolved in 1.95 mL 1 N NaOH. This was followed by the addition of 30 mL acetone and 5 g of anhydrous $MgSO_4$. The mixture was stirred for 3 h, followed by the removal of $MgSO_4$ by filtration. FFDNB (334.0 mg, 1,5-difluoro-2,4-dinitrobenzene) was dissolved in 7.5 mL acetone. To this solution was added drop-wise under magnetic stirring the acetone solution of *D*-Ala-NH_2. After addition, contents were stirred for an additional 30 min. About 30 mL of H_2O was added, resulting in formation of golden-yellow scales which were filtered,

washed first with a little 2:1 H_2O-acetone mixture, then with H_2O and finally dried in the air, kept in the dark. The yield obtained for the *D*-Marfey reagent was 150.0 mg (33 %).

Stereochemical Determination of Wewakamide (153). Compound **153** (0.2 mg) was treated with 1 mL of 6 N HCl and the suspension was heated at 110 °C for 18 h. Excess HCl were removed *in vacuo* and the resulting hydrolysate was resuspended in 100 μL of H_2O. This was divided into two equal portions and subjected to Marfey analysis and GC-MS on a chiral column using the same method as for clairamide B (**152**). The standard *L-N,O*-diMeTyr was derivatized with *D*-Marfey, which gave retention time identical to *D-N,O*-diMeTyr derivatized with *L*-Marfey. This was used as the *D-N,O*-diMeTyr equivalent in the amino acid analysis in **153**. The following amino acids were observed in wewakamide: *L-N*-MeVal (36.43 min; *D-N*-MeVal, 38.33 min) and *D-N,O*-diMeTyr (38.33 min; *L-N,O*-diMeTyr, 37.26 min). From the chiral column GC-MS analyses, only *L*-Hiv was observed from the acid hydrolysate of **153**.

Stereochemical Determination of Guinamides A (155) and B (156). Absolute stereochemical determination of amino acid units in guinamide A (**155**, 0.1 mg) was carried out using the same method outlined for clairamide B (**152**) and gave the corresponding amino acids from Marfey analysis: *L*-Pro (22.33 min; *D*-Pro, 25.79 min), *L-N*-MeVal (36.45 min; *D-N*-MeVal, 40.12 min), *L*-Ala (20.63 min; *D*-Ala, 25.98 min), and *D-N*-MePhe (39.32 min; *L-N*-MePhe, 38.38 min). Hiv unit in **155** was determined as *L*-form in the chiral GC-MS analysis. Similar method was also used for the absolute stereochemical determination of amino acid units present in guinamide B (**156**). Marfey analysis gave the following results: *L*-Pro (22.32 min; *D*-Pro, 25.78 min), *L*-Val (28.22 min; *D*-Val, 35.53 min), and *L-N*-MePhe (38.38 min; *D-N*-MePhe, 39.32 min).

Epimerization of 2(*S*)-Methyl-3(*R*)-Amino-Pentanoic acid (Mapa). 1.0 mg of 2*S*,3*R*-Mapa (**143**) was dissolved in 1 mL of 6 N HCl and transferred into a high-pressure tube. The content was heated at 130 °C for 3 days. After 3 days the excess HCl was dried under a stream of N_2 and redissolved in 1 mL of H_2O. The aqueous solution was divided into two equal portions and derivatized with either *L*- or *D*-Marfey according to procedure outlined in clairamide B (**152**).

Marfey Analysis of 2(*S*)-Methyl-3(*R*)-Amino-Pentanoic acid (Mapa). Pure samples of 2*S*,3*R*-Mapa (**143**, 0.5 mg) were derivatized with *L*-Marfey and analyzed on

HPLC using RP-18 column to give a retention time of 40.7 min. Derivatization of the pure sample (0.5 mg) with *D*-Marfey and analyzed in a similar way gave a retention time of 35.9 min. Contents from the epimerization experiments above were also derivatized with either *L*- or *D*-Marfey and analyzed on HPLC. Four peaks were observed and these are attributable to *L*-Marfey-2*S*,3*R*-Mapa (40.7 min), *L*-Marfey-2*R*,3*R*-Mapa (39.3 min), *D*-Marfey-2*S*,3*R*-Mapa (35.9 min), and *D*-Marfey-2*R*,3*R*-Mapa (36.4 min). By coinjection with the derivatized Mapa unit from clairamide A, the retention time was found to be 40.7 min, concluding the stereochemistry of 2*S*,3*R* in **151**.

CHAPTER FIVE

A NOVEL CYTOTOXIC MACROLIDE AND CYCLIC DEPSIPEPTIDES FROM A PAPUA NEW GUINEA MARINE CYANOBACTERIUM *LYNGBYA BOUILLONII* HOFFMANN AND DEMOULIN

ABSTRACT

Three novel cytotoxic natural products were isolated from a marine cyanobacterium *Lyngbya bouillonii* collected from Papua New Guinea. These metabolites comprised of two structural classes; the cyclic depsipeptides bouillonamides A (**161**) and B (**162**) and a macrolide, lyngbouilloside (**163**). In addition to these metabolites, a recently described cyanobacterial molecule, apratoxin (**164**) was also isolated from this marine blue-green alga. The isolation of these compounds was aided by a bioassay-guided fractionation based on a cytotoxicity assay using neuro 2a mouse neuroblastoma cells. Planar structures of **161** to **163** were established by 1D and 2D NMR experiments, including the multi-edited HSQC, TOCSY, HMBC, and ROESY experiments. Absolute stereochemistries of the α-amino acids in **161** and **162** were determined mainly by Marfey analysis. Bouillonamide A (**161**), a 25-membered cyclic depsipeptide, contains two unique moieties: a 2-methyl-6-methylamino-hex-5-enoic acid (Mmaha) moiety and a polyketide synthase-derived unit of 5-hydroxy-3-methyl-heptanoic acid (Hmha). In addition, bouillonamide A contained four α-amino acids residues (two *N*-MePhe, one Val, and one *N*-MeThr). A β-amino acid, Maha (2-methyl-3-amino-hexanoic acid) was present in bouillonamide B (**162**) along with an Ala-Thiazole, a *N*-MePhe, a *N*-MeVal, and a Lac (lactic acid) residue. The macrolide, lyngbouilloside (**163**), is a 14-membered lactone which contained a unique sugar unit of 2,4-di-*O*-methylrhamnopyranoside. Bouillonamides A (**161**), B (**162**), and lyngbouilloside (**163**) exhibited IC_{50}'s of 6.0 μM, 16.0 μM, and 17.0 μM, respectively, against neuro 2a mouse neuroblastoma cells. Apratoxin (**164**) was also cytotoxic with an IC_{50} of 1.0 μM.

INTRODUCTION

In nature, marine blue-green algae are found in brackish waters as well as in shallow coastal tidal pools. Some species of marine cyanobacteria, such as *Lyngbya* species, occur as filamentous tufts, forming extensive algal mats. With the exception of some species of nudibranchs which feed on these microalgae, these cyanobacteria appear to be largely undisturbed. It has been rationalized that they produce secondary metabolites that confer protection from predation by herbivorous fishes. Such ecological observations have prompted natural products chemists to examine marine cyanobacteria for their chemical constituents in the hope of discovering molecules with unique biological properties. In recent years, such endeavors have rewarded natural products chemists with a plethora of unique and biologically active molecules from marine cyanobacteria. As highlighted in the introduction and in the preceding chapter of this thesis, a majority of these secondary metabolites belong to the lipopeptide structural class.

As part of our drug discovery program at OSU, we have been making several trips to Papua New Guinea for the purpose of collecting marine cyanobacteria. It was in one of these trips that we chanced upon an intriguing subtidal and filamentous species of *Lyngbya* having cobweb-like morphology (Figure V.1). Closer examination of this species in the laboratory identified this microalga as *Lyngbya bouillonii* Hoffmann and Demoulin (Oscillatoriacea), formally described in 1991 with type locality from Hansa Bay, Laing Island, Papua New Guinea.[178] This cyanobacterium is readily recognized in nature by its thallus morphology where it forms tenacious mats, attaching to either dead corals of the *Acropora* varieties or to other calcareous matter, covering small pockets or cavities in the reef. In the course of collecting this marine cyanobacterium, we often encountered commensal snapping shrimps entangled with the microalga. Presumably, these invertebrates are found living in close association with the cyanobacterium, especially in cavities covered by the cyanobacterial mats.

Since the discovery of *Lyngbya bouillonii* in 1991, a number of interesting secondary metabolites have been characterized from this species (Figure V.2). These include four macrolides; lyngbyaloside (**68** in Figure I.13),[80] laingolide A (**157**),

laingolide (**158**),[179] and madangolide (**159**),[180] and a linear tetrapeptide, lyngbyapeptin (**160**).[181] However, due to the small amount of these compounds that were isolated as well as the unstable nature of these metabolites, no biological activities have been reported. The absolute stereoconfiguration of lyngbyapeptin (**160**), recently isolated from another cyanobacterial species, *L. majuscula* Gomont at Apra Harbor, Guam, was resolved by Moore's group.[91] Interestingly, their collection of cyanobacterium resembled the description for *L. bouillonii* but they choose to use the description by Gomont for *L. majuscula* due to the lack of genetic information for direct comparison.

The biosynthesis of the laingolides (**157** and **158**) and madangolide (**159**) could be rationalized by having the 2,2-dimethylpropionic acid as the starter unit for a PKS (polyketide synthase), followed by three (madangolide) or four (laingolides) units of acetate extension, an unit of glycine added by an NRPS (non-ribosomal polypeptide synthetase), and finally one (laingolides) or three further units (madangolide) of acetate extension. Cyclization to the final products could coincide with cleavage from the final PKS module.

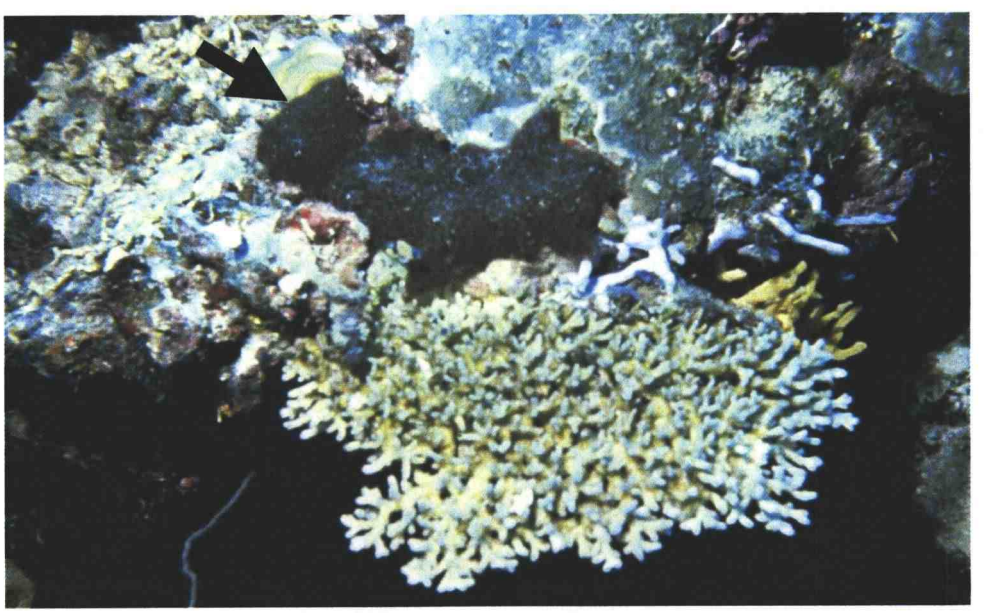

Figure V.1 Picture of *Lyngbya bouillonii* Hoffmann and Demoulin in nature.

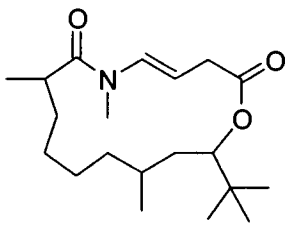

Laingolide A (**157**)

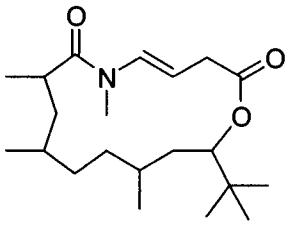

Laingolide (**158**)

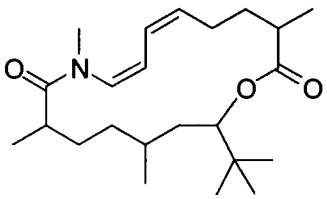

Madangolide (**159**)

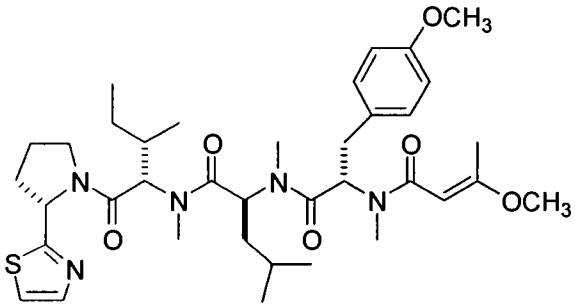

Lyngbyapeptin (**160**)

Figure V.2 Secondary metabolites isolated from *Lyngbya bouillonii*.

RESULTS AND DISCUSSION

The present sample of *Lyngbya bouillonii* Hoffmann and Demoulin from Papua New Guinea began with an initial collection in 1999. After it was found that the organic extract of this species possessed unique secondary metabolites by ^{1}H NMR, a second extensive recollection was made in the following year from the northern part of Papua New Guinea. Preliminary in-house bioassay screening of the organic extract of this cyanobacterium using the neuro-2a mouse neuroblastoma cell assay indicated cytotoxic activity. The organic extract was subjected through various chromatographic steps, including VLC and HPLC, coupled with a bioassay-guided fractionation to yield three novel cytotoxic molecules. These were two cyclic depsipeptides, bouillonamides A (**161**) and B (**162**), and a glycosidic macrolide, lyngbouilloside (**163**) (Figure V.3). A known cytotoxic compound, apratoxin (**164**), was also isolated from the organic extract (Figure V.4). The planar structure of apratoxin was recently disclosed by the Moore group at the Pacifichem conference, held in Honolulu Hawaii (14 – 19 December 2000). The gross structures of the new molecules reported in this thesis (**161** to **163**) were established mainly through detailed analyses of 1D as well as 2D NMR data. Marfey analysis was used to determine the absolute stereoconfigurations of the α-amino acids present in the cyclic depsipeptides (**161** and **162**).

Bouillonamide A (**161**) showed an $[M + H]^+$ peak at *m/z* 818.5068 for a molecular formula of $C_{46}H_{67}N_5O_8$ by high resolution FABMS (16 degrees of unsaturation). The ^{1}H NMR spectrum of **161** suggested a peptidic molecule due to the presence of an exchangeable *N*H proton at δ 6.02 as well as four CH_3 singlet protons observed between 2.6 - 3.2 ppm, which were indicative of *N*-methylation groups (Figure V.5). The IR spectrum of **161** gave strong absorption bands at 1726 and 1637 cm^{-1}, suggestive of ester and amide functionalities, respectively. A strong absorption band was also observed at 3440 cm^{-1}, indicating the presence of an –OH group in **161** involved in intramolecular hydrogen bonding. A total of 46 carbon signals could be observed from the ^{13}C NMR spectrum of **161** (Figure V.6). From the multi-edited HSQC data, these carbon signals were defined as six carbonyls, twelve olefinic

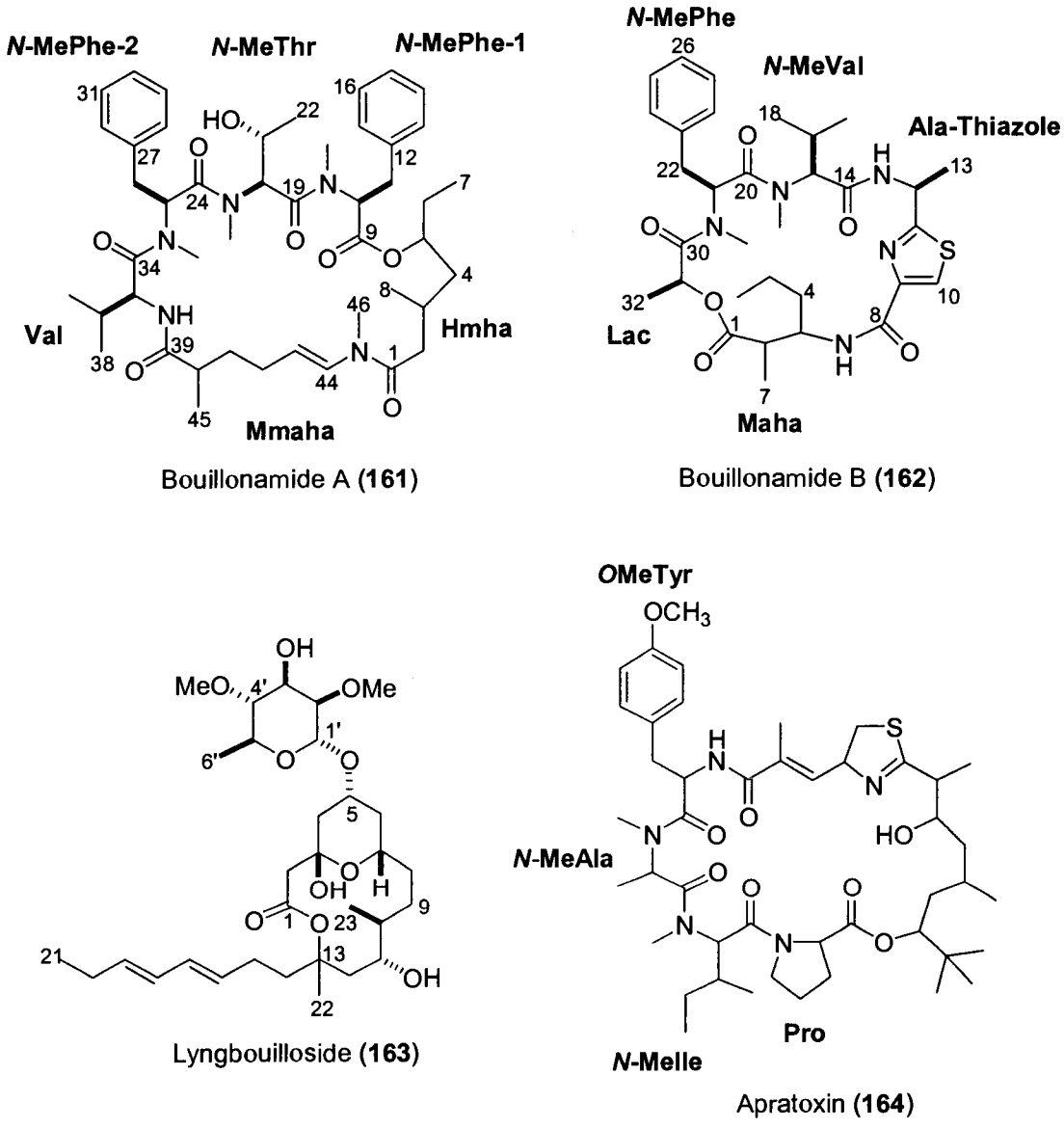

Figure V 3. Natural products from *Lyngbya bouillonii* (PNGRD 21/Aug/00-2).

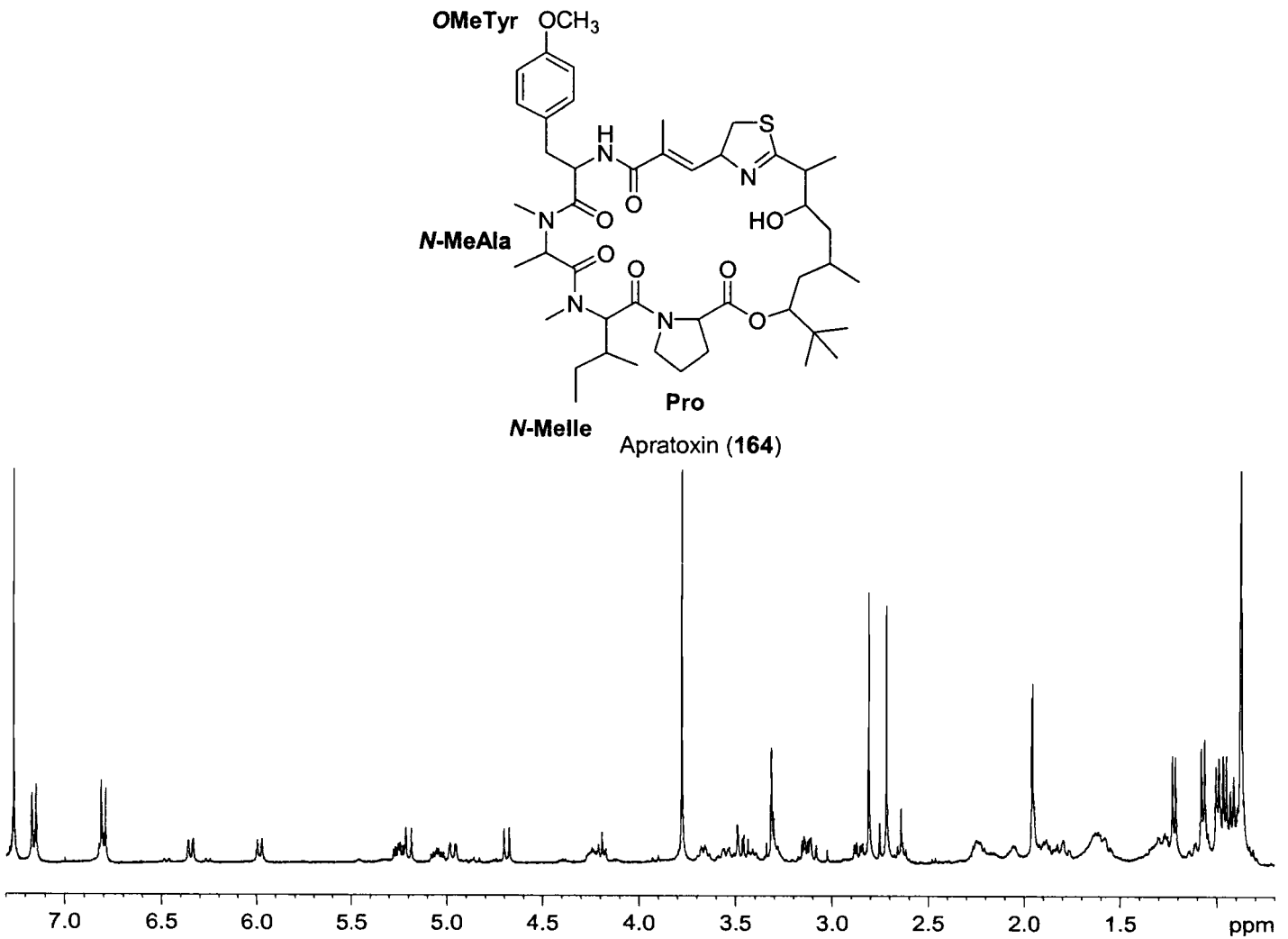

Figure V.4 ^{1}H NMR spectrum of apratoxin (**164**) in $CDCl_3$.

methines, two quaternary carbons (δ 138.0 and δ 136.5), nine sp^3 methines (two bearing oxygen, δ 67.8 and δ 76.6), seven methylenes, and ten methyls.

Six partial structures (A to F in Figure V.7) were generated using a combination of HSQC, HMBC, and TOCSY experiments. These include two *N*-MePhe residues, one *N*-MeThr residue, one Val residue, a 2-methyl-6-methylamino-hex-5-enoic acid (Mmaha) moiety, and a 5-hydroxy-3-methyl-heptanoic acid (Hmha) moiety. Evidence for two mono-substituted phenyl groups was obtained from ^{13}C NMR data which showed two sets of carbon signals attributable to these aromatic ring systems. HMBC correlations of proton signals, such as the α-Hs and β-Hs, to the aromatic carbon signals of these phenyl groups confirmed two *N*-MePhe units in **161**. These HMBC correlations were H_α-10/C_β-11, H_α-10/C-18; H_β-11/C-12, H_β-11/C-13 and C-17 in *N*-MePhe-1 and H_α-25/C_β-26, H_α-25/C-33, H_β-26/C-28 and C-32 in *N*-MePhe-2.

The key correlations in establishing an *N*-MeThr unit came from TOCSY and HMBC data. A proton doublet at δ 3.34 was assigned as a hydroxy proton due to the absence of any correlations in the HSQC data. TOCSY and HMBC data showed correlations from this hydroxy proton (δ 3.34) to H-20 (δ 4.54 d), H-21 (δ 3.85 m), and H-22 (δ 0.84 d) in the former data and to C-21 (δ 67.8) and C-22 (δ 19.9) in the latter spectrum. HMBC correlations from the α-proton (H-20) to the *N*Me group at C-23 (δ 32.8) and C-21 (δ 67.8) established the *N*-MeThr structural unit in **161**.

The presence of an enamide functionality in bouillonamide A (**161**) was deduced from HMBC correlations between the *N*Me signal (H-46, δ 3.08 s) and the carbonyl carbon at C-1 (δ 171.3) and the vinyl carbons at C-43 (δ 109.6) and C-44 (δ 130.5). Additional HMBC correlation data indicated that the enamide was part of a 2-methyl-6-methylamino-hex-5-enoic acid (Mmaha) moiety. The Mmaha unit in **161** was constructed from careful analyses of HMBC and TOCSY data. In the latter data, a proton spin system from H-41 to H-43 could be detected. Additional correlations from HMBC data confirmed the Mmaha substructure (Figure V.7). The configuration of the C-43-44 double bond was assigned as *E* on the basis of a 13.4 Hz $^3J_{HCH}$ coupling constant.

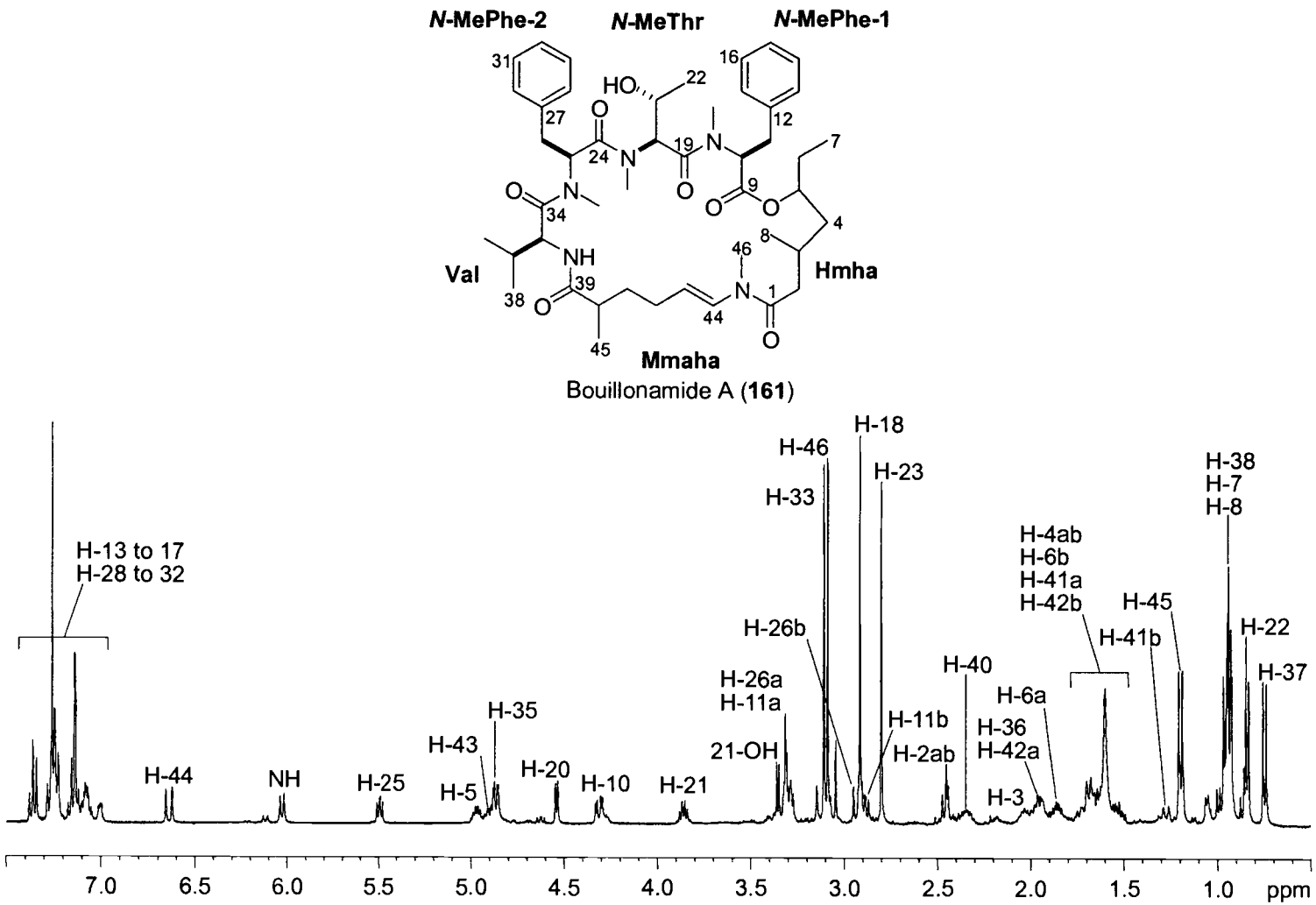

Figure V.5 ^{1}H NMR spectrum of bouillonamide A (**161**) in $CDCl_3$.

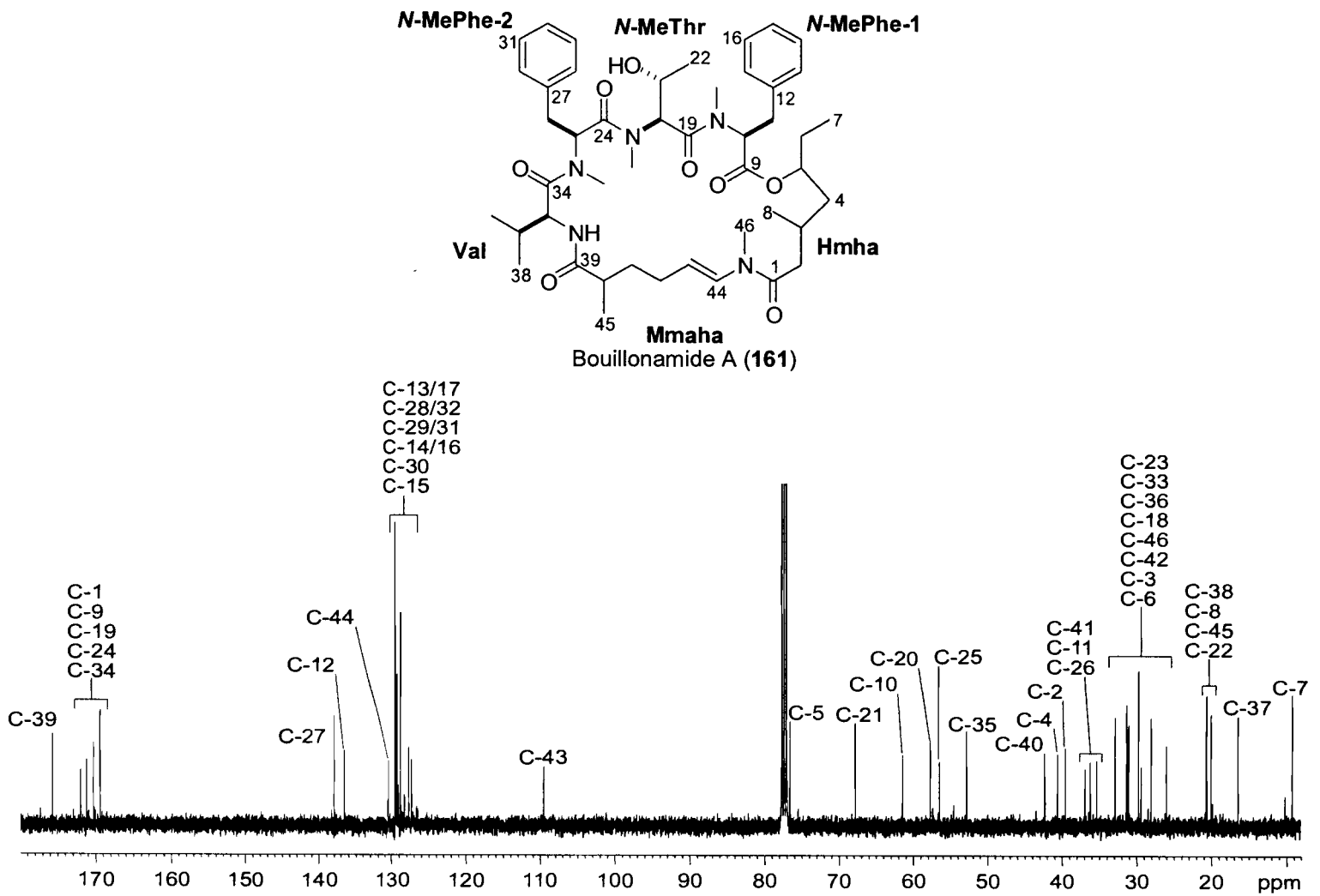

Figure V.6 ^{13}C NMR spectrum of bouillonamide A (**161**) in $CDCl_3$.

Table V.1 NMR spectral data for bouillonamide A (**161**) at 400 MHz (^{1}H) and 100 MHz (^{13}C) in $CDCl_3$.

Unit	Position	δH mult (*J* in Hz)	δC	HMBC
Hmha	1		171.3 s	
	2ab	2.44 m	39.5 t	C-1, C-3, C-4, C-8
	3	2.03 m	28.0 d	
	4a	1.64 m	40.5 t	C-2, C-3, C-5, C-6, C-7, C-8
	4b	1.52 m		C-2, C-3, C-5, C-6, C-8
	5	4.96 m	76.6 d	C-7
	6a	1.85 m	25.9 t	
	6b	1.62 m		
	7	0.94 t (7.4)	9.2 q	C-5, C-6
	8	0.94 m	20.6 q	C-2, C-3, C-4
N-MePhe-1	9		169.5 s	
	10	4.31 dd (11.5, 3.8)	61.4 d	C-9, C-11, C-18, C-19
	11a	3.28 m	36.1 t	C-10, C-12, C-13/17
	11b	2.90 m		C-10, C-12, C-13/17
	12		136.5 s	
	13/17	7.13 m	129.5 d	
	14/16	7.35 m	128.8 d	
	15	7.06 m	127.4 d	
	18 *N*Me	2.91 s	30.9 q	C-10, C-19
N-MeThr	19		171.3 s	
	20	4.54 d (4.7)	57.7 d	C-21, C-22, C-23
	21	3.85 m	67.8 d	
	21-OH	3.34 d (4.7)		C-21, C-22
	22	0.84 d (6.2)	19.9 q	C-20, C-21
	23 *N*Me	2.79 s	32.8 q	C-24, C-20
N-MePhe-2	24		170.4 s	
	25	5.49 dd (8.4, 5.6)	56.4 d	C-24, C-26, C-33, C-34
	26a	3.28 m	35.3 t	C-24, C-25, C-27, C-28/32, C-34
	26b	2.90 m		C-24, C-25, C-27, C-28/32, C-34
	27		138.0 s	
	28/32	7.23 m	129 5 d	
	29/31	7.35 m	129.3 d	
	30	7.24 m	127.7 d	
	33 *N*Me	3.10 s	31.3 q	C-25, C-34
Val	34		172.1 s	
	35	4.86 dd (8.6, 3.0)	52.8 d	C-34, C-36, C-37, C-38
	36	1.96 m	31.2 d	
	37	0.74 d (6.7)	16.4 q	C-35, C-36, C-38
	38	0.95 d (6.8)	20.6 q	C-35, C-36, C-37
	*N*H	6.02 d (8.6)		C-34, C-39
Mmaha	39		175.7 s	
	40	2.34 m	42.3 d	C-39, C-45
	41a	1.68 m	36.9 t	
	41b	1.27 m		
	42a	1.93 m	29.3 t	

Table V.1 (*continued*)

42b	1.69 m		
43	4.89 m	109.6 d	
44	6.64 d (13.4)	130.5 d	C-42, C-43, C-46, C-1
45	1.19 d (7.1)	20.5 q	C-39, C-40, C-41

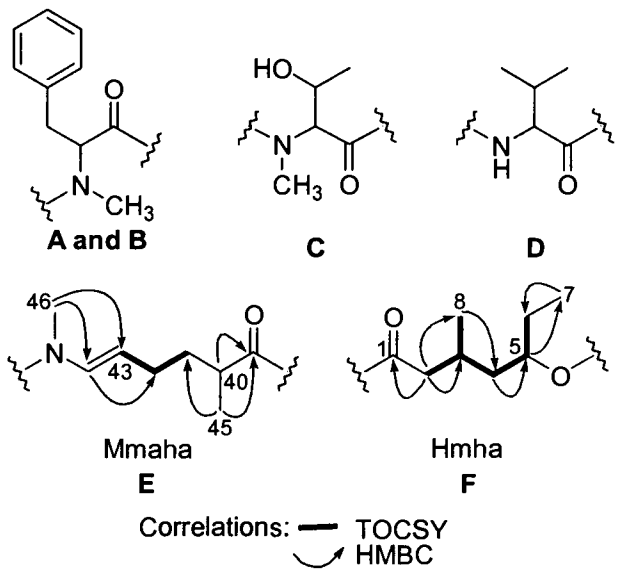

Figure V.7 Partial structures of bouillonamide A (**161**).

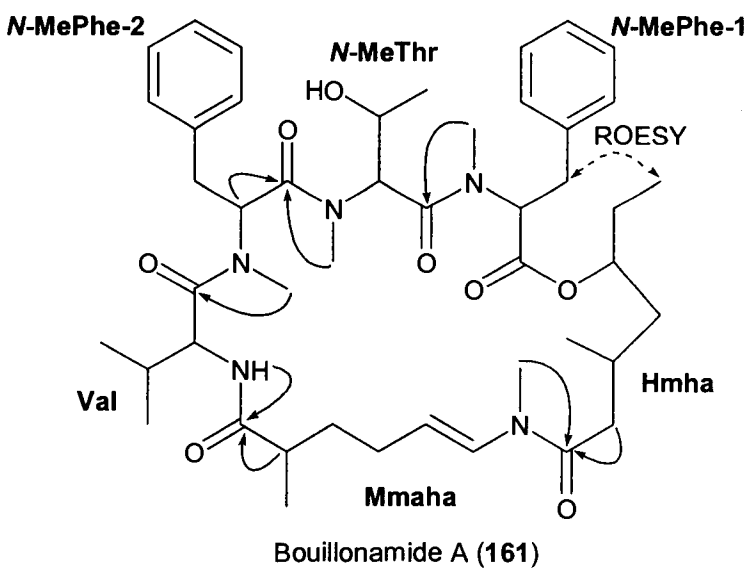

Figure V.8 Key HMBC correlations used to sequence the linkage of residues in bouillonamide A (**161**).

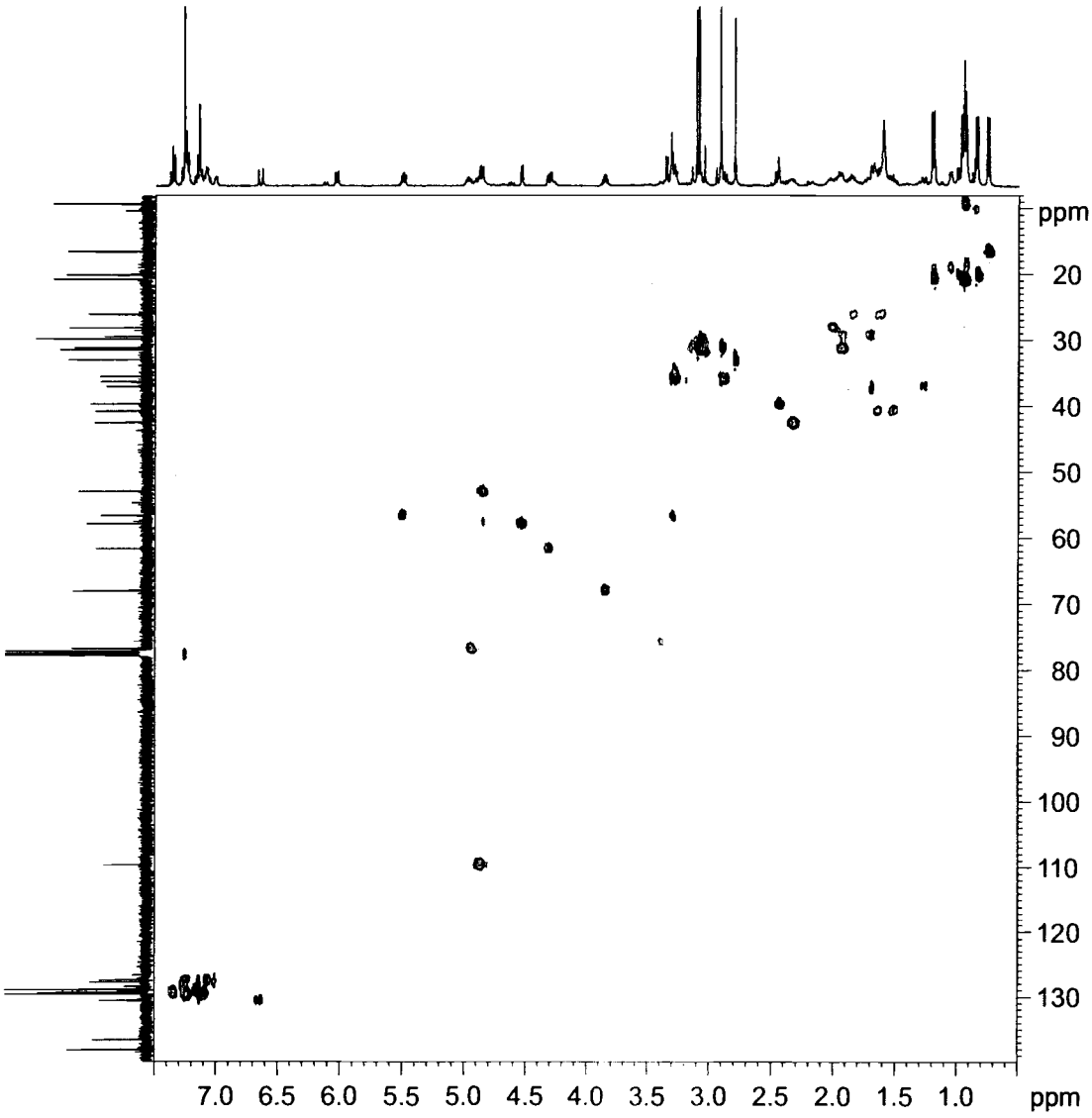

Figure V.9 HSQC spectrum of bouillonamide A (**161**) in $CDCl_3$.

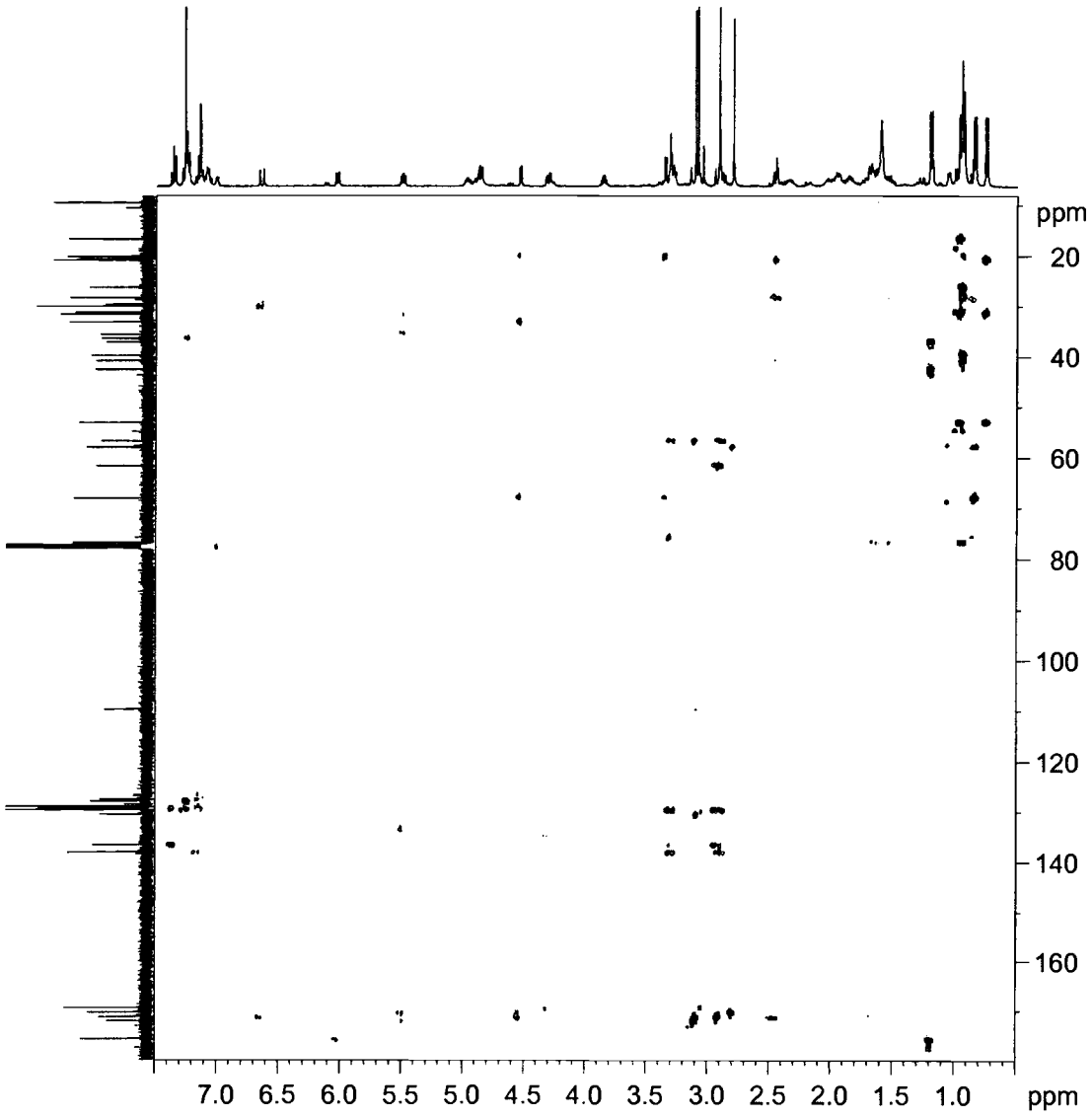

Figure V.10 HMBC spectrum of bouillonamide A (**161**) in $CDCl_3$.

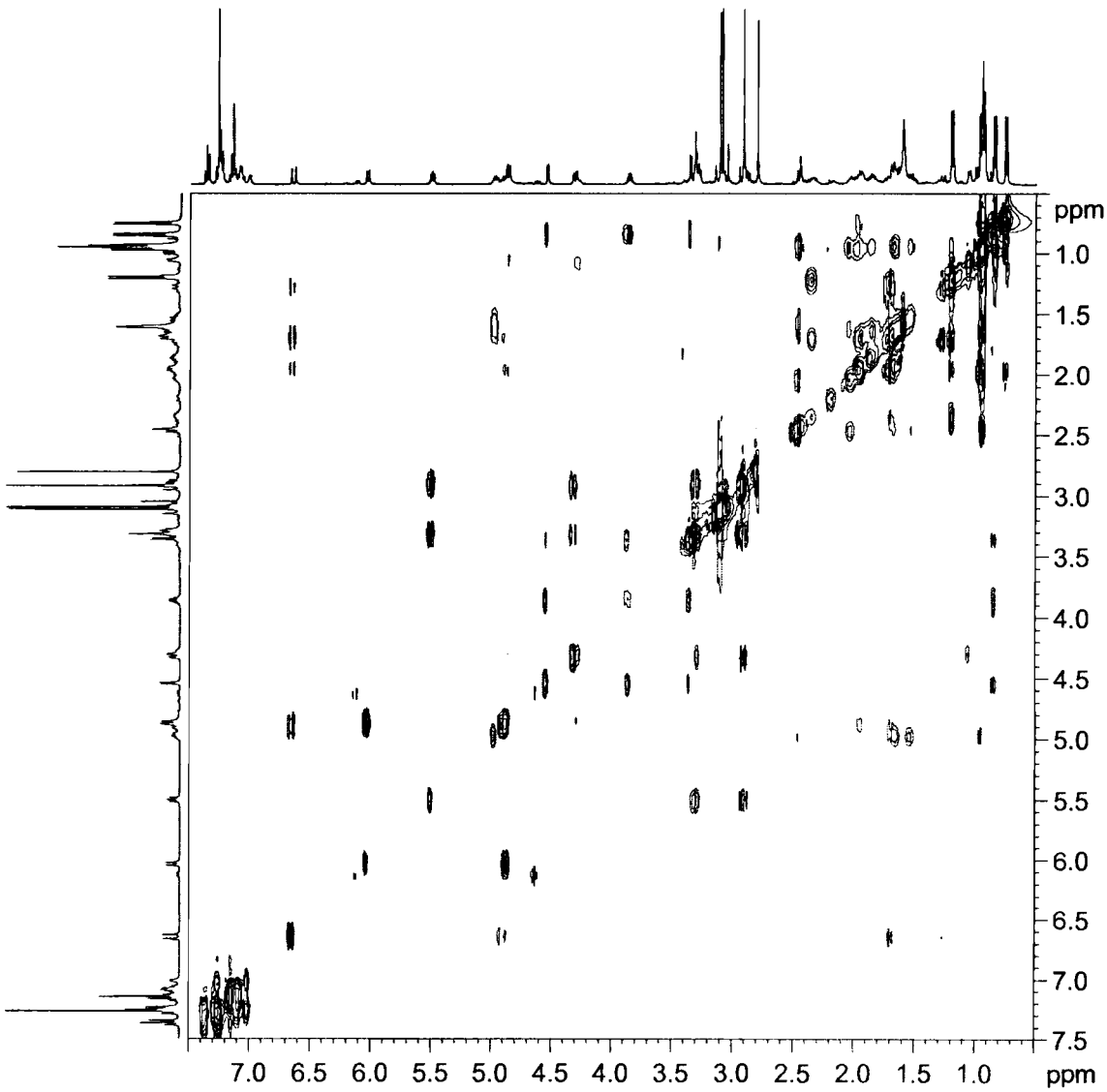

Figure V.11 TOCSY spectrum of bouillonamide A (**161**) in $CDCl_3$.

A polyketide synthase-derived unit of 5-hydroxy-3-methyl-heptanoic acid (Hmha) in **161** could also be deduced from TOCSY and HMBC data. Proton spin system from H-2/H-3/H-8/H-4/H-5/H-6 could be detected in the TOCSY data. Additional information from HMBC data indicated the presence of the Hmha unit in **161** (Figure V.7).

Connectivity of these six partial structures was achieved mainly through HMBC and ROESY data (Figure V.8). Useful correlations from either the *N*H or *N*Me proton signals to carbonyls of adjacent partial structures were observed in the HMBC data. Sequential HMBC correlations were observed between H-46 (*N*-Me of Mmaha)/C-1; *N*H (Val)/C-39; H-33 (*N*-Me of Phe-2)/C-34; H-23 (*N*-Me of Thr)/C-24; and H-18 (*N*-Me of Phe-1)/C-19 revealing the sequence of *N*-MePhe-1/*N*-MeThr/*N*-MePhe-2/Val/Mmaha. The final linkage between Hmha and *N*-MePhe-1 was established from observation of a ROESY correlation between H-7 of Hmha and the H-11 methylene protons of *N*-MePhe-1.

The absolute configurations of the two *N*-MePhe and Val residues in bouillonamide A (**161**) were determined by hydrolysis, derivatization with Marfey reagent, and analysis by HPLC on a reversed-phase column, yielding *L*-Val and only *L*-*N*-MePhe. The relative stereochemistry of the *N*-MeThr unit in **161** was established using ROESY data which showed strong correlations between the αH (H-43) of *N*-MeThr and the –OH as well as the αH (H-33) of *N*-MePhe-2, indicating that they lie on the same side in the molecule and hence have the relative configuration as indicated in **161**. Shortage of material prevented our determining the stereochemistry of the Mmaha (C-40) and Hmha (C-3 and C-5) groups.

HR FABMS of bouillonamide B (**162**) indicated a molecular composition of $C_{32}H_{45}N_5O_6S$ (13 degrees of unsaturation). The IR spectrum of **162** displayed strong absorption bands at 1632 and 1733 cm^{-1}, suggesting the presence of amide and ester groups, respectively. The peptidic nature of **162** could be implied from the ^1H NMR spectrum which indicated the presence of two *N*H resonances at δ 8.94 and δ 8.16, α-hydrogen signals between 4.0 and 6.5 ppm, two NCH_3 singlets at δ 3.20 and δ 2.98, and aromatic multiplets between 7.0 and 7.4 ppm (Figure V.12). A characteristic proton singlet at δ 8.02 indicated the presence of a thiazole functionality in **162**. A similar

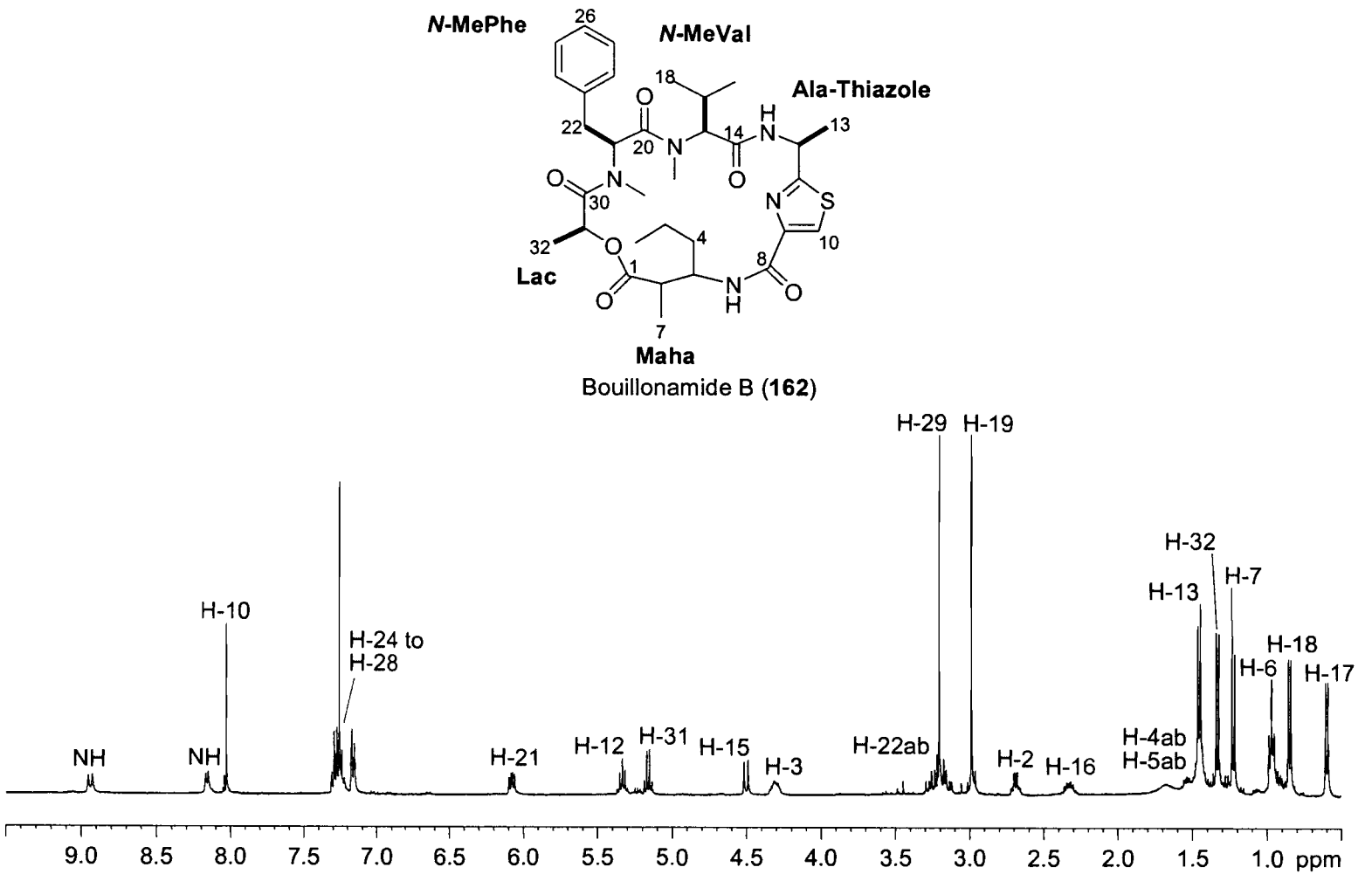

Figure V.12 ^{1}H NMR spectrum of bouillonamide B (**162**) in $CDCl_3$.

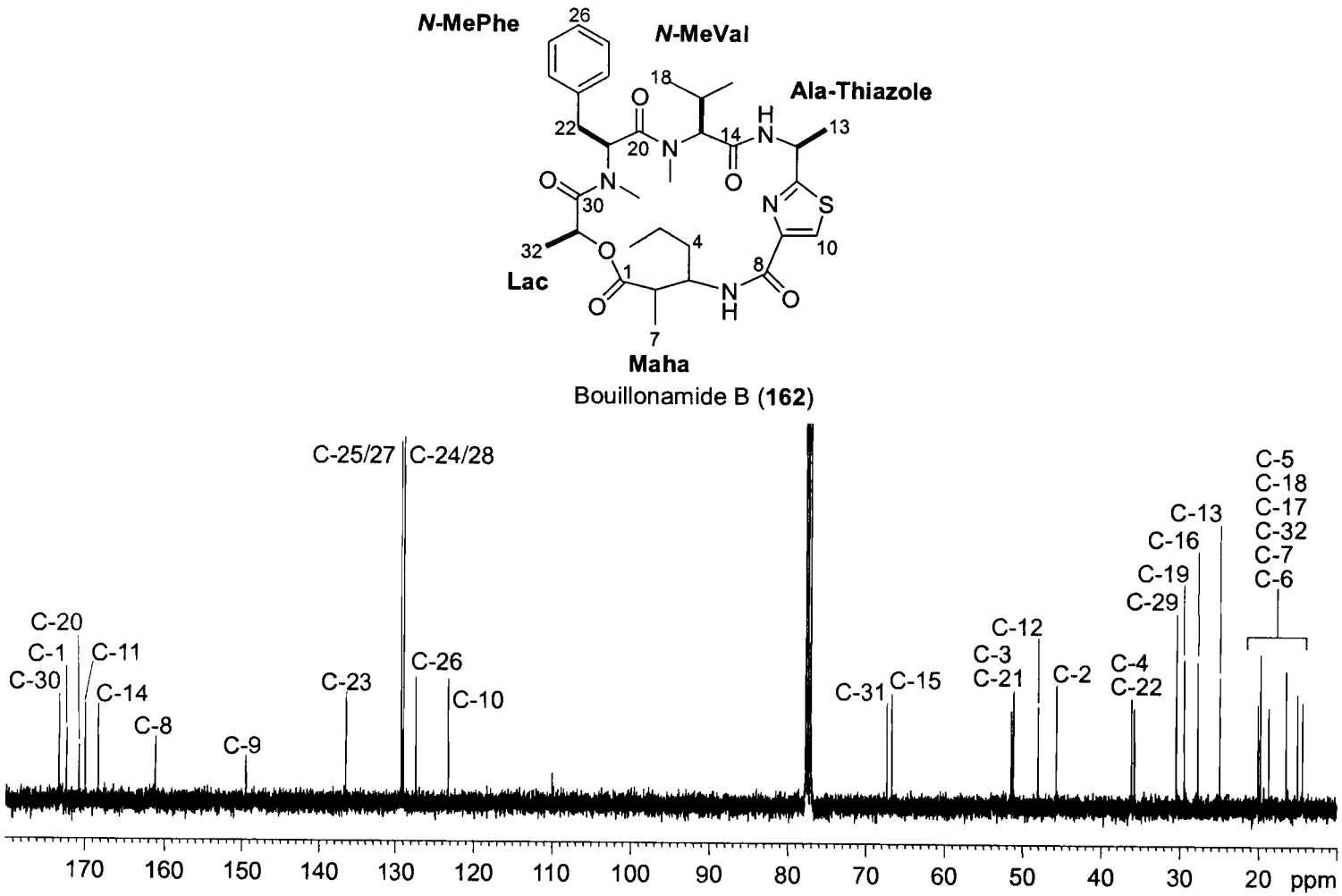

Figure V.13 ^{13}C NMR spectrum of bouillonamide B (**162**) in $CDCl_3$.

Table V.2 NMR spectral data for bouillonamide B (**162**) at 400 MHz (^{1}H) and 100 MHz (^{13}C) in $CDCl_3$.

Unit	Position	^{1}H mult (*J* in Hz)	^{13}C	HMBC
Maha	1		172.3	
	2	2.68 dt (9.8, 7.2)	45.7	C-1, C-3, C-7
	3	4.31 m	51.4	
	4a	1.53 m	36.1	C-3, C-5
	4b	1.44 m		C-3, C-5
	5ab	1.44 m	20.0	C-4, C-6
	6	0.96 t (6.9)	14.4	C-4, C-5
	7	1.22 d (7.0)	15.0	C-1, C-2, C-3
	*N*H	8.94 d (10.7)		C-8
Thiazole-Ala	8		161.2	
	9		149.5	
	10	8.02 s	123.3	C-8, C-9, C-11
	11		170.0	
	12	5.33 m	48.0	C-11, C-13, C-14
	13	1.45 d (6.7)	24.9	C-11, C-12
	*N*H	8.16 d (6.8)		C-11, C-12, C-14
MeVal	14		168.3	
	15	4.50 d (10.7)	66.7	C-20, C-14, C-16, C-17, C-18, C-19
	16	2.33 m	27.7	C-15, C-17, C-18
	17	0.59 d (6.8)	18.6	C-15, C-16, C-18
	18	0.84 d (6.4)	19.7	C-15, C-16, C-17
	19 *N*Me	2.98 s	29.4	C-20, C-15
MePhe	20		170.8	
	21	6.07 dd (9.3, 5.7)	51.1	C-20, C-22, C-23, C-29, C-30
	22a	3.26 dd (15.5, 9.3)	35.7	C-20, C-21, C-23, C-24/28
	22b	3.14 dd (15.0, 6.2)		C-20, C-21, C-23, C-24/28
	23		136.5	
	24/28	7.16 m	129.0	C-26
	25/27	7.28 m	129.3	C-23
	26	7.24 m	127.4	C-24/28
	29 *N*Me	3.20 s	30.4	C-21, C-30
Lac	30		173.3	
	31	5.15 q (6.8)	67.3	C-30, C-32, C-1
	32	1.33 d (6.8)	16.4	C-30, C-31

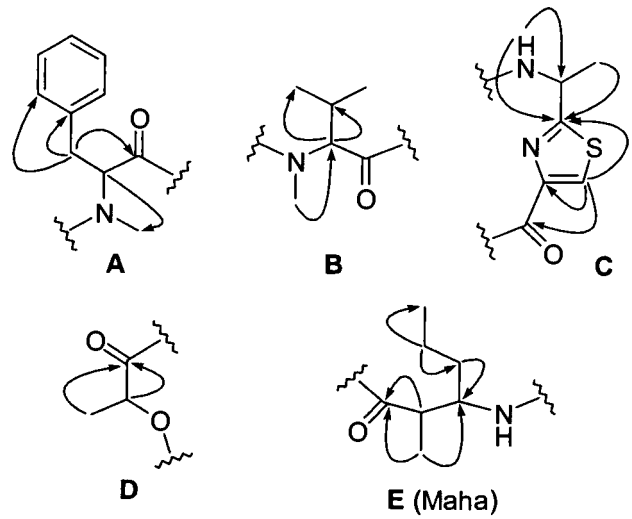

Figure V.14 Partial structures of bouillonamide B (**162**) showing selected HMBC correlations.

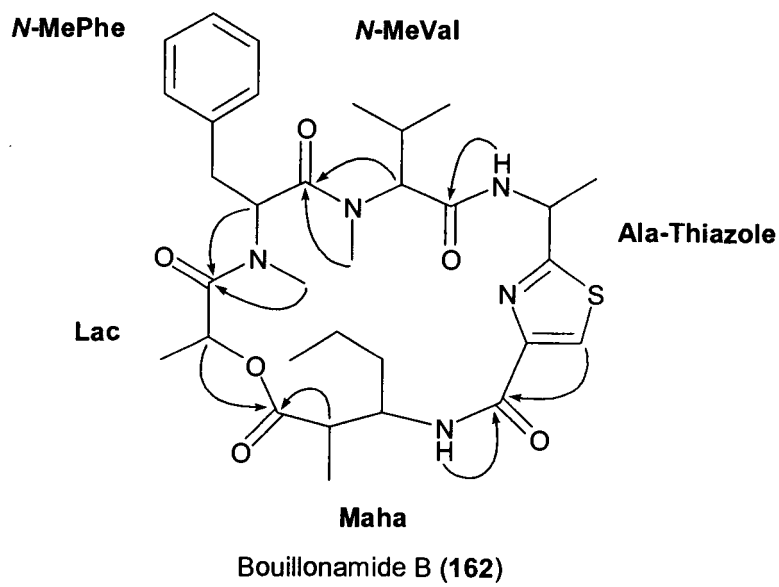

Figure V.15 Key HMBC correlations used to sequence the linkage of residues in bouillonamide B (**162**).

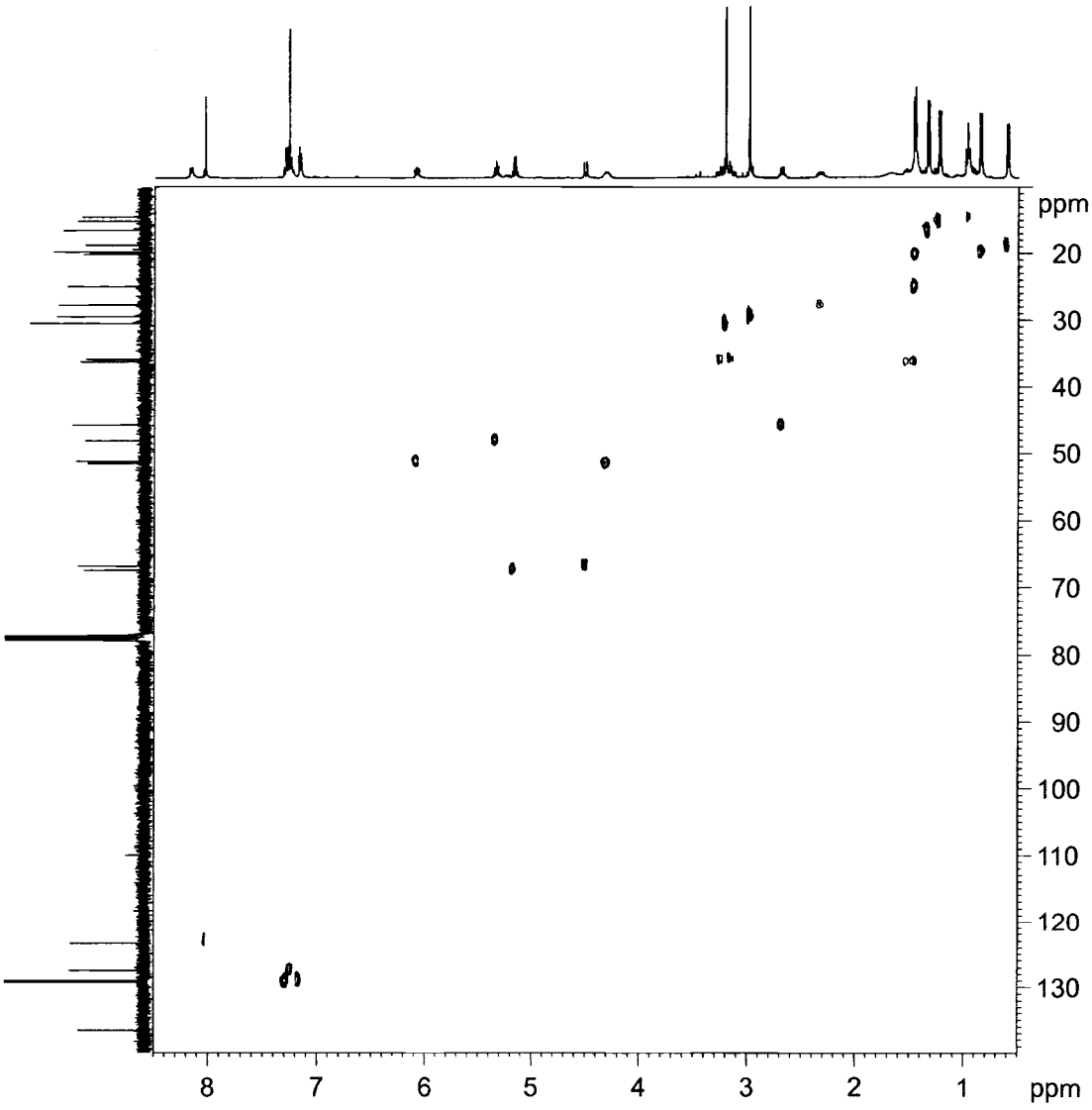

Figure V.16 HSQC spectrum of bouillonamide B (**162**) in $CDCl_3$.

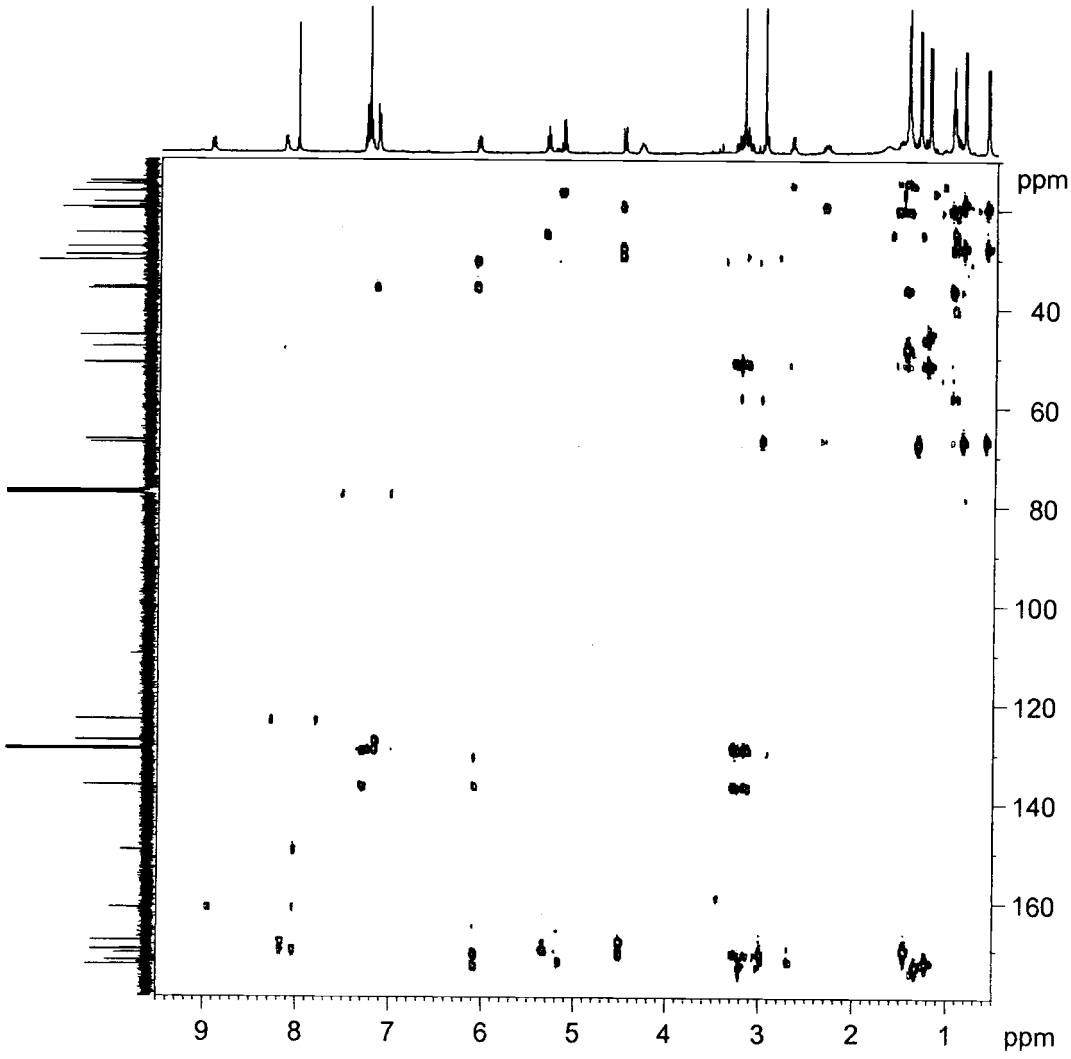

Figure V.17 HMBC spectrum of bouillonamide B (**162**) in $CDCl_3$.

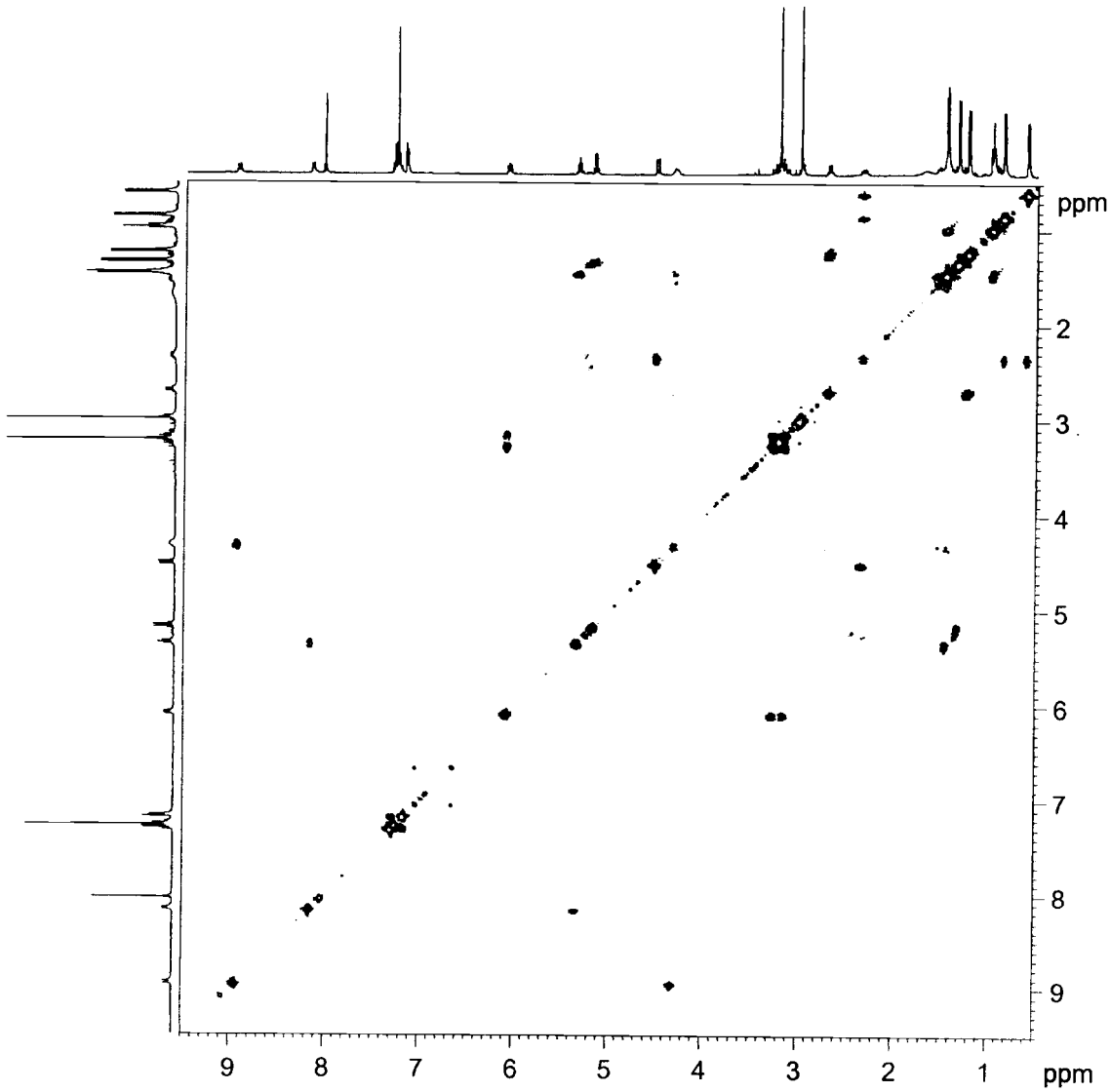

Figure V.18 COSY spectrum of bouillonamide B (**162**) in $CDCl_3$.

conclusion could also be deduced from the ^{13}C NMR of **162** which indicated a total of 32 carbon signals (Figure V.13). These included characteristic low field carbonyls (160.0 to 175.0 ppm) and aromatic resonances (120.0 to 140.0 ppm). Of the 13 degrees of unsaturation implied by the molecular formula, 12 were defined from ^{13}C NMR spectrum as five amide/ester carbonyls, a mono-substituted phenyl group, and a thiazole group. The remaining degree of unsaturation dictates the cyclic nature of **162**.

Four partial structures, A to D (Figure V.14), in **162** were constructed as *N*-MePhe, *N*-MeVal, Ala-Thiazole unit, and lactic acid (Lac) based on analyses of 1D and 2D NMR data (Table V.2). An additional partial structure E, a β-amino acid, was deduced from both COSY and HMBC data. COSY correlations were observed for H-7/H-2/H-3/*N*H/H-4 and H-5/H-6. The spin system was interrupted by overlapping signals for H-4 and H-5. However, HMBC correlations between H-4 to C-3 and C-5, and H-5 to C-4 and C-6 established the 2-methyl-3-amino-hexanoic acid (Maha) unit in **162**. This unusual β-amino acid was first reported as a moiety in malevamide B (**141**) from *Lyngbya majuscula*.[89]

The residual sequence of **162** was determined mainly from HMBC correlations. Correlations from the different α-protons of individual residue to neighboring carbonyl carbons were used to deduce the sequence of Maha/Lac/*N*-MePhe/*N*-MeVal/Ala-Thiazole. Additional proton correlations of NCH_3 or *N*H to adjacent carbonyl carbons were also observed for the Lac/*N*-MePhe/*N*-MeVal/Ala-Thiazole sequence. Closure to the cyclic system at Maha/Ala-Thiazole was observed from HMBC correlations which included the *N*H (Maha)/C-8 (δ 161.2) and H-10 (Ala-Thiazole)/C-8.

Acid hydrolysis of **162** followed by Marfey analysis revealed the *L* configurations of *N*-MePhe, *N*-MeVal. Ozonolysis of **162** followed by acid hydrolysis and Marfey analysis indicated the presence of *L*-Ala. The absolute configuration of the Lac unit was deduced as the *L*-form by comparing retention time and co-injections with both *L*- and *D*-lactic acid using a chiral HPLC column.

Lyngbouilloside (**163**) gave a quasimolecular ion at *m/z* 607 ($[M + Na]^+$) in the positive ion FABMS spectrum (Figure V.19). In EIMS, the molecular ion was not detected. However, when the compound was measured by negative ion FABMS (Figure

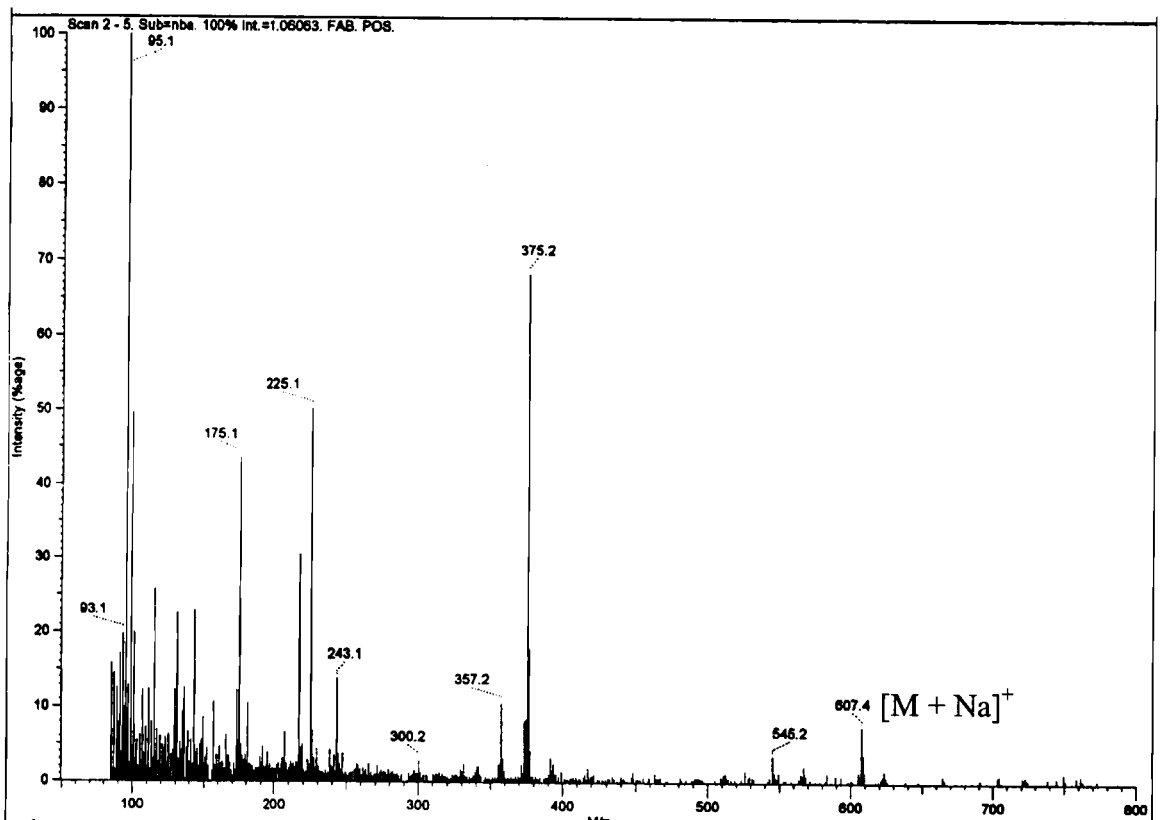

Figure V.19 LR positive ion FABMS spectrum of lyngbouilloside (**163**).

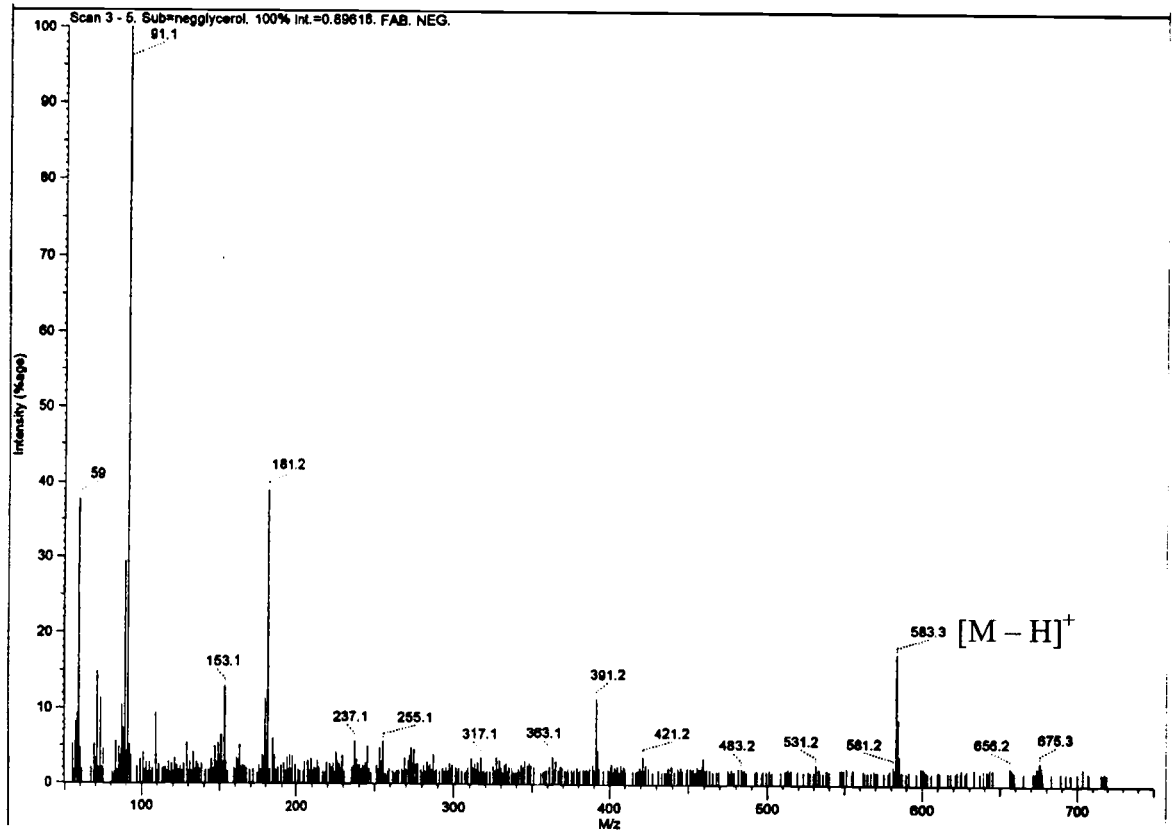

Figure V.20 LR negative ion FABMS spectrum of lyngbouilloside (**163**).

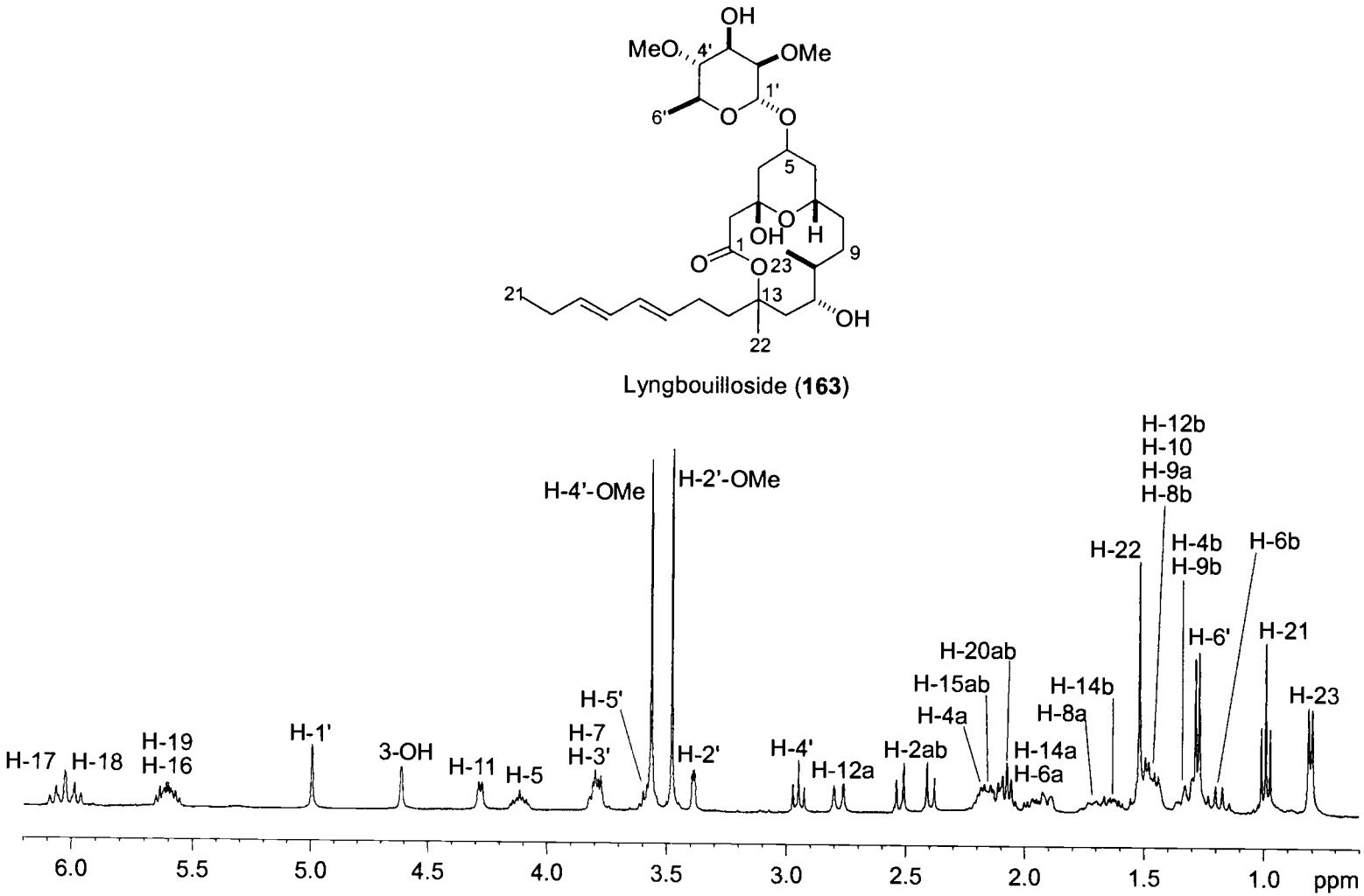

Figure V.21 ^{1}H NMR spectrum of lyngbouilloside (**163**) in $CDCl_3$.

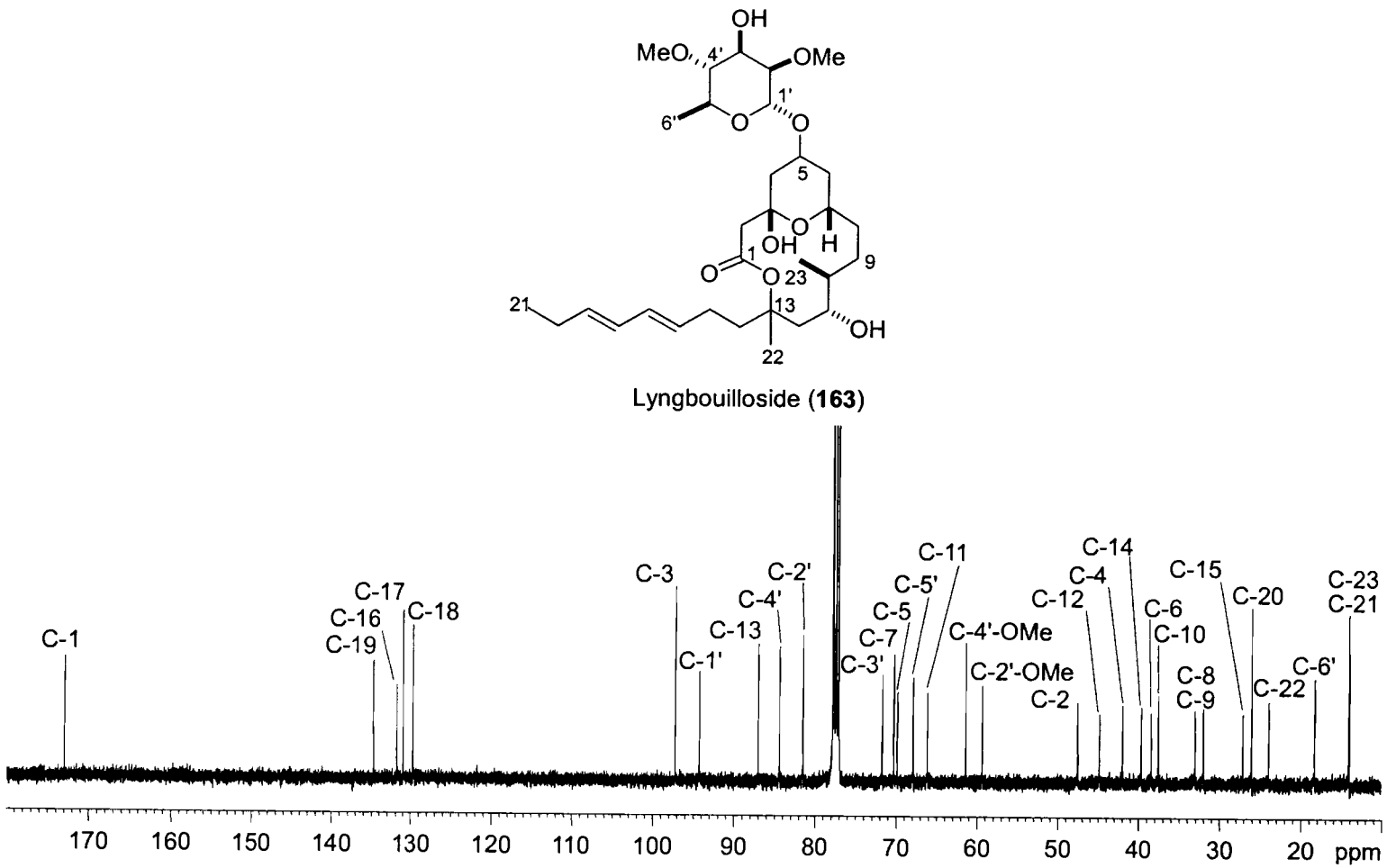

Figure V.22 ^{13}C NMR spectrum of lyngbouilloside (**163**) in $CDCl_3$.

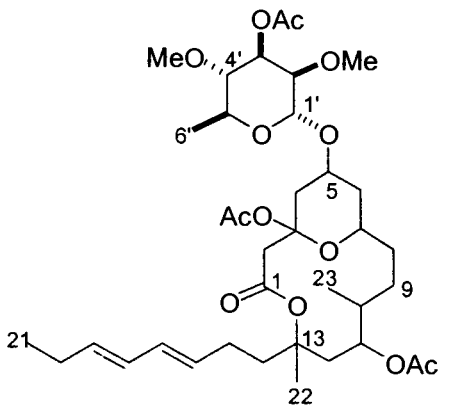

3,11,3'-Triacetyl-lyngbouilloside (**169**)

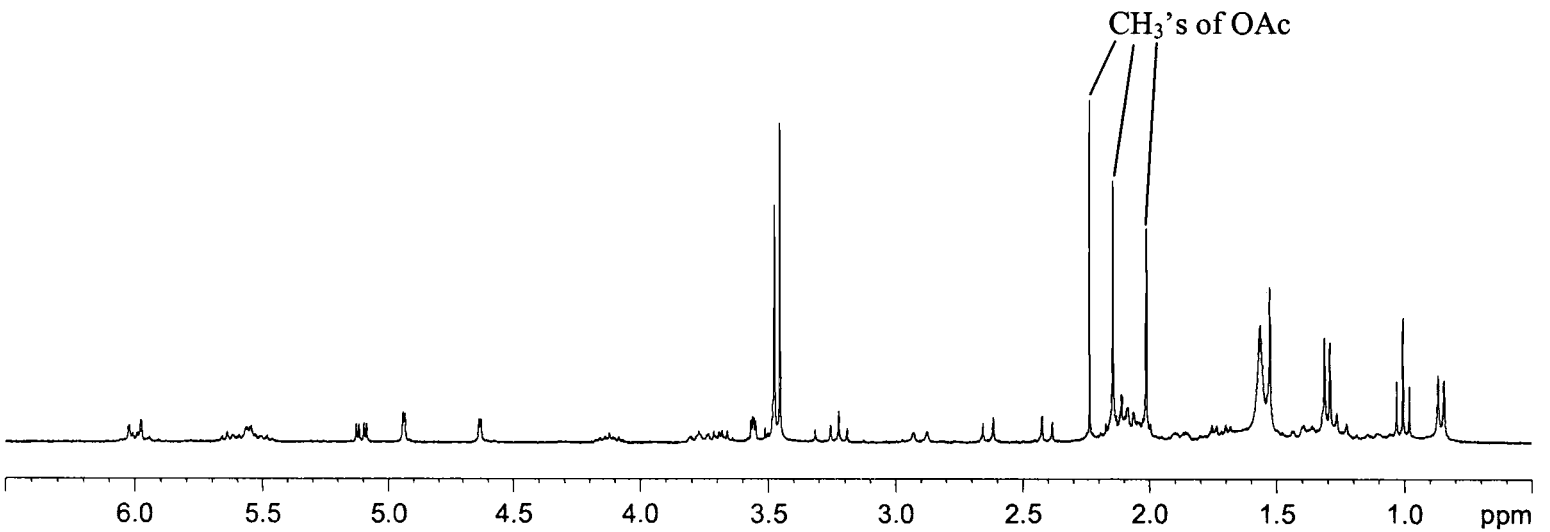

Figure V.23 ^{1}H NMR spectrum of acetylated lyngbouilloside (**169**) in $CDCl_3$.

Table V.3 NMR spectral data for lyngbouilloside (**163**) at 400 MHz (^{1}H) and 100 MHz (^{13}C) in $CDCl_3$.

Position	^{1}H mult (*J* in Hz)	^{13}C	HMBC
1		172.9	
2a	2.52 d (12.2)	47.5	C-1, C-3, C-4
2b	2.39 d (12.2)		C-1, C-3, C-4, C-7
3		97.2	
3-OH	4.61 brd (2.3)		C-3, C-4
4a	2.13 dd (12.5, 2.9)	41.9	C-3, C-5, C-6
4b	1.29 m		C-3, C-5, C-6
5	4.11 dddd (11.1, 4.5)	69.8	C-1′, C-4
6a	1.90 brd (12.5)	38.4	C-4, C-5
6b	1.18 ddd (11.1)		C-4, C-5, C-7, C-8
7	3.79 m	70.2	
8a	1.71 m	31.9	C-7, C-9
8b	1.45 m		C-9
9a	1.49 m	33.0	C-10, C-11
9b	1.33 m		C-8, C-10
10	1.49 m	37.5	C-11, C-23
11	4.28 brd (5.9)	66.0	C-9, C-10, C-12, C-13, C-23
12a	2.78 d (15.5)	44.7	C-10, C-11, C-13, C-14, C-23
12b	1.46 m		
13		86.9	
14a	1.96 dt (13.9, 5.9)	39.6	C-12, C-13, C-15, C-16, C-22
14b	1.63 m		C-12, C-13, C-15, C-16, C-22
15a	2.17 m	27.0	C-13, C-14, C-16
16	5.58 m	131.9	C-14, C-15, C-18
17	6.06 m	131.0	C-15, C-18, C-19
18	5.98 m	129.6	C-16, C-17, C20
19	5.61 m	134.8	C-17, C-20, C-21
20ab	2.07 dq (7.4)	26.0	C-18, C-19, C-21
21	0.99 t (7.4)	14.0	C-19, C-20
22	1.52 s	23.8	C-12, C-13, C-14
23	0.80 d (6.2)	14.0	C-9, C-10, C-11
1′	4.99 d (1.5)	94.2	C-5, C-2′, C-3′, C-5′
2′	3.38 dd (3.7, 1.5)	81.4	C-4′, C-3′, 2′-*O*Me
3′	3.78 m	71.6	C-4′, C-5′
4′	2.94 t (9.4)	84.3	C-3′, C-5′, 4′-*O*Me
5′	3.58 m	67.9	C-1′, C-3′, C-6′
6′	1.28 d (6.2)	18.2	C-4′, C-5′
2′ *O*Me	3.47 s	59.3	C-2′
4′ *O*Me	3.56 s	61.3	C-4′

V.20), an $[M - H]^+$ peak at *m/z* 583 was observed and calculated to have the molecular formula of $C_{31}H_{52}O_{10}$ (six degrees of unsaturation). Four olefinic carbons and one carbonyl carbon were observed in the ^{13}C NMR spectrum of **163**, accounting for three degrees of unsaturation (Figure V.22). The molecule had to be tricyclic in order to account for all the degrees of unsaturation. The IR spectrum of **163** suggested the presence of hydroxy (3461 cm^{-1}) and ester (1696 cm^{-1}) groups. The number of hydroxy functionalities in **163** was determined to be three, as revealed by three diagnostic CH_3 singlets clustered at about 2 ppm in the ^1H NMR spectrum of the acetylated molecule (Figure V.23). A conjugated diene system was also present in **163** as deduced from a UV absorbance at λ_{max} 235 (ϵ 26 200).

The gross structure of lyngbouilloside (**163**) was established from analyses of one- and two-dimensional NMR spectral data. The presence of a 2,4-di-*O*-methylrhamnopyranoside moiety in **163** was readily revealed by the coupling constants in the ^1H NMR spectrum, correlations in the ^1H-^1H COSY, and the HMBC spectral data as well as comparison with identical sugar unit in the sea-hare metabolite, auriside A (Figure V.24).[101] The α-anomeric structure was determined by correlations in the ROESY spectrum (H-1'/2'-OMe in Figure V.24).

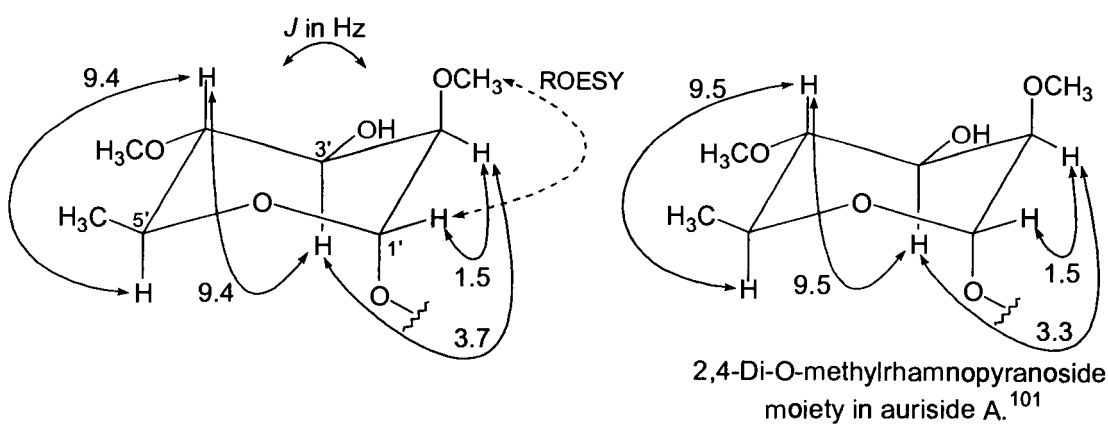

Figure V.24 2,4-Di-*O*-methylrhamnopyranoside moiety in lyngbouilloside (**163**).

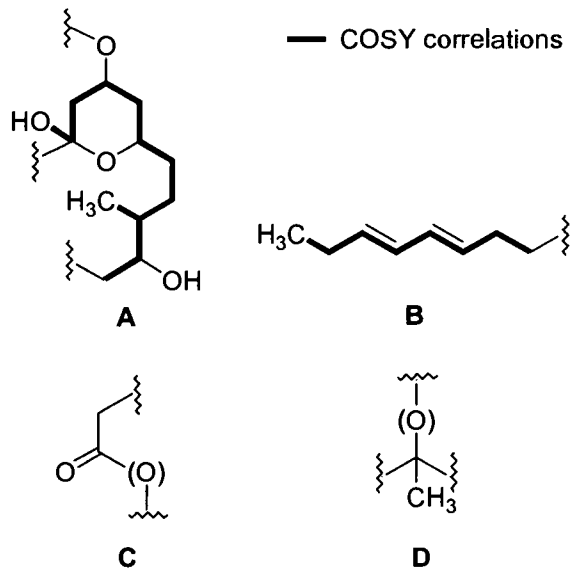

Figure V.25 Partial structures of lyngbouilloside (**163**).

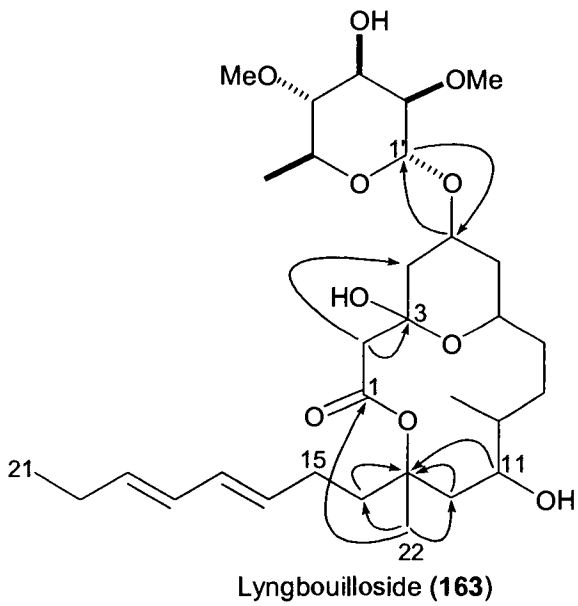

Figure V.26 Selected HMBC correlations in lyngbouilloside (**163**).

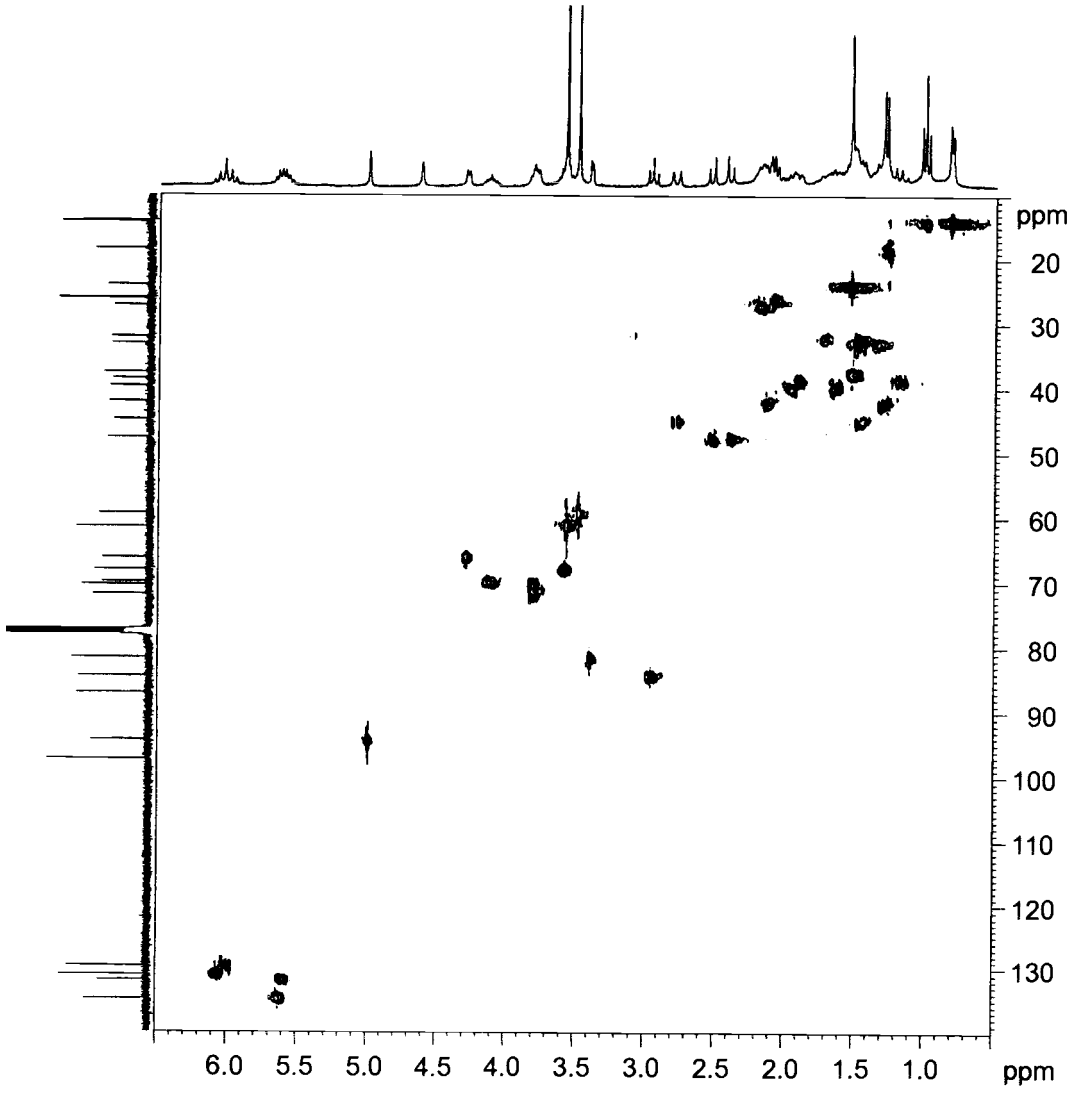

Figure V.27 HSQC spectrum of lyngbouilloside (**163**) in $CDCl_3$.

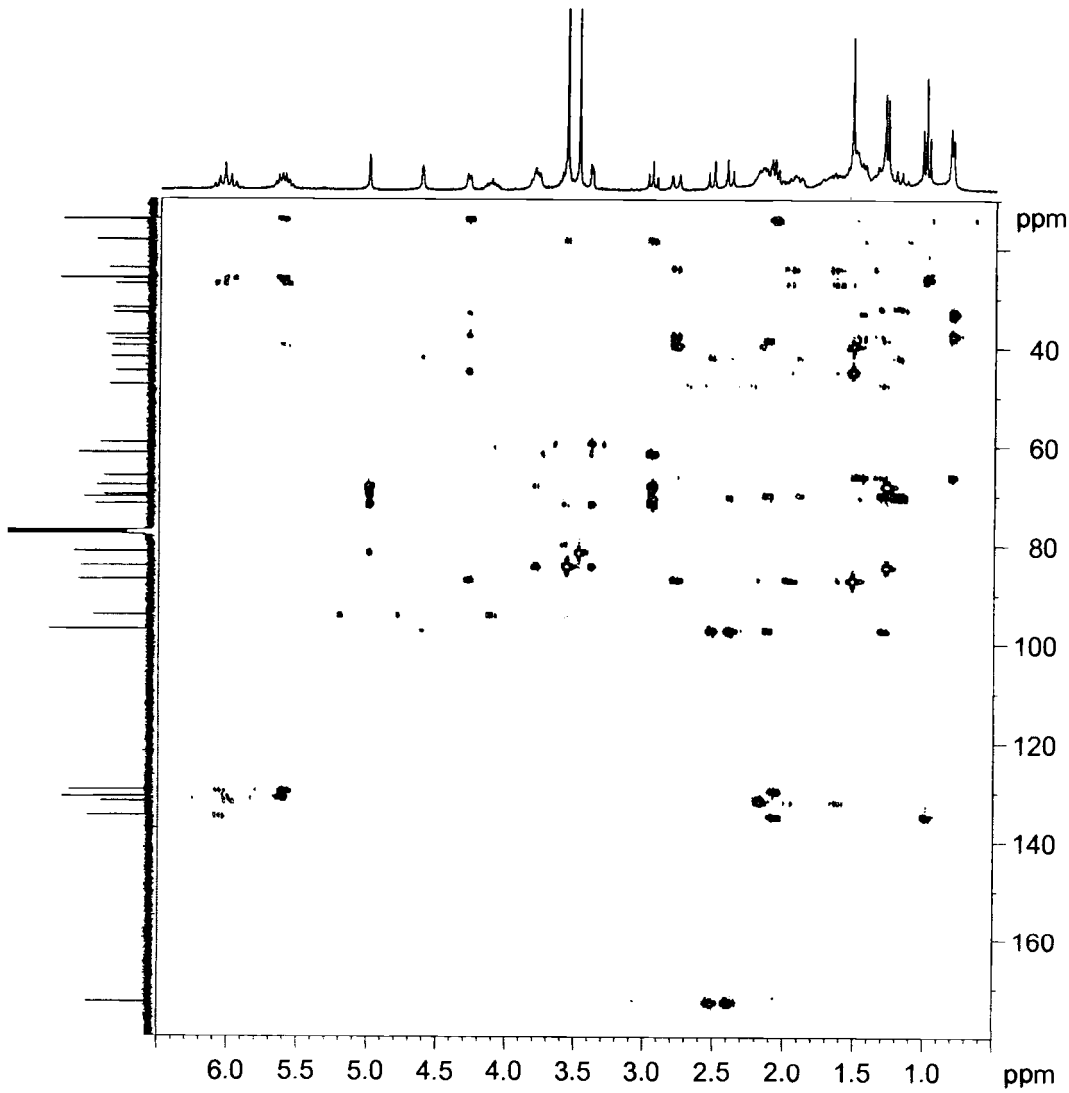

Figure V.28 HMBC spectrum of lyngbouilloside (**163**) in $CDCl_3$.

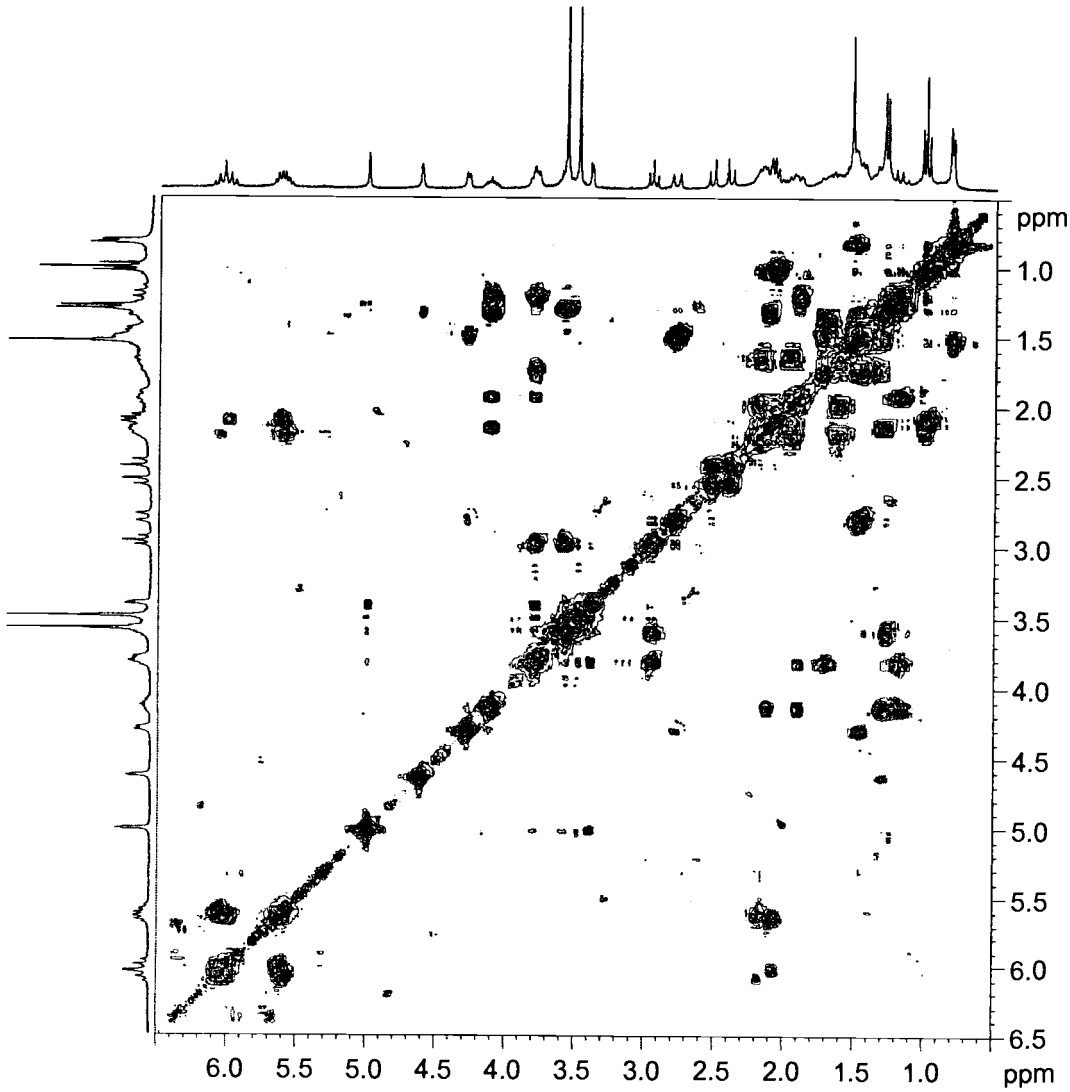

Figure V.29 COSY spectrum of lyngbouilloside (**163**) in $CDCl_3$.

For the macrolide moiety, two sets of proton spin systems were detected in the ^{1}H-^{1}H COSY spectrum, giving rise to substructures A and B (Figure V.25). These two substructures were confirmed by correlations in the HMBC data of **163**. It was noted from the COSY spectrum that one of the methylene protons at δ 1.29 (H-4b) exhibited *W*-type coupling with the 3-OH proton (δ 4.61). The *trans,trans*-stereostructure of the conjugated diene system in **163** was easily determined by the proton-proton coupling constants of 13.1 and 13.4 Hz when the sample was measured in C_6D_6. In addition to the partial structures A and B of the aglycon, lyngbouilloside had two more quaternary carbons, one methylene carbon, and one singlet methyl group. Connectivities of these units (Figure V.26) were determined by correlations in the HMBC spectral data optimized at 4 and 8 Hz. These correlations include H-2ab/C-3, H2ab/C-4, H-11/C-13, H-12a/C-13, H-22/C-12, H-22/C-14, H-14ab/C-13, and H-22/C-1, revealing all carbon connectivities of the macrolide moiety of **163**. The position of the linkage between the macrolide and the rhamnopyranoside unit was determined by key correlations in the HMBC spectrum, H-5/C-1′ and H-1′/C-5, establishing the gross structure of lyngbouilloside (**163**).

The relative stereochemistry and conformation of the macrolide moiety of **163** were determined by analyses of the vicinal spin-spin coupling constants, ROESY data, as well as the use of *J*-based NMR anaylsis[184] for the vicinal pair at C-10 and C-11. The proton-proton coupling constant ($J_{4b,5} = J_{5,6b} = J_{6b,7} = 11.1$ Hz) dictated a chair conformation in the six-membered hemiacetal ring and that the substituents at C-5 and C-7 were equatorial. The 3-hydroxy group was positioned as axial which allowed a *W*-type coupling with H-4b. Of the six possible conformers for the vicinal asymmetric carbons at C-10 and C-11, only two conformers were possible using the *J*-based configuration analysis.[184] However, additional data from ROESY experiment showed correlations between the methyl protons at H-23 and the methylene protons at C-12, suggesting the erythro relationship of the hydroxy and methyl groups at C-11 and C-10. A strong ROESY correlation was also observed between the methyl protons at H-22 and H-11, implying that the methyl group, attaching at C-13, lies on the same side of the molecule as H-11.

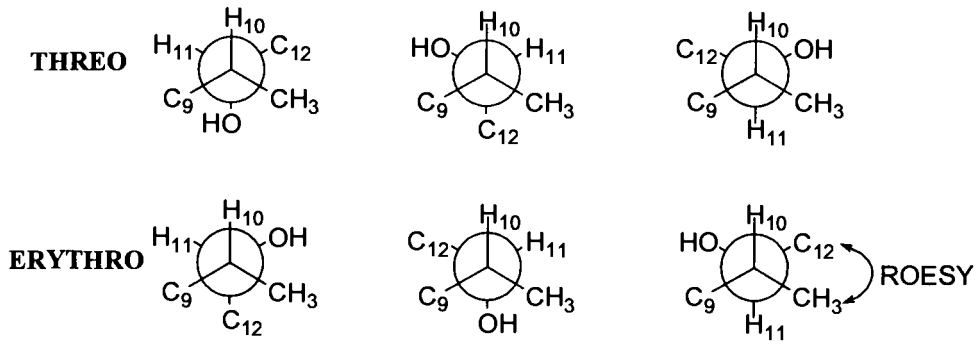

Figure V.30 Six possible conformers for the asymmetric carbons at C-10 and C-11 of lyngbouilloside (**163**).

These novel compounds from the present sample of *Lyngbya bouillonii* are new additions to metabolites reported from this species. It is interesting to note that the enamide functionality in **161** is also present in two other *L. bouillonii* compounds; laingolide (**158**) and laingolide A (**157**), while a dienamide system is present in madangolide (**159**).[179-181] The enamide group is also present in other cyanobacterial metabolites, such as the scytophycins and the tolytoxins.[99]

The cyclic depsipeptides, bouillonamides A (**161**) and B (**162**), are products of a mixed PKS and NRPS biosynthetic pathway. The presence of the two unusual units of Mmaha and Hmha in **161** posed intriguing questions concerning their biosyntheses. One could postulate that the former unit is derived from a deaminated lysine. An alternative hypothesis involves propionate as the starter unit for a PKS gene module which is then extended by two additional acetate units, followed by condensation with a Gly unit from an NRPS module, and a further extension with two units of acetate. This could then be followed by condensation with three more amino acids from an NRPS. Cyclization to the final product, **161**, might coincide with the cleavage from NRPS. A similar rationale could also be applied to apratoxin (**164**), where the starter unit could be a *t*-butyl group that is extended by three units of acetate from a PKS, followed by a unit of cysteine on from an NRPS. A unit of acetate would then be added to this growing chain before final addition of four more amino acids (i.e. *N*-MeTyr, *N*-MeAla, *N*-MeIle, and Pro) and cyclization to give apratoxin (**164**).

Bouillonamide B (**162**) resembles the clairamides (**151** and **152**) discussed in chapter four. The main differences are the additional methylene in the β-amino acid and the amino acid sequence of *N*-MePhe/*N*-MeVal/Ala-Thiazole in **162** instead of the *N*-MeVal/*N*-MePhe/Ala-Thiazole sequence in the clairamides (**151** and **152**). Such differences in residue sequence were observed in the ^{1}H NMR spectra of these molecules (Figure V.31). For instance, the α-protons signals of *N*-MePhe and *N*-MeVal in bouillonamide B (**162**) were shifted to lower and higher fields, respectively, when compared of those in the clairamides.

The isolation of lyngbouilloside (**163**) represents the second glycosidic macrolide reported from a marine blue-green algae [lyngbyaloside (**68**) was the first report]. It is also interesting to note that other glycosidic macrolides, aurisides[101] (**68** and **165**) and the callipeltosides (**166** to **168**),[182,183] from marine invertebrates bear strong structural similarities to lyngbouilloside (**163**), indicating their likely cyanobacterial origin, either sequestered through the animal's diet (e.g. mollusk) or living in symbiotic association, such as in sponges (Figure V.32). In addition, structural similarities of **163** to the toxic polycavernosides (**55** to **59**) reported from a red alga gives further evidence to the cyanobacterial origin of these toxins as well.[71,72]

Bouillonamides A (**161**) and B (**162**) were evaluated for biological activities in both the brine shrimp (*Artemia salina*) toxicity and the neuro-2a mouse neuroblastoma cells cytotoxicity assays. In the former assay, **161** and **162** exhibited LD_{50}'s of 9 μM and 18 μM, respectively, while IC_{50}'s of 6 μM and 16 μM were observed in the latter assay. Lyngbouilloside (**163**) has moderate cytotoxicity with an IC_{50} of 17 μM against the neuro-2a mouse neuroblastoma cell line. The known compound, apratoxin (**164**), was also evaluated and found to have significant cytotoxicity with an IC_{50} of 1.0 μM. The isolation of these novel and biologically active molecules from *Lyngbya bouillonii* attests to the rich and diverse natural product chemistries of marine cyanobacteria as well as demonstrates the biosynthetic potential of these ancient prokaryotes.

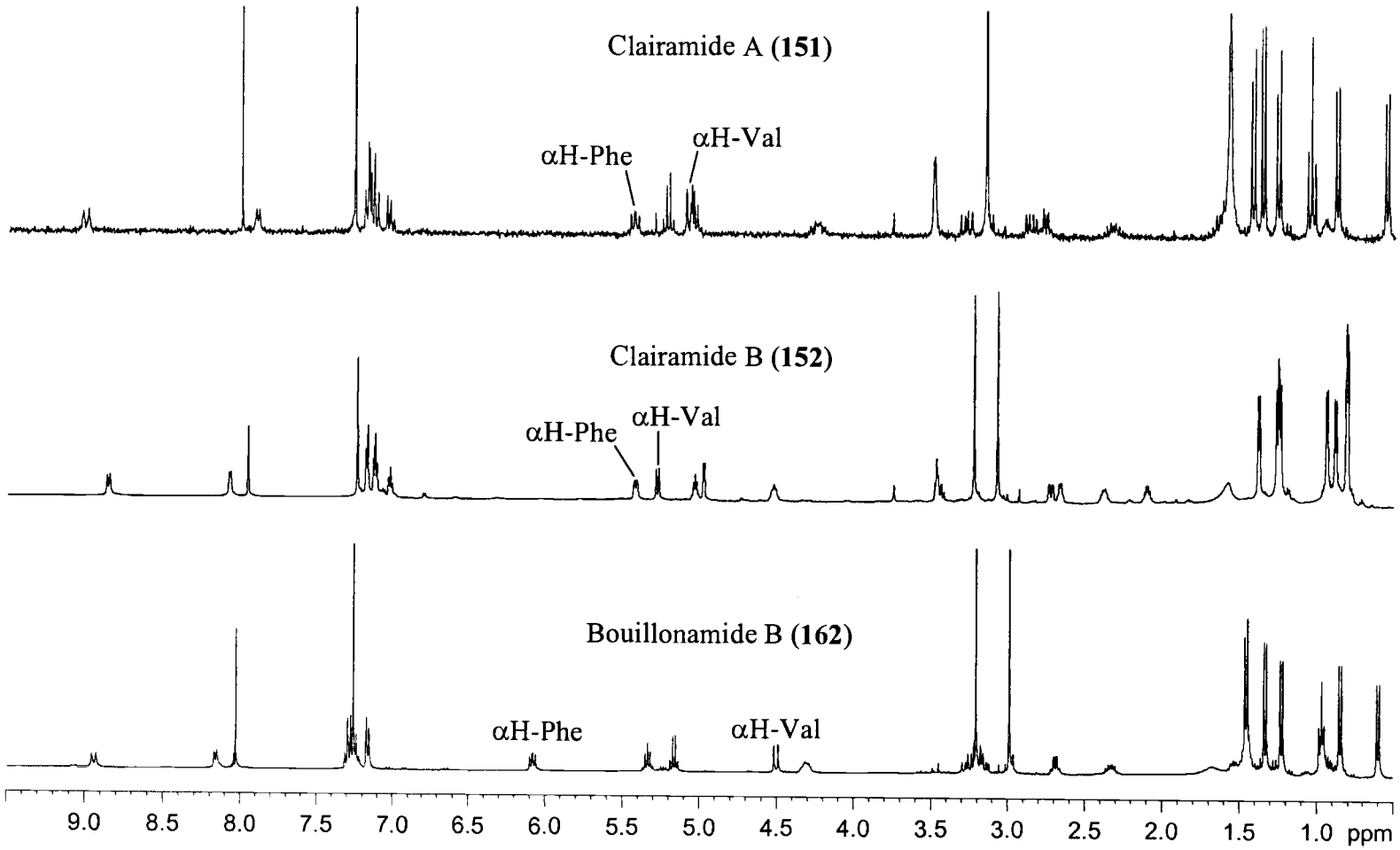

Figure V.31 ^{1}H NMR spectra of clairamides A (**151**, top), B (**152**, middle), and bouillonamide B (**162**, bottom) in $CDCl_3$.

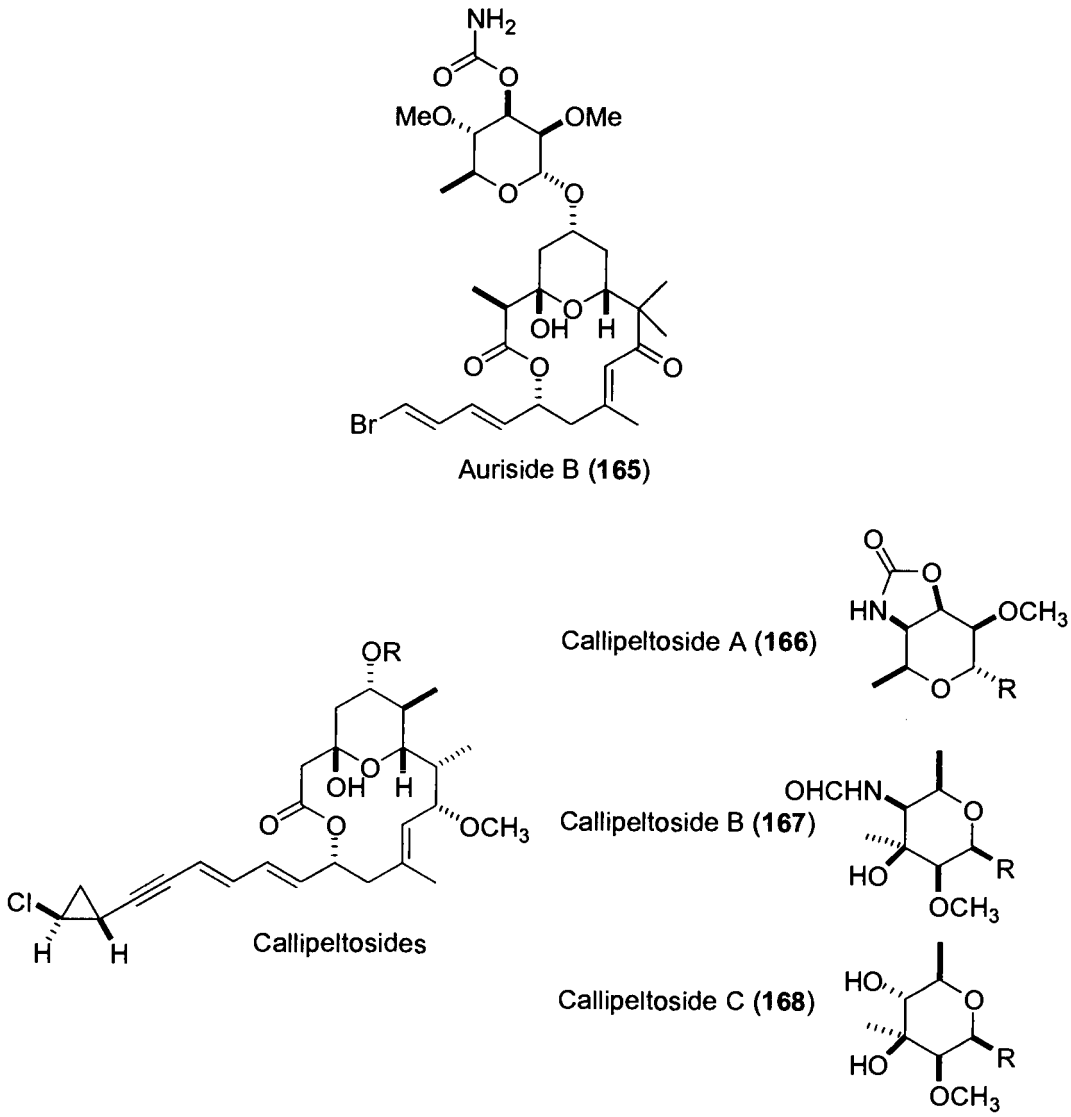

Figure V.32 Glycosidic macrolides from marine invertebrates.

EXPERIMENTAL

General Experimental Procedures. NMR experiments were measured on a Bruker AM 400 MHz NMR spectrometer in $CDCl_3$ as an internal standard. Chemical shifts are reported in ppm and coupling constants (*J*) are reported in Hz. High resolution mass spectra were recorded on a Kratos MS50TC mass spectrometer. Optical rotation was measured on a Perkin-Elmer 141 polarimeter. UV and IR spectra were recorded on Beckman DU® 640B and Nicolet 510 spectrophotometers, respectively. The isolation of compounds **161** to **164** was performed on a Waters Millipore® Model 590 Pump and detected with a Waters Millipore® Lambda-Max Model 480 LC spectrophotometer. All Marfey derivatized products were analyzed on a Waters 515 HPLC Pump and a Waters 996 Photodiode Array Detector.

Biological Material. The first collection of *Lyngbya bouillonii* Hoffman and Demoulin was made from the Eastern Fields, Papua New Guinea (5 December 1999) and given the collection number of PNGE9 5/Dec/99-1. A more extensive collection of this cyanobacterium was made the following year from the northern part of Papua New Guinea. In the second collection, samples of the cyanobacterium were hand collected at 8 – 15 m water depth using SCUBA from various reefs located on the northern coast of Papua New Guinea from the period 21 – 27 August 2000. These localities were: Bangkok Pass (*S* 4° 15.758′, *E* 151° 28.547′), Father's Reef (*S* 4° 55.153′, *E* 150° 54.554′), May Reef (*S* 5° 13.692′, *E* 150° 30.078′), Unea Island (*S* 4° 50.783′, *E* 149° 09.174′), and Long Island (*S* 5° 14.528′, *E* 147° 02.058′). Upon collection, the pooled marine cyanobacterium was preserved in 50% isopropyl alcohol and seawater and stored at low temperature until work-up. Voucher specimens are available from WHG as collection number PNGRD 21/Aug/00-2.

Extraction and Isolation of Bouillonamides A (161), B (162), and Lyngbouilloside (163). The thawed cyanobacterial material (PNGRD 21/Aug/00-2) was homogenized in CH_2Cl_2/MeOH (2:1, v/v), filtered, and the solvents removed *in vacuo* to yield a residue which was partitioned between CH_2Cl_2 and H_2O. The marc was extracted repeatedly (× 4) with CH_2Cl_2/MeOH (2:1, v/v) and the combined CH_2Cl_2 layers reduced *in vacuo* to yield about 2.0 g of a dark green extract. The crude extract

was fractionated using normal phase silica gel (TLC grade) vacuum liquid chromatography (VLC) through a step-wise gradient solvent system of increasing polarity starting from EtOAc in hexanes to EtOAc in MeOH. Fractions eluting with 2% MeOH in EtOAc were found to be active at 10 ppm in the brine shrimp toxicity assay. This fraction was refractionated using Mega Bond RP-18 Sep Pak. The most active fraction (82% cytotoxicity at 10 μg/mL to neuro-2a neuroblastoma cell line) was eluted with 20% H_2O in MeOH. This active fraction was further purified by HPLC [Phenomenex LUNA 5μ Phenyl-hexyl 250 × 4.60 mm, CH_3CN/H_2O (61:39); detection at 220 nm] to give an almost pure metabolite **161** and apratoxin (**164**, 2.2 mg). Two more HPLC purification steps [(a) Phenomenex SYNERGI 4 μ MAX-RP 80 A 250 × 4.60 mm, $MeOH/H_2O$ (83:17); (b) Phenomenex SPHERECLONE 5μ ODS (2) 250 × 10.00 mm, $MeOH/H_2O$ (90:10); detection at 220 nm] were necessary to give pure bouillonamide A (**161**, 1.5 mg). A second active fraction obtained from Mega Bond RP-18 Sep Pak was subjected to further HPLC purification on Phenomenex Sphereclone 5μ ODS (2); $MeOH/H_2O$ (82:18) to yield bouillonamide B (**162**, 3.5 mg) and the macrolide, lyngbouilloside (**163**, 4.5 mg).

Bouillonamide A (161): white amorphous solid; $[\alpha]^{25}_D$ –180° (c = 0.19, $CHCl_3$); UV (MeOH) λ_{max} 240 nm (∈ 12400); IR (neat) 3440, 2964, 2933, 1726, 1637, 1457, 1403, 1082, 1044 cm^{-1}; LR FABMS *m/z* 818 (93), 800 (21), 774 (10), 140 (42), 134 (100); HR FABMS (positive ion, 3-nitrobenzyl alcohol) *m/z* obs. $[M + H]^+$ 818.5067 ($C_{46}H_{68}N_5O_8$, –0.3 mmu dev.); ^1H NMR (400 MHz, $CDCl_3$) and ^{13}C NMR (100 MHz, $CDCl_3$) see Table V.1.

Bouillonamide B (162): white amorphous solid; $[\alpha]^{25}_D$ +11° (c = 0.35, $CHCl_3$); UV (EtOH) λ_{max} 224 nm (∈ 32600); IR (neat) 3317, 2962, 2934, 1733, 1632, 1553, 1269, 1080, 753 cm^{-1}; LR FABMS *m/z* 628 (45), 594 (75), 216 (60), 134 (50), 86 (100); HR FABMS (positive ion, 3-nitrobenzyl alcohol) *m/z* obs. $[M + H]^+$ 628.3163 ($C_{32}H_{46}N_5O_6S$, –0.6 mmu dev.); ^1H NMR (400 MHz, $CDCl_3$) and ^{13}C NMR (100 MHz, $CDCl_3$) see Table V.2.

Lyngbouilloside (163): amorphous solid; $[\alpha]^{25}_D$ –38° (c = 0.46, $CHCl_3$); UV (EtOH) λ_{max} 235 nm (∈ 26200); IR (neat) 3461, 2931, 1696, 1207, 1103, 1045, 755 cm^{-}

[1]; LR FABMS *m/z* 583 (19), 391 (12), 181 (39), 91 (100), 59 (38); HR FABMS (negative ion, 3-nitrobenzyl alcohol) *m/z* obs. $[M - H]^+$ 583.3486 ($C_{31}H_{51}O_{10}$, –0.4 mmu dev.); ^1H NMR (400 MHz, $CDCl_3$) and ^{13}C NMR (100 MHz, $CDCl_3$) see Table V.3.

Acid Hydrolysis and Marfey Analysis of Bouillonamide A (161). Bouillonamide A (**161**, 200 μg) was placed in a pressure tube with 1 mL of 6 N HCl and hydrolyzed in a microwave oven (setting at high) for 1 min. Upon cooling and concentrated to dryness under a stream of N_2 gas, the hydrolysate was dissolved in 50 μL of H_2O, followed by a 1% (w/v) solution of 1-fluoro-2,4-dinitrophenyl-5-*L*-alanine amide (Marfey reagent) in acetone (100 μL) and 20 μL of 1M $NaHCO_3$. After heating the mixture at 38 °C for 1 h, the reaction was cooled and acidified with 20 μL of 2 N HCl, and evaporated to dryness under N_2 gas. The resulting products were redissolved in DMSO/H_2O (1:1, 100 μL), and aliquots were subjected to reverse-phase HPLC analysis (Waters Nova-Pak® C_{18}, 3.9 × 150 mm) using two different solvent systems: **A** CH_3CN-0.05% TFA in H_2O linear gradient (10-50% over 60 min) and **B** CH_3CN-50 mM NH_4OAc linear gradient (10-50% over 60 min). The retention time (t_R, min) of the derivatized amino acids in the hydrolysate of **161** matched those of *L*-Val (29.1; *D*-Val, 35.2 in solvent system **A**) and *L-N*Me Phe (34.2; *D-N*Me Phe, 34.9 in solvent system **B**).

Ozonolysis of Bouillonamide B (162). A stream of O_3 was carefully bubbled into a vial containing 1 mL of CH_2Cl_2 solution of **162** (300 μg) at 25 °C for about 10 min. Solvent was removed under a stream of N_2 and the resulting residue was subjected to acid hydrolysis and Marfey derivatization.

Acid Hydrolysis and Marfey Analysis of Bouillonamide B (162). About 0.3 mg of the ozonolyzed **162** was subjected to acid hydrolysis using the same method described for bouillonamide A (**161**). After removal of excess 6 N HCl, the hydrolysate was redissolved in 100 μL of H_2O and one half of the aqueous hydrolysate was derivatized with Marfey reagent as described for **161**. Marfey analysis, using solvent system **B** on RP-HPLC, of the derivatized amino acids in **162** yielded the following: *L*-Ala (23.8 min; *D*-Ala, 27.0 min), *L-N*-MePhe (34.4 min; *D-N*-MePhe, 35.0 min), and *L-N*-MeVal (36.1 min; *D-N*-MeVal, 39.3 min). The other 50 μL of the hydrolysate of **162** was subjected to chiral column (Chirex (*D*)-penicillamine 50 × 4.60 mm, in 100% 2 mM $CuSO_4$ H_2O) analysis on HPLC to detect *L*-Lac (6.1 min; *D*-Lac, 6.5 min).

Acetylation of Lyngbouilloside (163). To 0.9 mg of **163** was added three drops of pyridine following by six drops of acetic anhydride. The mixture was stirred in a two dram vial at RT for 19 h. The solution was then dried down *in vacuo* and subjected to ^{1}H NMR analysis in $CDCl_3$.

Cytotoxicity Assay.[165] Neuro-2a mouse neuroblastoma cells (ATCC CCL-131) were grown in RPMI 1640 medium supplemented with 10% heat-inactivated fetal bovine serum, 1 mM sodium pyruvate, 50 μg/mL streptomycin, and 50 units/mL penicillin in an atmosphere of 5% CO_2 at 37 °C. Growth medium (200 μL) containing the cell suspension (1×10^5 cells/mL) was placed in 96-well culture plates. After 24 h, 30 μL of the samples were added to the cells. The sample was dissolved in EtOH and serially diluted with medium to make the final concentration of EtOH less than 1%. Cultures were incubated for 24 h, and cytotoxicity determined by the MTT (3-[4,5-dimethylthiazol-2-yl]-2,5-diphenyltetrazolium bromide) assay with colorimetric measurement at 570 nm.

CHAPTER SIX

CONCLUSIONS

A total of three species of marine organisms have been examined for their chemical constituents in this thesis. These were a red alga, *Ceratodictyon spongiosum* Zanardini, from Indonesia and two species of marine cyanobacteria, two different collections of *Lyngbya majuscula* Gomont, from Papua New Guinea and *L. bouillonii* Hoffmann and Demoulin, also from Papua New Guinea. Thirteen new natural products were identified from the organic extracts of these marine algae. The isolations and purifications of these molecules were achieved by using different chromatographic techniques, including VLC and HPLC, and their structure determinations established by extensive 1D and 2D NMR experiments. All of the secondary metabolites, except for lyngbouilloside (**163**), are nitrogen-containing with molecular sizes ranging from 359 MW [hermitamide A (**123**)] to 817 MW [bouillonamide A (**161**)]. In addition to being new chemical structures, these molecules possessed various bioactivities including anti-inflammatory, antifungal, and cytotoxic activities (Table VI.1).

The organic extract of the red alga, *Ceratodictyon spongiosum*, yielded two new cyclic heptapeptides, *cis,cis*- (**96**) and *trans,trans*-ceratospongamide (**97**). These metabolites have identical planar structures with the main difference being the conformation of the Pro amide bonds in each of the molecules. Evidence for such conformational difference was obtained from comparing the $\Delta\delta_{\beta\gamma}$ of the carbon chemical shifts in the Pro unit between these molecules, from ROESY data, as well as chemical transformation from the *cis*-form (**96**) to the *trans*-form (**97**). This subtle difference in conformation translates into a dramatic effect in bioactivity as the *trans*-form (**97**) is a potent anti-inflammatory agent, inhibiting $sPLA_2$ expression in a cell-based model with ED_{50} 32 nM, whereas the *cis,cis* isomer (**96**) was inactive. The true producer of these cyclopeptides is not known as the alga has a sponge symbiont as well as other microorganism associations. However, cyanobacteria are implicated as the true

producer due to structural similarities of these molecules with those isolated from other blue-green algae.

Hermitamides A (**123**) and B (**124**) were isolated from a collection of *Lyngbya majuscula* from reefs off of the Hermit Village Islands, Papua New Guinea. These are new additions to a growing class of marine cyanobacterial metabolites known as the malyngamides. Semi-syntheses of these molecules were achieved by three different methods, mainly through the coupling of the naturally occurring lyngbic acid (**98b**), isolated from the organic extract, with different free amines. Two synthetic methods, involving the generation of acid chloride derivatives, gave higher yields of the hermitamides. These natural molecules possessed biological activities, ranging from brine-shrimp toxicity, ichthyotoxicity, and cytotoxicity. Two new *N*-methylated derivatives of the hermitamides, *N*-Me-hermitamides A (**125**) and B (**126**), were also synthesized and exhibited biological activities similar to the natural compounds.

The organic extract of a species of the marine cyanobacterium, *Lyngbya majuscula* from Papua New Guinea, is a rich source of a series of novel cyclic depsipeptides. Each of these molecules contained unique structural moieties, including α-hydroxy acids (2-hydroxy-isovaleric acid and lactic acid), β-amino acids [clairamides A (**151**) and B (**152**), wewakamide (**153**), and carliamide (**154**)], and β-hydroxy acids [guinamides A (**155**) and B (**156**)]. The β-hydroxy acid unit of 2,2-dimethyl-hexanoic acid in the guinamides is a new structural unit to be found in marine natural products. There were also a high occurrence of *N*-methylated α-amino acids, especially Val, in these natural products. Structural similarities between these cyanobacterial molecules to those reported from marine mollusks gave further support to the hypothesis that many metabolites from the latter organisms are diet-derived. Analyses using Marfey's method (using both *L*- and *D*-Marfey's reagent) were used extensively for stereochemical determination in these compounds. Carliamide (**154**) and clairamide B (**152**) had only moderate activities with IC_{50} values of 16 μM and 15 μM, respectively.

Lyngbya bouillonii is rapidly becoming recognized as an important species of marine cyanobacteria for the production of novel secondary metabolites. Three new compounds were isolated from the organic extract of this species collected from Papua New Guinea. Bouillonamide A (**161**), the largest new molecule reported in this thesis, is

a product of a mixed PKS and NRPS biosynthetic gene clusters. The second depsipeptide, bouillonamide B (**162**) is structurally related to the clairamides (**151** and **152**), differing in the amino acids sequence and in the β-amino acid unit. The 14-membered glycosidic macrolide, lyngbouilloside (**163**), contained a unique sugar of 2,4-di-*O*-methylrhamnopyranoside. It is also the second glycosidic macrolide to be reported from a marine cyanobacterium. All three metabolites showed moderate cytotoxicity against the mouse neuro-2a neuroblastoma cells.

This thesis has shown that marine algae, especially marine cyanobacteria, are indeed a prolific and important source of new and bioactive natural products. Some of these molecules have potential to be pharmaceuticals or as chemical leads in generating new pharmaceuticals. It is therefore a worthwhile pursuit to carry out natural products research on these phenomenal microorganisms.

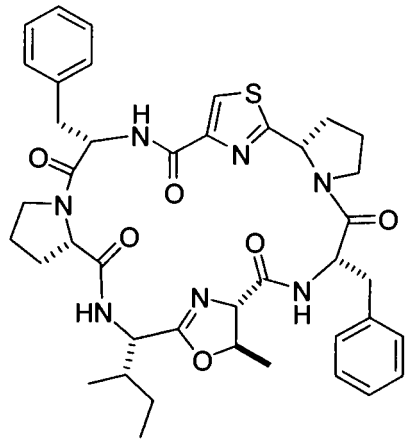

Cis,cis-ceratospongamide (**96**)

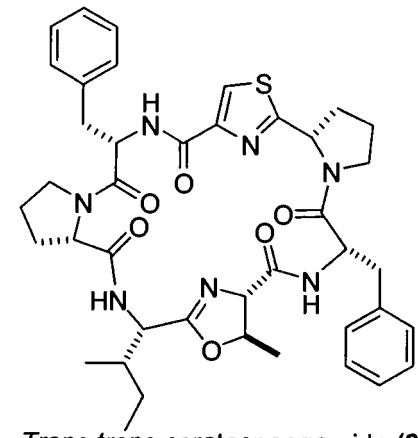

Trans,trans-ceratospongamide (**97**)

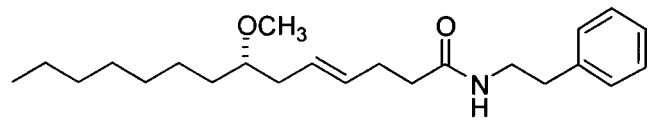

Hermitamide A (**123**)

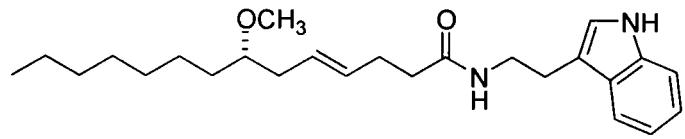

Hermitamide B (**124**)

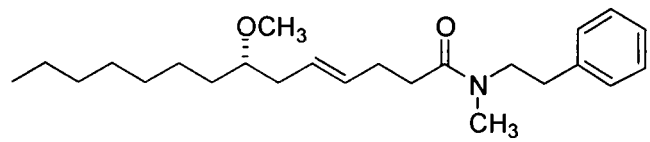

N-Methyl-hermitamide A (**125**)

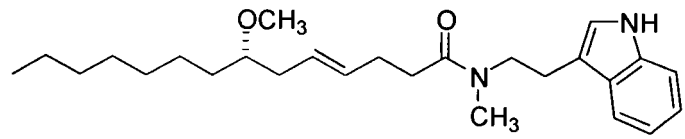

N-Methyl-hermitamide B (**126**)

Figure VI.1 Natural products from *Ceratodictyon spongiosum* (**96** and **97**) and *Lyngbya majuscula* (**123** and **124**). [Compounds **125** and **126** are synthetic *N*-methylated derivatives of the natural hermitamides]

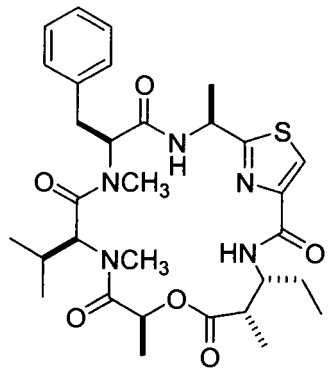

Clairamide A (**151**)

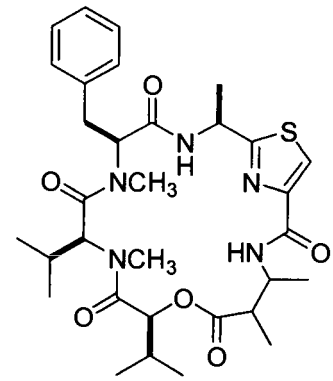

Clairamide B (**152**)

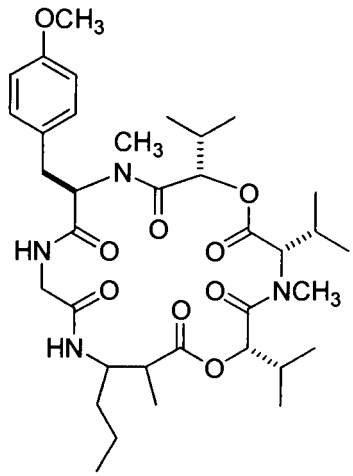

Wewakamide (**153**)

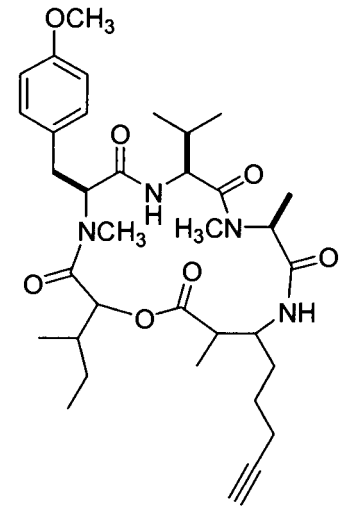

Carliamide (**154**)

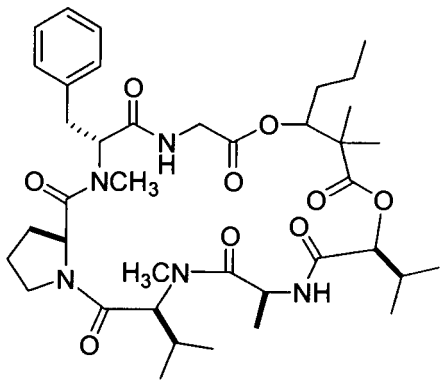

Guinamide A (**155**)

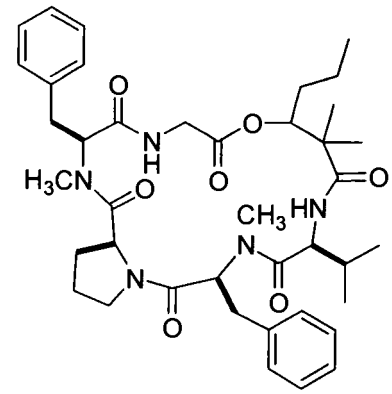

Guinamide B (**156**)

Figure VI.2 Natural products isolated and defined in this thesis from Papua New Guinea collections of *Lyngbya majuscula* (**151** to **156**).

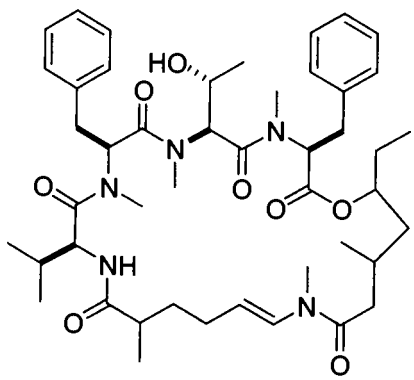

Bouillonamide A (**161**)

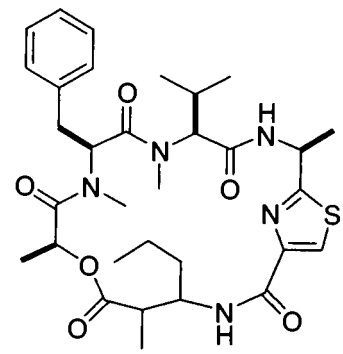

Bouillonamide B (**162**)

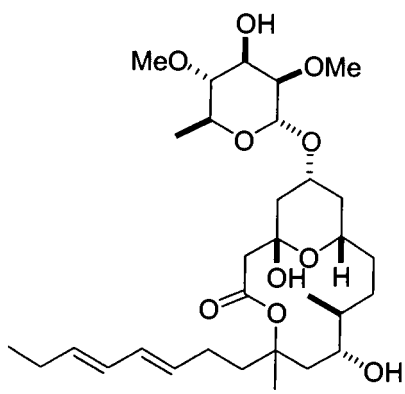

Lyngbouilloside (**163**)

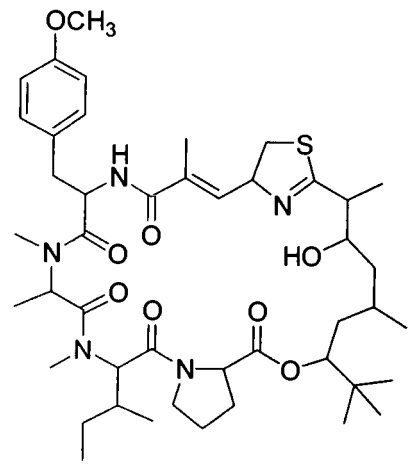

Apratoxin (**164**)

Figure VI.3 Natural products isolated and defined in this thesis from Papua New Guinea collections of *Lyngbya bouillonii* (**161** to **164**).

Table VI.1 Biological activities of natural and semi-synthetic molecules presented in the thesis.

Organisms & ID numbers	Compounds	Biological Activities				
		Antiinflammatory[a] (ED_{50})	Cytotoxicity[b] (IC_{50})	Antifungal	Brine shrimp[c] (LD_{50})	Ichthyotoxicity[d] (LD_{50})
Ceratodictyon spongiosum IBI 4/Nov/94-15	*cis,cis*-Ceratospongamide (**96**)	inactive			*ca.* 13-19 μM	
	trans,trans-Ceratospongamide (**97**)	32 nM			*ca.* 13-19 μM	
Lyngbya Majuscula PNHV 11/Sep/98-04	Hermitamide A (**123**)		2.2 μM		5 μM	19 μM
	Hermitamide B (**124**)		5.5 μM		18 μM	inactive at 25 μM
	N-Me-Hermitamide A (**125**)				6 μM	
	N-Me-Hermitamide B (**126**)				18 μM	
L. majuscula PNSM 4/Sep/98-01	Clairamide A (**151**)			inactive[e]		
	Clairamide B (**152**)		15 μM	active[e]		
	Wewakamide (**153**)			not tested		
	Carliamide (**154**)		16 μM	active[e]		
	Guinamide A (**155**)			inactive[e]		
	Guinamide B (**156**)			inactive[e]		
L. bouillonii PNGRD 21/Aug/00-2	Bouillonamide A (**161**)		6.0 μM		9.0 μM	
	Bouillonamide B (**162**)		16.0 μM		18.0 μM	
	Lyngbouilloside (**163**)		17.0 μM			
	Apratoxin (**164**)		1.0 μM			

[a] inhibition of $sPLA_2$ expression in a cell-based model for anti-inflammation. [b] cytotoxicity against the neuro-2a neuroblastoma cell in tissue culture. [c] toxicity against the brine shrimp *Artemia salina*. [d] toxicity against the goldfish *Carassius auratus*. [e] proprietary bioassay results from industrial collaborator.

BIBLIOGRAPHY

1. Grifo, F. T.; Newman, D.; Fairfield, A. S. *Biodiversity and Human Health*; Grifo, F. T., Rosenthal, J., Eds.; Island Press: Washington D. C., 1997; pp 131–163.

2. Bergman, W.; Feeney, R. J. *J. Org. Chem.* **1951**, *16*, 981–987.

3. Bodey, G. P.; Freirich, E. J.; Monto, R. W.; Hewlett, J. S. *Cancer Chemother.* **1969**, *53*, 59–66.

4. Buchanan, R. A.; Hess, F. *Science* **1980**, *127*, 143–171.

5. Culotta, E. *Science* **1994**, *263*, 918–920.

6. Jaspars, M. *Advances in Drug Discovery Techniques*; Harvey, A. L., Ed.; Wiley: New York, 1998; pp 65–84.

7. Faulkner, D. J. *Nat. Prod. Rep.* **2001**, *18*, 1–49.

8. Lin, Y.–Y.; Risk, M.; Ray, S. M.; Van Engen, D.; Clardy, J.; Golik, J.; James, J. C.; Nakanishi, K. *J. Am. Chem. Soc.* **1981**, *103*, 6773–6775.

9. Murata, M.; Legrand, A.–M.; Ishibashi, Y.; Yasumoto, T. *J. Am. Chem. Soc.* **1989**, *111*, 8927–8931.

10. Murata, M.; Nakoi, H.; Iwashita, T.; Matsunaga, S.; Sasaki, M.; Yokoyama, A.; Yasumoto, T. *J. Am. Chem. Soc.* **1993**, *115*, 2060–2062.

11. Norimura, T.; Sasaki, M.; Matsumori, N.; Miata, M.; Tachibana, K.; Yasumoto, T. *Angew. Chem. Int. Ed. Engl.* **1996**, *35*, 1675–1678.

12. Yasumoto, T.; Oshima, Y.; Sugawara, W.; Fukuyo, Y.; Oguri, H.; Igarashi, T.; Fujita, N. *Nippon Suisan Gakkaishi* **1980**, *46*, 1405–1411.

13. Murakami, Y.; Oshima, Y.; Yasumoto, T. *Nippon Suisan Gakkaishi* **1982**, *48*, 69–72.

14. Moore, R. E.; Scheuer, P. J. *Science* **1971**, *172*, 495–498.

15. Pettit, G. R.; Herald, C. L.; Doubek, D. L.; Herald, D. L.; Arnold, E.; Clardy, J. *J. Am. Chem. Soc.* **1982**, *104*, 6846–6848.

16. May, W. S.; Sharkis, S. J.; Esa, A. H.; Gebbia, V.; Kraft, A. S.; Pettit, G. R.; Sensenbrenner, L. L. *Proc. Natl. Acad. Sci. USA* **1987**, *84*, 8483–8487.

17. Kraft, A. S. *J. Natl. Cancer Inst.* **1993**, *85*, 1790–1792.

18. Kraft, A. S.; Woodley, S.; Pettit, G. R.; Gao, F.; Coll, J. C.; Wagner, F. *Cancer Chemother. Pharmacol.* **1996**, *37*, 271–278.

19. Schaufelberger, D. E.; Pettit, G. R. *J. Nat. Prod.* **1991**, *54*, 1265–1270.

20. Haygood, M. G.; Schmidt, E. W.; Davidson, S. K.; Faulkner, D. J. *J. Mol. Microbiol. Biotechnol.* **1999**, *1*, 33–43.

21. Wright, A. E.; Forleo, D. A.; Gunawardana, G. P.; Gunasekera, S. P.; Koehn, F. E.; McConnell, O. J. *J. Org. Chem.* **1990**, *55*, 4508–4511.

22. Rinehart, K. L.; Holt, T. G.; Fregeau, N. L.; Stroh, J. G.; Kiefer, P. A.; Sun, F.; Li, L. H.; Martin, D. G. *J. Org. Chem.* **1990**, *55*, 4512–4515.

23. Sakai, R.; Rinehart, K. L.; Kishore, V.; Kundu, B.; Faircloth, G.; Gloer, J. B.; Carney, J. R.; Namikoshi, M.; Sun, F.; Hughes, R. G.; Garcia Gravalos, D.; de Quesada, T. G.; Wilson, G. R.; Heid, R. M. *J. Med. Chem.* **1996**, *39*, 2819–2834.

24. Pettit, G. R.; Kamano, Y.; Herald, C. L.; Tuinamn, A. A.; Boettner, F. E.; Kizu, H.; Schmidt, J. M.; Baczynskyj, L.; Tomer, K. B.; Bontems, R. *J. Am. Chem. Soc.* **1987**, *109*, 6883–6885.

25. Hirata, Y.; Uemura, D. *Pure Appl. Chem.* **1986**, *58*, 701–710.

26. Litaudon, M.; Hart, J. B.; Blunt, J. W.; Lake, R. J.; Munro, M. H. G. *Tetrahedron Lett.* **1994**, *35*, 9435–9438.

27. Yamada, K.; Ojika, M.; Ishigaki, T.; Yoshida, Y.; Ekimoto, H.; Arakawa, M. *J. Am. Chem. Soc.* **1993**, *115*, 11020–11021.

28. Gunasekera, S. P.; Gunasekera, M.; Longley, R. E.; Schulte, G. K. *J. Org. Chem.* **1990**, *55*, 4912–4915.

29. Lindel, T.; Jensen, P. R.; Fenical, W.; Long, B. H.; Casazza, A. M.; Carboni, J.; Fairchild, C. R. *J. Am. Chem. Soc.* **1997**, *119*, 8744–8745.

30. D'Ambrosio, M.; Guerriero, A.; Pietra, F. *Helv. Chim. Acta* **1987**, *70*, 2019–2027.

31. Gerwick, W. H.; Proteau, P. J.; Nagle, D. G.; Hamel, E.; Blokhin, A, Slate, D. L. *J. Org. Chem.* **1994**, *59*, 1243–1245.

32. Hamann, M. T.; Scheuer, P. J. *J. Am. Chem. Soc.* **1993**, *115*, 5825–5826.

33. Kobayashi, E.; Motoki, K.; Uchida, T.; Fukushima, H.; Koezuka, Y. *Oncol. Res.* **1995**, *7*, 529–534.

34. Jordan, A.; Hadfield, J. A.; Lawrence, N. J.; McGown, A. T. *Med. Res. Rev.* **1998**, *18*, 259–296.

35. Wylie, B. L.; Ernst, N. B.; Grace, K. J. S.; Jacobs, R. S. *Prog. Surg.* **1997**, *24*, 146–152.

36. Bartik, K.; Braekman, J.–C.; Daloze, D.; Stoller, C.; Huysecom, J.; Vandevyver, G.; Ottinger, R. *Can. J. Chem.* **1987**, *65*, 2118–2121.

37. Cimino, G.; De Stefano, S.; Minale, L. *Experientia* **1974**, *30*, 846–847.

38. Proteau, P.; Gerwick, W. H.; Garcia–Pichel, F.; Castenholz, R. *Experientia* **1993**, *49*, 825–829.

39. De Silva, E. D.; Scheuer, P. J. *Tetrahedron Lett.* **1980**, *21*, 1611–1614.

40. Look, S. A.; Fenical, W.; Matsumoto, G. K.; Clardy, J. *J. Org. Chem.* **1986**, *51*, 5140–5145.

41. Roussis, V.; Wu, Z, Fenical, W.; Strobel, S. A.; Van Duyne, G. D.; Clardy, J. *J. Org. Chem.* **1990**, *55*, 4916–4922.

42. Anger, T.; Madge, D. J.; Mulla, M.; Riddall, D. *J. Med. Chem.* **2001**, *44*, 115–137.

43. Takai, A.; Bialojan, C.; Troschka, M.; Ruegg, J. C. *FEBS Lett.* **1987**, *217*, 81–84.

44. Spector, I.; Shochet, N. R.; Kashman, Y.; Groweiss, A. *Science* **1983**, *219*, 493–495.

45. Kitagawa, I.; Kobayashi, M.; Katori, T.; Yamashita, M.; Tanaka, J.; Doi, M.; Ishida, T. *J. Am. Chem. Soc.* **1990**, *112*, 3710–3712.

46. Zabriskie, T. M.; Klocke, J. A.; Ireland, C. M.; Marcus, A. H.; Molinski, T. F.; Faulkner, D. J.; Xu, C.; Clardy, J. C. *J. Am. Chem. Soc.* **1986**, *108*, 3123–3124.

47. Crews, P.; Manes, L. V.; Boehler, M. *Tetrahedron Lett.* **1986**, *27*, 2797–2800.

48. Luibrand, R. T.; Erdman, T. R.; Vollmer, J. J.; Scheuer, P. J.; Finer, J.; Clardy, J. *Tetrahedron* **1979**, *35*, 609–612.

49. Blackburn, C. L.; Hopmann, C.; Sakowicz, R.; Berdelis, M. S.; Goldstein, L. S. B.; Faulkner, D. J. *J. Org. Chem.* **1999**, *64*, 5565–5570.

50. Wright, A. D.; Konig, G. M. *J. Nat. Prod.* **1996**, *59*, 710–716.

51. Ang, K. K. H.; Holmes, M. J.; Higa, T.; Hamann, M. T.; Kara, U. A. K. *Antimicrob. Agents Chemother.* **2000**, *44*, 1645–1649.

52. El Sayed, K. A.; Kelly, M.; Kara, U. A. K.; Ang, K. K. H.; Katsuyama, I.; Dunbar, D. C.; Khan, A. A.; Hamann, M. T. *J. Am. Chem. Soc.* **2001**, *123*, 1804–1808.

53. El Sayed, K. A.; Bartyzel, P.; Shen, X.; Perry, T. L.; Zjawiony, J. K.; Hamann, M. T. *Tetrahedron* **2000**, *56*, 949–953.

54. De Clercq, E. *Med. Res. Rev.* **2000**, *20*, 323–349.

55. Reddy, M. V. R.; Rao, M. R.; Rhodes, D.; Hansen, M. S. T.; Rubins, K.; Bushman, F. D.; Venkateswarlu, Y.; Faulkner, D. J. *J. Med. Chem.* **1999**, *42*, 1901–1907.

56. Thale, Z.; Kinder, F. R.; Bair, K. W.; Bontempo, J.; Czuchta, A. M.; Versace, R. W.; Phillips, P. E.; Sanders, M. L.; Wattanasin, S.; Crews, P. *J. Org. Chem.* **2001**, *66*, 1733–1741.

57. El Sayed, K. A.; Dunbar, D. C.; Bartyzel, P.; Zjawiony, J. K.; Day, W.; Hamann, M. T. *Biologically Active Natural Products: Pharmaceuticals*; Cutler, S. J., Cutler, H. G., Eds.; CRC Press: 1999; pp 233–252.

58. Keifer, P. A.; Rinehart, K. L.; Hooper, I. R. *J. Org. Chem.* **1986**, *51*, 4450–4454.

59. Walker R. P.; Faulkner, D. J. *J. Org. Chem.* **1981**, *46*, 1098–1102.

60. Kashman, Y.; Zviely, M. *Experientia* **1980**, *36*, 1279–1279.

61. Manefield, M.; de Nys, R.; Kumar, N.; Read, R.; Givskov, M.; Steinberg, P.; Kjelleberg, S. *Microbiology* **1999**, *145*, 283–291.

62. Hay, M. E.; Fenical, W. *Oceanography* **1996**, *9*, 10–20.

63. Gribble, G. W. *Chem. Soc. Rev.* **1999**, *28*, 335–346.

64. Fuller, R. W.; Cardellina, J. H.; Kato, Y.; Brinen, L. S.; Clardy, J.; Snader, K. M.; Boyd, M. R. *J. Med. Chem.* **1992**, *35*, 3007–3011.

65. Fuller, R. W.; Cardellina, J. H.; Jurek, J.; Scheuer, P. J.; Alvarado–Lindner, B.; McGuire, M.; Gray, G. N.; Steiner, J. R.; Clardy, J.; Menez, E.; Shoemaker, R. H.; Newman, D. J.; Snader, K. M.; Boyd, M. R. *J. Med. Chem.* **1994**, *37*, 4407–4411.

66. Murakami, S.; Takemoto, T.; Shimizu, Z. *J. Pharm. Soc. Japan* **1953**, *73*, 1026–1028.

67. Daigo, K. *Yakugaku Zasshi* **1959**, *79*, 356–360.

68. Wright, J. L.; Bird, C. J.; de Freitas, A. S.; Hampson, D.; McDonald, J.; Quilliam, M. A. *Can. Dis. Wkly. Rep.* **1990**, *1E*, 21–26.

69. Gerwick, W. H.; Bernart, M. W. *Marine Biotechnology, Volumn 1: Pharmaceutical and Bioactive Natural Products*; Attaway, D. H., Zaborsky, O. R., Eds.; Plenum Press: New York, 1993; pp 101–151.

70. Fusetani, N.; Hashimoto, K. *Bull. Jpn. Soc. Sci.* **1984**, *50*, 465–469.

71. Yamashita, M. Y.; Haddock, R. L.; Yasumoto, T. *J. Am. Chem. Soc.* **1993**, *115*, 1147–1148.

72. Yamashita, M. Y.; Seki, T.; Paul, V. J.; Naoki, H.; Yasumoto, T. *Tetrahedron Lett.* **1995**, *36*, 5563–5566.

73. Nagai, H.; Yasumoto, T.; Hokama, Y. *J. Nat. Prod.* **1997**, *60*, 925–928.

74. Nagai, H.; Yasumoto, T.; Hokama, Y. *Toxicon* **1996**, *37*, 753–761.

75. Rice, S. A.; Givskov, M.; Steinberg, P.; Kjelleberg, S. *J. Mol. Microbiol. Biotechnol.* **1999**, *1*, 23–31.

76. Panda, D.; Ananthnarayan, V.; Larson, G.; Shih, C; Jordan, M. A.; Wilson, L. *Biochemistry* **2000**, *39*, 14121–14127.

77. Gerwick, W. H.; Roberts, M. A.; Proteau, P. J.; Chen, J.–L. *J. Applied Phycology* **1994**, *6*, 143–149.

78. Ojala, J.; Nagle, D. G.; Hsu, V. L.; Gerwick, W. H. *J. Am. Chem. Soc.* **1995**, *117*, 8281–8282.

79. Nagle, D. G.; Paul, V. J. Roberts, M. A. *Tetrahedron Lett.* **1996**, *37*, 6263–6266.

80. Klein, D.; Braekman, J. C.; Daloze, D.; Hoffmann, L.; Demoulin, V. *J. Nat. Prod.* **1997**, *60*, 1057–1059.

81. Nagle, D. G.; Park, P. U.; Paul, V. J. *Tetrahedron Lett.* **1997**, *38*, 6969–6972.

82. Harrigan G. G.; Luesch, H.; Yoshida, W. Y.; Moore, R. E.; Nagle, D. G.; Paul, V. J.; Mooberry, S. L.; Corbett, T. H.; Valeriote, F. A. *J. Nat. Prod.* **1998**, *61*, 1075–1077.

83. Harrigan G. G.; Luesch, H.; Yoshida, W. Y.; Moore, R. E.; Nagle, D. G.; Paul, V. J. *J. Nat. Prod.* **1999**, *62*, 655–658.

84. Harrigan G. G.; Yoshida, W. Y.; Moore, R. E.; Nagle, D. G.; Park, P. U.; Biggs, J.; Paul, V. J.; Mooberry, S. L.; Corbett, T. H.; Valeriote, F. A. *J. Nat. Prod.* **1998**, *61*, 1221–1225.

85. Luesch, H.; Yoshida, W. Y.; Moore, R. E.; Paul, V. J. *J. Nat. Prod.* **1999**, *62*, 1702–1706.

86. Harrigan G. G.; Luesch, H.; Yoshida, W. Y.; Moore, R. E.; Nagle, D. G.; Biggs, J.; Park, P. U.; Paul, V. J. *J. Nat. Prod.* **1999**, *62*, 464–467.

87. Sitachitta, N.; Williamson, R. T.; Gerwick, W. H. *J. Nat. Prod.* **2000**, *63*, 197–200.

88. Berman F. W.; Gerwick, W. H.; Murray, T. F. *Toxicon* **1999**, *37*, 1645–1648.

89. Horgen, F. D.; Yoshida, W. Y.; Scheuer, P. J. *J. Nat. Prod.* **2000**, *63*, 461–467.

90. Luesch, H.; Yoshida, W. Y.; Moore, R. E.; Paul, V. J.; Mooberry, S. L. *J. Nat. Prod.* **2000**, *63*, 611–615.

91. Luesch, H.; Yoshida, W. Y.; Moore, R. E.; Paul, V. J. *J. Nat. Prod.* **2000**, *63*, 1437–1439.

92. Milligan, K. E.; Marquez, B. L.; Williamson, R. T.; Gerwick, W. H. *J. Nat. Prod.* **2000**, *63*, 1440–1443.

93. Paul, V. J.; Pennings, S. C. *J. Exp. Mar. Biol. Ecol.* **1991**, *151*, 227–243.

94. Rose, A. F.; Scheuer, P. J.; Springer, J. P.; Clardy, J. *J. Am. Chem. Soc.* **1978**, *100*, 7665–7670.

95. Poncet, J. *Curr. Pharm. Des.* **1999**, *5*, 139–162.

96. Pettit, G. R.; Kamano, Y.; Herald, C. L.; Cerny, R. L.; Herald, D. L.; Schmidt, J. M.; Kizu, H. *J. Am. Chem. Soc.* **1989**, *111*, 5015–5017.

97. Ishida, K.; Matsuda, H.; Murakami, M.; Yamaguchi, K. *J. Nat. Prod.* **1997**, *60*, 184–187.

98. Pettit, G. R.; Kamano, Y.; Dufresne, C.; Cerny, R. L.; Herald, C. L.; Schmidt, J. M. *J. Org. Chem.* **1989**, *54*, 6005–6006.

99. Carmeli, S.; Moore, R. E.; Patterson, G. M. L. *J. Nat. Prod.* **1990**, *53*, 1533–1542.

100. Nakao, Y.; Yoshida, W. Y.; Szabo, C. M.; Baker, B. J.; Scheuer, P. J. *J. Org. Chem.* **1998**, *63*, 3272–3280.

101. Sone, H.; Kigoshi, H.; Yamada, K. *J. Org. Chem.* **1996**, *61*, 8956–8960.

102. Kobayashi, M.; Aoki, S. J.; Ohyabu, N.; Kurosu, M.; Wang, W. Q.; Kitagawa, I. *Tetrahedron Lett.* **1994**, *35*, 7969–7972.

103. Kobayashi, M.; Kurosu, M.; Ohyabu, N.; Wang, W. Q.; Fujii, S.; Kitagawa, I. *Chem. Pharm. Bull.* **1994**, *42*, 2196–2198.

104. Dilip de Silva, E.; Williams, D. E.; Andersen, R. J.; Klix, H.; Holmes, C. F. B.; Allen, T. M. *Tetrahedron Lett.* **1992**, *33*, 1561–1564.

105. Moroder, L.; Rudolph–Bohner, S. *Stud. Nat. Prod. Chem.* **1998**, *20*, 887–920.

106. Unson, M. D.; Holland, N. D.; Faulkner, D. J. *Mar. Biol.* **1994**, *119*, 1–11.

107. Flowers, A. E.; Garson, M. J.; Webb, R. I.; Dumdei, E. J.; Charan, R. D. *Cell Tissue Res.* **1998**, *292*, 597–607.

108. Orjala, J.; Gerwick, W. H. *J. Nat. Prod.* **1996**, *59*, 427–430.

109. Sings, H. L.; Rinehart, K. L. *J. Ind. Microbiol.* **1996**, *17*, 385–396.

110. Hambley, T. W.; Hawkins, C. J.; Lavin, M. F.; Van den Brenk, A.; Watters, D. J. *Tetrahedron* **1992**, *48*, 341–348.

111. Prinsep, M. R.; Moore, R. E.; Levine, I. A.; Patterson, G. M. L. *J. Nat. Prod.* **1992**, *55*, 140–142.

112. Price, I. R.; Kraft, G. T. *Phycologia* **1991**, *30*, 106–116.

113. Lo, J.–M.; Wang, W.–L.; Chiang, Y.–M.; Chen, C.–M. XVIth International Seaweed Sym., Cebu City, Philippines, Apr. 12–17, 1998.

114. Olivier, J. L.; Fan, Q.; Salavat, C.; Ziari, M.; Kong, L.; Manageney, M.; Bereziat, G. *Biochemistry* **1994**, *33*, 7134–7145.

115. Vadas, P.; Pruzanski, W. *Lab. Invest.* **1986**, *55*, 391–404.

116. Vadas, P.; Pruzanski, W.; Stefanski, E. *Agents Actions* **1988**, *24*, 320–325.

117. Pruzanski, W.; Bogoch, E.; Wloch, M.; Vadas, P. *J. Rheumatology* **1991**, *18*, 117–119.

118. Crowl, R. M.; Stoller, T. J.; Conroy, R. R.; Stoner, R. R. *J. Biol. Chem.* **1991**, *266*, 2647–2651.

119. Cao, Z.; Xiong, J.; Takeuchi, M.; Kurama, T.; Goeddel, D. *Nature* **1996**, *383*, 443–446.

120. O'Neill, L. A. J. *Biochem. Soc. Trans.* **1996**, *24*, 207–211.

121. Potts, B. C. M.; Faulkner, D. J.; Jacobs, R. S. *J. Nat. Prod.* **1992**, *55*, 1701–1717.

122. Ireland, C. M.; Scheuer, P. J. *J. Am. Chem. Soc.* **1980**, *102*, 5688–5691.

123. Williamson, R. T.; Marquez, B.; Gerwick, W. H. *Tetrahedron* **1999**, *55*, 2881–2888.

124. Martin, G. E.; Crouch, R. C.; Sharaf, M. H. M.; Schiff, P. L. *J. Nat. Prod.* **1996**, *59*, 2–4.

125. Fukuzawa, S.; Matsunaga, S.; Fusetani, N. *Tetrahedron Lett.* **1996**, *37*, 1447–1448.

126. Williamson, M. P. *Nat. Prod. Rep.* **1993**, *10*, 207–232.

127. Marfey, P. *Carlsberg Res. Commun.* **1984**, *49*, 591–596.

128. McDonald, L. A.; Ireland, C. M. *J. Nat. Prod.* **1992**, *55*, 376–379.

129. Siemion, I. Z.; Wieland, T.; Pook, K. *Angew. Chem. Int. Ed.* **1975**, *14*, 702–703.

130. Kessler, H. *Angew. Chem. Int. Ed.* **1982**, *21*, 512–523.

131. Schmidt, E. W.; Bewley, C. A.; Faulkner, D. J. *J. Org. Chem.* **1998**, *63*, 1254–1258.

132. Bewley, C.; Faulkner, D. J. *Angew. Chem. Int. Ed.* **1998**, *37*, 2162–2178.

133. Roshak, A. K.; Mochan, E.; Marshall, L. A. *J. Rheumatology* **1996**, *23*, 420–427.

134. Dauber–Osguthorpe, P.; Roberts, V. A.; Osguthorpe, D. J.; Wolff, J.; Genest, M.; Hagler, A. T. *Proteins: Structure, Function and Genetics* **1988**, *4*, 31–47.

135. Markley, J. L.; Bax, A.; Arata, Y.; Hilbers, C. W.; Kaptein, R.; Sykes, B. D.; Wright, P. E.; Wthrich, K. *Pure & Appl. Chem.* **1998**, *70*, 117–142.

136. Cardellina II, J. H.; Dalietos, D.; Marner, F.–J.; Mynderse, J.S.; Moore, R.E. *Phytochemistry* **1978**, *17*, 2091–2095.

137. Cardellina II, J. H.; Marner, F.–J.; Moore, R. E. *J. Am. Chem. Soc.* **1978**, *101*, 240–242.

138. Ainslie, R. D.; Barchi, J. J.; Kuniyoshi, M.; Moore, R. E.; Mynderse, J.S. *J. Org. Chem.* **1985**, *50*, 2859–2862.

139. Wright, A. D.; Coll, J. C.; Price, I. R. *J. Nat. Prod.* **1990**, *53*, 845–861.

140. Mynderse, J. S.; Moore, R. E. *J. Org. Chem.* **1978**, *43*, 4359–4363.

141. Gerwick, W. H.; Reyes, S.; Alvarado, B. *Phytochemistry* **1987**, *26*, 1701–1704.

142. Praud, A.; Valls, R.; Piovetti, L.; Banaigs, B. *Tetrahedron Lett.* **1993**, *34*, 5437–5440.

143. Mesguiche, V.; Valls, R.; Piovetti, L.; Peiffer, G. *Tetrahedron Lett.* **1999**, 7473–7476.

144. Orjala, J.; Nagle, D.; Gerwick, W. H. *J. Nat. Prod.* **1995**, *58*, 764–768.

145. Todd, J. S.; Gerwick, W. H. *Tetrahedron Lett.* **1995**, *36*, 7837–7840.

146. Wu, M.; Milligan, K. E.; Gerwick, W. H. *Tetrahedron Lett.* **1997**, *53*, 15983–15990.

147. Kan, Y.; Fujita, T.; Nagai, H.; Sakamoto, B.; Hokama, Y. *J. Nat. Prod.* **1998**, *61*, 152–155.

148. Gallimore, W. A.; Scheuer, P. J. *J. Nat. Prod.* **2000**, 1422–1424.

149. Milligan, K. E.; Marquez, B.; Williamson, R. T.; Davies–Coleman, M.; Gerwick, W. H. *J. Nat. Prod.* **2000**, *63*, 965–968.

150. Wan, F.; Erickson, K. L. *J. Nat. Prod.* **1999**, *62*, 1696–1699.

151. Kan, Y.; Sakamoto, B.; Fujita, T.; Nagai, H. *J. Nat. Prod.* **2000**, *63*, 1599–1602.

152. Fryhle, C. B.; Willard, P. G.; Rybak, C. M. *Tetrahedron Lett.* **1992**, *33*, 2327–2330.

153. Sankaranarayanan, S.; Sharma, A.; Chattopadhyay, S. *Tetrahedron Asymm.* **1996**, 2639–2643.

154. Muller, C.; Voss, G.; Gerlach, H. *Liebigs Ann. Chem.* **1995**, 673–675.

155. Wylie, C. R.; Paul, V. J. *Mar. Ecol. Prog. Ser.* **1988**, *45*, 23–32.

156. Pennings, S. C.; Paul, V. J. *Mar. Biol.* **1993**, *117*, 535–546.

157. Nagle, D. G.; Camacho, F. T.; Paul, V. J. *Mar. Biol.* **1998**, *132*, 267–273.

158. Pennings, S. C.; Carefoot, T. H. *Comp. Biochem. Physiol.* **1995**, *111C*, 249–256.

159. Klausner, Y. S.; Bodansky, M. *Synthesis* **1972**, *9*, 453–463.

160. Jang, D. O.; Park, D. J.; Kim, J. *Tetrahedron Lett.* **1999**, *40*, 5323–5326.

161. Fletcher, R. L. *J. Appl. Phycol.* **1995**, *7*, 325–333.

162. Meyer, B. N.; Ferrigni, N. R.; Putnam, J. E.; Jacobsen, L. B.; Nichols, D. E.; McLaughlin, J. L. *Planta Med.* **1982**, *45*, 31–34.

163. Bakus, G. J.; Green, G. *Science* **1974**, *185*, 951–953.

164. Hostettmann, K.; Kizu, H.; Tomimori, T. *Planta Med.* **1982**, *44*, 34–35.

165. Manger, R. L.; Leja, L. S.; Lee, S. Y.; Hungerford, J. M.; Hokama, Y.; Dickey, R. W.; Granade, H. R.; Lewis, R.; Yasumoto, T.; Wekell, M. M. *J. AOAC International* **1995**, *78*, 521–527.

166. Reese, M. T.; Gulavita, N. K.; Nakao, Y.; Hamann, M. T.; Yoshida, W. Y.; Coval, S. J.; Scheuer, P. J. *J. Am. Chem. Soc.* **1996**, *118*, 11081–11084.

167. Sitachitta, N., Ph.D. Thesis, Oregon State University, Corvallis, **2000**.

168. Rodriquez, J.; Fernandez, R.; Quinoa, E.; Riguera, R.; Debitus, C.; Bouchet, P. *Tetrahedron Lett.* **1994**, *35*, 9239–9242.

169. Rodriquez, J.; Fernandez, R.; Quinoa, E.; Riguera, R.; Munoz, L.; Fernandez–Suarez, M.; Debitus, C. *J. Am. Chem. Soc.* **1996**, *118*, 11635–11643.

170. Pettit, G. R.; Kamano, Y.; Kizu, H.; Dufresne, C.; Herald, C. L.; Bontems, R.; Schmidt, J. M.; Boettner, F. E.; Nieman, R. A. *Heterocycles* **1989**, *28*, 553–558.

171. Williams, D. E.; Burgoyne, D. L.; Rettig, S. J.; Andersen, R. J. *J. Nat. Prod.* **1993**, *56*, 545–551.

172. Carter, D. C.; Moore, R. E.; Mynderse, J. S.; Niemczura, W. P.; Todd, J. S. *J. Org. Chem.* **1984**, *49*, 236–241.

173. Mynderse, J. S.; Hunt, A. H.; Moore, R. E. *J. Nat. Prod.* **1988**, *51*, 1299–1301.

174. Bates, R.; Gangwar, S. *Tetrahedron Asymm.* **1993**, *4*, 69–72.

175. Sone, H.; Nemoto, T.; Ishiwata, H.; Ojika, M.; Yamada, K. *Tetrahedron Lett.* **1993**, *34*, 8449–8452.

176. Fernandez–Suarez, M.; Munoz, L.; Fernandez, R.; Riguera, R. *Tetrahedron Asymm.* **1997**, *8*, 1847–1854.

177. Luesch, H.; Pangilinan, R.; Yoshida, W. Y.; Moore, R. E.; Paul, V. J. *J. Nat. Prod.* **2001**, *64*, 304–307.

178. Hoffmann, L.; Demoulin, V. *Belg. J. Bot.* **1991**, *124*, 82–88.

179. Klein, D.; Braekman, J. C.; Daloze, D.; Hoffmann, L.; Demoulin, V. *Tetrahedron Lett.* **1996**, *37*, 7519–7520.

180. Klein, D.; Braekman, J. C.; Daloze, D.; Hoffmann, L.; Castillo, G.; Demoulin, V. *J. Nat. Prod.* **1999**, *62*, 934–936.

181. Klein, D.; Braekman, J. C.; Daloze, D.; Hoffmann, L.; Castillo, G.; Demoulin, V. *Tetrahedron Lett.* **1999**, *40*, 695–696.

182. Zampella, A.; Valeria D'Auria, M.; Minale, L.; Debitus, C.; Roussakis, C. *J. Am. Chem. Soc.* **1996**, *118*, 11085–11088.

183. Zampella, A.; Valeria D'Auria, M.; Minale, L.; Debitus, C. *Tetrahedron* **1997**, *53*, 3243–3248.

184. Matsumori, N.; Kaneno, D.; Murata, M.; Nakamura, H.; Tachibana, K. *J. Org. Chem.* **1999**, *64*, 866-876.

APPENDICES

APPENDIX A

ISOLATION OF MALYNGAMIDE C AND DERIVATIVES FROM A MARINE CYANOBACTERIUM, *LYNGBYA* SPECIES, COLLECTED FROM PAPUA NEW GUINEA

An organic extract (# 1233) of a marine cyanobacterium, *Lyngbya* species, collected from Heina Lagoon, Papua New Guinea (PNHL 9 Sep 98-02) yielded a series of known malyngamides. These were malyngamide C (**1**), malyngamide C acetate (**2**), 8'-deacetoxymalyngamide C (**3**), and dideoxymalyngamide C (**4**) (= malyngamide K).[1]

Fraction 7, eluted with 70% EtOAc:Hexanes and 100% EtOAc from normal phase Si gel VLC of the organic extract (ca. 4.0 g), was subjected through a series of chromatographic techniques, including Mega Bond Sep Pak RP-18 and HPLC to give these natural products. The condition used for HPLC was 33% H_2O in CH_3CN on Phenomenex Sphereclone 5μ ODS (2) and detected at 215 nm on the UV detector.

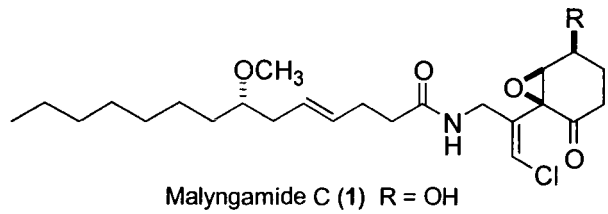

Malyngamide C (**1**) R = OH
Malyngamide C acetate (**2**) R = OAc
8'-Deacetoxymalyngamide C (**3**) R = H

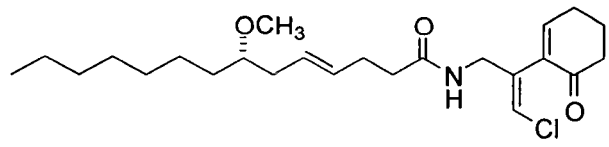

Dideoxymalyngamide C (**4**) (= Malyngamide K)

Reference

1. Ainslie, R. D.; Barchi, J. J.; Kuniyoshi, M.; Moore, R. E.; Mynderse, J.S. *J. Org. Chem.* **1985**, *50*, 2859–2862.

APPENDIX B

DETECTION OF DEBROMOAPLYSIATOXIN IN A MARINE CYANOBACTERIAL ASSEMBLAGE COLLECTED FROM FIJI

The aqueous extract (# 1067) of a marine cyanobacterial assemblage consisting of *Lyngbya/Schizothrix* mix (VYI 5 Feb 97-2) contained the tumor-promoting agent, debromoaplysiatoxin (**1**).[1] A fraction, obtained from extensive fractionation of the aqueous extract, showed it contain the known metabolite, debromoaplysiatoxin (**1**) after comparison with sample of the pure molecule on 1D as well as 2D normal phase TLC plates.

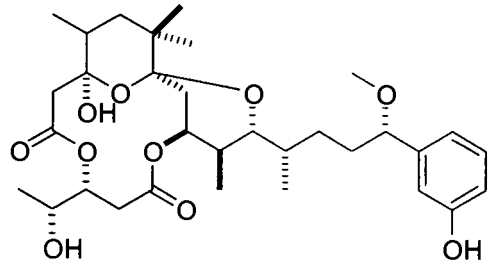

Debromoaplysiatoxin (**1**)

Reference

1. Kato, Y.; Scheuer, P. J. *J. Am. Chem. Soc.* **1974**, *96*, 2245-2246.

APPENDIX C

ISOLATION AND STRUCTURE DETERMINATION OF KNOWN ANTIFUNGAL NATURAL PRODUCTS FROM THE RED ALGA, *GELIDIUM PRISTIODES*

An organic extract (# 1060) of about 1.3 g was made on a collection of marine red agla, *Gelidium pristoides* (ZAK 27 Mar 97-02) obtained from South Africa. The organic extract was taken through several tiers of chromatography including VLC and HPLC to afford known halogenated furanones (**1** and **2**).[1,2] The separation was guided by antifungal bioassay data, tested against three strains of fungi, *Phytophthora infestans*, *Septoria nodorum*, and *Septoria tritici*.

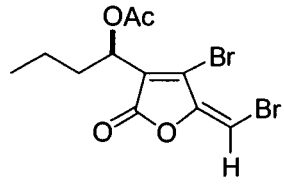

1

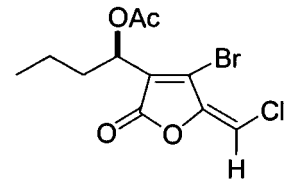

2

References

1. Kazlauska, R.; Murphy, P. T.; Quinn, R. J.; Wells, R. J. *Tetrahedron Lett.* **1977**, 37-40.

2. Pettus, J. A.; Wing, R. M.; Sims, J. J. *Tetrahedron Lett.* **1977**, 41-44.